

UNIVERSITÀ  
DEGLI STUDI  
DI PADOVA

Head Office: Università degli Studi di Padova

Department

**BIOLOGY**

Ph.D. COURSE IN: **BIOCIENCES**

CURRICULUM: **EVOLUTION, ECOLOGY & CONSERVATION**

SERIES **XXX**

**Population structure, connectivity and ecological dynamics of the Antarctic silverfish,  
*Pleuragramma antarctica***

Thesis written with the financial contribution of Fondazione Casse di Risparmio di Padova e Rovigo

**Coordinator:** Prof. Ildikò Szabò

**Supervisor:** Prof. Lorenzo Zane

**Co-Supervisor:** Dr. Chiara Papetti

**Ph.D. student :** JILDA ALICIA CACCAVO



# Contents

Thesis structure . . . . .	iv
Summary . . . . .	vi
Riassunto . . . . .	x
<b>1 Background and aims</b>	<b>1</b>
<b>2 Brooks <i>et al.</i> 2018</b>	<b>17</b>
Supplementary Information <b>Brooks <i>et al.</i> 2018</b> . . . . .	32
<b>3 Caccavo <i>et al.</i> 2018a</b>	<b>41</b>
Supplementary Information <b>Caccavo <i>et al.</i> 2018a</b> . . . . .	73
<b>4 Caccavo <i>et al.</i> 2018b</b>	<b>97</b>
<b>5 Discussion and conclusion</b>	<b>143</b>
<b>Appendix 1</b>	<b>151</b>
<b>Appendix 2</b>	<b>161</b>

SO LONG, AND THANKS FOR ALL THE FISH.

Douglas Adams

*The Hitchhiker's Guide to the Galaxy*

## Thesis structure

The thesis you are about to enjoy is presented as a paper collection, describing the research undertaken during the three years of my PhD under the supervision of Prof. Lorenzo Zane. I endeavored to characterize the population structure and life history connectivity of the keystone Southern Ocean forage species the Antarctic silverfish (*Pleuragramma antarctica*). To this end, I spent the first two years of my PhD using population genetics techniques to assess levels of gene flow as a proxy for connectivity between populations on a local and circumpolar scale. At the end of my second year, thanks to an Antarctic Science Bursary award, I was able to delve into the use of alternative techniques to describe fish population structure, namely otolith chemistry, during a 2-month period at the Center for Quantitative Fisheries at Old Dominion University (Virginia, USA) under the supervision of Dr. Julian Ashford. Thanks to an additional fellowship awarded by the Scientific Committee on Antarctic Research (SCAR), I spent the first 3-months of the third year of my PhD exploring the connection between population structure and trophic ecology by employing lipid-based analyses of diet composition at the Laboratoire d'Océanographie de Villefranche-sur-Mer (France) under the supervision of Ingénieur Marc Boutoute and Directeur de Recherche Émérite Patrick Mayzaud. This thesis follows the trajectory of my body of research, and is presented in the following manner:

- A main section detailing the work carried out to describe the population structure and life history connectivity in Antarctic silverfish through three manuscripts at various stages of drafting, revision and publication.
- Two appendices, the first describing the preliminary results of work on the trophic ecology of Antarctic silverfish carried out in collaboration with the laboratory in Villefranche-sur-Mer, and the second a published manuscript on which I collaborated utilizing the populations genetics techniques developed in my silverfish studies.

This thesis provides a wholistic approach to defining population structure in Antarctic silverfish, combining multidisciplinary techniques in order to understand how the complex interplay between life history and hydrography modulate connectivity in this critical forage species of the Southern Ocean.



## Summary

The Antarctic silverfish (*Pleuragramma antarctica*) is a keystone species in the continental shelf waters around the Antarctic, performing an essential role of connecting higher and lower trophic levels in the Southern Ocean ecosystem. Its early life history is dependent on the platelet ice layer found below sea ice, thus intimately intertwining its fate with that of sea ice extent.

Antarctic silverfish belong to the family Nototheniidae, part of the Notothenioidei suborder whose species radiation in the Southern Ocean 24 million years ago is one of the most expansive among teleost fish. Most notothenioids inhabit a benthic niche as adults, though many experience a pelagic egg and larval phase. Antarctic silverfish are unique among notothenioids in that they are pelagic throughout their life history. Larvae develop in the platelet ice layer near the surface beneath sea ice, descending into deeper waters as they grow in size as juveniles, finally reaching their maximum depth range as adults at 400 – 700 m below the surface. While they lack a swim bladder, Antarctic silverfish manage to remain in the water column as adults by a type of pedomorphy in which they retain lipids from larval and juvenile life stages, allowing them to achieve neutral buoyancy. Despite their presence in the water column as adults, they practice a similar energy-efficient life strategy to their benthic counterparts. Their feeding strategy involves hanging in the water column and passively consuming prey. Remaining in the water column throughout their life history combined with their passive life strategy renders Antarctic silverfish especially susceptible to transport via local and circumpolar current systems. Thus, local and circumpolar current systems form the hydrographic framework in which hypotheses regarding Antarctic silverfish population connectivity must be tested.

How populations of fish are defined, and the extent to which separate populations exchange individuals forms the basis of marine fish population biology. The extent to which Antarctic silverfish, which have a circumpolar distribution, represent one fully connected, panmictic population around the Antarctic continent, remains an open question. It is reasonable to presume that, given their pelagic larval phase, many species of notothenioids with a circumpolar distribution represent large, homogeneous populations. This presumption remains the null hypothesis to test when investigating population structure in notothenioids, and it is especially salient when considering the fully pelagic Antarctic silverfish.

The first investigation into Antarctic silverfish population structure employed mitochondrial DNA markers on a circumpolar scale and did not find evidence to reject the null hypothesis of panmixia throughout the Southern Ocean. Intriguingly, while comparisons between regions failed to indicate differentiation, comparisons within regions between years hinted at inter-annual variation in patterns of connectivity. Genetic differentiation within the same geographic area that is lost and gained between sampling years due to variations in recruitment, mortality

and hydrography is known as chaotic genetic patchiness. The extent to which chaotic genetic patchiness is relevant to understanding Antarctic silverfish population structure was further studied in a more recent investigation, restricting its geographic focus to the Antarctic Peninsula, and employing a set of highly polymorphic EST-linked microsatellite markers to understand population connectivity around the Antarctic Peninsula. Based on both its more focused regional scale and sampling scheme, as well as the use of genetic markers more adept at capturing population differentiation, this study was able to detect genetic structuring on the scale of the Antarctic Peninsula.

Building upon these initial studies, this thesis aimed to characterize the circumpolar population structure of Antarctic silverfish, integrating aspects of life history and hydrography in order to describe mechanisms of connectivity between populations.

The first aim was to understand the hydrography underlying life history connectivity on the scale of the Ross Sea region in order to better understand what may be occurring on the circumpolar level. Silverfish larvae were collected from areas in the Ross Sea coincident with hydrographic features hypothesized to influence their connectivity. While a microsatellite-based analysis was precluded due to the poor state of preservation of the larvae, it was possible to confirm species identification using mitochondrial sequence analysis. The genetic confirmation of species was especially important given that this study proposed a new spawning ground for silverfish in the Ross Sea based on size at collection and established growth rates from the time of hatching. Importantly, this study provided renewed support for the life history hypothesis in silverfish, emphasizing the impact of trough circulation in transporting early life stage fish from the ice shelf edge to the continental slope, where retention back towards the coast or entrainment in shelf-long currents modulates connectivity between neighboring populations of silverfish.

The Ross Sea investigation was then expanded on a circumpolar scale, now carried out using a suite of highly polymorphic EST-linked microsatellite markers developed in a closely related notothenioid species and shown to successfully amplify in silverfish in a previous study. This analysis was carried out on fish collected over 25 years from six different regions: the western Ross Sea, the eastern Weddell Sea, Larsen Bay, the northern Antarctic Peninsula, the South Orkney Islands, and the western Antarctic Peninsula. The data analyzed included samples from the two previous investigations of silverfish population structure described earlier, the first using mitochondrial markers on a circumpolar scale that had not found evidence of population structuring, and the second using the same suite of microsatellite markers employed in this thesis on a regional scale around the Antarctic Peninsula. The integration of these previous datasets into the present analysis allowed for an increase in the resolving power of the previous mitochondrial marker-based study, as well as for the integration of the Antarctic Peninsular work into the greater circumpolar context.



The circumpolar investigation of Antarctic silverfish population structure confirmed that the population structure of silverfish on a circumpolar scale is characterized by high levels of gene flow, and suggested that the Antarctic Slope Front and Current System (AFS) plays an integral role in connecting populations in the Southern Ocean. The importance of the AFS was evident in that reductions in gene flow were only observed in the South Orkney Islands and west Antarctic Peninsula, which were the only two areas in the study where the AFS has not been shown to arrive. This result also expanded to a circumpolar scale the earlier Ross Sea study, which had emphasized the importance of the AFS in connecting Ross Sea populations between local trough systems.

It remained however, that small scale population differentiation which had been observed in the Ross Sea based on larval distributions, as well as in the eastern Weddell Sea based on the distribution of older and younger cohorts between sampling areas, was unable to be resolved using genetic techniques. Thus, the final aim of the main project of this thesis was carried out in order to resolve population structure on the regional scale, this time in the Weddell Sea, employing otolith chemistry. Analysis of trace element deposition in otolith nuclei, reflective of oceanographic conditions to which fish were exposed in early life, has been shown to delineate population structure in the Southern Ocean, in both silverfish and related notothenioids. Of the stations for which samples were available in the Weddell Sea, five stations were selected based on their locations with respect to hydrographic features hypothesized to influence population structuring in the region, in Atka Bay, Halley Bay, off of Coats Land, and west and east of the Filchner Trough. Previous studies, as well as data on biomass and abundance from the sampling expedition during which the silverfish were collected, emphasized the importance of the Filchner Trough in supporting a local population of silverfish in the eastern Weddell Sea continental shelf area. Furthermore, hydrographic data collected in the Weddell Sea emphasized the importance of warm water mass intrusion onto the continental shelf carried from the east into the Weddell Sea region by the AFS. These warm water intrusions from the AFS not only have the potential to carry fish from other regions into the Weddell Sea area, but regulate circulation patterns and the strength and directionality of coastal currents in the region, modulating local connectivity. The results of the otolith nucleus chemistry analysis revealed significant population structuring along the eastern Weddell Sea, in contrast to the structure revealed using genetics. The population structure revealed by the otolith chemistry analysis supported the importance of warm water intrusions from the AFS in transporting fish between areas, while highlighting the role of the Filchner Trough circulation in supporting a coherent population in the southeast Weddell Sea. These results emphasize the importance of the integration of multidisciplinary techniques in the context of local hydrography in addressing questions of population structure and life history connectivity in Antarctic silverfish in the Southern Ocean, and for that matter, any pelagic species inhabiting a continental shelf ecosystem.



## Riassunto

L'*antarctic silverfish* (*Pleuragramma antarctica*) è una specie chiave nelle acque della piattaforma continentale antartica, dove svolge un ruolo essenziale nel collegare i diversi livelli trofici. La sua life history dipende, nella prima fase, dal cosiddetto "ghiaccio a placchette" (*platelet ice*), che si forma all'interfaccia tra l'acqua marina e lo strato di ghiaccio superficiale, legando strettamente il destino di questa specie all'estensione del ghiaccio antartico.

L'*antarctic silverfish* appartiene alla famiglia Nototheniidae, che fa parte del sottordine dei Nototeniioidei, la cui radiazione, avvenuta nell'oceano Antartico a partire da 24 milioni di anni fa, rappresenta una delle più spettacolari radiazioni adattative nei pesci teleostei. I nototeniioidei comprendono, nella maggior parte dei casi, specie demersali in fase adulta, ma caratterizzate da uova e larve pelagiche; l'*antarctic silverfish* è unico sotto questo punto di vista perché è pelagico durante tutto il ciclo vitale. Le larve si sviluppano nello strato di *platelet ice* sotto il ghiaccio marino superficiale e scendono verso acque più profonde durante la maturazione, arrivando come adulti a profondità massime di 400 – 700 m. Nonostante l'assenza di vescica natatoria, l'*antarctic silverfish* riesce a mantenersi nella colonna d'acqua nello stadio adulto grazie a un tipo di pedomorfia caratterizzato dal mantenimento e dall'aumento dei lipidi presenti nelle fasi larvali e giovanili, che ne aumenta il potere di galleggiamento. Malgrado l'*habitus* pelagico da adulto, il *silverfish* è molto efficiente dal punto di vista energetico, possedendo una strategia alimentare simile alle controparti bentoniche, che consiste in questo caso nel galleggiare passivamente nella colonna d'acqua, consumando le prede che capitano nei paraggi, ma senza investire energia in una vera e propria ricerca attiva delle prede.

Il fatto di rimanere nella colonna d'acqua durante tutto il ciclo vitale, in combinazione con la strategia di vita passiva, rende l'*antarctic silverfish* particolarmente suscettibile al trasporto da parte dei sistemi di correnti locali e circumpolari. Questo aspetto lo rende particolarmente interessante nel contesto della biologia di popolazione dei pesci marini, dove risulta importante identificare la presenza di diverse popolazioni e definire l'entità con cui popolazioni separate scambiano individui. In particolare, il fatto che l'*antarctic silverfish*, che ha una distribuzione circumpolare, presenti o meno una singola popolazione panmittica attorno al continente antartico, rimane una questione aperta. Dato che le fasi larvali sono pelagiche, è ragionevole presupporre che molte specie di nototeniioidei siano organizzate in grandi popolazioni omogenee su scala geografica più o meno ampia. Questo presupposto fornisce l'ipotesi nulla da testare quando si investiga la struttura di popolazione di questo gruppo, ed è specialmente rilevante se si considera l'*habitus* pelagico dell'*antarctic silverfish*.

Il primo studio della struttura genetica di popolazione dell'*antarctic silverfish* è stato svolto con marcatori del DNA mitocondriale; questa indagine, svolta su una scala circumpolare, non ha fornito evidenze tali da confutare l'ipotesi nulla di panmissia per l'intero oceano antartico. Tuttavia, mentre i confronti svolti tra diverse regioni non sono riusciti a dimostrare la presenza di differenziamento genetico, i confronti svolti entro regioni tra diversi anni di campionamento hanno suggerito l'esistenza di variazione inter-annuale del grado di connettività. Il differenziamento genetico tra anni di campionamento entro la stessa area geografica è riconducibile al fenomeno della *chaotic genetic patchiness* e può essere dovuto a variazioni nel tasso di reclutamento e mortalità e nell'idrografia. La presenza di differenziamento genetico di popolazione e di *chaotic genetic patchiness* nell'*antarctic silverfish* sono stati recentemente confermati mediante genotipizzazione di microsatelliti EST-linked in uno studio focalizzato su campioni provenienti dalla Penisola Antartica. In questo caso, l'utilizzo di marcatori genetici ipervariabili caratterizzati da un elevato potere risolutivo ha permesso di rilevare una significativa struttura genetica sulla scala regionale della Penisola Antartica.

Questa tesi di dottorato mira a caratterizzare la struttura di popolazione circumpolare dell'*antarctic silverfish*, integrando l'informazione fornita dagli studi iniziali con nuovi campioni ed interpretando i risultati alla luce dei diversi aspetti di life history ed idrografia al fine di descrivere i meccanismi di connettività tra popolazioni.

Nel primo studio prodotto nell'ambito di questa tesi di dottorato, sono stati analizzati dei campioni di larve dell'*antarctic silverfish* provenienti dal Mare di Ross, con l'obiettivo di legare l'idrografia locale alla connettività della specie. Lo stato di conservazione dei campioni non ha permesso di utilizzare marcatori molecolari nucleari (microsatelliti) per studiare il differenziamento tra siti geografici entro il Mare di Ross. Nonostante questo, è stato possibile sequenziare un frammento di DNA mitocondriale che ha permesso di identificare univocamente le larve come appartenenti alla specie *P. antarctica*. Questo risultato è particolarmente rilevante perché conferma, grazie all'utilizzo di metodi genetici, la presenza di larve della specie *P. antarctica* in alcune aree del Mare di Ross che erano state precedentemente solo ipotizzate essere zone preferenziali di nursery del *silverfish*, sulla base di tempi di raccolta dal momento della schiusa delle uova e del tasso di crescita ipotizzato. Sulla base dell'idrografia locale, questo studio ipotizza che la circolazione legata alle depressioni del fondale sia essenziale per il trasporto delle fasi di vita iniziali dalle zone più costiere fino alla scarpata continentale, mentre l'idrografia costiera potrebbe controllare il trasporto lungo i margini della piattaforma continentale modulando la connettività tra popolazioni adiacenti.

In un secondo studio prodotto nell'ambito di questa tesi di dottorato sono stati analizzati campioni raccolti nell'arco di 25 anni da sei regioni antartiche diverse: la parte ovest del Mare di Ross, la parte est del Mare di Weddell, la Baia di Larsen, la parte nord della Penisola Antartica, le Isole di South Orkney, e la parte ovest della Penisola Antartica. Questo studio su scala circumpolare è stato condotto utilizzando un pannello di 18 loci microsatellite isolati in precedenza per varie specie di nototenioidi antartici. Questi loci sono risultati polimorfici anche in *P. antarctica* e informativi per gli obiettivi di questa tesi di dottorato. Alcuni dei campioni inclusi in questo studio sono stati analizzati in due studi precedenti: un primo studio non aveva evidenziato segnali di differenziamento genetico a livello circumpolare (analisi di un marcatore mitocondriale) mentre un secondo studio, più recente e focalizzato sulla Penisola Antartica, aveva segnalato *chaotic genetic patchiness* e differenziamento genetico utilizzando lo stesso pannello di 18 microsatelliti genotipizzati in questa tesi di dottorato.

Questo secondo studio ha confermato che la struttura di popolazione del *silverfish* sulla scala circumpolare è caratterizzato da alti livelli di flusso genico suggerendo che il sistema di correnti, in particolare l'*Antarctic Slope Front and Current System* (AFS), abbia un ruolo critico nel collegamento delle popolazioni nell'oceano Antartico. L'importanza del AFS è suggerita dal limitato flusso genico tra le aree ad ovest della Penisola Antartica e le South Orkneys, le due uniche zone non raggiunte dall'AFS. Questa considerazione è ulteriormente supportata dall'ipotesi che l'AFS mantenga la connettività tra depressioni del fondale anche nel Mare di Ross.

Per comprendere se l'assenza di differenziamento nell'area ad est del Mare di Weddell fosse effettivamente un fatto biologico o fosse dovuta alla scarsa sensibilità dei marcatori microsatellite a piccole differenze, è stato condotto un ulteriore studio utilizzando l'analisi della chimica degli otoliti di *silverfish*. La quantificazione delle tracce di elementi deposti nel centro (*nucleus*) degli otoliti è indicativa delle condizioni chimiche oceanografiche alle quali gli individui sono stati esposti nelle fasi iniziali dello sviluppo. Questa metodologia permette di conseguenza di testare se gli individui siano stati esposti a masse d'acqua diverse nelle prime fasi di vita e di dimostrare l'esistenza di popolazioni con diversa origine.

Tra i campioni disponibili per il Mare di Weddell, sono state scelte 5 aree sulla base degli aspetti idrografici che potrebbero influire sulla struttura di popolazione locale (Baia di Atka, Baia di Halley, vicino alla costa di Coats, ad est ed ovest del Filchner Trough). Dati di abbondanza e biomassa raccolti in parallelo durante il campionamento del *silverfish* nel Mare di Weddell avevano già evidenziato l'importanza del Filchner Trough nel sostenere la popolazione locale dell'*antarctic silverfish*. Inoltre, l'idrografia locale, attraverso l'intrusione di acqua più calda dall'AFS verso il Mare di Weddell, permetterebbe sia di trasportare il *silverfish* verso il Mare di Weddell sia di regolare direzionalità e tasso di connettività locale.

In contrasto con quanto evidenziato dall'approccio genetico, le analisi di microchimica degli otoliti segnalano differenze statisticamente significative tra gruppi di individui all'interno del mare di Weddell, in particolare tra nordest e sudest del Mare di Weddell.

Questi studi suggeriscono un ruolo chiave dell'idrografia sia su scala circumpolare che locale nel modulare la connettività delle popolazioni dell'*antarctic silverfish*. Inoltre, questa tesi di dottorato evidenzia come un approccio multidisciplinare possa chiarire questioni di connettività di popolazione proponendo una metodologia applicabile a diversi organismi sia antartici che non.

# Chapter 1

Background and aims

## Background and aims

### The Antarctic silverfish (*Pleuragramma antarctica*)

The Antarctic silverfish (*Pleuragramma antarctica*) (Fig. 1) is an essential part of the continental shelf ecosystem in the Southern Ocean (Duhamel et al. 2014, Koubbi et al. 2017). Together with krill, they are the main forage species that transfer energy up the trophic hierarchy from primary producers to larger fish predators, birds and mammals (Mintenbeck et al. 2012). In areas where krill is less prevalent, Antarctic silverfish are often the main prey item for krill-dependent species such as Adélie penguins (La Mesa et al. 2004). This vital role that the Antarctic silverfish plays in the Southern Ocean ecosystem makes it an important target species of study in seeking to understand the health and resilience of the Southern Ocean ecosystem (Koubbi et al. 2017). The relevance of Antarctic silverfish is further underpinned by its dependence on sea ice in its life history (Vacchi et al. 2012). Early life stages of Antarctic silverfish are associated with the platelet ice layer beneath fast ice (Vacchi et al. 2004). This environment not only provides protection from predators (Guidetti et al. 2014), but is rich in plankton species upon which silverfish depend during early development (Arrigo & Thomas 2004, Guidetti et al. 2014). While eggs and larvae are found close to the surface, older larvae and juveniles begin to descend deeper into the water column as they grow and develop (La Mesa & Eastman 2012). Adult silverfish are found in the deepest depths of their range at 400 – 700 m (La Mesa & Eastman 2012).



**Figure 1** The Antarctic silverfish (*Pleuragramma antarctica*). Photo Credit: Joel Bellucci, [goo.gl/BEx4L9](https://goo.gl/BEx4L9).

Antarctic silverfish belong to the family Nototheniidae, part of the Notothenioidei suborder which includes most Antarctic and sub-Antarctic fish (Near et al. 2004). The notothenioid lineage can be traced back to 24 million years ago, after the origination and strengthening of



the Antarctic Circumpolar Current (Dalziel et al. 2013, Chenuil et al. 2018). Notothenioids have a variety of adaptations which allowed them to dominate the waters of the Southern Ocean in one of the greatest species radiations among teleost fish (Eastman 2005, Near et al. 2012). Principal among these adaptations is the development of Antifreeze Glycoproteins (AGFPs), which allow notothenioids to thrive in subzero waters that hover between  $-2 - 0^{\circ}\text{C}$  (Eastman 1993, Matschiner et al. 2011). While many notothenioids have pelagic egg and larval phases, Antarctic silverfish are unique in that they are pelagic throughout their life history (La Mesa & Eastman 2012). Though they lack a swim bladder, silverfish maintain their neutral buoyancy by the pedomorphic retention of lipids from earlier life stages (Wöhrmann et al. 1997). Most notothenioids occupy benthic niches as adults, and practice a relatively efficient, energy-saving life strategy (Eastman 2005). There is no evidence of migrations in Antarctic silverfish, as their life history is spatially constrained to the shelf ecosystem (Vacchi et al. 2004, La Mesa et al. 2010). The only regular activity observed in silverfish are diel vertical migrations in the presence of seasonal light, in which adult fish are found in the shallower range of their distribution by night and in the deeper portions by day (Lancraft et al. 2004, La Mesa & Eastman 2012). Early life stages are also characterized by a lack of evidence of active swimming, movements across the shelf instead enabled by passive transport (Hubold 1984, La Mesa et al. 2010, La Mesa & Eastman 2012). These aspects of their life history have important implications for silverfish population structure and connectivity.

#### Population structure and connectivity – relevance

The extent to which marine populations form coherent units, exchange individuals and are dependent on one another impacts the health, resilience and eventual management of a species (Jones et al. 2007). Given their pelagic nature and the ability of circumpolar current systems to transport eggs and larvae large distances, the null hypothesis for population structure in many notothenioid species has been one of panmixia, in which species with a circumpolar distribution represent one large, homogeneous population unit (Matschiner et al. 2009). This was first demonstrated in Zane et al. (2006), which found no evidence of population structuring on a circumpolar scale using mitochondrial markers. This result was echoed among multiple species of the families Nototheniidae and Channichthyidae (Damerau et al. 2012, Papetti et al. 2012).

However, some nuance is required in the interpretation of the lack of genetic differentiation found in Antarctic silverfish. While Zane et al. (2006) did not find genetic differentiation between sampling areas as geographically distant as the Weddell and Ross Seas, they did find evidence of genetic differentiation between years. Such patterns of genetic differentiation which vary over time have been referred to as chaotic genetic patchiness (Johnson & Black 1982), and is thought to be caused by variability in recruitment, mortality and hydrography

over time (Selwyn et al. 2016). Chaotic genetic patchiness was also observed more recently in an investigation of Antarctic silverfish focused on the Antarctic Peninsula region using microsatellite markers (Agostini et al. 2015). The results of Agostini et al. (2015) further challenged the null hypothesis of panmixia in silverfish by finding evidence for significant genetic differentiation between populations along the western, northern and eastern peninsula. Both the regional scale of Agostini et al. (2015) and the use of more discerning genetic markers (Cuéllar-Pinzón et al. 2016) likely contributed to these contrasting results.

### Population structure and connectivity – methodologies

The methodologies used to define population structure and connectivity have changed over time, and life history and scale are both important to consider when assessing the strength and validity of methods (Cuéllar-Pinzón et al. 2016). The assessment of genetic differentiation between populations sampled from different areas is a powerful tool that serves as a proxy for the exchange of individuals and thus gene flow among populations (Waples & Gaggiotti 2006). While mitochondrial markers are useful in their ability to recreate demographic histories (Antoniou & Magoulas 2014) ancestral matrilineages (Bernatchez 2007), their mutation rate and thus level of polymorphism limits their ability to define population structure in species with high basal levels of gene flow (Cuéllar-Pinzón et al. 2016). Microsatellites in contrast, exhibit elevated rates of mutation resulting in highly polymorphic markers that allow them to distinguish population structure on small scales (Li et al. 2008). Microsatellites are regions of tandem repeats in nuclear DNA whose increased mutation rate is generally attributed to replication slippage, resulting in alleles which vary in base pair length (Zane et al. 2002, Ellegren 2004). While next-generation sequencing methods offer a similar, and depending on the study context, more powerful means of diving genetic structure, they remain cost prohibitive, especially in species for which microsatellite markers have already been developed (Hodel et al. 2016).

While genetic tools remain a powerful and important technique in the population biology toolbox, it is important to recognize their limitations (Lowe & Allendorf 2010). Especially in pelagic species exposed to strong current systems, the exchange of small numbers of individuals between otherwise independent populations would effectively result in genetic homogenization (Begg et al. 1999, Hawkins et al. 2016). While such high basal levels of gene flow are important to preclude genetic isolation and its negative impacts on species resilience (Jones et al. 2007), variation in mechanisms of connectivity have the potential to erase observed connectivity over time (Hellberg 2009, Eldon et al. 2016). Thus, it is essential that any investigation of population structure and connectivity in marine populations include multidisciplinary modes of inquiry (Welch et al. 2015). In addition to taking important life history measures such as size at capture, age, sex and maturity into account, several

methodologies in fisheries biology function well to complement genetics in the investigation of population structure, including tagging, parasitology and otolith chemistry (Begg et al. 1999, Welch et al. 2015, Taillebois et al. 2017). Both parasitology and otolith chemistry are especially useful in that they both describe population structure on the shortened scale of the individual lifetime as opposed to the generational perspective provided by measures of genetic differentiation (Taillebois et al. 2017). Otolith chemistry has the potential to resolve population structure where gene flow homogenizes genetic differences, and throw light on the mechanisms explaining spatial length distributions and genetic connectivity (Ashford et al. 2006, Taillebois et al. 2017).

Otolith chemistry, while originally developed to distinguish between estuarine and oceanic environments in anadromous species (Thresher 1999), has been shown to elucidate provenance in fully oceanic species (Miller et al. 2005), including in the Southern Ocean (Ashford et al. 2006). The fish otolith is composed of an aragonite lattice of Ca overlaid on a protein matrix (Campana 1999). Ambient conditions to which fish are exposed influence the extent to which divalent elements are substituted for Ca in the otolith (Thorrold & Swearer 2009). Validating studies have demonstrated the relationship between trace element deposition and environmental concentrations experimentally by manipulating ambient levels of divalent elements and measuring their resulting deposition in otoliths (Bath et al. 2000). Some of the most common divalent elements measured to assess environmental exposure in marine fish are Sr and Ba, driven by temperature and salinity (Izzo et al. 2017), and Mg, driven by physiological processes (Loewen et al. 2016). Otolith chemistry has been shown population structure delineated by genetics in the Patagonian toothfish (*Dissostichus eleginoides*) (Ashford et al. 2006), as well as to reflect frontal systems in the Antarctic Circumpolar Current (ACC) (Ashford et al. 2007). Population structuring due to large-scale ocean circulation has been revealed by otolith chemistry in both the Patagonian and Antarctic (*Dissostichus mawsoni*) toothfish (Ashford et al. 2008, Ashford et al. 2012). It has also been shown that otolith chemistry can distinguish population structure in Antarctic silverfish between the Antarctic Peninsula and the South Orkney Islands (Ferguson 2012).

### The role of hydrography in local and circumpolar connectivity

In considering what methods to utilize and how to create a framework for testing hypotheses describing population structure in Antarctic silverfish, it is essential to consider the mechanisms underlying connectivity, principal among which is hydrography (Ashford et al. 2017). The Antarctic Circumpolar Current (ACC) has long been considered the principal transport mechanisms by which circumpolar species are distributed (Matschiner et al. 2009). Having formed between 34 and 25 million years ago (Dalziel et al. 2013) and forming the principal barrier which separates the Southern Ocean from the world's oceans (Orsi et al.

1995), it is the largest current system in the world, carrying over nearly  $150 \text{ million m}^3\text{s}^{-1}$  of water over 24,000 km (Carter et al. 2008). The ACC has been shown to be relevant in the population connectivity of several notothenioids (Damerau et al. 2012). In Antarctic silverfish, the ACC has been implicated in connectivity between the Amundsen Sea and the Antarctic Peninsula (Kellermann 1996), the one section of its circumpolar extent where it approaches the continental slope (Orsi et al. 1995, Savidge & Amft 2009). However, its distance from the continental shelf and slope throughout the rest of its extent (Fig. 2)(Orsi et al. 1995) renders the ACC less relevant to connectivity generally among Antarctic silverfish, whose range is restricted to the shelf/slope ecosystem (Ashford et al. 2017).

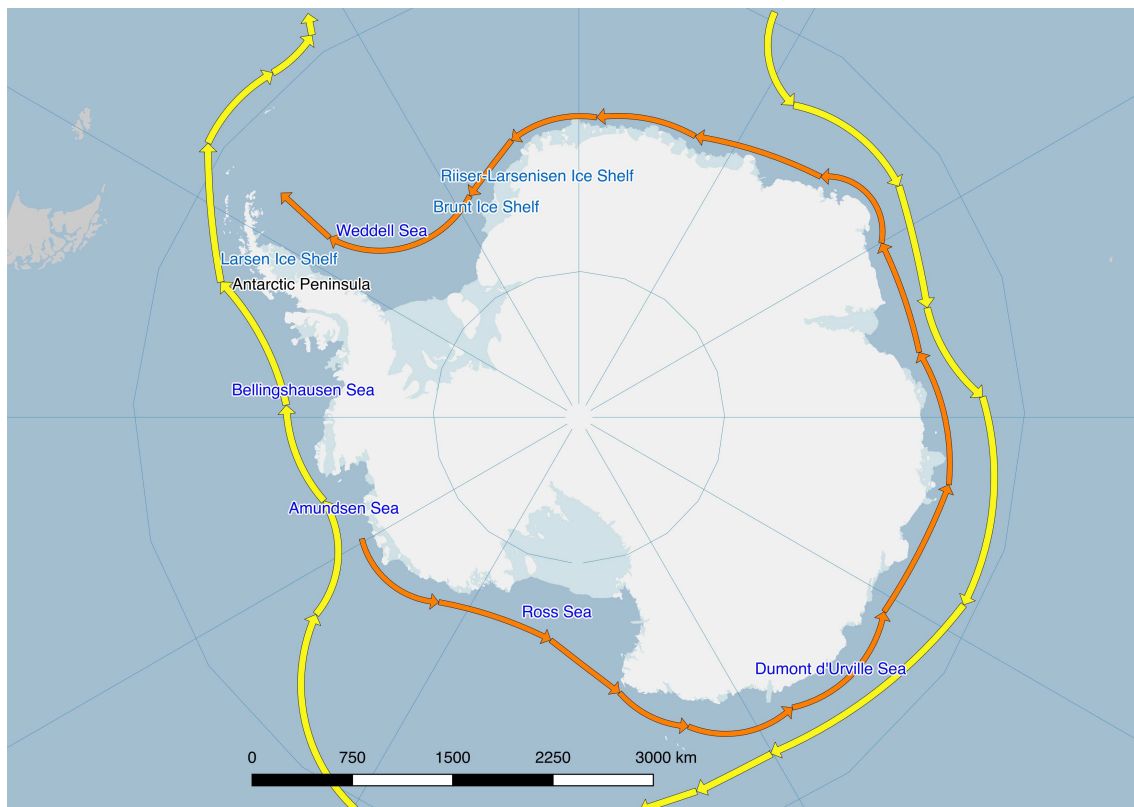


**Figure 2** Map of the Antarctic. Yellow arrows approximate the ACC, Antarctic Circumpolar; Orange arrows approximate the AFS, Antarctic Slope Front and Current System. Inferred position of the ACC and AFS approximated based on Orsi et al. (1995) Fig. 7 and Whitworth et al. (1998), respectively. Map created using the Norwegian Polar Institute's Quantarctica 2.0 package (Matsuoka et al. 2018) in the software QGIS version 2.18.9 <http://qgis.osgeo.org> (QGIS Development Team 2018).

While not entirely circumpolar in their extents, the Antarctic Slope Front and Current System (AFS) and the Antarctic Coastal Current (AACC) are thought to play an important role in facilitating connectivity between Antarctic silverfish populations (Agostini et al. 2015, La Mesa et al. 2015, Ashford et al. 2017). The AFS is first identifiable in the western Amundsen Sea, from where it flows westward along the slope of the Ross Sea, East Antarctica and the

Weddell Sea (Fig. 2)(Whitworth et al. 1998, Heywood et al. 2004). In the western Weddell Sea, the AFS rounds the tip of the Antarctic Peninsula off Joinville Island, before entering the Hesperides Trough, where it mixes with Weddell-Scotia Confluence waters (Azaneu et al. 2017). Further inshore, the AACC is typical of coastal buoyant plumes, occupying the upper part of the water column close inshore (Moffat et al. 2008). It is influenced by freshwater input from precipitation, run-off, sea-ice and glacial melt, its presence and strength varying spatially, seasonally and between years (Dutrieux et al. 2014). It merges with the AFS around Joinville Island at the northern tip of the Antarctic Peninsula before separating to continue along the Trinity Peninsula (Thompson et al. 2009). There, it forms the southern boundary of the Bransfield Gyre (Savidge & Amft 2009), which carries water past the South Shetland Islands.

Large-scale circulation impacts local connectivity by its interaction with glacial trough systems. The Antarctic continental shelf bathymetry is characterized by troughs created by glacial retreat since the Last Glacial Maximum (Anderson et al. 2002). Glacial troughs span the continental shelf in many places, with the trough heads located inshore at the ice shelf rim, while trough mouths open onto the slope at the continental shelf edge (Ashford et al. 2017). Warm Deep Water (WDW) entrained in slope currents penetrates the shelf via trough inflows, mixing with colder shelf waters to form Modified Warm Deep Water (MWDW) which is carried inshore towards the shelf (Dinniman et al. 2003, Nicholls et al. 2009). Cold shelf waters defined by ice dynamics near the coast, mix with MWDW eventually forming Antarctic Bottom Water which flows equatorward in gravity currents towards the slope (Gordon et al. 2009). This inflow and outflow characterizes trough circulation, and provides a mechanisms for cross-shelf transport of fish to and from the continental shelf edge (Ashford et al. 2017).

The Antarctic silverfish life history hypothesis integrates aspects of large-scale circulation with local trough circulation to propose a physical-biological mechanism for local and circumpolar connectivity among populations (Ashford et al. 2017). Distributions of early life stages associated with ice shelves in the western Ross Sea (Ghigliotti et al. 2017), Antarctic Peninsula (Kellermann 1986), Dumont d'Urville Sea (Koubbi et al. 2011) and eastern Weddell Sea (Hubold 1984, Knust R 2014) support the hypothesis that early life stages are associated with inshore areas supported by the sea ice edge ecosystem (Ashford et al. 2017). Larval dispersal predicted by particle tracking simulations combined with otolith age data (La Mesa et al. 2015), as well as observed inshore adult movements (Daniels & Lipps 1982) suggest a life cycle in which ontogenic dispersion culminates in adult return to coastal spawning areas (Ashford et al. 2017). Trough circulation provides a retention mechanism to support local silverfish populations throughout its life history, while also explaining the process by which populations may exchange individuals on a local and circumpolar scale by exposure to along-shelf current systems (AFS, ACC) as well as inshore buoyancy plumes (AACC) (Ashford et al. 2017).

### Thesis goals

The present thesis aims to test the life history hypothesis in Antarctic silverfish by integrating multidisciplinary methods in order to address questions regarding population structure and connectivity in a hydrographic framework. This was done using a multipronged approach in both scale and mode of inquiry. Both circumpolar and regional scales were considered in order to assess how circumpolar connectivity may impact regional population structure, as well as to understand the different connectivity mechanisms functioning at these scales. Multidisciplinary techniques including life history traits, genetics and otolith chemistry were used in tandem to utilize their synergies and maximize their descriptive capabilities in addressing population structure and connectivity of Antarctic silverfish. Finally, these analyses of silverfish were combined with and contextualized by regional and circumpolar hydrography to get at the underlying mechanisms of the observed patterns of connectivity. In detail:

- The Antarctic silverfish life history hypothesis was first tested in larvae from the Ross Sea using abundance indices and life history traits to determine length distributions, growth rates and hatching dates. These data were used to assess the extent to which connectivity via trough circulation and westward movement along the shelf impacted the population structure of silverfish in the Ross Sea. Furthermore, mitochondrial DNA analysis was used to verify morphological species assessment, which confirmed the presence of a new potential spawning ground in the eastern Ross Sea at the Bay of Whales.
- Expanding the Ross Sea investigation to a circumpolar scale, over 1000 samples from 19 different sampling areas collected over 25 years were analyzed using microsatellite markers to assess temporal and spatial genetic differentiation. This analysis integrated samples and data from the previous two investigations of silverfish population structure on a circumpolar scale using mitochondrial markers (Zane et al. 2006) and on the regional scale around the Antarctic Peninsula using microsatellites (Agostini et al. 2015). Given the high basal rate of gene flow in silverfish, the available analysis tools were assessed in order to determine how best to characterize genetic differentiation. This optimization of the tools available to assess differentiation in high gene flow species culminated in a collaboration on the population structure of a Mediterranean clam species *Chamelea gallina* (Appendix 2). Spatial comparisons between silverfish sampling areas were considered in the context of connectivity via the AFS, as well as other hydrographic and bathymetric features relevant to the silverfish life history hypothesis.

- In an effort to deepen our understanding of population structure on the regional scale of the Weddell Sea in Antarctic silverfish, an otolith chemistry analysis was conducted on the same samples on which genetics work had been carried out. An otolith chemistry follow-up to the genetics work was especially relevant in the Weddell Sea where, despite results indicative of a single homogeneous population from the genetics, there were strong indications of population structuring from life history and abundance data. CTD measurements collected at the time of fish sampling were used to identify the water masses occupied by fish from the various sampling areas compared. Considering the interplay of water mass movements allowed for greater specificity in the interpretation of the otolith chemistry results and resultant elaborations on the silverfish life history hypothesis.

Taken together, the research composing the present thesis represents a significant contribution to our knowledge of population structure in this critical forage species underpinning the Southern Ocean ecosystem. The integration of multiple techniques in a hydrographical context to test the life history hypothesis of Antarctic silverfish have made this leap forward in our understanding of population connectivity possible, and represent a framework for future investigations of population structure in species in the Southern Ocean and beyond.

#### Following contents

- **CHAPTER 2 – Population structure and connectivity of Antarctic silverfish in the Ross Sea using life history traits**

This chapter reports the study of Antarctic silverfish larvae associated with trough systems in the Ross Sea. The chapter includes the main article and Supporting Information published in the journal Fisheries Oceanography as:

Brooks CM, **Caccavo JA**, Ashford J, Dunbar R, Goetz K, La Mesa M, Zane L (2018) Early life history connectivity of Antarctic silverfish (*Pleuragramma antarctica*) in the Ross Sea. Fisheries Oceanography 00:1-14. doi: [10.1111/fog.12251](https://doi.org/10.1111/fog.12251).

My role in this work involved performing the genetics experiments and analyses, writing the genetics portion of the paper, and reviewing and editing the paper in its entirety.

- **CHAPTER 3 – Circumpolar population genetic structure and mechanisms of connectivity in Antarctic silverfish**

This Chapter reports the culmination of my doctoral research using genetics to test life history connectivity in Antarctic silverfish. This Chapter includes the main article and Supporting information accepted with revisions to the journal Scientific Reports as:

**Caccavo JA**, Papetti C, Wetjen M, Knust R, Ashford JR, Zane L (2018) Along-shelf connectivity and circumpolar gene flow in Antarctic silverfish (*Pleuragramma antarctica*). *Scientific Reports: Accepted*.

My role in this work was to carry out all experiments and analyses, and write, review, and edit the paper.

- **CHAPTER 4 – Population structure and connectivity of Antarctic silverfish in the Weddell Sea using otolith chemistry**

This Chapter reports the study of connectivity of Antarctic silverfish associated with water masses structured by trough systems in the southern Weddell Sea. This Chapter includes the manuscript draft to be submitted to the journal *Marine Ecology Progress Series (MEPS)* as:

**Caccavo JA**, Ashford J, Ryan S, Papetti C, Schröder M, Zane L (2018) Spatially-based population structure and life history connectivity of the Antarctic silverfish along the southern Weddell Sea shelf. *In preparation*.

My role in this work was to carry out all experiments, assist with the analyses, and write, review, and edit the paper.

- **CHAPTER 5 – Discussion and conclusion**

This Chapter synthesizes the results of the studies described in Chapters 2 – 4 in the context of the Background and aims presented in the present Chapter, as well as the Antarctic silverfish life history hypothesis.

- **Appendix 1 – Trophic ecology in the Antarctic silverfish (*Pleuragramma antarctica*)**

This Chapter reports the background and aims, extended summary, and preliminary results from a study on the trophic ecology of Antarctic silverfish using lipids-based analyses.

- **Appendix 2 – Using population genetics to assess the population structure and connectivity of the striped venus *Chamelea gallina***

This Chapter reports a study on which I collaborated, which includes many of the techniques and considerations eventually honed in the silverfish genetics analysis. This Chapter includes the main article and Supporting information published in the journal *Fisheries Research* as:

Papetti C, Schiavon L, Milan M, Lucassen M, **Caccavo JA**, Paterno M, Boscari E, Marino IAM, Congiu L, Zane L (2018) Genetic variability of the striped venus *Chamelea gallina* in the northern Adriatic Sea. *Fisheries Research* 201:68-78. doi: [10.1016/j.fishres.2018.01.006](https://doi.org/10.1016/j.fishres.2018.01.006).

My role in this work was to assist with the analyses, and review and edit the paper in its entirety.

## References



- Agostini C, Patarnello T, Ashford JR, Torres JJ, Zane L, Papetti C (2015) Genetic differentiation in the ice-dependent fish *Pleuragramma antarctica* along the Antarctic Peninsula. *Journal of Biogeography* 42:1103-1113
- Anderson JB, Shipp SS, Lowe AL, Wellner JS, Mosola AB (2002) The Antarctic Ice Sheet during the Last Glacial Maximum and its subsequent retreat history: a review. *Quaternary Science Reviews* 21:49-70
- Antoniou A, Magoulas A (2014) Chapter Thirteen - Application of Mitochondrial DNA in Stock Identification A2 - Cadrin, Steven X. In: Kerr LA, Mariani S (eds) *Stock Identification Methods (Second Edition)*. Academic Press, San Diego
- Arrigo KR, Thomas DN (2004) Large scale importance of sea ice biology in the Southern Ocean. *Antarctic Science* 16:471-486
- Ashford J, Dinniman M, Brooks C, Andrews AH, Hofmann E, Cailliet G, Jones C, Ramanna N (2012) Does large-scale ocean circulation structure life history connectivity in antarctic toothfish (*Dissostichus mawsoni*)? *Canadian Journal of Fisheries and Aquatic Sciences* 69:1903-1919
- Ashford J, Zane L, Torres JJ, La Mesa M, Simms AR (2017) Population Structure and Life History Connectivity of Antarctic Silverfish (*Pleuragramma antarctica*) in the Southern Ocean Ecosystem. In: Vacchi M, Pisano E, Ghigliotti L (eds) *The Antarctic Silverfish: a Keystone Species in a Changing Ecosystem*. Springer International Publishing, Cham
- Ashford JR, Arkhipkin AI, Jones CM (2006) Can the chemistry of otolith nuclei determine population structure of Patagonian toothfish *Dissostichus eleginoides*? *Journal of fish biology* 69:708-721
- Ashford JR, Arkhipkin AI, Jones CM (2007) Otolith chemistry reflects frontal systems in the Antarctic Circumpolar Current. *Marine Ecology Progress Series* 351:249-260
- Ashford JR, Jones CM, Hofmann EE, Everson I, Moreno CA, Duhamel G, Williams R (2008) Otolith chemistry indicates population structuring by the Antarctic Circumpolar Current. *Canadian Journal of Fisheries and Aquatic Sciences* 65:135-146
- Azaneu M, Heywood KJ, Queste BY, Thompson AF (2017) Variability of the Antarctic Slope Current System in the Northwestern Weddell Sea. *Journal of Physical Oceanography* 47:2977-2997
- Bath GE, Thorrold SR, Jones CM, Campana SE, McLaren JW, Lam JWH (2000) Strontium and barium uptake in aragonitic otoliths of marine fish. *Geochimica et Cosmochimica Acta* 64:1705-1714
- Begg GA, Friedland KD, Pearce JB (1999) Stock identification and its role in stock assessment and fisheries management: An overview. *Fisheries Research* 43:1-8
- Bernatchez L (2007) THE EVOLUTIONARY HISTORY OF BROWN TROUT (*SALMO TRUTTA* L.) INFERRED FROM PHYLOGEOGRAPHIC, NESTED CLADE, AND MISMATCH ANALYSES OF MITOCHONDRIAL DNA VARIATION. *Evolution* 55:351-379
- Campana SE (1999) Chemistry and composition of fish otoliths: Pathways, mechanisms and applications. *Marine Ecology Progress Series* 188:263-297
- Carter L, McCave IN, Williams MJM (2008) Chapter 4 Circulation and Water Masses of the Southern Ocean: A Review. *Developments in Earth and Environmental Sciences, Book 8*

- Chenuil A, Saucède T, Hemery Lenaïg G, Eléaume M, Féral JP, Améziane N, David B, Lecointre G, Havermans C (2018) Understanding processes at the origin of species flocks with a focus on the marine Antarctic fauna. *Biological Reviews* 93:481-504
- Cuéllar-Pinzón J, Presa P, Hawkins SJ, Pita A (2016) Genetic markers in marine fisheries: Types, tasks and trends. *Fisheries Research* 173, Part 3:194-205
- Dalziel IWD, Lawver LA, Pearce JA, Barker PF, Hastie AR, Barfod DN, Schenke H-W, Davis MB (2013) A potential barrier to deep Antarctic circumpolar flow until the late Miocene? *Geology* 41:947-950
- Damerau M, Matschiner M, Salzburger W, Hanel R (2012) Comparative population genetics of seven notothenioid fish species reveals high levels of gene flow along ocean currents in the southern Scotia Arc, Antarctica. *Polar Biology* 35:1073-1086
- Daniels RA, Lipps JH (1982) Distribution and Ecology of Fishes of the Antarctic Peninsula. *Journal of Biogeography* 9:1-9
- Dinniman MS, Klinck JM, Smith Jr WO (2003) Cross-shelf exchange in a model of the Ross Sea circulation and biogeochemistry. *Deep Sea Research Part II: Topical Studies in Oceanography* 50:3103-3120
- Duhamel G, Hulley P-A, Causse R, Koubbi P, Vacchi M, Pruvost P, Vignetta S, Irisson J-O, Mormède S, Belchier M, Dettai A, Detrich HW, Gutt J, Jones CD, Koch K-H, Lopez Abellan LJ, Van de Putte AP (2014) Biogeographic patterns of fish. In: De Broyer C., Koubbi P., Griffiths H.J., Raymond B., d' UdAC, Van De Putte A, Danis B, David B, Grant S, Gutt J, Held C, Hosie G, Huettmann F, Post A, Ropert-Coudert Y (eds) *Biogeographic Atlas of the Southern Ocean*. Scientific Committee on Antarctic Research, Cambridge
- Dutrieux P, De Rydt J, Jenkins A, Holland PR, Ha HK, Lee SH, Steig EJ, Ding Q, Abrahamsen EP, Schröder M (2014) Strong Sensitivity of Pine Island Ice-Shelf Melting to Climatic Variability. *Science* 343:174
- Eastman JT (1993) *Antarctic fish biology: evolution in a unique environment*. Academic Press, San Diego, CA
- Eastman JT (2005) The nature of the diversity of Antarctic fishes. *Polar Biology* 28:93-107
- Eldon B, Riquet F, Yearsley J, Jollivet D, Broquet T (2016) Current hypotheses to explain genetic chaos under the sea. *Current Zoology* 62:551-566
- Ellegren H (2004) Microsatellites: simple sequences with complex evolution. *Nature Reviews Genetics* 5:435
- Ferguson JW (2012) Population structure and connectivity of an important pelagic forage fish in the Antarctic ecosystem, *Pleuragramma antarcticum*, in relation to large scale circulation. MS Thesis, Old Dominion University, Norfolk, VA.
- Ghigliotti L, Ferrando S, Carlig E, Di Blasi D, Gallus L, Pisano E, Hanchet S, Vacchi M (2017) Reproductive features of the Antarctic silverfish (*Pleuragramma antarctica*) from the western Ross Sea. *Polar Biology* 40:199-211
- Gordon A, Orsi A, Muench R, A. Huber B, Zambianchi E, Visbeck M (2009) *Western Ross Sea continental slope gravity currents*, Vol 56
- Guidetti P, Ghigliotti L, Vacchi M (2014) Insights into spatial distribution patterns of early stages of the Antarctic silverfish, *Pleuragramma antarctica*, in the platelet ice of Terra Nova Bay, Antarctica. *Polar Biology* 38:333-342
- Hawkins SJ, Bohn K, Sims DW, Ribeiro P, Faria J, Presa P, Pita A, Martins GM, Neto AI, Burrows MT, Genner MJ (2016) Fisheries stocks from an ecological perspective: Disentangling ecological connectivity from genetic interchange. *Fisheries Research* 179:333-341

- Hellberg ME (2009) Gene flow and isolation among populations of marine animals. Annual Review of Ecology, Evolution, and Systematics, Book 40
- Heywood KJ, Naveira Garabato AC, Stevens DP, Muench RD (2004) On the fate of the Antarctic Slope Front and the origin of the Weddell Front. Journal of Geophysical Research: Oceans 109:C06021
- Hodel RGJ, Segovia-Salcedo MC, Landis JB, Crowl AA, Sun M, Liu X, Gitzendanner MA, Douglas NA, Germain-Aubrey CC, Chen S, Soltis DE, Soltis PS (2016) The Report of My Death was an Exaggeration: A Review for Researchers Using Microsatellites in the 21st Century. Applications in Plant Sciences 4
- Hubold G (1984) Spatial distribution of *Pleuragramma antarcticum* (Pisces: Nototheniidae) near the Filchner- and Larsen ice shelves (Weddell sea/antarctica). Polar Biology 3:231-236
- Izzo C, Reis-Santos P, Gillanders BM (2017) Otolith chemistry does not just reflect environmental conditions: A meta-analytic evaluation. Fish and Fisheries:n/a-n/a
- Johnson MS, Black R (1982) Chaotic genetic patchiness in an intertidal limpet, *Siphonaria* sp. Marine Biology 70:157-164
- Jones GP, Srinivasan M, Almany GR (2007) Population connectivity and conservation of marine biodiversity. Oceanography 20:100-111
- Kellermann A (1986) Geographical distribution and abundance of postlarval and juvenile *Pleuragramma antarcticum* (Pisces, Notothenioidei) off the Antarctic Peninsula. Polar Biology 6:111-119
- Kellermann AK (1996) Midwater Fish Ecology. In: Ross RM, Hofmann EE, Quetin LB (eds) Foundations for Ecological Research West of the Antarctic Peninsula, Book 70. American Geophysical Union, Washington
- Knust R SM (2014) The expedition PS82 of the Research Vessel Polarstern to the southern Weddell Sea in 2013/14. Ber Polarforsch Meeresforsch, Book 680
- Koubbi P, Grant S, Ramm D, Vacchi M, Ghigliotti L, Pisano E (2017) Conservation and Management of Antarctic Silverfish *Pleuragramma antarctica* Populations and Habitats. In: Vacchi M, Pisano E, Ghigliotti L (eds) The Antarctic Silverfish: a Keystone Species in a Changing Ecosystem. Springer International Publishing, Cham
- Koubbi P, O'Brien C, Loots C, Giraldo C, Smith M, Tavernier E, Vacchi M, Vallet C, Chevallier J, Moteki M (2011) Spatial distribution and inter-annual variations in the size frequency distribution and abundances of *Pleuragramma antarcticum* larvae in the Dumont d'Urville Sea from 2004 to 2010. Polar Science 5:225-238
- La Mesa M, Catalano B, Russo A, Greco S, Vacchi M, Azzali M (2010) Influence of environmental conditions on spatial distribution and abundance of early life stages of antarctic silverfish, *Pleuragramma antarcticum* (Nototheniidae), in the Ross Sea. Antarctic Science 22:243-254
- La Mesa M, Eastman JT (2012) Antarctic silverfish: Life strategies of a key species in the high-Antarctic ecosystem. Fish and Fisheries 13:241-266
- La Mesa M, Eastman JT, Vacchi M (2004) The role of notothenioid fish in the food web of the Ross Sea shelf waters: A review. Polar Biology 27:321-338
- La Mesa M, Piñones A, Catalano B, Ashford J (2015) Predicting early life connectivity of Antarctic silverfish, an important forage species along the Antarctic Peninsula. Fisheries Oceanography 24:150-161

- Lancraft TM, Reisenbichler KR, Robison BH, Hopkins TL, Torres JJ (2004) A krill-dominated micronekton and macrozooplankton community in Croker Passage, Antarctica with an estimate of fish predation. *Deep-Sea Research Part II: Topical Studies in Oceanography* 51:2247-2260
- Li YC, Korol Abraham B, Fahima T, Beiles A, Nevo E (2008) Microsatellites: genomic distribution, putative functions and mutational mechanisms: a review. *Molecular ecology* 11:2453-2465
- Loewen TN, Carriere B, Reist JD, Halden NM, Anderson WG (2016) Review: Linking physiology and biomineralization processes to ecological inferences on the life history of fishes. *Comparative Biochemistry and Physiology -Part A : Molecular and Integrative Physiology* 202:123-140
- Lowe WH, Allendorf FW (2010) What can genetics tell us about population connectivity? *Molecular ecology* 19:3038-3051
- Matschiner M, Hanel R, Salzburger W (2009) Gene flow by larval dispersal in the Antarctic notothenioid fish *Gobionotothen gibberifrons*. *Molecular ecology* 18:2574-2587
- Matschiner M, Hanel R, Salzburger W (2011) On the origin and trigger of the notothenioid adaptive radiation. *PloS one* 6
- Matsuoka K, Skoglund A, Roth G (2018) Quantarctica [Data set]. Norwegian Polar Institute
- Miller JA, Banks MA, Gomez-Uchida D, Shanks AL (2005) A comparison of population structure in black rockfish (*Sebastes melanops*) as determined with otolith microchemistry and microsatellite DNA. *Canadian Journal of Fisheries and Aquatic Sciences* 62:2189-2198
- Mintenbeck K, Barrera-Oro ER, Brey T, Jacob U, Knust R, Mark FC, Moreira E, Strobel A, Arntz WE (2012) Impact of Climate Change on Fishes in Complex Antarctic Ecosystems. Book 46
- Moffat C, Beardsley RC, Owens B, van Lipzig N (2008) A first description of the Antarctic Peninsula Coastal Current. *Deep Sea Research Part II: Topical Studies in Oceanography* 55:277-293
- Near TJ, Dornburg A, Kuhn KL, Eastman JT, Pennington JN, Patarnello T, Zane L, Fernández DA, Jones CD (2012) Ancient climate change, antifreeze, and the evolutionary diversification of Antarctic fishes. *Proceedings of the National Academy of Sciences of the United States of America* 109:3434-3439
- Near TJ, Pesavento JJ, Cheng CH (2004) Phylogenetic investigations of Antarctic notothenioid fishes (Perciformes: Notothenioidei) using complete gene sequences of the mitochondrial encoded 16S rRNA. *Mol Phylogenet Evol* 32:881-891
- Nicholls KW, Østerhus S, Makinson K, Gammelsrød T, Fahrbach E (2009) Ice-ocean processes over the continental shelf of the southern Weddell Sea, Antarctica: A review. *Reviews of Geophysics* 47:RG3003
- Orsi AH, Whitworth Iii T, Nowlin Jr WD (1995) On the meridional extent and fronts of the Antarctic Circumpolar Current. *Deep-Sea Research Part I* 42:641-673
- Papetti C, Pujolar JM, Mezzavilla M, La Mesa M, Rock J, Zane L, Patarnello T (2012) Population genetic structure and gene flow patterns between populations of the Antarctic icefish *Chionodraco rastrispinosus*. *Journal of Biogeography* 39:1361-1372
- QGIS Development Team (2018) QGIS Geographic Information System. Open Source Geospatial Foundation Project.

- Savidge DK, Amft JA (2009) Circulation on the West Antarctic Peninsula derived from 6 years of shipboard ADCP transects. *Deep-Sea Research Part I: Oceanographic Research Papers* 56:1633-1655
- Selwyn JD, Hogan JD, Downey-Wall AM, Gurski LM, Portnoy DS, Heath DD (2016) Kin-aggregations explain chaotic genetic patchiness, a commonly observed genetic pattern, in a marine fish. *PLoS one* 11
- Taillebois L, Barton DP, Crook DA, Saunders T, Taylor J, Hearnden M, Saunders RJ, Newman SJ, Travers MJ, Welch DJ, Greig A, Dudgeon C, Maher S, Ovenden JR (2017) Strong population structure deduced from genetics, otolith chemistry and parasite abundances explains vulnerability to localized fishery collapse in a large Sciaenid fish, *Protonibea diacanthus*. *Evolutionary Applications*
- Thompson AF, Heywood KJ, Thorpe SE, Renner AHH, Trasviña A (2009) Surface Circulation at the Tip of the Antarctic Peninsula from Drifters. *Journal of Physical Oceanography* 39:3-26
- Thorrold SR, Swearer SE (2009) Otolith Chemistry. In: Green BS, Mapstone BD, Carlos G, Begg GA (eds) *Tropical Fish Otoliths: Information for Assessment, Management and Ecology*. Springer Netherlands, Dordrecht
- Thresher RE (1999) Elemental composition of otoliths as a stock delineator in fishes. *Fisheries Research* 43:165-204
- Vacchi M, DeVries AL, Evans CW, Bottaro M, Ghigliotti L, Cutroneo L, Pisano E (2012) A nursery area for the Antarctic silverfish *Pleuragramma antarcticum* at Terra Nova Bay (Ross Sea): First estimate of distribution and abundance of eggs and larvae under the seasonal sea-ice. *Polar Biology* 35:1573-1585
- Vacchi M, La Mesa M, Dalu M, Macdonald J (2004) Early life stages in the life cycle of Antarctic silverfish, *Pleuragramma antarcticum* in Terra Nova Bay, Ross Sea. *Antarctic Science* 16:299-305
- Waples RS, Gaggiotti O (2006) What is a population? An empirical evaluation of some genetic methods for identifying the number of gene pools and their degree of connectivity. *Molecular ecology* 15:1419-1439
- Welch DJ, Newman SJ, Buckworth RC, Ovenden JR, Broderick D, Lester RJG, Gribble NA, Ballagh AC, Charters RA, Stapley J, Street R, Garrett RN, Begg GA (2015) Integrating different approaches in the definition of biological stocks: A northern Australian multi-jurisdictional fisheries example using grey mackerel, *Scomberomorus semifasciatus*. *Marine Policy* 55:73-80
- Whitworth T, Orsi AH, Kim SJ, Nowlin WD, Locarnini RA (1998) Water Masses and Mixing Near the Antarctic Slope Front. *Ocean, Ice, and Atmosphere: Interactions at the Antarctic Continental Margin*. American Geophysical Union
- Wöhrmann APA, Hagen W, Kunzmann A (1997) Adaptations of the Antarctic silverfish *Pleuragramma antarcticum* (Pisces: Nototheniidae) to pelagic life in high-Antarctic waters. *Marine Ecology Progress Series* 151:205-218
- Zane L, Bargelloni L, Patarnello T (2002) Strategies for microsatellite isolation: A review. *Molecular ecology* 11:1-16
- Zane L, Marcato S, Bargelloni L, Bortolotto E, Papetti C, Simonato M, Varotto V, Patarnello T (2006) Demographic history and population structure of the Antarctic silverfish *Pleuragramma antarcticum*. *Molecular ecology* 15:4499-4511



# Chapter 2

## Population structure and connectivity of Antarctic silverfish in the Ross Sea using life history traits

Published as:

Brooks CM, **Caccavo JA**, Ashford J, Dunbar R, Goetz K, La Mesa M, Zane L (2018) Early life history connectivity of Antarctic silverfish (*Pleuragramma antarctica*) in the Ross Sea. Fisheries Oceanography 00:1-14. doi: 10.1111/fog.12251.


Received: 8 April 2017 | Accepted: 4 October 2017

DOI: 10.1111/fog.12251

## ORIGINAL ARTICLE

WILEY FISHERIES OCEANOGRAPHY

# Early life history connectivity of Antarctic silverfish (*Pleuragramma antarctica*) in the Ross Sea

Cassandra M. Brooks<sup>1,2</sup>  | Jilda Alicia Caccavo<sup>3</sup> | Julian Ashford<sup>4</sup> | Robert Dunbar<sup>1</sup> | Kimberly Goetz<sup>5</sup> | Mario La Mesa<sup>6</sup> | Lorenzo Zane<sup>3</sup>

<sup>1</sup>School of Earth, Energy and Environmental Sciences, Stanford University, Stanford, CA, USA

<sup>2</sup>Environmental Studies, Sustainability, Energy and Environment Complex, University of Colorado Boulder, Boulder, CO, USA

<sup>3</sup>Dipartimento di Biologia, Università di Padova, Padova, Italy

<sup>4</sup>Department of Ocean, Earth and Atmospheric Sciences, Center for Quantitative Fisheries Ecology, Old Dominion University, Norfolk, VA, USA

<sup>5</sup>National Institute of Water and Atmospheric Research, Wellington, New Zealand

<sup>6</sup>Istituto di Scienze Marine, UOS di Ancona, Ancona, Italy

## Correspondence

C. M. Brooks

Email: cassandra.brooks@colorado.edu

## Funding information

National Science Foundation, Grant/Award Number: 1043454, 0741348; Emmett Interdisciplinary Program in Environment and Resources at Stanford University; Switzer Foundation; Biosciences Program in Evolution, Ecology and Conservation at the Università di Padova

## Abstract

A recent population hypothesis for Antarctic silverfish (*Pleuragramma antarctica*), a critical forage species, argued that interactions between life history and circulation associated with glacial trough systems drive circumpolar distributions over the continental shelf. In the Ross Sea, aggregations of eggs and larvae occur under fast ice in Terra Nova Bay, and the hypothesis predicted that dispersing larvae encounter outflow along the western side of Drygalski Trough. The outflow advects larvae towards the shelf-break, and mixing with trough inflow facilitates return toward the inner shelf. To examine the hypothesis, we compared samples of *P. antarctica* collected near Coulman Island in the outflow, along Cray Bank in the inflow, and a third set taken over the rest of the Ross Sea. We ruled out misidentification using an innovative genetic validation. Silverfish larvae comprised 99.5% of the catch, and the highest population densities were found in Drygalski Trough. The results provided no evidence to reject the population hypothesis. Abundance indices, back-calculated hatching dates, length distributions and growth were congruent with a unified early life history in the western Ross Sea, constrained by cryopelagic early stages in Terra Nova Bay. By contrast, a sample in the Bay of Whales revealed much smaller larvae, suggesting either a geographically separate population in the eastern Ross Sea, or westward connectivity with larvae spawned nearby by fish sourced from troughs upstream in the Amundsen Sea. These results illustrate how hypotheses that integrate population structure with life history can provide precise spatial predictions for subsequent testing.

## KEYWORDS

Ross Sea, Antarctic silverfish, physical-biological interactions, large-scale circulation, glacial trough systems, Circumpolar Deep Water, life history connectivity, population structure

## 1 | INTRODUCTION

In the Southern Ocean ecosystem, Antarctic silverfish (*Pleuragramma antarctica*) are a critical forage species that, with Antarctic krill (*Euphausia superba*), typically connect producer trophic levels to those of higher predators (Granata, Zagami, Vacchi, & Guglielmo, 2008; La Mesa & Eastman, 2012; La Mesa, Eastman, & Vacchi,

2004; Smith, Ainley, & Cattaneo-Vietti, 2007; Smith, Ainley, Cattaneo-Vietti, & Hofmann, 2012). The connections occur throughout its life history, which is exclusively pelagic, and the species has a circumpolar distribution over the continental shelves around the Antarctic, including the sub-antarctic South Shetland and South Orkney Islands. In the western Ross Sea (Figure 1a), *P. antarctica* dominates the ichthyoplankton comprising up to 99% of the total



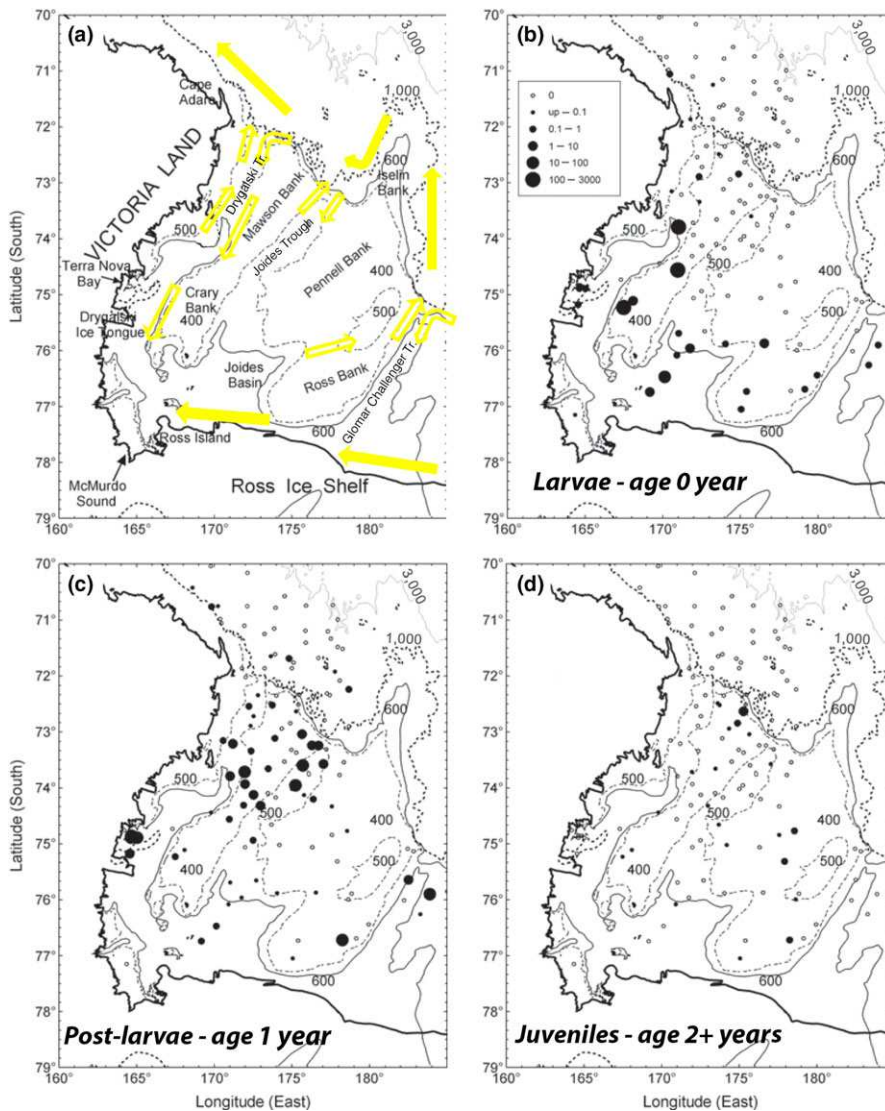


**FIGURE 1** Distribution of young silverfish in the upper water column of the western Ross Sea in relation to the shelf circulation, reproduced from La Mesa et al. (2010) and Ashford et al. (2017). Geographically labelled schematic of westward flow along the Ross Ice Shelf and in the Antarctic Slope Current and Front system (filled arrows), and cross-shelf inflows and outflows along troughs (transparent arrows; [a]). Standardized abundances of silverfish at larvae (b), post-larval (c), and juvenile stages (d) in net tows that sampled to a maximum depth of between 130 and 300 m

catch in research surveys over the continental shelf (Granata et al., 2002; Guglielmo, Granata, & Greco, 1998; La Mesa et al., 2010; Vacchi, La Mesa, & Greco, 1999), and occurring in concentrations that extend over the shelf-break and slope (La Mesa et al., 2010; O'Driscoll, Macaulay Gavin, Gauthier, Pinkerton, & Hanchet, 2011).

Aggregations of *P. antarctica* eggs and larvae are consistently found inshore, under winter fast ice in Terra Nova Bay (Guidetti, Ghigliotti, & Vacchi, 2015; Vacchi, La Mesa, Dalu, & Macdonald, 2004; Vacchi et al., 2012) and the species relies on an inactive, energy-efficient strategy (La Mesa & Eastman, 2012), especially in older stages. Lipid sequestration in large sacs composed of adipocytes (Eastman & DeVries, 1989) results in neutral buoyancy and low-energy behavior in which fish are suspended in the water column to feed (La Mesa & Eastman, 2012). *P. antarctica* distribution can be explained by dispersal in regional circulation over the continental shelf (Agostini et al., 2015; Ferguson, 2012; Hubold, 1984; La Mesa, Piñones, Catalano, & Ashford, 2015; La Mesa et al., 2010; Parker et al., 2015). In Terra Nova Bay, the eggs occupy a layer of platelet ice under the fast ice and hatch from mid-November

through December (Vacchi et al., 2004, 2012). A potential second hatching extends into early January (Granata et al., 2002). The larvae have a mean hatching length of 9–9.3 mm standard length (SL; Vacchi et al., 2004, 2012). La Mesa et al. (2010) found distributions of young stages in the upper water column during summer surveys of the western Ross Sea between December and early February (Figure 1). Larvae (SL 7–18 mm, age 0; Figure 1b) were found in large numbers along the western side of the Mawson and Crary Banks, and in smaller numbers in Terra Nova Bay and the Joides Basin. In contrast, post-larvae (SL 30–57 mm, age 1; Figure 1c) occurred in concentrations over the outer shelf corresponding to the Drygalski and Joides Troughs and the Mawson Bank, and along the Glomar Challenger Trough further east (La Mesa et al., 2010). La Mesa et al. (2010) also noted that most *P. antarctica* captured were in areas characterized by a layer of warmer Circumpolar Deep Water (CDW); and the young stages were generally confined to the surface 100 m in the water column, where a productive environment provides favorable conditions for growth (La Mesa & Eastman, 2012). Early growth rates were estimated at 0.15–0.25 mm/day (Guglielmo et al.,

1998; Hubold, 1985; La Mesa et al., 2010), and juveniles aged 2+ were also found near the shelf-break before moving to depth with age.

In a subsequent review of the population structure of *P. antarctica*, Ashford, Zane, Torres, La Mesa, and Simms (2017) developed this life history hypothesis further, arguing that distributions across and along the shelf are maintained by interactions between life history and the circulation associated with glacial trough systems. The circulation in the Ross Sea is generally bathymetrically controlled and the trough systems are oriented north/south, connecting the shelf-break to the inner shelf (Figure 1a). Intrusions of warm CDW from the continental slope are carried along the eastern side of the troughs (Dinniman, Klinck, & Smith, 2003; Orsi & Wiederwohl, 2009) and modified by mixing with Antarctic Surface Water. The modified CDW (MCDW) meets equatorward flow of dense, cold Shelf Water, mixing to form Modified Shelf Water and eventually Antarctic Bottom Water that flows in gravity currents down the slope (Gordon et al., 2009). In the Drygalski and Joides Troughs, southward jets carry the MCDW towards the inner shelf at velocities of 0.3 m/s and disperse it across the neighbouring Mawson and Pennell Banks (Kohut, Hunter, & Huber, 2013). Although reports indicate larvae of *P. antarctica* in McMurdo Sound and off Ross Island (summarized in Ghigliotti, Herasymchuk, Kock, & Vacchi, 2017), the existence of nursery grounds remains undetermined with no evidence so far of consistent aggregations such as those observed in Terra Nova Bay (Ghigliotti et al., 2017). Moreover, otolith chemistry from adults showed no evidence of

mixing, implying a single population in the western Ross Sea (Ferguson, 2012). Developing the life history hypothesis, Ashford et al. (2017) suggested that larvae dispersing from Terra Nova Bay encounter the shelf outflow along the western side of the Drygalski Trough, which advects them toward the shelf-break and productive areas associated with nutrient-rich MCDW. As they grow older, they either mix with the trough inflow, which facilitates return toward the inner shelf (Figure 1a), or reach the slope front (Hubold, 1984) and become entrained in westward flow along the Antarctic Slope Current and Front system (AFS; Ashford et al., 2017).

During February and March of 2013, a United States National Science Foundation (NSF) research cruise in the Ross Sea provided an opportunity to examine cross-shelf dispersal via the trough circulation predicted by the life history hypothesis. By February, larvae of *P. antarctica* are considered to have largely dispersed from Terra Nova Bay to be entrained in flows along the Drygalski Trough. In this paper, we compare three sets of samples; the first taken along Cray Bank corresponding to the inflow including MCDW with a second set taken in the outflow near Coulman Island, and a third set of samples taken from the rest of the Ross Sea: over the Joides and Glomar Challenger Troughs, south of Cray Bank and in the Joides Basin, and at the southern end of the Little America Trough in the Bay of Whales (Figure 2). We examine relative abundances between the three sets of samples in relation to water structure, and length frequency distributions in the context of reported early growth rates and hatching times from the nursery ground at Terra Nova Bay. We also report on a recently hatched group of larvae found late in the

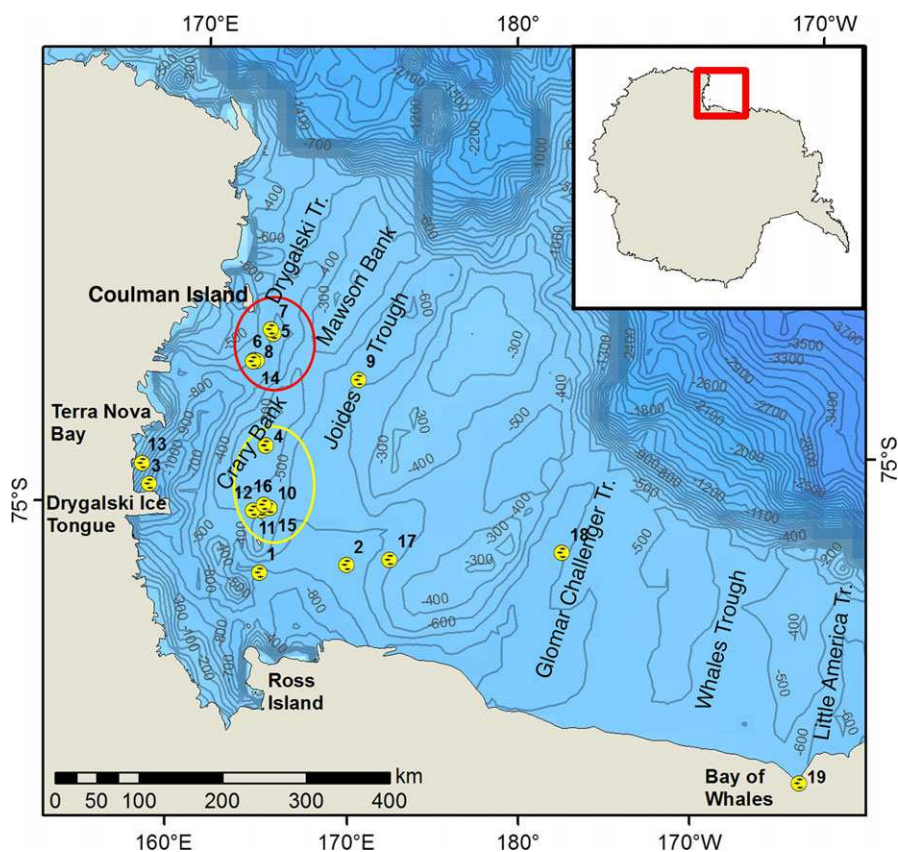


**FIGURE 2** Map of the Ross Sea showing locations sampled by Tucker trawl during February and March 2013. Inflow locations along Cray Bank (yellow circle; Locations 4, 10, 11, 12, 15, 16); outflow locations near Coulman Island (red circle; Locations 5, 6, 7, 8, 14)

cruise in the Bay of Whales; a validation method that used genetic markers to test species identifications based on morphological characteristics; and sea-ice distribution in relation to connectivity during early life.

## 2 | MATERIALS AND METHODS

NSF research cruise NBP13-02 deployed during February–March 2013 to measure the carbon flux in the Ross Sea towards the end of the Antarctic summer, in particular along the edge of the Ross Sea polynya. During these operations, larval fish were sampled at 19 different locations (Table 1, Figure 2) using a Tucker Trawl equipped with either of two nets, one 2 × 2 m mouth and mesh size 700 µm, the other 1 × 1 m mouth and mesh size 300 µm. Thirteen locations were successfully sampled using both nets, towed in succession off the stern of the vessel diagonally through the water column. Tows using the 700 µm net targeted the top 100 m of the water column, while operations using the 300 µm net targeted depths between the surface and ca 300 m; however, this varied with conditions and depth of the water column. The volume of water sampled was measured using a General Oceanics Digital Flowmeter (Model 2030 series), and abundance indices were calculated by normalizing the number of fish caught by volume sampled.

Tows deployed at Locations 4, 10, 11, 12, 15 and 16 corresponded to inflow along the Drygalski Trough and western side of Cray Bank; Locations 5, 6, 7, 8 and 14 corresponded to the outflow along the trough; and Locations 1, 3, 9, 13, 17, 18, and 19 elsewhere in the Ross Sea provided a spatial comparison (Figure 2). Hydrographic data including temperature, salinity and oxygen were collected at each location using CTD casts. At all locations, the presence or absence of MCDW, detected via the CTD casts, was used to confirm that tows corresponded to trough inflow and outflow, respectively. Sea ice data, at 6.25 km resolution, was also examined at sampling locations. This was obtained from the daily Advanced Microwave Scanning Radiometer sea ice concentration data from the University of Bremen (<http://www.iup.uni-bremen.de/seaice/amsr/>). All larval fish were sampled from each tow and identified according to morphological characteristics using the guide developed by Kellermann (1989). Standard length (SL) of specimens was measured to the nearest mm. In the case of large catches (>100) of *P. antarctica*, subsamples were selected by thoroughly mixing the catch in a container of seawater and pouring off a volume containing approximately 100 individuals. All fish selected in this way were measured except a small number that were damaged by the net. An adult (SL 171 mm) and a juvenile fish (SL 62 mm) were captured in the 700 µm net at Location 4; an adult (SL 120 mm) in the 700 µm net at Location 12; and two juveniles (SL 49 mm, 52 mm) at Location 18. These individuals were not included in the analysis.

Location no.	Latitude	Longitude	700		300	300 V	
			Date	Depth (m)	Date	Date	Depth (m)
1	–76.417500	167.940300	13 Feb	80	13 Feb		180
2	–76.502152	171.995050	16 Feb	100	16 Feb		195
3	–75.193183	164.177433	22 Feb	91	22 Feb		291
4	–75.082350	169.338017	25 Feb	138	25 Feb		283
5	–73.914742	170.429200	26 Feb	136	26 Feb		386
6	–74.152610	169.506485				27 Feb	379
7	–73.861473	170.368683				28 Feb	348
8	–74.163972	169.604202				1 Mar	334
9	–74.531800	173.530030	2 Mar	83	2 Mar		376
10	–75.750870	169.001587	2 Mar	172	2 Mar		343
11	–75.758728	168.604355	4 Mar	151	4 Mar		325
12	–75.746433	168.239333	5 Mar	264	5 Mar		414
13	–74.956133	164.137667			6 Mar		408
14	–74.165317	169.457317				7 Mar	278
15	–75.752200	168.998400	8 Mar	135	8 Mar		355
16	–75.706467	168.773333	9 Mar	312	9 Mar		151
17	–76.500833	174.010133	10 Mar	143	10 Mar		326
18	–76.492900	–177.968383				11 Mar	338
19	–78.587250	–164.365677	13 Mar	155	13 Mar		320

**TABLE 1** Sampling locations in the Ross Sea

Tucker trawl net type 700 and 300 refers to mesh size (µm); V indicates vertical tow off the starboard side; Depths (m) refer to deepest part of the water column sampled.

To test that identification of *P. antarctica* larvae by morphological characteristics was correct, samples were frozen for later genetic analysis. A total of 70 larvae were selected for DNA extraction from tows using the 700  $\mu\text{m}$  net for which frozen larvae were preserved. For locations in the western Ross Sea, 44 larvae ranging from 15 to 26 mm SL were selected by stratified random sampling from the nine tows with the largest catches. For Location 19 in the Bay of Whales, 26 whole larvae were adequately preserved for analysis, and all were used. Genomic DNA was extracted from whole larvae using a standard salting-out protocol. Total genomic DNA was diluted to approximately 100 ng/ $\mu\text{l}$  for use in PCR amplification, and stored at  $-20^{\circ}\text{C}$ . The 16S large ribosomal unit and the D-Loop control region of mitochondrial DNA were amplified by PCR (see Figure S1 for details). Approximately 528 base pairs (bp) of 16S rDNA and 349 bp of the D-Loop region were amplified and sequenced (See Figure S1 and Table S1 legends for details). The resultant mitochondrial DNA sequences were then aligned against seven 16S rDNA and sixteen D-Loop region corresponding to sequences of *P. antarctica* retrieved from the nucleotide database NCBI (see Table S1 for GenBank accession numbers). GenBank sequences from three of the most closely related notothenioids *Aethotaxis mitopteryx*, *Dissostichus mawsoni* and *D. eleginoides* (Near et al., 2012) were also included as outgroups (see Table S1 for GenBank accession numbers). The proportion of nucleotide positions at which two sequences differed represented by the p distance was used to calculate genetic distance in MEGA. In addition, a neighbour-joining tree was drawn using the Kimura 2-parameter substitution model, with tree robustness confirmed by 1,000 bootstrap replications.

To describe the growth rate of the larvae, an exponential model was applied to the length frequency distributions over the period of sampling, as reported in previous studies (Hubold, 1985; Keller, 1983; Kellermann, 1986). The model was fitted by linear regression on  $\log_e$  transformed data in the form:

$$\log_e \text{SL} = \log_e a + gt,$$

where SL is the standard length in mm,  $a$  is the initial SL,  $g$  is the instantaneous growth rate and  $t$  is time in days. Specific growth rate representing the daily percentage change in size ( $G$ , % SL/day) was calculated by multiplying the instantaneous growth rate  $g$  by 100, allowing comparison with growth rates from different geographical areas and size ranges. The distribution of hatching dates was back-calculated by applying the growth model to individual size of survivors and date of capture, and pooled by week. We assumed no selective mortality related to different hatching periods (Campana & Jones, 1992) and a minimum size at hatching of 8 mm, corresponding to the minimum size found during field operations.

### 3 | RESULTS

Tows using both the 700 and 300  $\mu\text{m}$  nets were completed for Locations 4, 10, 11, 12, 15 and 16 along Cray Bank, Location 5 off

Coulman Island, and Locations 1, 2, 3, 9, 17 and 19 over the rest of the Ross Sea. Because of severe winds near Coulman Island, towing operations using the 700  $\mu\text{m}$  net were suspended at Locations 6, 7, 8 and 14, and the 300  $\mu\text{m}$  net was towed vertically off the starboard side of the vessel. At Location 13, the 700  $\mu\text{m}$  net failed and was not retrieved; at Location 18, only the 300  $\mu\text{m}$  net was deployed using a vertical tow (Table 1).

#### 3.1 | Hydrography and sea-ice

Along Cray Bank in the trough inflow, stratification occurred at approximately 30–50 m, with a well defined mixed layer at Locations 11, 12, 15 and 16, although not at Location 4 (Figure 3a). As expected, a layer of warm water was found between 40 and 100 m at all the Cray Bank locations, which was associated with a pronounced oxygen minimum indicating MCDW (Figure 3a). Off Coulman Island in the outflow, surface mixing reached ca 30 m at Location 5 and there was strong stratification at 40–60 m at Locations 6, 8 and 14 with relatively low salinity in the surface layer (Figure 3b). As expected, the hydrographic data showed no evidence of MCDW. A layer of warm water was found at a depth of 30–60 m at Location 5, which was warmer and somewhat deeper at Locations 6, 8 and 14, but this was not associated with an oxygen minimum. However, at the northernmost Location 7, a temperature maximum and oxygen minimum was found between depths of 40–80 m, indicating MCDW (Figure 3b).

Elsewhere, mixing reached 80 m at Location 3 in Terra Nova Bay near the Drygalski Ice Tongue, and more than 140 m at Location 13 in front of the Reeves Glacier (Figure 3c). At Location 1 south of Cray Bank, a warm mixed layer reached ca 50 m; colder water beneath was associated with an oxygen minimum at 60 m. Further east in the Joides Basin, the warm surface layer reached 100 m at Location 2 with a layer of warm water below showing an oxygen minimum between 100 and 150 m, indicating MCDW. At Location 17, the mixed surface layer was colder and MCDW was present but slightly deeper. The temperature in the surface layer was warmer at Location 9 in the Joides Trough, and MCDW was present deeper than at the Drygalski Trough locations, with an oxygen minimum between 80 and 100 m (Figure 3c). MCDW was deeper still at Location 18 in the Glomar Challenger Trough, with surface mixing down to nearly 100 m. Finally, Location 19 in the Bay of Whales showed much less variation in oxygen and temperature over the water column, and lower oxygen at the surface compared to elsewhere (Figure 3c).

Locations along Cray Bank and near Coulman Island were close to the ice edge (Figure 4), with a sharper transition near Coulman Island. Sea-ice covered most of the Drygalski Trough between Coulman Island and Terra Nova Bay, and the western side of Cray Bank. Ice cover was much less dense at sampling locations in the rest of the Ross Sea; Locations 3 and 13 were in the Terra Nova Bay polynya, and open water at Location 19 was consistent with the Ross Ice Shelf polynya. Locations 1, 2, 3 and 9, sampled earlier in the season, showed a relatively warm, well mixed surface layer, whereas the

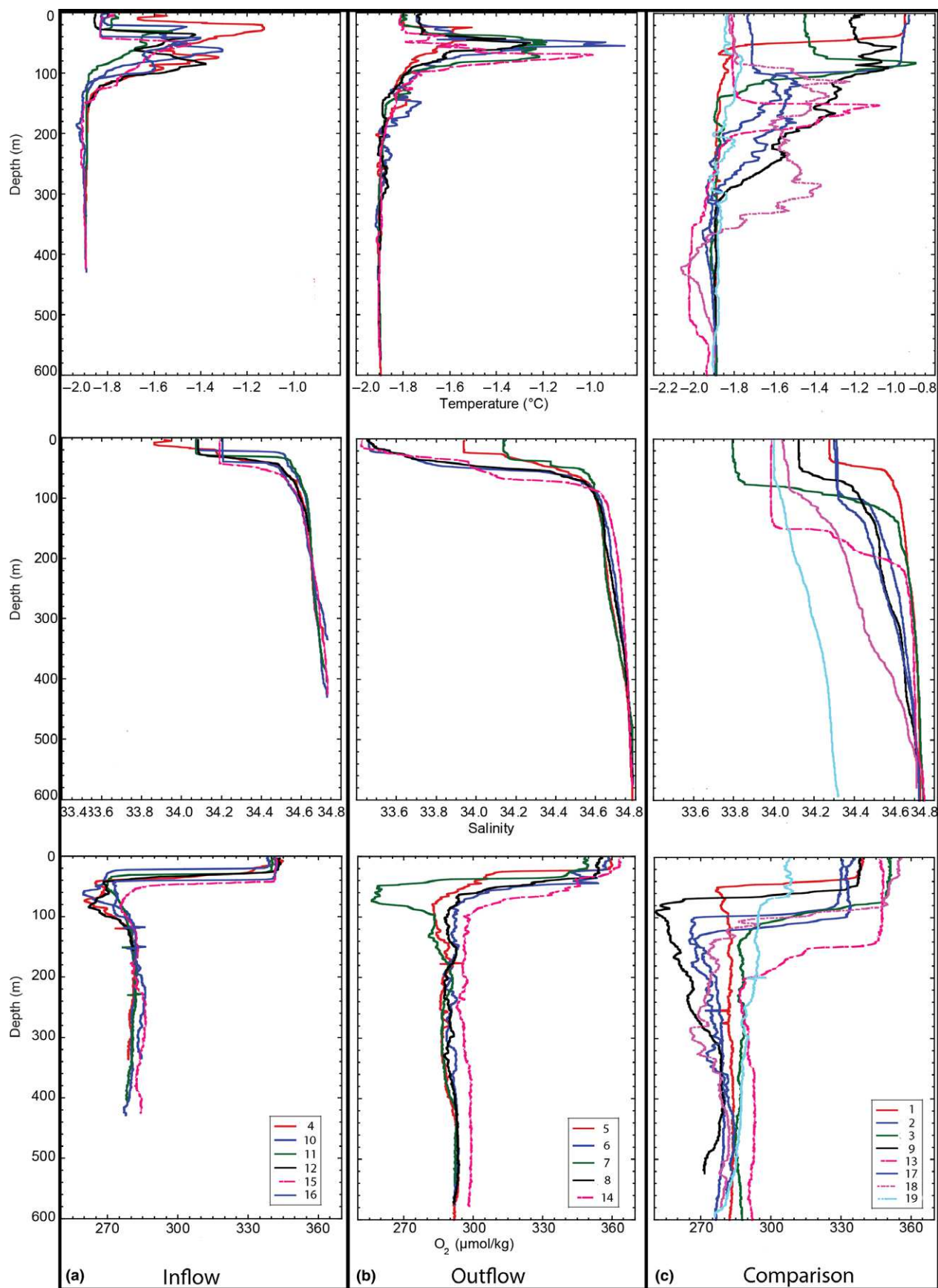


**FIGURE 3** CTD profiles showing temperature, salinity and dissolved oxygen for inflow (a) and outflow (b) locations, and locations in the rest of the Ross Sea (c) for comparison

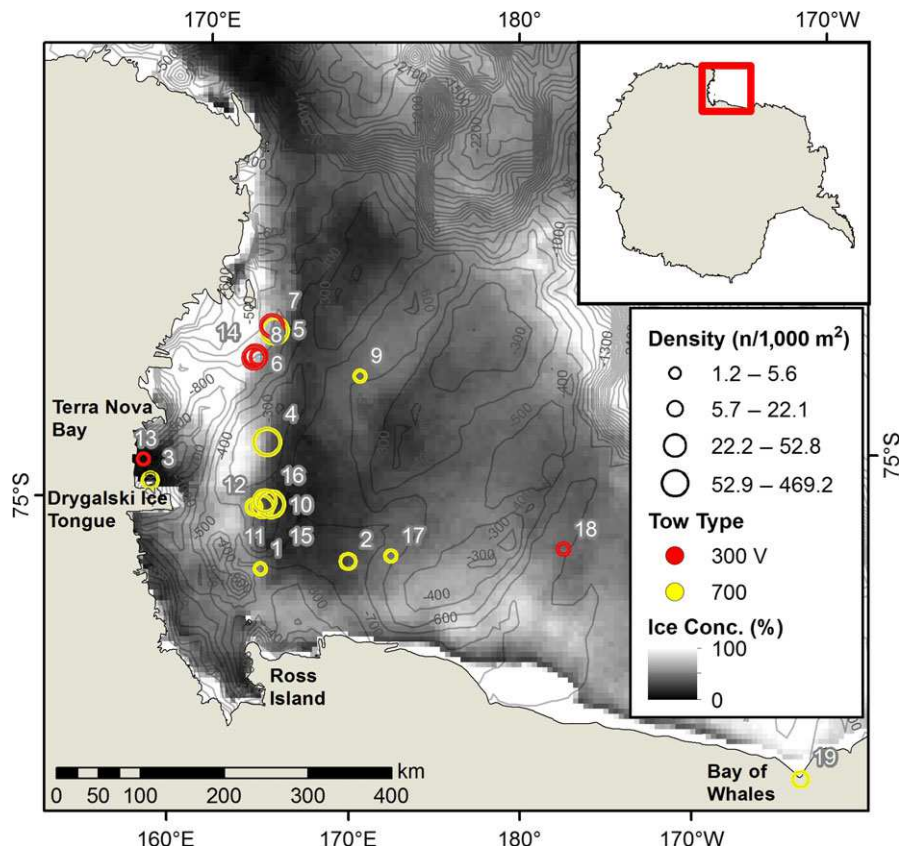


**FIGURE 4** Bathymetric map of the Ross Sea, Antarctica showing average ice cover over the duration of the sampling period (13 February–16 March), in relation to abundance indices measured using the 700  $\mu\text{m}$  net (yellow). Abundance indices for vertical tows with the 300  $\mu\text{m}$  net (red) are shown at locations where the 700  $\mu\text{m}$  net could not be deployed due to wind conditions. Since the 700  $\mu\text{m}$  net failed at Location 13, the abundance index shown is for the corresponding diagonal tow of the 300  $\mu\text{m}$  net. Shading represents 100% ice cover (white) to 0% (black)

surface was colder at Locations 13, 17 and 18 sampled later in the season, indicating seasonal cooling. However, freshening in the surface layer contributed strongly to stratification, notably at Locations 6, 8 and 14 near Coulman Island, consistent with melting sea-ice. By contrast at Location 19, weak stratification and freshening throughout the water column (Figure 3c) was consistent with upwelling from deeper melting processes along the front of the ice shelf.

### 3.2 | Genetic validation

The genetic analyses confirmed the identification of *P. antarctica* larvae by morphological characteristics. As detailed in Table S3, the newly obtained Ross Sea larval sequences were extremely similar to the existing GenBank sequences for *P. antarctica* (uncorrected divergence 0.001 with 16S and 0.004 with D-Loop) and different from those of the outgroups included in the analysis (minimum uncorrected divergence 0.048 with 16S and 0.139 with D-loop). In a neighbour-joining tree, the larval sequences from both the western Ross Sea and Bay of Whales clustered in a single clade with the *P. antarctica* sequences from the NCBI database with 100% bootstrap support, and were clearly differentiated from the D-loop sequences of the phylogenetically closest species (Figure S2, 16S rDNA and Figure S3, D-Loop).

### 3.3 | Spatial distribution

Based on the validated morphological identifications, more than 99% of the overall catch from all combined tows consisted of larvae of *P. antarctica*. Species from other families were represented, including Channichthyidae, *Trematomus* spp., Bathydraconidae, Paralepididae and Artedidraconidae (Table 2), but these contributed only 50 fish out of a total of 9,519 individuals caught.

For *P. antarctica*, abundance indices were higher using the 700  $\mu\text{m}$  net than the 300  $\mu\text{m}$  net, which sampled much deeper in the water column (Table 3). Using the 700  $\mu\text{m}$  net, the indices varied from 22 to 469/1,000  $\text{m}^3$  off Coulman Island and along Cary Bank; with the 300  $\mu\text{m}$  net, they varied between 12 and 32/1,000  $\text{m}^3$  off Coulman Island and were <7/1,000  $\text{m}^3$  everywhere else (Table 3). Only at Location 1 was the abundance index lower using the 700  $\mu\text{m}$  net. Although weather conditions prevented direct quantitative comparison between the three sample sets, the abundance index along Cary Bank reached 430 fish/1,000  $\text{m}^3$  at Location 4 using the 700  $\mu\text{m}$  net, and was still high further south (22–96/1,000  $\text{m}^3$ ) relative to areas in the rest of the Ross Sea (2–21 fish/1,000  $\text{m}^3$ ). Indices at Locations 10, 15 and 16 were higher (53–96 fish/1,000  $\text{m}^3$ ) than further west at Locations 11 and 12 (28 fish/1,000  $\text{m}^3$  and 22 fish/1,000  $\text{m}^3$  respectively). However, the highest

Family	Taxa	Tows present	Total no.	Total %
Nototheniidae	<i>Pleuragramma antarctica</i>	1–19	9,469	99.47
	<i>Trematomus</i> spp.	3, 4, 6	5	0.05
Channichthyidae	Unid.	1, 3, 4,	5	0.05
	<i>Chaenodraco wilsoni</i>	4	2	0.02
	<i>Chionobathyscus dewitti</i>	8	1	0.01
	<i>Chionodraco</i> spp.	5, 6, 11, 12, 14, 16	10	0.11
	<i>Cryodraco antarcticus</i>	11	1	0.01
	<i>Pagetopsis macropterus</i>	4	2	0.02
	<i>Pagetopsis maculatus</i>	3, 15	9	0.09
Artedidraconidae	<i>Dacodraco hunteri</i>	3, 4, 15, 19	7	0.07
	<i>Dolloidraco longedorsalis</i>	8, 11	2	0.02
Bathydraconidae	Unid.	9, 10	3	0.03
	<i>Racovitzia glacialis</i>	17	1	0.01
Paralepididae	Unid.	10, 17	2	0.02
Total collected specimens			9,519	

**TABLE 2** Total larval fish abundance and composition from the 19 tow locations

abundance index using the 700  $\mu\text{m}$  net was at Location 5 (469 fish/1,000  $\text{m}^3$ ) and the highest using the 300  $\mu\text{m}$  net were all similarly off Coulman Island (Table 3).

In the rest of the Ross Sea, abundance indices using the 700  $\mu\text{m}$  net were low at Locations 1, 2 and 17 south of the Crary Bank and in the Joides Basin, and at Location 9 in Joides Trough (2–10 fish/1,000  $\text{m}^3$ ). At Location 18 in the Glomar Challenger Trough, no tow was taken using the 700  $\mu\text{m}$  net and the abundance index for the 300  $\mu\text{m}$  tow was very low (1 fish/1,000  $\text{m}^3$ ). Indices were only higher in Terra Nova Bay at Location 3 (21 fish/1,000  $\text{m}^3$  using the 700  $\mu\text{m}$  net) and Location 13 (6 fish/1,000  $\text{m}^3$  using the 300  $\mu\text{m}$  net; Table 3).

### 3.4 | Length, growth rate and hatch dates

The average length of larvae caught at Locations 1–17 between 13 February and 10 March was 17.4 mm (Figure 5). Almost all sampled specimens (99.94%, 1,654 specimens measured) were less than 30 mm, indicating they were hatched during the current season (Figure 5; La Mesa, Piñones, et al., 2015). The average size sampled by both nets increased over the sampling period. Pooling larvae sampled by both nets (Figure 5) and estimating the growth rate from larvae smaller than 30 mm SL based on the exponential model fitted to the length frequency distributions (Figure 5a), the daily percentage change in size (G) was 1.25%/day, and the growth rate at the mean size of 18.3 mm was 0.23 mm/day. Hatch dates were spread over two months (December and January), with a single peak occurring in the last week of December (Figure 5b).

By contrast, the tow in the Bay of Whales (Location 19) using the 700  $\mu\text{m}$  net yielded *P. antarctica* with a mean SL of 10.59 mm, and the fish were significantly smaller than those caught at Locations 1–17 (*t* test; *p* value < .001). Larger fish (19 mm and 41 mm) were

also sampled in the tow at Location 19, which may have hatched earlier in the current season or in the previous one. When these were excluded, the mean SL was 9.80 mm (*SD* = 0.86 mm). Assuming the same growth curve as for the western Ross Sea, the larvae would have hatched from 15 February to 13 March.

## 4 | DISCUSSION

### 4.1 | Examining the life history hypothesis

As observed in earlier studies, *P. antarctica* larvae dominated the ichthyoplankton in the western Ross Sea, comprising more than 99% of the fish sampled. As reported by La Mesa et al. (2010), the highest population densities were in the Drygalski Trough, along Crary Bank and near Coulman Island. Despite sampling relatively late in the summer, larvae were also present in Terra Nova Bay. Relatively few were found elsewhere. The results provided no evidence to reject dispersal via the trough circulation as predicted by the life history hypothesis, demonstrating high concentrations in the outflow and inflow that were consistent with expected transport from spawning inshore at Terra Nova Bay.

Length distributions were larger than La Mesa et al. (2010), consistent with sampling later in the summer, and the average length of the larvae increased over the course of the sampling period at a rate similar to that reported in the literature (Guglielmo et al., 1998; Hubold, 1985; La Mesa et al., 2010). Back-calculated hatching dates covered the range previously found from mid-December to early January, and largely matched reported hatching events in Terra Nova Bay (Granata et al., 2002; Vacchi et al., 2004, 2012). Overall, the abundance and size data supported a unified early life history expected for a single population of *P. antarctica* in the western Ross Sea, constrained by cryopelagic early stages under fast ice in Terra Nova Bay.

**TABLE 3** Standard length (SL, mean  $\pm$  SD, and range), number caught and abundance indices ( $n/1,000\text{ m}^3$ ) for *Pleuragramma antarctica*, caught by (a) 300 micron nets, (b) 700 micron nets

Location	No. caught	Abundance index	No. measured	Average SL (mm)	Range SL (mm)
(a)					
1	31	3	31	15.54 ( $\pm 3.59$ )	12–34
2	48	5	48	17.9 ( $\pm 1.72$ )	14–22
3	1	0	1	19	19
4	23	7	23	13 ( $\pm 1.98$ )	10–18
5	93	28	93	16.25 ( $\pm 1.95$ )	13–22
6	76	33	72	16.14 ( $\pm 1.96$ )	13–22
7	55	29	53	15.64 ( $\pm 1.55$ )	13–20
8	22	12	20	17.5 ( $\pm 1.91$ )	13–21
9	2	1	2	22.5 ( $\pm 3.54$ )	20–25
10	24	7	23	19.57 ( $\pm 1.34$ )	17–22
11	1	0	1	12	12
12	6	2	6	19.67 ( $\pm 0.52$ )	19–20
13	16	6	16	23.31 ( $\pm 1.85$ )	21–28
14	50	32	48	17.81 ( $\pm 1.68$ )	14–22
15	13	5	13	19.62 ( $\pm 2.02$ )	15–22
16	1	0	1	23	23
17	1	1	0		
18	2	1	2		
19	0	0	0		
Tow	No. caught	Abundance index	No. measured	Average SL (mm)	Range SL (mm)
(b)					
1	7	2	6	10.17 ( $\pm 1.83$ )	8–12
2	60	10	58	16.5 ( $\pm 1.54$ )	13–36
3	144	21	131	18.77 ( $\pm 2.11$ )	14–31
4	3,402	430	77	16.23 ( $\pm 1.95$ )	11–21
5	3,538	469	97	17.54 ( $\pm 1.63$ )	14–22
9	35	5	35	20.34 ( $\pm 1.66$ )	16–23
10	668	96	296	17.5 ( $\pm 1.67$ )	14–22
11	213	28	206	19.56 ( $\pm 1.89$ )	15–23
12	141	22	108	20.01 ( $\pm 1.83$ )	16–25
15	435	67	105	21.09 ( $\pm 3.54$ )	15–49
16	291	53	109	21.39 ( $\pm 2.36$ )	15–35
17	10	2	9	21.11 ( $\pm 4.43$ )	16–26
19	59	11	51	10.59 ( $\pm 4.61$ )	8–41

However, in the eastern Ross Sea, sampling in the Bay of Whales showed a clear discontinuity. Only a single tow was undertaken, but the mean length of larvae (SL 9.8 mm) indicated strong spatial structuring. There is considerable uncertainty over the distribution of egg and larval aggregations around the Antarctic (Ashford et al., 2017; Ghigliotti et al., 2017). Nevertheless, recently hatched larvae of 10 mm in length have previously been reported in the Bay of Whales, earlier in the season between mid-December and mid-

January (Biggs, 1982). *Pleuragramma antarctica* show remarkable consistency in reproductive timing and behavior under a variety of environmental conditions (La Mesa, Riginella, Mazzoldi, & Ashford, 2015), yet hatch dates in December and January for fish in our sample would demand virtual cessation of growth until their capture in mid-March. Instead, recent hatching in the vicinity of the Bay of Whales appears a better explanation. Late hatching may reflect multiple hatching events (Granata et al., 2002; Keller, 1983), the longer season and higher productivity of the Ross Ice Shelf polynya (Arrigo, van Dijken, & Strong, 2015), or the southern location of the Bay of Whales (78.5°S) relative to Terra Nova Bay (74.83°S).

#### 4.2 | Cross-shelf dispersal in the western Ross Sea

Refining the scenario for dispersal using our results during the 2013 summer, eggs incubated under the fast ice between Gerlache Inlet and Cape Washington (shown in Figure 6 in relation to sampling locations 3 and 13) would have been initially retained in association with platelet ice. Based on back-calculation, most larvae hatched during the last three weeks of December and first two weeks of January. Moving into the water column, the larvae would have encountered surface Ekman transport induced by the katabatic wind field (Hubold, 1984; La Mesa et al., 2010) notably off the Reeves Glacier that, flowing past Cape Washington to the offshore edge of the Terra Nova Bay polynya and the western Drygalski Trough, would have exposed them to northward transport in the trough outflow to Coulman Island. The distribution of ice cover made it unlikely that the katabatic winds over Terra Nova Bay advected larvae eastward as far as Cray Bank.

Considering the timing of these events, advection northward from Cape Washington at a velocity of 0.1 m/s, similar to that found in the surface layer in the Joides Trough (Kohut et al., 2013), would have taken in the order of 14 days, suggesting that fish sampled between 26 February–1 March off Coulman Island were originally entrained in the trough circulation in mid-February. The timing coincided with a series of strong wind events recorded at Mario Zucchelli Station after 5 February (Figure 7), consistent with enhanced connectivity between the fast ice stretching from Gerlache Inlet to Cape Washington and the outer edge of the polynya. Earlier series of wind events in the last week of December and commencing 15 January suggest similar periods of enhanced dispersal (Figure 7). From Coulman Island, subsequent advection in southward jets, documented at velocities of 0.2 m/s in the surface layer by Kohut et al. (2013), would have taken in the order of seven days to pass along the Cray Bank. As a result, fish sampled off the southern Cray Bank may have been part of the same advection event out of Terra Nova Bay as those caught off Coulman Island.

However, the high concentration of larvae at Location 4 were caught too early to have been advected in the same event. Instead, the period of high katabatic winds commencing on 15 January was associated with open water off southern Victoria Land (Figure 7) and, prior to our sampling period, a pulse of wind-



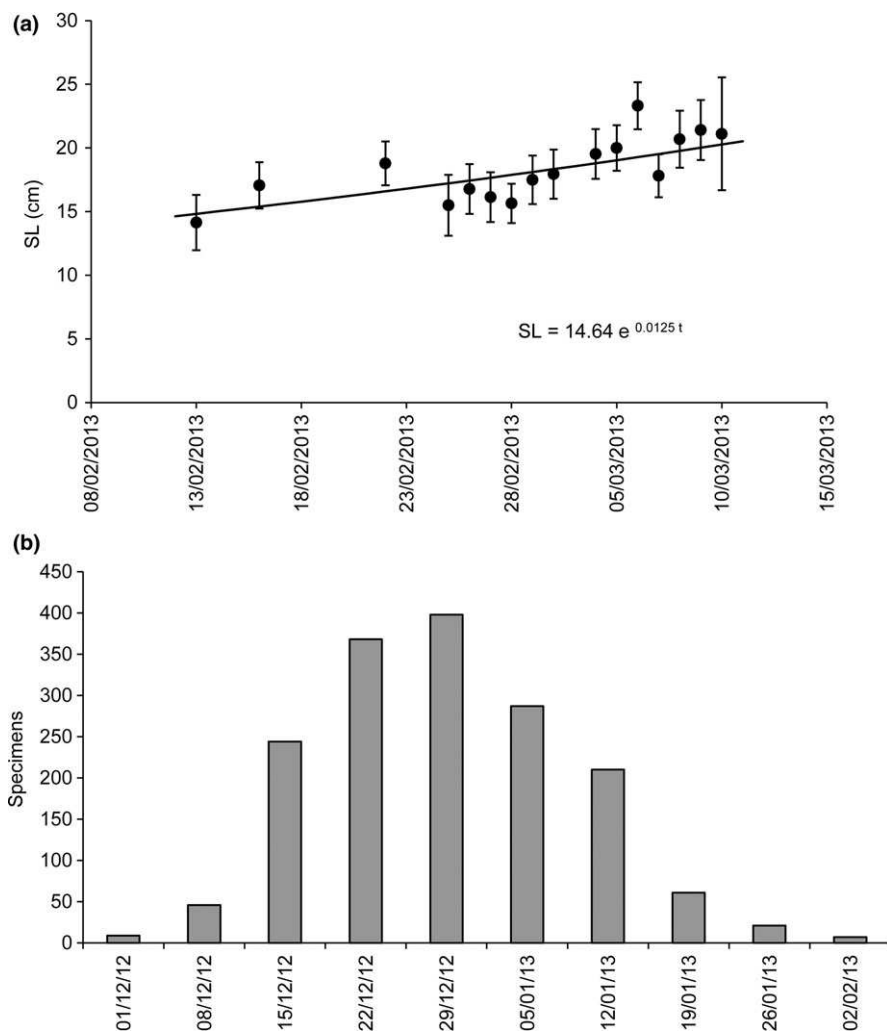


**FIGURE 5** Length distributions for *Pleuragramma antarctica* sampled between 13 February to 13 March 2013 in the Ross Sea. Standard length (mean  $\pm$  SD) all larvae pooled, with estimated exponential equation growth relationship (a), and back-calculated hatch dates (b). First day of sampling 13 February 2013; all dates reported in day/month/year (DD/MM/YY). Locations reflect order of sampling; with the Bay of Whales sampled last on 13 March

induced Ekman transport in the surface layer may have carried larvae past Cape Washington, reaching across the trough to generate an alternative, episodic pathway to the Cray Bank. Notably, the congruence in length distributions between Location 4 and locations off Coulman Island indicated that the dispersal events were from the same pool of larvae, presumably accumulating during the hatching period under the fast ice between Gerlache Inlet and Cape Washington.

Sea ice distribution may also be important. The trajectory northward from the edge of the Terra Nova Bay polynya was covered with ice during sampling: transported northward to emerge from under the ice near Coulman Island, the water at Locations 6, 8 and 14 was characterized by freshening near the surface, whereas a pronounced mixed layer was found further from the ice margin at Locations 5 and 7. Similarly over southern Cray Bank, more open conditions were associated with a well developed mixed layer above MCDW. The ice distribution may have had other effects as well. Meltwater from sea-ice is one of the largest sources of dissolved iron to the euphotic zone (McGillicuddy et al., 2015). Melting, especially near the ice edge, combined with wind action at the surface, is likely to strongly influence conditions for growth and survival of *P. antarctica* larvae. Such sea-ice interactions with the circulation

and life history suggest an important development to the scenario, in which growth and survival decline when the ice edge does not lie over Drygalski Trough and larval trajectories are geographically separated from meltwater inputs. In years when the two coincide, successful recruitment may result in strong cohorts connecting production to higher trophic levels.

#### 4.3 | Retention by trough systems and transport along shelf

The life history hypothesis predicted that trough circulation facilitates retention of fish in populations of *P. antarctica*, and that advection across and along the shelf helps to maintain distributions around the Antarctic (Ashford et al., 2017). In the western Ross Sea, La Mesa et al. (2010) found post-larvae (age 1+ yr) and juveniles (2+ yr) on the outer shelf (Figure 1c,d). Cross-shelf transport northward reaching the AFS, would result in advection westward to areas of the shelf along East Antarctica past Cape Adare, similar to the description by Hubold (1984) for the south-east Weddell Sea. The hypothesis suggested a mechanism by which fish mixing between trough outflows and inflows regulates along-shelf advection, versus retention and return toward the inner shelf.



**FIGURE 6** Geography of Terra Nova Bay, including Mario Zucchelli Station (MZS) and showing sampling Locations 3 and 13

Our results suggest physical effects that are potentially involved. The trough near Coulman Island is notable for its curvature and narrowing, as well as a reverse slope and glacial discontinuities like grounding zone wedges (Anderson et al., 2014) that may help promote mixing both in vertical and horizontal directions. The unexpected presence of MCDW at Location 7 may have been due to a meander or eddy. Given the proximity of the coast, wind events like those encountered during sampling may also be involved. These potential effects, concentrated near Coulman Island, argue for the importance of the area for entrainment in southward flow. Dilution with increasing dispersal along the trough, rates of mixing between outflowing and inflowing water, and variation in the outflow to the outer shelf, would then help account for spatial variation in abundance indices, as well as retention within the population and advective losses along the continental shelf.

Predictions of population structure and connectivity are less straightforward for the Bay of Whales. In much the same way as for the western Ross Sea, dispersal by katabatic winds off the Ross Ice

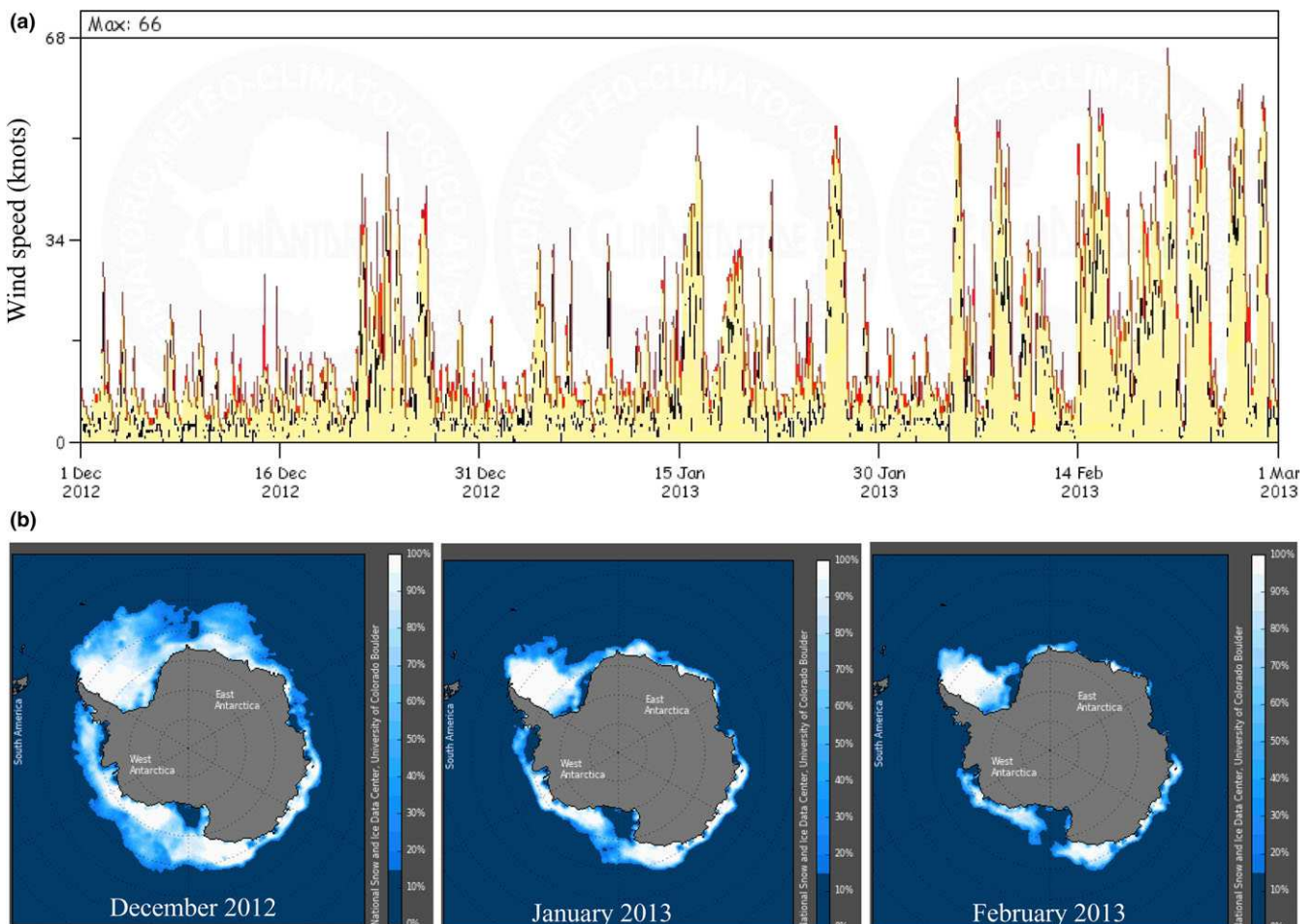


**FIGURE 7** Wind velocities at Terra Nova Bay station (a), and sea ice concentration around the Antarctic during the months December 2012–February 2013 (b). Data and information for the wind velocities were obtained from the Meteo Climatological Observatory at Mario Zucchelli Station and Victoria Land of PNRA -<http://www.climantartide.it>. Sea ice concentrations were obtained from Fetterer, F., Knowles, K., Meier, W., & Savoie, M. (2016) updated daily. Sea Ice Index, Version 2. Boulder, Colorado USA. NSIDC: National Snow and Ice Data Center. <https://doi.org/10.7265/n5736nv7>

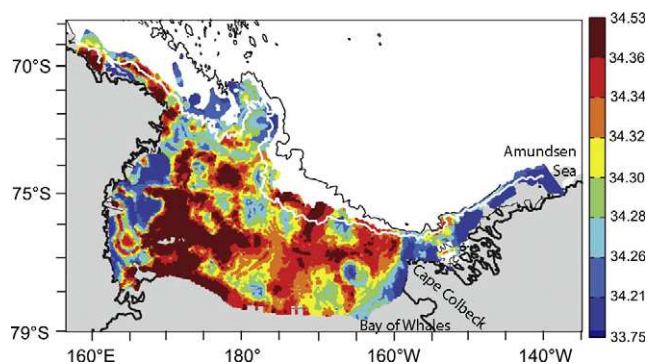


**FIGURE 8** Average salinity for the surface density layer in the Ross Sea, reproduced from Orsi and Wiederwohl (2009) in their Figure 5. Fresher AASW that flows south of Cape Colbeck corresponds to the Antarctic Coastal Current. Isobaths: 1,000 m (white); 3,000 m (black)

Shelf may connect the nursery ground of a geographically discrete population (Brooks & Goetz, 2014) to outflowing water along the Whales Trough (Orsi & Wiederwohl, 2009) consistent with a coherent early life history spatially constrained by incubation under fast ice in the vicinity of the Bay of Whales. However, late hatching, or lack of growth, raises questions over subsequent larval survival and recruitment. In addition, how fish would close their life history is unclear: water is transported poleward along Little America Trough, located east of Whales Trough (Orsi & Wiederwohl, 2009), but connectivity is limited. Flow along the slope is westward, constraining return to potential nursery grounds under fast ice in the vicinity of the Bay of Whales. Considerable uncertainty remains over whether the larvae represent a true nursery ground (Ghigliotti et al., 2017), and more work is required to resolve the physical-biological interactions by which retention and self-recruitment could support a discrete population in the eastern Ross Sea.

Moreover, the life history hypothesis suggests a competing explanation based on along-shelf advection. In contrast to the AFS, the westward Antarctic Coastal Current (AACC, e.g., Moffat, Beardsley, Owens, & van Lipzig, 2008; Núñez-Riboni & Fahrbach, 2009) is a feature typical of coastal buoyant plumes, with freshwater inputs from precipitation over the ocean, meltwater run-off from land and sea-ice and glacial melting (Dutrieux et al., 2014; Moffat et al., 2008). The AACC is thought to be involved in the delivery of larvae spawned in the western Weddell Sea to adult assemblages in the Bransfield Strait (La Mesa, Piñones, et al., 2015), and from Marguerite Bay to Charcot Island (Agostini et al., 2015; Ferguson, 2012). It is also located inshore along the Amundsen Sea, flowing around Cape Colbeck and sharply south towards the eastern Ross Ice Shelf (Orsi & Wiederwohl, 2009; Figure 8). Larvae in the Bay of Whales were too small to have been advected themselves, but large aggregations of older *P. antarctica* occur inshore along the western Amundsen Sea and around Cape Colbeck (Donnelly, Torres, Sutton, & Simoniello, 2004). As in the western Weddell Sea, advective losses in the AACC past Cape Colbeck may survive to join adult assemblages downstream. Such vagrants (Sinclair, 1988) may still spawn as adults where they encounter suitable conditions along the Ross Ice Shelf, including in the Bay of Whales, but the

lack of a coherent spatial trajectory to underpin their life cycle inhibits their ability to self-recruit successfully.

Further research is needed to address these questions, especially since multi-decadal freshening of shelf water in the southwestern Ross Sea has been linked to melting of continental ice in the Amundsen Sea and transport westward along the shelf (Jacobs & Giulivi, 2010; Jacobs, Giulivi, & Mele, 2002). Strengthening connectivity over time, with larger and more stable spawning events, may lead to colonization if changing conditions allow life cycle closure and a stable population to form (Ashford et al., 2017). Due to heavy ice conditions and difficulties of access and sampling, the eastern Ross Sea is understudied compared to western areas. However, multi-disciplinary approaches combining techniques that include genetics (Agostini et al., 2015), otolith chemistry (Ferguson, 2012), age distributions and circulation modelling (La Mesa, Piñones, et al., 2015), reproduction (La Mesa, Riginella, et al., 2015), and community studies (Parker et al., 2015) successfully tested population hypotheses along the Antarctic Peninsula. Spatial heterogeneity between discrete populations contrasts strongly to homogeneity between exported fish and their parent population, providing a useful test around which field sampling can be designed. Resolving life history and population structure in a critical forage species can help unravel the complex physical-biological interactions that link producers and higher predators in the Southern Ocean ecosystem.

#### ACKNOWLEDGEMENTS

We thank the crew and science personnel aboard the research cruise NBP13-02, especially from the laboratory of Dr Alexander Bochdansky at Old Dominion University. We also thank Dr Christian Reiss at NOAA who assisted with calculations of the abundance indices and provided useful feedback on the manuscript; Dr Joseph Eastman and Dr David Ainley for insightful comments concerning *P. antarctica* in the Ross Sea; Dr Chiara Papetti at the Università di Padova for assistance in genetic data analysis and interpretation; and an anonymous reviewer. Funding and logistic support were provided by the National Science Foundation (Grant No. 1043454). C. Brooks was supported by the Emmett Interdisciplinary Program in Environment and Resources at Stanford University, the Price Fellowship and the Switzer Foundation. J. Caccavo was supported by the Biosciences Program in Evolution, Ecology and Conservation at the Università di Padova, and the Cariparo Fellowship. Funding for J. Ashford was provided by the National Science Foundation (Grant No. 0741348).

#### ORCID

Cassandra M. Brooks  <http://orcid.org/0000-0002-1397-0394>

#### REFERENCES

Agostini, C., Patarnello, T., Ashford, J. R., Torres, J. J., Zane, L., & Papetti, C. (2015). Genetic differentiation in the icedependent fish

- Pleuragramma antarctica* along the Antarctic Peninsula. *Journal of Biogeography*, 42, 1103–1113. <https://doi.org/10.1111/jbi.12497>
- Anderson, J. B., Conway, H., Bart, P. J., Witus, A. E., Greenwood, S. L., McKay, R. M., ... Stone, J. O. (2014). Ross Sea paleo-ice sheet drainage and deglacial history during and since the LGM. *Quaternary Science Reviews*, 100, 31–54. <https://doi.org/10.1016/j.quascirev.2013.08.020>
- Arrigo, K. R., van Dijken, G. L., & Strong, A. L. (2015). Environmental controls of marine productivity hot spots around Antarctica. *Journal of Geophysical Research: Oceans*, 120, 5545–5565.
- Ashford, J., Zane, L., Torres, J., La Mesa, M., & Simms, A. (2017). Population structure and life history connectivity of Antarctic silverfish (*Pleuragramma antarctica*) in the Southern Ocean ecosystem. In M. Vacchi, E. Pisano, & L. Ghigliotti (Eds.), *The Antarctic silverfish: A keystone species in a changing ecosystem* (pp. 193–234). Berlin, Germany: Springer. <https://doi.org/10.1007/978-3-319-55893-6>
- Biggs, D. C. (1982). Zooplankton excretion and NH<sub>4</sub> cycling in near-surface water of the Southern Ocean. I. Ross Sea, austral summer 1977–1978. *Polar Biology*, 1, 55–67. <https://doi.org/10.1007/BF00568755>
- Brooks, C., & Goetz, K. (2014). *Pleuragramma antarcticum* distribution in the Ross Sea during late austral summer 2013. CCAMLR WG-EMM-14/38.
- Campana, S. E., & Jones, C. (1992). Analysis of otolith microstructure data. *Canadian Special Publication of Fisheries and Aquatic Sciences*, 117, 73–100.
- Dinniman, M. S., Klinck, J. M., & Smith, W. O. (2003). Cross-shelf exchange in a model of the Ross Sea circulation and biogeochemistry. *Deep-Sea Research II*, 50, 3103–3120. <https://doi.org/10.1016/j.dsr2.2003.07.011>
- Donnelly, J., Torres, J. J., Sutton, T. T., & Simoniello, C. (2004). Fishes of the eastern Ross Sea, Antarctica. *Polar Biology*, 27, 637–650. <https://doi.org/10.1007/s00300-004-0632-2>
- Dutrieux, P., De Rydt, J., Jenkins, A., Holland, P. R., Kyung Ha, H., Hoon Lee, S., ... Schroder, M. (2014). Strong sensitivity of Pine Island ice-shelf melting to climatic variability. *Science*, 343, 174–178. <https://doi.org/10.1126/science.1244341>
- Eastman, J. T., & DeVries, A. L. (1989). Ultrastructure of the lipid sac wall in the Antarctic nototheniid fish *Pleuragramma antarcticum*. *Polar Biology*, 9, 333–335. <https://doi.org/10.1007/BF00287433>
- Ferguson, J. W. (2012). Population structure and connectivity of an important pelagic forage fish in the Antarctic ecosystem, *Pleuragramma antarcticum*, in relation to large scale circulation. Masters Thesis, Old Dominion University, United States.
- Ghigliotti, L., Herasymchuk, V. V., Kock, K.-H., & Vacchi, M. (2017). Reproductive Strategies of the Antarctic Silverfish: Known Knowns, Unknowns and Unknown Unknowns. In M. Vacchi, E. Pisano, & L. Ghigliotti (Eds.), *The Antarctic silverfish: A keystone species in a changing ecosystem* (pp. 173–192). Berlin, Germany: Springer.
- Gordon, A. L., Orsi, A. H., Muench, R., Huber, B., Zambianchi, E., & Visbeck, M. (2009). Western Ross Sea continental slope gravity currents. *Deep-Sea Research II*, 56, 796–817. <https://doi.org/10.1016/j.dsr2.2008.10.037>
- Granata, A., Cubeta, A., Guglielmo, L., Sidoti, O., Greco, S., Vacchi, M., & La Mesa, M. (2002). Ichthyoplankton abundance and distribution in the Ross Sea during 1987–1996. *Polar Biology*, 25, 187–202.
- Granata, A., Zagami, G., Vacchi, M., & Guglielmo, L. (2008). Summer and spring trophic niche of larval and juvenile *Pleuragramma antarcticum* in the Western Ross Sea, Antarctica. *Polar Biology*, 3, 369–382.
- Guglielmo, L., Granata, A., & Greco, S. (1998). Distribution and abundance of postlarval and juvenile *Pleuragramma antarcticum* (Pisces, Nototheniidae) off Terra Nova Bay (Ross Sea, Antarctica). *Polar Biology*, 19, 37–51.
- Guidetti, P., Ghigliotti, L., & Vacchi, M. (2015). Insights into spatial distribution patterns of early stages of the Antarctic silverfish, *Pleuragramma antarctica*, in the platelet ice of Terra Nova Bay, Antarctica. *Polar Biology*, 38, 333–342. <https://doi.org/10.1007/s00300-014-1589-4>
- Hubold, G. (1984). Spatial distribution of *Pleuragramma antarcticum* (Pisces: Nototheniidae) near the Filchner and Larsen ice shelves (Weddell Sea, Antarctica). *Polar Biology*, 3, 231–236. <https://doi.org/10.1007/BF00292628>
- Hubold, G. (1985). The early life history of the high-Antarctic silverfish, *Pleuragramma antarcticum*. In W. R. Siegfried, P. R. Condy, & R. M. Laws (Eds.), *Antarctic nutrient cycles and food webs* (pp. 445–451). Berlin, Germany: Springer. <https://doi.org/10.1007/978-3-642-82275-9>
- Jacobs, S. S., & Giulivi, C. F. (2010). Large multidecadal salinity trends near the Pacific-Antarctic continental margin. *Journal of Climate*, 23, 4508–4524. <https://doi.org/10.1175/2010JCLI3284.1>
- Jacobs, S. S., Giulivi, C. F., & Mele, P. (2002). Freshening of the Ross Sea during the late 20th Century. *Science*, 297, 386–389. <https://doi.org/10.1126/science.1069574>
- Keller, R. (1983). Contributions to the early life history of *Pleuragramma antarcticum* Boulenger 1902 (Pisces, Nototheniidae) in the Weddell Sea. *Meeresforschung*, 30, 10–24.
- Kellermann, A. (1986). Geographical distribution and abundance of post-larval and juvenile *Pleuragramma antarcticum* (Pisces, Notothenioidei) off the Antarctic Peninsula. *Polar Biology*, 6, 111–119. <https://doi.org/10.1007/BF00258262>
- Kellermann, A. (1989). Identification key and catalogue of larval Antarctic fishes. *BIOMASS Scientific Series*, 10, 1–136.
- Kohut, J., Hunter, E., & Huber, B. (2013). Small-scale variability of the cross-shelf flow over the outer shelf of the Ross Sea. *Journal of Geophysical Research: Oceans*, 118, 1863–1876.
- La Mesa, M., Catalano, B., Russo, A., Greco, S., Vacchi, M., & Azzali, M. (2010). Influence of environmental conditions on spatial distribution and abundance of early life stages of Antarctic silverfish, *Pleuragramma antarcticum* (Nototheniidae), in the Ross Sea. *Antarctic Science*, 22, 243–254. <https://doi.org/10.1017/S0954102009990721>
- La Mesa, M., & Eastman, J. T. (2012). Antarctic silverfish: Life strategies of a key species in the high-Antarctic ecosystem. *Fish and Fisheries*, 13, 241–266. <https://doi.org/10.1111/j.1467-2979.2011.00427.x>
- La Mesa, M., Eastman, J. T., & Vacchi, M. (2004). The role of nototheniid fish in the food web of the Ross Sea shelf waters: A review. *Polar Biology*, 27, 321–338. <https://doi.org/10.1007/s00300-004-0599-z>
- La Mesa, M., Piñones, A., Catalano, B., & Ashford, J. (2015). Predicting early life connectivity of Antarctic silverfish, an important forage species along the Antarctic Peninsula. *Fisheries Oceanography*, 24, 150–161. <https://doi.org/10.1111/fog.12096>
- La Mesa, M., Riginella, E., Mazzoldi, C., & Ashford, J. (2015). Reproductive resilience of ice-dependent Antarctic silverfish in a rapidly changing system along the Western Antarctic Peninsula. *Marine Ecology*, 36, 235–245. <https://doi.org/10.1111/maec.12140>
- McGillicuddy, D. J., Sedwick, P. N., Dinniman, M. S., Arrigo, K. R., Bibby, T. S., Greenan, B. J., ... van Dijken, G. L. (2015). Iron supply and demand in an Antarctic shelf ecosystem. *Geophysical Research Letters*, 42, 8088–8097. <https://doi.org/10.1002/2015GL065727>
- Moffat, C., Beardsley, R. C., Owens, B., & van Lipzig, N. (2008). A first description of the Antarctic Peninsula Coastal Current. *Deep-Sea Research II*, 55, 277–293. <https://doi.org/10.1016/j.dsr2.2007.10.003>
- Near, T. J., Dornburg, A., Kuhn, K. L., Eastman, J. T., Pennington, J. N., Patarnello, T., ... Jones, C. D. (2012). Ancient climate change, anti-freeze, and the evolutionary diversification of Antarctic fishes. *Proceedings of the National Academy of Sciences of the United States of America*, 109, 3434–3439. <https://doi.org/10.1073/pnas.1115169109>
- Núñez-Riboni, I., & Fahrback, E. (2009). Seasonal variability of the Antarctic Coastal Current and its driving mechanisms in the Weddell

- Sea. *Deep Sea Research I*, 56, 1927–1941. <https://doi.org/10.1016/j.dsr.2009.06.005>
- O'Driscoll, R. L., Macaulay Gavin, J., Gauthier, S., Pinkerton, M., & Hanchet, S. (2011). Distribution, abundance and acoustic properties of Antarctic silverfish (*Pleuragramma antarcticum*) in the Ross Sea. *Deep-Sea Research II*, 58, 181–195. <https://doi.org/10.1016/j.dsr2.2010.05.018>
- Orsi, A. H., & Wiederwohl, C. L. (2009). A recount of Ross Sea waters. *Deep-Sea Research II*, 56, 778–795. <https://doi.org/10.1016/j.dsr2.2008.10.033>
- Parker, M. L., Fraser, W. R., Ashford, J., Patarnello, T., Zane, L., & Torres, J. J. (2015). Assemblages of micronektonic fishes and invertebrates in a gradient of regional warming along the Western Antarctic Peninsula. *Journal of Marine Systems*, 152, 18–41. <https://doi.org/10.1016/j.jmarsys.2015.07.005>
- Sinclair, M. (1988). *Marine populations: An essay on population regulation and speciation* (p. 252). Washington, DC: University of Washington Press.
- Smith, W. O., Ainley, D. G., & Cattaneo-Vietti, R. (2007). Trophic interactions within the Ross Sea continental shelf ecosystem. *Philosophical Transactions of the Royal Society of London B: Biological Sciences*, 362, 95–111. <https://doi.org/10.1098/rstb.2006.1956>
- Smith, W. O., Ainley, D. G., Cattaneo-Vietti, R., & Hofmann, E. E. (2012). The Ross Sea continental shelf: Regional biogeochemical cycles, trophic interactions, and potential future changes. In A. D. Rogers, N. M. Johnston, E. J. Murphy, & A. Clarke (Eds.), *Antarctic ecosystems: An extreme environment in a changing world* (pp. 213–242). London, UK: J. Wiley and Sons. <https://doi.org/10.1002/9781444347241>
- Vacchi, M., DeVries, A. L., Evans, C. W., Bottaro, M., Ghigliotti, L., Cutroneo, L., & Pisano, E. (2012). A nursery area for the Antarctic silverfish *Pleuragramma antarcticum* at Terra Nova Bay (Ross Sea): First estimate of distribution and abundance of eggs and larvae under the seasonal sea-ice. *Polar Biology*, 35, 1573–1585. <https://doi.org/10.1007/s00300-012-1199-y>
- Vacchi, M., La Mesa, M., Dalu, M., & Macdonald, J. (2004). Early life stages in the life cycle of Antarctic silverfish, *Pleuragramma antarcticum* in Terra Nova Bay, Ross Sea. *Antarctic Science*, 16, 299–305. <https://doi.org/10.1017/S0954102004002135>
- Vacchi, M., La Mesa, M., & Greco, S. (1999). Summer distribution and abundance of larval and juvenile fishes in the western Ross Sea. *Antarctic Science*, 11, 54–60.

## SUPPORTING INFORMATION

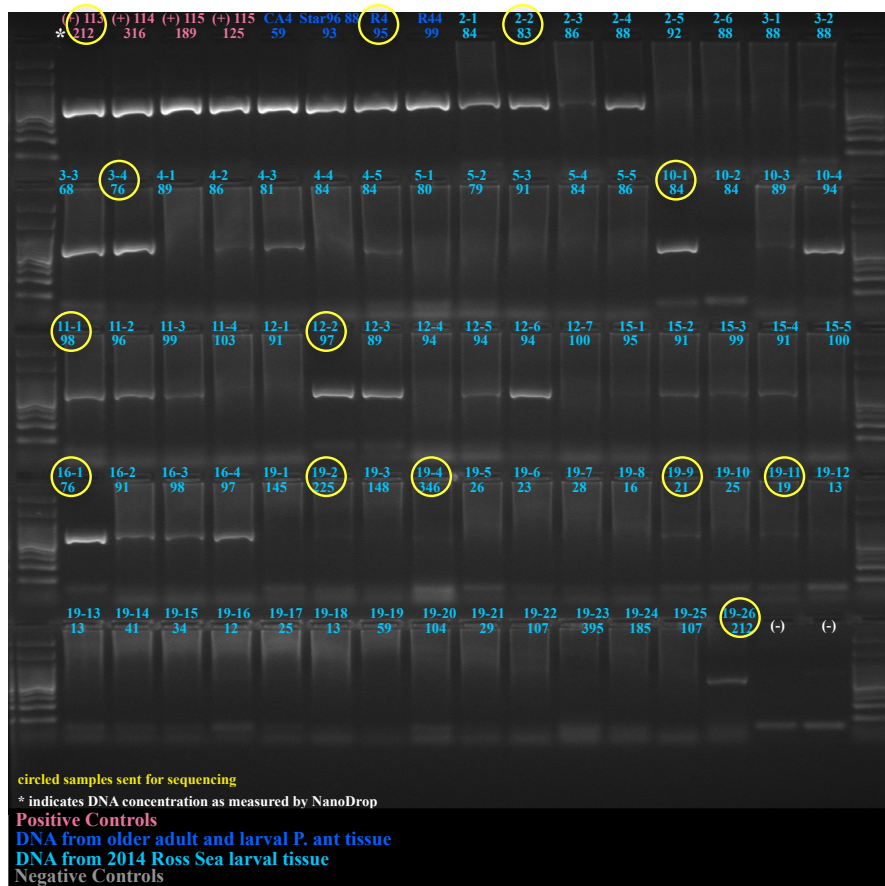
Additional Supporting Information may be found online in the supporting information tab for this article.

**How to cite this article:** Brooks CM, Caccavo JA, Ashford J, et al. Early life history connectivity of Antarctic silverfish (*Pleuragramma antarctica*) in the Ross Sea. *Fish Oceanogr.* 2018;00:1–14. <https://doi.org/10.1111/fog.12251>

Supplementary Information **Brooks *et al.* 2018**

**Figure S1. PCR results of 16S rDNA and D-Loop region amplification.** Amplicons from seventy-eight *P. antarctica* samples visualized on a 1.8% agarose gel with a 1 kb ladder are shown for 16S rDNA (a) and the D-Loop region (b). Forward and reverse fish universal primers 16ar and 16br were used for the amplification of approximately 528 base pairs (bp) of 16S rDNA (Palumbi et al. 2002). Forward and reverse primers LPRO2 and HDL1 were used to amplify approximately 349 bp of the D-Loop region (Patarnello et al. 2003). Singleplex PCRs were performed on 2  $\mu$ L of DNA in a total volume of 20  $\mu$ L consisting of 0.04 U/ $\mu$ L of Promega *Taq* polymerase, 1x Promega reaction buffer (with MgCl<sub>2</sub>), 0.1  $\mu$ M of each dNTPs, and 0.25 nM of each primer. The thermal profile for 16S rDNA amplification was: (1) predenaturation: 94°C for 3 min; (2) 6 touchdown cycles: denaturation at 94°C for 40 s, annealing at 56°C for 1 min decreased by 1°C each cycle, extension at 72°C for 1 min; (3) 30 cycles: denaturation at 94°C for 40 s, annealing at 50°C for 1 min and extension at 72°C for 1 min; (4) final extension: 72°C for 5 min. The D-Loop thermal cycle was: (1) predenaturation: 94°C for 3 min; (2) 30 cycles: denaturation at 94°C for 1 min, annealing at 52°C for 45 s and extension at 72°C for 45 s; (3) final extension: 72°C for 5 min. Amplification of mtDNA from larvae showed evidence of DNA damage that can be seen in the smear signatures of the majority of larval samples compared to the absence of such signatures in positive controls. Six western Ross Sea (WRS) larvae from six different tows and five eastern Ross Sea (ERS) larvae had bands clear enough to indicate adequate quantities of amplified mtDNA to proceed with sequencing. Two of the positive controls (one adult from the Weddell Sea and one larva from the Ross Sea) were also included for sequencing. Yellow circles indicate samples subsequently submitted for sequencing.

a) 16S



b) D-Loop

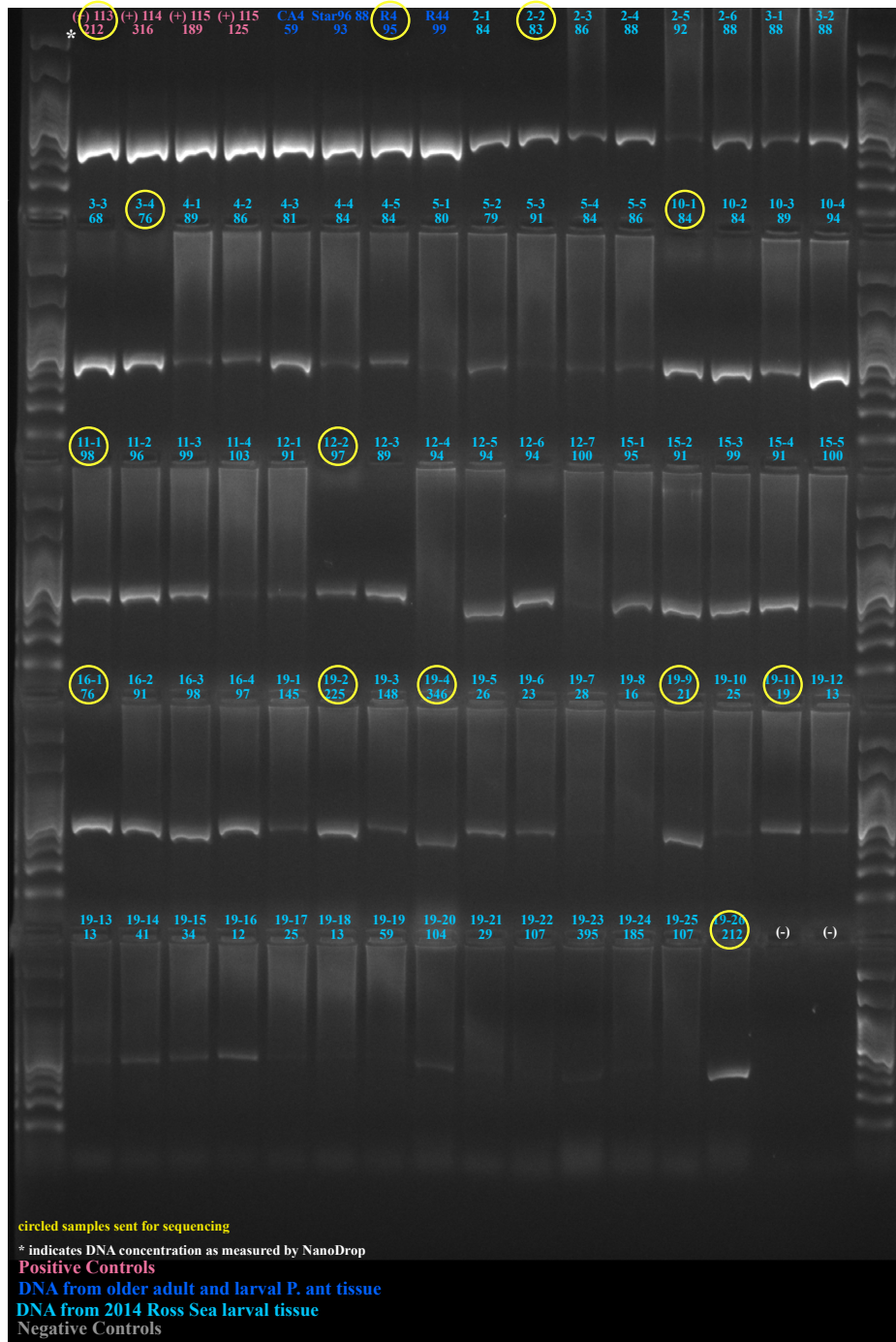




**Figure S2. Neighbour-joining tree based on Kimura 2-parameter genetic distance between 16S sequences.** Eight new sequences of 16S rDNA from *P. antarctica* are presented below in a neighbour-joining tree with seven existing *P. antarctica* and nine outgroup sequences from the NCBI database (see Table S1 for full sequence details). Bootstrap values are adjacent to nodes. Values of 100 where nodes indicate separate species are circled in red. The tree is not meant to represent true phylogenetic relationships within the taxa shown, but to visualize the clear coincidence of the six western Ross Sea (WRS, purple text) larvae with existing *P. antarctica* sequences, and the divergence of the *P. antarctica* clade from the outgroup species with 100% bootstrap support. Visual inspection of raw fluorograms resulted in the elimination of all five 16S rDNA sequences from the eastern Ross Sea (ERS) due to poor or inconsistent signal precluding accurate nucleotide calling. Thus the 16S neighbour-joining tree does not include sequences from ERS larvae. The majority of 16S sequences from the NCBI database did not indicate sample provenance.

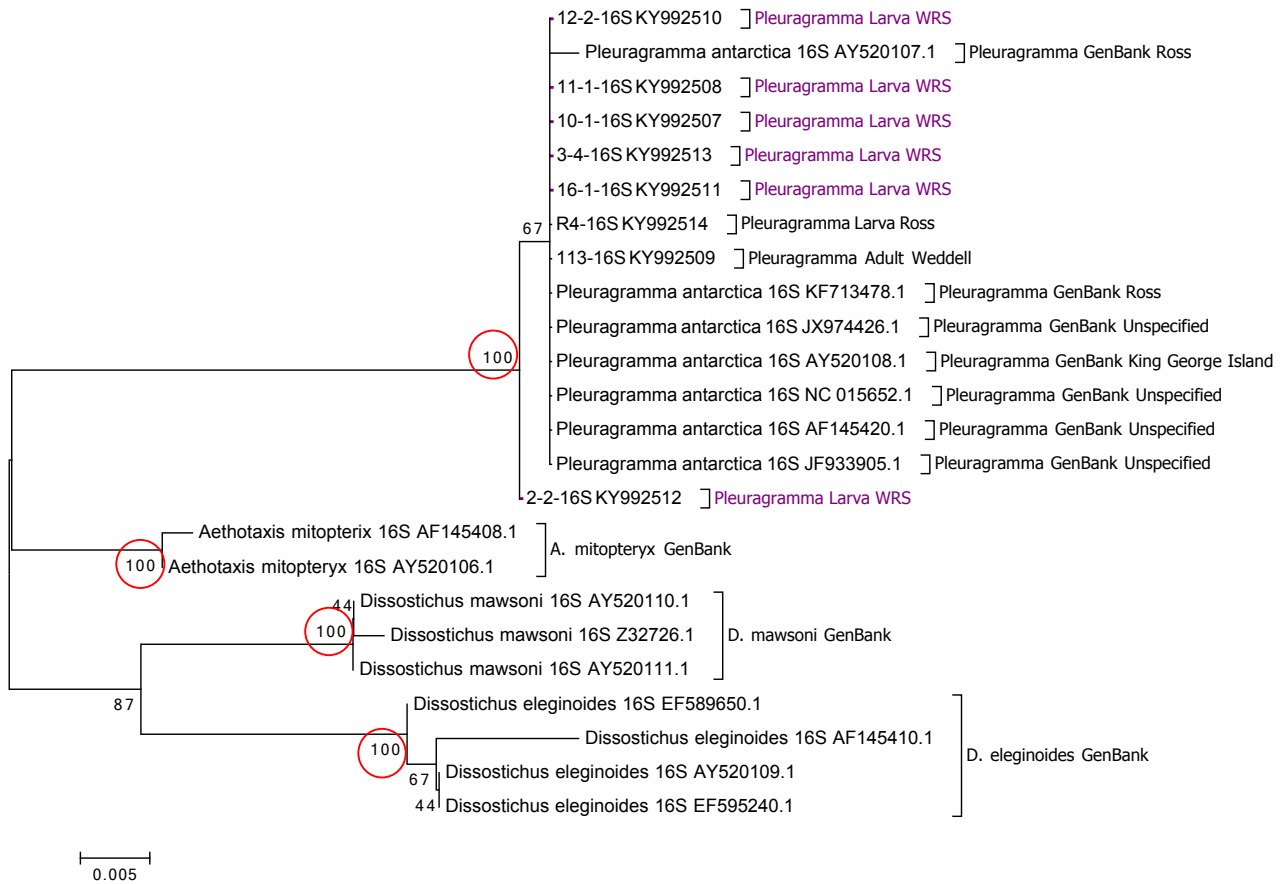


**Figure S3. Neighbour-joining tree based on Kimura 2-parameter genetic distance between D-Loop sequences.** Twelve new sequences of the D-Loop region from *P. antarctica* are presented below in a neighbour-joining tree with sixteen existing *P. antarctica* and seven outgroup sequences from the NCBI database (see Table S1 for full sequence details). Bootstrap values are adjacent to nodes. Values of 100 where nodes indicate separate species are circled in red. The tree is not meant to represent true phylogenetic relationships within the taxa shown, but to visualize the unmistakable clustering together in a single clade of the six larval sequences from the western Ross Sea (WRS, purple text) and the four larval sequences from the eastern Ross Sea (ERS, pink text) with the existing *P. antarctica* sequences from the NCBI database with 100% bootstrap support, clearly differentiating them from the phylogenetically closest species. D-Loop sequences from the NCBI database did not indicate sample provenance.

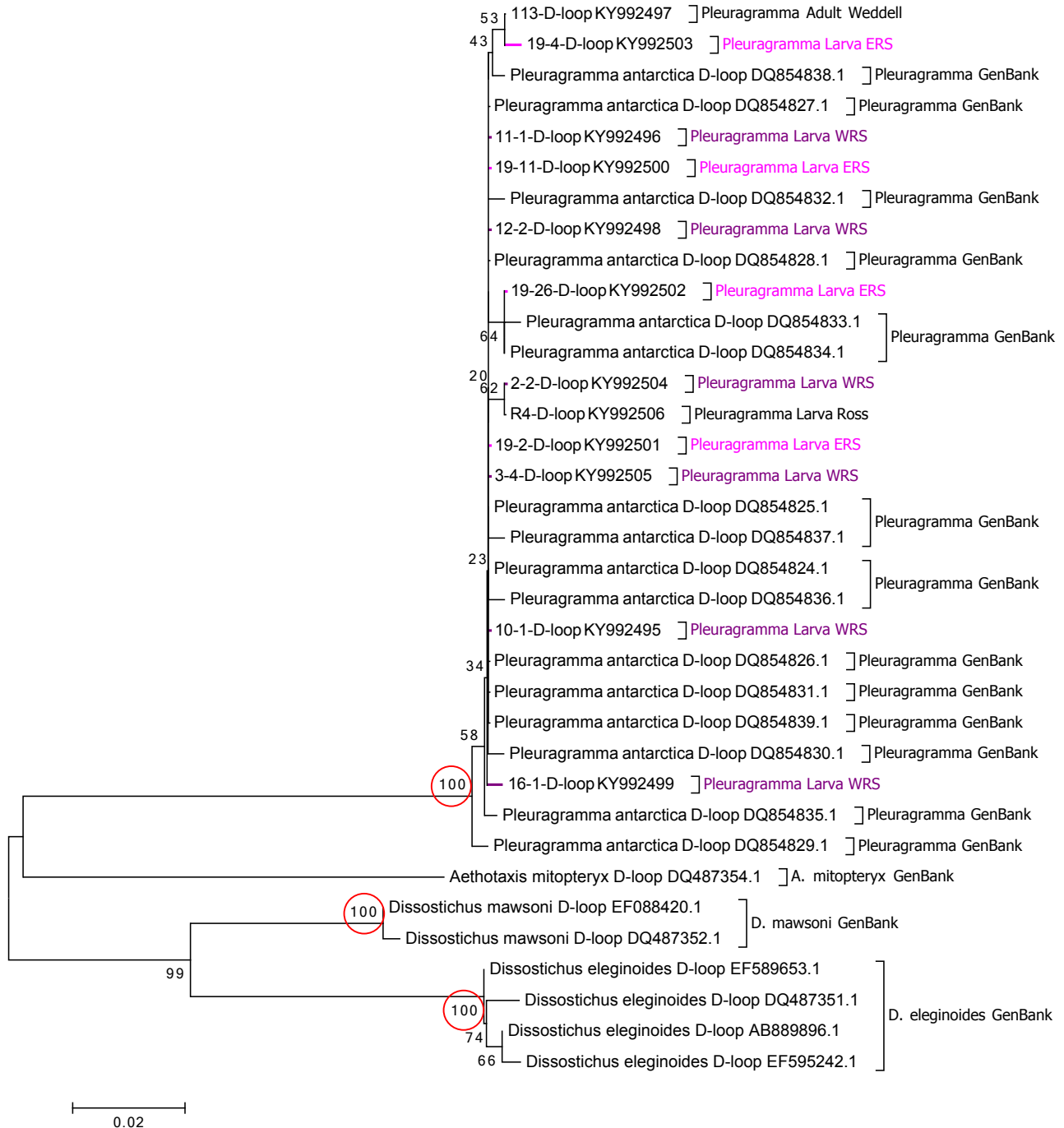


**Table S1. Sequence information.** Year and area collected, study ID and GenBank accession number are indicated for the twelve 16S and eight D-Loop sequences newly obtained from *P. antarctica* (a). Accession numbers for sequences from *P. antarctica* and closely related notothenioids pulled from the NCBI database are also shown with associated reference number adjacent in brackets where applicable (b). The new sequences were obtained from amplicons reported in Fig. S1. To prepare for Sanger sequencing, unincorporated dNTPs and primers were removed from PCR products using the pre-sequencing kit USB® ExoSAP-IT® PCR Product Cleanup (Affymetrix) according to the manufacturer's instructions. Fragments were sequenced using an internal service, BMR Genomics ([www.bmr-genomics.it](http://www.bmr-genomics.it)). Prior to alignment, the raw fluorogram sequences were visually inspected and cleaned up using Chromas LITE Version 2.1.1. Alignment was then performed by MUSCLE (<http://www.ebi.ac.uk/Tools/msa/muscle/>) using MEGA 6.06 (Tamura et al. 2013).

a)

16S alignment sequences					D-Loop alignment sequences				
Species	GenBank Accession numbers	Year	Area	ID	Species	GenBank Accession numbers	Year	Area	ID
<i>Pleuragramma</i> larva	KY992512	2014	WRS	2-2	<i>Pleuragramma</i> larva	KY992504	2014	WRS	2-2
<i>Pleuragramma</i> larva	KY992513	2014	WRS	3-4	<i>Pleuragramma</i> larva	KY992505	2014	WRS	3-4
<i>Pleuragramma</i> larva	KY992507	2014	WRS	10-1	<i>Pleuragramma</i> larva	KY992495	2014	WRS	10-1
<i>Pleuragramma</i> larva	KY992508	2014	WRS	11-1	<i>Pleuragramma</i> larva	KY992496	2014	WRS	11-1
<i>Pleuragramma</i> larva	KY992510	2014	WRS	12-2	<i>Pleuragramma</i> larva	KY992498	2014	WRS	12-2
<i>Pleuragramma</i> larva	KY992511	2014	WRS	16-1	<i>Pleuragramma</i> larva	KY992499	2014	WRS	16-1
<i>Pleuragramma</i> larva	KY992514	1998	Ross	R4	<i>Pleuragramma</i> larva	KY992506	1998	Ross	R4
<i>Pleuragramma</i> adult	KY992509	2007	Weddell	113	<i>Pleuragramma</i> adult	KY992497	2007	Weddell	113
					<i>Pleuragramma</i> larva	KY992501	2014	ERS	19-2
					<i>Pleuragramma</i> larva	KY992503	2014	ERS	19-4
					<i>Pleuragramma</i> larva	KY992500	2014	ERS	19-11
					<i>Pleuragramma</i> larva	KY992502	2014	ERS	19-26

b)

16S alignment sequences		D-Loop alignment sequences	
Species NCBI database	GenBank Accession numbers	Species NCBI database	GenBank Accession numbers
<i>Pleuragramma antarctica</i>	KF713478.1 [2]	<i>Pleuragramma antarctica</i>	DQ854824.1 [8]
<i>Pleuragramma antarctica</i>	JX974426.1	<i>Pleuragramma antarctica</i>	DQ854825.1 [8]
<i>Pleuragramma antarctica</i>	AY520108.1 [3]	<i>Pleuragramma antarctica</i>	DQ854826.1 [8]
<i>Pleuragramma antarctica</i>	AY520107.1 [3]	<i>Pleuragramma antarctica</i>	DQ854827.1 [8]
<i>Pleuragramma antarctica</i>	NC 015652.1	<i>Pleuragramma antarctica</i>	DQ854828.1 [8]
<i>Pleuragramma antarctica</i>	AF145420.1 [1]	<i>Pleuragramma antarctica</i>	DQ854829.1 [8]
<i>Pleuragramma antarctica</i>	JF933905.1	<i>Pleuragramma antarctica</i>	DQ854830.1 [8]
<i>Aethotaxis mitopteryx</i>	AF145408.1 [1]	<i>Pleuragramma antarctica</i>	DQ854831.1 [8]
<i>Aethotaxis mitopteryx</i>	AY520106.1 [3]	<i>Pleuragramma antarctica</i>	DQ854832.1 [8]
<i>Dissostichus eleginoides</i>	AY520109.1 [3]	<i>Pleuragramma antarctica</i>	DQ854833.1 [8]
<i>Dissostichus eleginoides</i>	EF589650.1	<i>Pleuragramma antarctica</i>	DQ854834.1 [8]
<i>Dissostichus eleginoides</i>	AF145410.1 [1]	<i>Pleuragramma antarctica</i>	DQ854835.1 [8]
<i>Dissostichus eleginoides</i>	EF595240.1	<i>Pleuragramma antarctica</i>	DQ854836.1 [8]
<i>Dissostichus mawsoni</i>	AY520111.1 [3]	<i>Pleuragramma antarctica</i>	DQ854837.1 [8]
<i>Dissostichus mawsoni</i>	AY520110.1 [3]	<i>Pleuragramma antarctica</i>	DQ854838.1 [8]
<i>Dissostichus mawsoni</i>	Z32726.1	<i>Pleuragramma antarctica</i>	DQ854839.1 [8]
		<i>Aethotaxis mitopteryx</i>	DQ487354.1 [6]
		<i>Dissostichus eleginoides</i>	AB889896.1
		<i>Dissostichus eleginoides</i>	DQ487351.1 [6]
		<i>Dissostichus eleginoides</i>	EF589653.1
		<i>Dissostichus eleginoides</i>	EF595242.1
		<i>Dissostichus mawsoni</i>	EF088420.1
		<i>Dissostichus mawsoni</i>	DQ487352.1 [6]

**Table S2. Within group genetic distance.** Reported are the average 16S (a) and D-Loop (b) p-distances and their standard errors for the newly obtained *P. antarctica* sequences and for *P. antarctica* and outgroup sequences from the NCBI database (see table S1 for full sequence details). Within group distance estimation tests revealed no greater variation amongst larval sequences from the western and eastern Ross Sea combined than seen amongst *P. antarctica* sequences from the NCBI database.

a)				b)			
16S	<i>n</i>	p-distance	standard error	D-Loop	<i>n</i>	p-distance	standard error
<i>P. antarctica</i> <b>new sequences</b>	8	0.00052	0.00048	<i>P. antarctica</i> <b>new sequences</b>	12	0.00314	0.00140
<i>P. antarctica</i> NCBI database	7	0.00059	0.00056	<i>P. antarctica</i> NCBI database	16	0.00386	0.00114
<i>A. mitopteryx</i> NCBI database	2	0.00207	0.00197	<i>A. mitopteryx</i> NCBI database	1	-	-
<i>D. eleginoides</i> NCBI database	4	0.00622	0.00243	<i>D. eleginoides</i> NCBI database	4	0.00616	0.00300
<i>D. mawsoni</i> NCBI database	3	0.00138	0.00139	<i>D. mawsoni</i> NCBI database	2	0.00284	0.00265

**Table S3. Pairwise genetic distance between groups.** Reported are the pairwise genetic distances between groups of 16S (a) and D-Loop (b) sequences from newly obtained *P. antarctica* and existing *P. antarctica* and outgroup sequences from the NCBI database (see table S1 for full sequence details). p-distance (below the diagonal) and standard error (above the diagonal) from 1000 bootstrap replications are shown. Sequences for the western and eastern Ross Sea larvae were included in the same group for between group distance tests, based on evidence of homogeneity revealed by within group distance estimation tests. Between group distance tests clearly showed that the Ross Sea larval sequences are extremely similar to silverfish sequences from the NCBI database and different from those of the various outgroups.

a)						
16S	<i>n</i>	<i>P. antarctica</i> <b>new sequences</b>	<i>P. antarctica</i> NCBI database	<i>A. mitopteryx</i> NCBI database	<i>D. eleginoides</i> NCBI database	<i>D. mawsoni</i> NCBI database
<i>P. antarctica</i> <b>new sequences</b>	8	-	0.000	0.010	0.011	0.010
<i>P. antarctica</i> NCBI database	7	0.001	-	0.010	0.011	0.010
<i>A. mitopteryx</i> NCBI database	2	0.048	0.049	-	0.008	0.009
<i>D. eleginoides</i> NCBI database	4	0.068	0.068	0.038	-	0.008
<i>D. mawsoni</i> NCBI database	3	0.061	0.061	0.041	0.038	-

b)						
D-Loop	<i>n</i>	<i>P. antarctica</i> <b>new sequences</b>	<i>P. antarctica</i> NCBI database	<i>A. mitopteryx</i> NCBI database	<i>D. eleginoides</i> NCBI database	<i>D. mawsoni</i> NCBI database
<i>P. antarctica</i> <b>new sequences</b>	12	-	0.001	0.018	0.018	0.018
<i>P. antarctica</i> NCBI database	16	0.004	-	0.018	0.018	0.018
<i>A. mitopteryx</i> NCBI database	1	0.144	0.143	-	0.018	0.017
<i>D. eleginoides</i> NCBI database	4	0.156	0.155	0.144	-	0.014
<i>D. mawsoni</i> NCBI database	2	0.139	0.139	0.135	0.084	-

**References**

- [1] Bargelloni, L., Marcato, S., Zane, L. and Patarnello, T. (2000) Mitochondrial phylogeny of notothenioids: A molecular approach to antarctic fish evolution and biogeography. *Systematic Biology*, **49**, 114-129.
- [2] Gallego, R., Lavery, S. and Sewell, M.A. (2013) The meroplankton community of the oceanic Ross Sea during late summer. *Antarctic Science*, **26**, 345-360.
- [3] Near, T.J., Pesavento, J.J. and Cheng, C.H. (2004) Phylogenetic investigations of Antarctic notothenioid fishes (Perciformes: Notothenioidei) using complete gene sequences of the mitochondrial encoded 16S rRNA. *Mol Phylogenet Evol*, **32**, 881-891.
- [4] Palumbi, S.R., Martin, A., Romano, S., McMillan, W.O., Stice, L. and Grabowski, G. (2002) *The Simple Fools Guide to PCR version 2.0* (University of Hawaii Press: Honolulu).
- [5] Patarnello, T., Marcato, S., Zane, L., Varotto, V. and Bargelloni, L. (2003) Phylogeography of the *Chionodraco* genus (Perciformes, Channichthyidae) in the Southern Ocean. *Mol. Phylogenet. Evol.* **28**:420-429.
- [6] Sanchez, S., Dettai, A., Bonillo, C., Ozouf-Costaz, C., Detrich, H.W. and Lecointre, G. (2007) Molecular and morphological phylogenies of the Antarctic teleostean family Nototheniidae, with emphasis on the Trematominae. *Polar Biology*, **30**, 155-166.
- [7] Tamura, K., Stecher, G., Peterson, D., Filipski, A. and Kumar, S. (2013) MEGA6: Molecular Evolutionary Genetics Analysis version 6.0. *Molecular biology and evolution*, **30**, 2725-2729.
- [8] Zane, L., Marcato, S., Bargelloni, L., Bortolotto, E., Papetti, C., Simonato, M., Varotto, V. and Patarnello, T. (2006) Demographic history and population structure of the Antarctic silverfish *Pleuragramma antarcticum*. *Molecular ecology*, **15**, 4499-4511.



# Chapter 3

## Circumpolar population genetic structure and mechanisms of connectivity in Antarctic silverfish

Published as:

**Caccavo JA**, Papetti C, Wetjen M, Knust R, Ashford JR, Zane L (2018) Along-shelf connectivity and circumpolar gene flow in Antarctic silverfish (*Pleuragramma antarctica*). Scientific Reports: *Accepted*.

1 Along-shelf connectivity and circumpolar gene flow in Antarctic silverfish (*Pleuragramma*  
2 *antarctica*)  
3

4 Jilda Alicia Caccavo<sup>1\*</sup>, Chiara Papetti<sup>1,2</sup>, Maj Wetjen<sup>3</sup>, Rainer Knust<sup>4</sup>, Julian R. Ashford<sup>5</sup>,  
5 Lorenzo Zane<sup>1,2</sup>  
6

7 <sup>1</sup> Department of Biology, University of Padua, Via G. Colombo 3, Padua 35121, Italy.

8 <sup>2</sup> Consorzio Nazionale Interuniversitario per le Scienze del Mare (CoNISMa), Piazzale Flaminio 9, Rome  
9 00196, Italy.

10 <sup>3</sup> Institute for Environmental Sciences, University of Koblenz-Landau, Fortstraße 7, Landau 76829, Germany.

11 <sup>4</sup> Helmholtz Center for Polar and Marine Research, Alfred Wegener Institute, Am Alten Hafen 26, Bremerhaven  
12 27568, Germany.

13 <sup>5</sup> Department of Ocean, Earth and Atmospheric Sciences, Center for Quantitative Fisheries Ecology, Old  
14 Dominion University, 800 West 46<sup>th</sup> Street, Norfolk, VA 23508, United States.

15  
16 **Corresponding author**

17 \* Jilda Alicia Caccavo, [ergo@jildacaccavo.com](mailto:ergo@jildacaccavo.com), ORCID: 0000-0002-8172-7855  
18

19 **ABSTRACT**

20 The Antarctic silverfish (*Pleuragramma antarctica*) is a critically important forage  
21 species with a circumpolar distribution and is unique among other notothenioid species for its  
22 wholly pelagic life cycle. Previous studies have provided mixed evidence of population  
23 structure over regional and circumpolar scales. The aim of the present study was to test the  
24 recent population hypothesis for Antarctic silverfish, which emphasizes the interplay between  
25 life history and hydrography in promoting connectivity. A total of 1067 individuals were  
26 collected over 25 years from different locations on a circumpolar scale. Samples were  
27 genotyped at fifteen microsatellites to assess population differentiation and genetic  
28 structuring using clustering methods, *F*-statistics, and hierarchical analysis of variance. A  
29 lack of differentiation was found between most locations, with significantly reduced gene  
30 flow observed at the South Orkney Islands and the western Antarctic Peninsula. This pattern  
31 of gene flow emphasized the relevance of the Antarctic Slope Front and Current System as a  
32 mechanism for circumpolar connectivity. Chaotic genetic patchiness characterized population  
33 structure over time, with varying patterns of differentiation observed between years,  
34 accompanied by heterogeneous standard length distributions. The present study supports a  
35 more nuanced version of the genetic panmixia hypothesis that reflects physical-biological  
36 interactions over the life history.  
37

38 **KEYWORDS**



39 Antarctic Slope Front and Current System, genetic patchiness, large-scale circulation, life  
40 history connectivity, notothenioids, physical-biological interactions.

41

## 42 INTRODUCTION

43

### 44 Silverfish life history and connectivity

45 The Antarctic silverfish (*Pleuragramma antarctica*) is a critically important forage  
46 species in the Southern Ocean that connects higher and lower trophic levels in the continental  
47 shelf ecosystem<sup>1,2</sup>. Having a circumpolar distribution, silverfish dominate the high-Antarctic  
48 neritic assemblage in terms of both biomass and abundance<sup>3</sup>. Atypical for a notothenioid,  
49 silverfish have a wholly pelagic life cycle, including a cryopelagic egg and larval phase<sup>4</sup>.  
50 Silverfish have adopted a relatively inactive, energy-conserving life strategy similar to related  
51 benthic species, in which their neutral buoyancy allows them to hover in the water column  
52 without active swimming<sup>3,5</sup>. Remaining in the water column throughout their life history  
53 exposes silverfish to current and front systems over the slope and shelf that have been  
54 hypothesized by Ashford *et al.*<sup>6</sup> to play an integral role in shaping their circumpolar  
55 distribution<sup>6</sup>.

56 The silverfish life history hypothesis predicts along-shelf connectivity facilitated  
57 principally by three major features of the large-scale circulation. The Antarctic Coastal  
58 Current (AACC) is typical of coastal buoyant plumes<sup>7</sup> and transports water westward  
59 between glacial trough systems along the inner shelf. Similarly, the Antarctic Slope Front and  
60 Current System (AFS) transports water westward. It is located over the continental slope and  
61 thought to be continuous from the Amundsen Sea along the Ross Sea continental shelf and  
62 East Antarctica, forming the southern limb of the Weddell Gyre and reaching waters north of  
63 the Antarctic Peninsula<sup>8,9</sup> (Fig. 1, overview). In contrast to the AACC and AFS, the Antarctic  
64 Circumpolar Current (ACC) transports water eastward. It approaches the continental shelf in  
65 the Amundsen Sea where it bifurcates, and its southern boundary and the Southern ACC  
66 Front (SACCF) are located over the slope off the western Antarctic Peninsula, before moving  
67 seaward west of the South Shetland Islands<sup>10,11</sup> (Fig. 1, overview).

68 Entrainment of silverfish in transport pathways is facilitated by a life history  
69 characterized by vertical migrations associated with different life stages<sup>12</sup>. Eggs and larvae  
70 are found from 0 – 100 m among the platelet ice layer beneath coastal fast ice<sup>13</sup>. Descent to  
71 deeper layers begins at the post-larval phase, and post-larvae and juveniles up to 2+ years are  
72 found at depths up to 400 m<sup>3</sup>. Adult silverfish are typically found at depths from 400 – 700  
73 m<sup>3</sup>, exhibiting a diel migration in which a greater abundance of fish are present in the  
74 shallower portion of their distribution by night, and in deeper waters by day<sup>14</sup>. These changes  
75 in habitat occupancy correlate with ontogenetic shifts in diet composition, such that silverfish  
76 may occupy several trophic levels throughout their lifetime<sup>15</sup>. While feeding almost  
77 exclusively on zooplankton, silverfish have been shown to exhibit dietary plasticity,

78 including cannibalism<sup>16-18</sup>. Thus, early-life dependence on coastal sea-ice zones and later  
79 movement into deeper waters in pursuit of prey and avoidance of predators expose fish to  
80 hydrographic features along the continental shelf. This results in a complex life history which  
81 generates the conditions for a dynamic population structure and underlying patterns of  
82 connectivity<sup>6</sup>.

83 The silverfish life history hypothesis incorporates these physical-biological  
84 interactions, predicting that cross-shelf circulation mediates retention within populations and  
85 exposure to along-shelf transport pathways<sup>6,19,20</sup>. Schools of adult silverfish have been  
86 observed moving inshore along the Antarctic Peninsula<sup>21</sup>. Assemblages of silverfish eggs and  
87 larvae have been found in the summer polynya of the eastern Weddell Sea<sup>22</sup>, in waters along  
88 the Antarctic Peninsula<sup>23</sup>, under sea ice in the western Ross Sea<sup>4,12,24</sup>, and in the Dumont  
89 d'Urville Sea<sup>25</sup> (see Fig. 1 for place names). These observations suggest a life cycle in which  
90 adults return to coastal areas each winter to spawn. This migration is facilitated by the  
91 circulation within glacial trough systems across the continental shelf. While trough outflows  
92 aid in the dispersal of developing fish away from hatching sites, inflows function to retain  
93 adults by transporting them back to spawning areas. The discovery of newly hatched larvae in  
94 trough systems along the Weddell Sea, Ross Sea, and Antarctic Peninsula<sup>6,13,22,26</sup> implies this  
95 cycle of dispersion and retention occurs in multiple areas around the Antarctic. However,  
96 such a cycle would be vulnerable to advective losses along the shelf in the AACC, and along  
97 the slope in the AFS or SACCF, resulting in transport to locations downstream<sup>6</sup>.

98

### 99 **Genetic structuring and gene flow around the Antarctic**

100 Estimates of genetic differentiation are a principal tool for defining population  
101 structure, by assessing gene flow between populations, as well as the extent to which  
102 inbreeding and genetic drift contribute to population differentiation<sup>27</sup>. The first hypotheses  
103 concerning population structure in silverfish arose from research carried out in the 1980s in  
104 the eastern Weddell Sea and Antarctic Peninsula<sup>22,23</sup>. Recent advances in our understanding  
105 of hydrography and physical-biological interactions provide a contemporary life history  
106 framework in which the population genetic structure of silverfish needs to be considered (see  
107 Ashford *et al.*<sup>6</sup>).

108 Highly connected populations resulting in genetic panmixia have previously been the  
109 null hypothesis to describe genetic structuring in notothenioids. This hypothesis is based on  
110 the expected influence of circumpolar currents on the transport of pelagic larvae, which  
111 would sustain high levels of gene flow<sup>28</sup>. This was supported by genetic homogeneity found  
112 among multiple species of the families Nototheniidae and Channichthyidae inhabiting the  
113 Scotia Arc<sup>29,30</sup>. At the same time however, this panmictic hypothesis was challenged by  
114 evidence of population structuring based on genetic heterogeneity in multiple other species,  
115 including *Dissostichus mawsoni*<sup>31,32</sup>, *Chionodraco hamatus*<sup>33</sup>, *Chaenocephalus aceratus*<sup>34,35</sup>,  
116 and *Champscephalus gunnari*<sup>35</sup>.

117 Evidence for gene flow and genetic panmixia has been similarly variable for  
118 silverfish. Using mitochondrial DNA markers, Zane *et al.*<sup>36</sup> found little indication of  
119 population structuring in silverfish on a circumpolar scale, although differences were found  
120 between sampling years in the eastern Weddell Sea, and between one sample in the eastern  
121 Weddell Sea and one of two taken in the western Ross Sea<sup>36</sup>. A more recent study on  
122 silverfish connectivity around the Antarctic Peninsula employing microsatellite markers  
123 revealed that fish taken from Marguerite Bay and Charcot Island along the western Antarctic  
124 Peninsula (WAP) were significantly different from those along the northern Antarctic  
125 Peninsula (NAP) at Joinville Island and on the eastern side of the peninsula at Larsen Bay  
126 (LB)<sup>19</sup> (see Fig. 1, WAP, NAP, and LB for place names). Samples were collected over  
127 multiple years, and as in Zane *et al.*<sup>36</sup>, evidence for restrictions to gene flow varied between  
128 years<sup>19</sup>.

129 Variation in recruitment and dispersal, which could explain the observed changes in  
130 silverfish distribution, is predicted by the hypothesis of chaotic genetic patchiness<sup>37</sup>,  
131 developed to explain the fluctuations in gene flow between sampling years<sup>19</sup>. Current theory  
132 emphasizes the role of physical-biological interactions in structuring populations and the  
133 potential for extensive along-shelf connectivity. Yet to date, there has been no comprehensive  
134 investigation of silverfish gene flow and population structure at different spatial scales and  
135 over time<sup>6</sup>, nor re-examination of earlier genetic evidence in the context of recent theoretical  
136 advances in understanding.

137 The present study builds upon the Matschiner *et al.*<sup>28</sup> hypothesis of genetic panmixia  
138 in the light of the physical-biological framework provided by Ashford *et al.*<sup>6</sup>. It aims to test  
139 for population structuring and along-shelf connectivity mediated by large-scale circulation.  
140 Employing microsatellite markers, we assessed gene flow between silverfish sampled over 25  
141 years from six different geographic regions around the Antarctic Continent. The following  
142 regions were investigated based on observed and predicted silverfish larval assemblages: the  
143 western Ross Sea<sup>4,12,24</sup>, eastern Weddell Sea<sup>22</sup>, Larsen Bay<sup>26</sup>, northern Antarctic Peninsula<sup>23</sup>,  
144 South Orkney Islands<sup>38</sup>, and western Antarctic Peninsula<sup>39</sup>. Inclusion of samples from  
145 previous studies allowed for a greater number of spatial and temporal comparisons. The  
146 expansion of the Agostini *et al.*<sup>19</sup> analysis of Antarctic Peninsular connectivity enables  
147 comparisons to be made on a circumpolar scale. Finally, the use of microsatellite markers  
148 increases the analytical power of the Zane *et al.*<sup>36</sup> mitochondrial DNA-based study<sup>40</sup>. With  
149 the present approach, we were able to compare shelf areas located along the AFS from the  
150 Ross Sea to the tip of the Antarctic Peninsula, as well as areas located along the SACCF from  
151 Charcot Island to the South Shetland Islands. In addition, we tested for potential gene flow  
152 downstream to the South Orkney Islands along the southern ACC and Weddell Gyre.

153

154

155 **RESULTS**

156

157 **Genotyping**

158 Genotypes from 16 microsatellite loci were successfully obtained for all 505 newly  
159 sequenced individuals, further supporting that microsatellites developed for *C. hamatus*<sup>19</sup> can  
160 be used in *P. antarctica*. While amplifying successfully in all individuals, one locus  
161 (Ch11230) was problematic in terms of accurate genotyping, due to stuttering and  
162 interference from the other fluorophores used to detect fragments in sequencing. Subsequent  
163 analyses were carried out on datasets both including and excluding this locus, and no major  
164 differences were obtained in the results. Thus, results are presented based on 15 microsatellite  
165 loci, excluding locus Ch11230, for verisimilitude. High levels of genetic variation were  
166 observed in comparable values of  $N_A$ ,  $A_R$ ,  $H_O$ , and  $H_E$  (Table 2, Table S2), showing no  
167 significant differences (one-way ANOVA,  $P > 0.05$ ) across all sampling locations. While no  
168 significant linkage disequilibrium was observed between loci, significant departures from  
169 Hardy Weinberg Equilibrium (HWE) were found at 22 of 304 tests after SGoF+ correction  
170 for multiple tests (threshold for significance with 304 comparisons 0.008) with no locus  
171 exhibiting Hardy Weinberg Disequilibrium (HWD) in more than 3 sampling locations and no  
172 sampling location containing more than 5 loci in HWD (Table S2). Of the 20 occasions in  
173 which the software Micro-Checker found evidence for null alleles at a locus in a given  
174 sampling location, only 3 of those coincided with an instance of HWD. Thus, it is likely that  
175 the 22 instances of HWD were not representative of an artifactual excess of homozygotes  
176 among sampling locations for the loci tested. Neither ARLEQUIN nor LOSITAN identified  
177 any locus as a putative outlier, with all simulated  $F_{ST}$  values falling within neutral  
178 expectations.

179

180 **Population structure**

181 Hierarchical AMOVA indicated that partitioning the 19 sampling locations into  $k = 6$   
182 groups based on geographic provenance (Ross Sea (RS), Weddell Sea (WS), Larsen Bay  
183 (LB), northern Antarctic Peninsula (NAP), South Orkney Islands (SOI), and western  
184 Antarctic Peninsula (WAP), Table 1) maximized between group heterogeneity (global  $F_{CT} =$   
185  $0.00159$ ;  $P = 0.00218 \pm 0.00050$ ) while minimizing within group heterogeneity (global  $F_{sc} =$   
186  $0.00002$ ;  $P = 0.63050 \pm 0.00429$ ). Genetic differentiation was present (global  $F_{ST} = 0.00161$ ;  
187  $P = 0.00644 \pm 0.00087$ ) but very low, with  $<1\%$  of the variation due to between sampling  
188 location variation. Only 0.16% of variation was attributed to variation among groups. Locus-  
189 by-locus AMOVA confirmed that no particular locus had a significantly outsized impact on  
190 the calculation of global  $F$ -statistics (Table S3).

191 Clustering methods failed to indicate a clear structure among the sampling locations  
192 analyzed. Clustering methods employed by FLOCK and DAPC (without pre-defined groups)  
193 randomly assigned individuals to groups, with no correlation to sampling location or

194 geographic provenance (Fig. 2, 3). DAPC run without *a priori* parameters suggested the  
195 existence of nine clusters (Fig. 3a), with  $k = 9$  selected based on cluster optimization plotted  
196 against Bayesian Information Criteria (Fig. S2a). The same DAPC based on the six  
197 geographic areas of provenance (RS, WS, LB, NAP, SOI, and WAP) run in an attempt to  
198 maximize variation between locality showed no evidence of cluster formation (Fig. 3b).  
199 PCoA on all 19 sampling locations provided limited support for geographic clustering, with  
200 the first principal coordinate accounting for 39.21% of the variance and clearly distinguishing  
201 the SOI and WAP samples from all others (Fig. 4a). PCoA on the six geographic groups (RS,  
202 WS, LB, NAP, SOI, and WAP) emphasized this delineation further, with the first principal  
203 coordinate accounting for 81.16% of the variance separating the SOI and WAP samples from  
204 the rest (Fig. 4b). However, in both cases PCoA failed to distinguish NAP, WS, and LB from  
205 one another, and also from the other geographic areas.

206 In contrast to clustering methods, pairwise  $F_{ST}$  provided support for geographic  
207 population clusters. Within sampling locations, there were no significant differences between  
208 samples collected over multiple years ( $F_{ST}$  ranged from -0.0025 to 0.0024,  $P > 0.05$  for all  
209 comparisons, Table 3), suggestive of genetic stability over time. In addition, within  
210 geographic areas (RS, WS, LB, NAP, SOI, and WAP), there was no significant difference  
211 between sampling locations ( $F_{ST}$  ranged from -0.0051 to 0.0024,  $P > 0.05$  for all  
212 comparisons, Table 3), indicative of single genetic populations within these areas.

213 Pairwise comparisons between years and different sampling locations among the  
214 geographic groupings displayed a less discernible structure. Patterns of significant  
215 differentiation previously found along the Antarctic Peninsula were maintained to some  
216 extent (4 significant comparisons out of 36 in the current study and 9 out of 36 in Agostini *et*  
217 *al.*<sup>19</sup> after SGoF+ correction for multiple tests, threshold for significance with 171  
218 comparisons 0.0332). Such discrepancies are likely due to the use of 15 loci instead of 16 loci  
219 as in Agostini *et al.*<sup>19</sup> (due to the removal of the unreliable locus Ch11230) as well as to  
220 changes in significance thresholds resulting from the increased number of comparisons in the  
221 present study (nineteen sampling locations versus nine). Variation in differentiation between  
222 years in comparisons from the same sampling location, as previously documented in the Ross  
223 Sea<sup>36</sup> and the Antarctic Peninsula<sup>19</sup>, was also obtained in the current study. For every location  
224 for which samples existed from multiple years, patterns of differentiation varied over  
225 sampling years (Table 3). This was especially evident at Marguerite Bay, Joinville Island, the  
226 South Orkney Islands, Larsen Bay, and the Ross Sea.

227 Grouping sampling locations based on geographic area provided evidence of weak  
228 genetic structuring ( $F_{ST}$  ranged from 0.0001 to 0.0153, Table 4). Significant pairwise  $F_{ST}$   
229 values were found between all groups and the western Antarctic Peninsula group (also seen  
230 in Agostini *et al.*<sup>19</sup>), as well as between the South Orkney Islands and all groups except for  
231 the Weddell Sea, where the comparison was not significant after SGoF+ correction for  
232 multiple tests (threshold for significance with 15 comparisons 0.0142, Table 4). In addition,

233 the comparison between Larsen Bay and the Ross Sea was not significant after correction ( $P$   
234 = 0.0312, Table 4).

235

### 236 **Comparison by length modes**

237 Standard length (SL) distributions varied considerably between sampling locations  
238 (Fig. S1). A pronounced bimodal SL distribution from the Joinville Island 2010 (JI10) sample  
239 (SL = 5 cm and SL = 10 cm) had spurred Agostini *et al.*<sup>19</sup> to divide the small and large SL  
240 modes of JI10 into two clusters. Pairwise  $F_{ST}$  analysis revealed that in addition to the two size  
241 modes being significantly different from each other, seven of the eight comparisons were  
242 significant between all groups and JI10 small, and three of the eight comparisons were  
243 significant between all groups and JI10 large after SGoF+ correction for multiple tests<sup>19</sup>  
244 (threshold for significance with 190 comparisons 0.0453). When this analysis was extended  
245 to the sampling locations considered in the current study, this result was largely replicated  
246 (six of the eight comparisons were significant between the original AP groups and JI10 small,  
247 and two of the eight comparisons were significant between the original AP groups and JI10  
248 large after SGoF+ correction for multiple tests, Table S4). Dividing the JI10 sample into  
249 small ( $F_{ST} = 0.0045$ ,  $P = 0.0265$ ) and large ( $F_{ST} = 0.0042$ ,  $P = 0.0312$ ) clusters, comparisons  
250 between these groups and the South Orkney Islands sample were significantly different, in  
251 contrast to the original analysis. Consistent with results seen in the initial and replicated AP  
252 analysis between JI10 small and Larsen Bay 2007, JI10 small significantly differentiated after  
253 SGoF+ correction for multiple tests from Larsen Bay 2011 ( $F_{ST} = 0.0037$ ,  $P = 0.0361$ ), a  
254 comparison that was not significant when analyzing the undivided JI10 group. Similarly, the  
255 comparison between JI10 small and Ross Sea 1997 was significant after SGoF+ correction  
256 for multiple tests ( $F_{ST} = 0.0044$ ,  $P = 0.0061$ ), despite no indication of differentiation with the  
257 undivided JI10 group. Finally, seven additional pairwise comparisons were significant after  
258 SGoF+ correction for multiple tests in the JI10 cluster analysis, despite not involving the  
259 newly introduced JI10 small or large clusters (see Table S4 for details).

260 Spatially recurring length modes among sampling locations collected in the eastern  
261 Weddell Sea in 2014 provided evidence for episodic connectivity (Fig. S1). Thus, a separate  
262 pairwise  $F_{ST}$  analysis was performed including only sampling locations collected in 2014  
263 within the eastern Weddell Sea. No significant differences were seen between any of the  
264 sampling areas, which included west Filchner Trough ( $n = 23$ ), east Filchner Trough ( $n = 27$ ),  
265 Coats Land ( $n = 29$ ), Halley Bay ( $n = 52$ ), and Atka Bay ( $n = 25$ ) ( $F_{ST}$  ranged from -0.0062 to  
266 0.0027,  $P > 0.05$  for all comparisons, Table S5). With such low levels of differentiation  
267 between areas despite the diverse SL distributions, a final pairwise  $F_{ST}$  analysis was  
268 performed on groupings of fish from the eastern Weddell Sea that were based solely on SL  
269 range, independent of sampling location. SL among specimens from the eastern Weddell Sea  
270 ranged from 7.0 – 21.5 cm. First, fish were divided into six SL-based groups (< 10 cm, 10 –  
271 12 cm, 12 – 14 cm, 14 – 16 cm, 16 – 18 cm, > 18 cm), with group  $n$  ranging from 14 – 43

272 individuals. When no significant differences were found between SL-based groups after  
273 SGoF+ correction for multiple tests ( $F_{ST}$  ranged from -0.0081 to 0.01019), an exploratory  
274 analysis of various pools of the six original SL-based groups was conducted. The smallest  
275 SL-based pool was defined as  $SL \leq 12$  cm and then subsequently as  $SL \leq 14$  cm. The largest  
276 SL-based pool was defined as  $SL < 16$  cm and various combinations of the intermediate  
277 groups were created. Testing these various pools of SL range allowed for the control of the  
278 influence of group size. None of the pairwise comparisons based on the various pools of the  
279 SL-based groups were significant after SGoF+ correction for multiple tests ( $F_{ST}$  ranged from  
280 -0.0081 to 0.0103).

281

## 282 **DISCUSSION**

283

284 The present study tests the hypothesis of genetic panmixia<sup>28</sup> in the light of the  
285 physical-biological framework provided by Ashford *et al.*<sup>6</sup> for Antarctic silverfish. Evidence  
286 of high gene flow between areas connected by the Antarctic Slope Front and Current System  
287 (AFS) on a circumpolar scale was accompanied by indications of reduced gene flow in areas  
288 not reached by the AFS. We corroborated the findings from Agostini *et al.*<sup>19</sup> that Charcot  
289 Island and Marguerite Bay represent a homogeneous population with significantly reduced  
290 gene flow from populations around the AP and beyond, while also discovering significant  
291 reductions in gene flow to the population at the South Orkney Islands. These results were  
292 broadly consistent with the Matschiner *et al.*<sup>28</sup> prediction of gene flow facilitated by the  
293 large-scale circulation. Nevertheless, genetic structuring corresponded to discontinuities  
294 between along-shelf major current systems. This structuring argues for a more nuanced  
295 version of the genetic panmixia hypothesis that reflects physical-biological interactions over  
296 silverfish life history.

297

### 298 **Along-shelf gene flow and connectivity**

299 Similarity between samples from the Ross Sea, eastern Weddell Sea, Larsen Bay and  
300 Joinville Island indicated gene flow along the shelf corresponding to the AFS. Pairwise  $F_{ST}$   
301 analysis provided evidence for six possible silverfish populations among the geographic areas  
302 analyzed. The Ross Sea did not differ from Larsen Bay. Joinville Island and the South  
303 Shetland Islands formed a cluster, which did not differ from any others, suggesting gene flow  
304 along the AFS into the Bransfield Strait. Notably, comparisons made by Agostini *et al.*<sup>19</sup>  
305 showed evidence of differentiation between Larsen Bay and Joinville Island, whereas in the  
306 present analysis, not a single comparison among sampling locations from Joinville (JI07,  
307 JI10, and JI12) and Larsen Bay (LB07 and LB11) revealed significant differentiation. This is  
308 consistent with the predictions made in La Mesa *et al.*<sup>26</sup> of connectivity between Larsen Bay  
309 and the Bransfield Strait. Thus, the inclusion of the additional samples from Larsen Bay

310 (LB11) clarified connectivity along the AFS between the western Weddell Sea and  
311 Bransfield Strait.

312 In contrast, areas not connected by the AFS showed evidence of reduced gene flow.  
313 Along the Antarctic Peninsula, where westward flow inshore along the AACC contrasts with  
314 eastward flow along the slope in the SACCF, Charcot Island (CI) and Marguerite Bay (MB)  
315 represented one cluster, which differentiated genetically from all other five areas. This  
316 possible discontinuity in silverfish distribution between the northern and southern regions of  
317 the western Antarctic Peninsula was first discussed in Agostini *et al.*<sup>19</sup> based in part on the  
318 decrease of silverfish in Adélie penguin diets at Palmer Station<sup>41</sup>. The loss of intermediate  
319 populations that may have previously facilitated connectivity between the northern and  
320 southern extents of the western Antarctic Peninsula was further supported by the total  
321 absence of silverfish in sampling surveys at Anvers and Renaud Islands and the Croker  
322 Passage midway up the western Antarctic Peninsula in 2010 (see Fig. 1, WAP for place  
323 names) despite having previously been the dominant fish species in these areas since the  
324 1980s<sup>14</sup>. The South Orkney Islands differentiated from all other areas except for the eastern  
325 Weddell Sea. Differentiation between years within certain locations echoed evidence for  
326 chaotic genetic patchiness seen in the Ross Sea by Zane *et al.*<sup>36</sup> and in the Antarctic Peninsula  
327 by Agostini *et al.*<sup>19</sup>. This was further supported by the variability in SL distributions between  
328 years in particular sampling locations.

329 The clearest example of interannual variability was seen in the western Antarctic  
330 Peninsula (WAP). Specimens from MB01 and MB02 exhibited a bimodal distribution of SL  
331 representative of both young and old fish, contrasting with specimens from MB10 and CI10  
332 which exhibited a much tighter unimodal distribution around SL = 15 cm, and MB11 which  
333 had a similarly tight unimodal distribution around SL = 10 cm (Fig. S1). This disparity  
334 between cohorts was reflected in patterns of genetic differentiation within the WAP area  
335 between years, with MB01 and MB02 differentiating from two of the nineteen other  
336 sampling locations, while MB11 differed from six of the nineteen other sampling locations  
337 (Table 3). However, position with respect to local hydrographic features must also be  
338 considered. Despite being collected only a year before the strongly differentiated MB11  
339 sample, MB10 shares the weak differentiation pattern of nearby MB01 and MB02, which  
340 were all collected in the Labeuf Fjord closer to the coast (Fig. 1, WAP, Table 3). This greater  
341 connectivity with populations outside of the WAP is consistent with gene flow down the  
342 Antarctic Peninsula promoted by the AACC<sup>19</sup>. Furthermore, the position of MB11 along the  
343 trough inflow in Marguerite Trough (Fig. 1, WAP) raises the possibility that the sample  
344 consisted of fish resulting from connectivity along the slope, where entrainment in the  
345 SAACF potentially transports fish from the Bellingshausen and Amundsen Seas<sup>23</sup>. The influx  
346 of migrants from populations further upstream may contribute to the stronger pattern of  
347 differentiation found between MB11 and sampling locations beyond the Antarctic Peninsula.



348 Differences between the previously published Antarctic Peninsula study<sup>19</sup> and the  
349 current results are likely attributable to changes in significance thresholds resulting from the  
350 increased number of comparisons in the present study, as well as the use of 15 instead of 16  
351 loci due to the removal of one problematic locus. In the original Antarctic Peninsula analysis,  
352 Agostini *et al.*<sup>19</sup> found 9 out of 36 significant comparisons around the Antarctic Peninsula,  
353 while in the current analysis, only four out of the thirty-six Antarctic Peninsula comparisons  
354 were significant. This was mainly due to weaker differentiation between Antarctic Peninsula  
355 populations and JI10 and JI12. Discrepancies in patterns of differentiation between the  
356 current study and the original investigation of population connectivity in Zane *et al.*<sup>36</sup> can be  
357 attributed to their use of mtDNA as opposed to microsatellite markers to resolve patterns of  
358 genetic heterogeneity<sup>40</sup>, in addition to differences in sample size (Table 3). Given the small  
359 differences between populations, stochasticity associated with reproduction, differential  
360 survival, and recruitment can lead to changes in resolution in subsequent investigations<sup>6</sup>. This  
361 highlights the importance of continued, targeted sampling, and the integration of  
362 multidisciplinary techniques (modelling<sup>42</sup>, otolith chemistry<sup>43</sup>, genomics<sup>44</sup>) in order to  
363 monitor changes in population structure over time.

364

### 365 **Population structure and life history connectivity**

366 The silverfish physical-biological population hypothesis<sup>6</sup> provides a mechanistic  
367 explanation consistent with the patterns of gene flow and genetic structuring we observed.  
368 When fish in outflows from local trough systems, for instance in the Ross Sea<sup>20</sup> and eastern  
369 Weddell Sea<sup>22</sup>, reach the shelf break, entrainment in the AFS and westward transport has the  
370 potential to introduce fish into trough systems downstream. Samples from Terra Nova Bay in  
371 the Ross Sea collected in 1996 and 1997 were genetically very similar to those collected in  
372 the Weddell Sea and Antarctic Peninsula, only differentiating from samples taken along the  
373 western Antarctic Peninsula and the South Orkney Islands. This high level of connectivity  
374 between areas on opposite sides of the continent may be attributed to two main factors. The  
375 first is related to the extent and importance of the Terra Nova Bay silverfish nursery, where  
376 silverfish comprise 98% of the ichthyoplankton<sup>4,13</sup>. The second is related to potential  
377 silverfish populations along East Antarctica. Substantial distributions of silverfish have been  
378 found across the continental shelf along East Antarctica<sup>3</sup>, as well as in association with the  
379 Ninnis and Adélie Troughs off Wilkes Land<sup>45</sup> (Fig. S3, East Antarctica). Other trough  
380 systems along East Antarctica in Lützw-Holm Bay, Iceberg Alley, Nielsen Basin, and Prydz  
381 Bay may also provide suitable habitats for coherent silverfish populations<sup>6</sup> (Fig. S3, East  
382 Antarctica). The existence of a network of local populations of silverfish associated with  
383 trough systems along East Antarctica provides a mechanism for the exchange of individuals  
384 via the westward-flowing AFS. Such a mechanism would explain the high levels of gene  
385 flow observed between sampling locations as geographically separated as Terra Nova Bay  
386 and Joinville Island.

387           Moreover, our results lend further support for connectivity beyond Joinville Island  
388 into the region around the Bransfield Strait. Fish at Joinville could theoretically be  
389 transported there by either: 1) the AACC, which could transport fish from Larsen Bay<sup>26,46</sup>; or  
390 2) the AFS, which could transport enough individuals from the eastern Weddell Sea and  
391 beyond to render the Joinville population genetically indistinguishable from upstream  
392 populations<sup>6,9,47</sup>. Although the path of the AACC south of Joinville Island is undefined,  
393 buoyancy forcing is likely to generate connectivity that is shallow and close to the coast<sup>7</sup>.  
394 This could result in larval transport north from Larsen Bay which would explain the  
395 differentiation between size modes in the Antarctic Sound (Fig 1., NAP).

396           The results of the current study raise the possibility of a coherent silverfish population  
397 at the South Orkney Islands. Surveys carried out between 1967 – 1981 revealed the presence  
398 of silverfish larvae at the South Orkney Islands<sup>38</sup>, consistent with a local breeding population.  
399 Furthermore, a recent bathymetric analysis of the South Orkney Islands microcontinent found  
400 seven trough systems on the northern and southern sides of the islands<sup>48</sup>. Features supportive  
401 of a locally breeding silverfish population were found in Signy Trough between Coronation  
402 and Signy Island<sup>48</sup>, including active glaciers at the trough head, thought to be necessary for  
403 early-life stages<sup>6</sup> (Fig. 1, SOI). Evidence from otolith chemistry analyses has revealed that  
404 fish from the northern Antarctic Peninsula significantly differed from those at the South  
405 Orkney Islands, indicating that fish in these areas were sourced from different breeding  
406 grounds<sup>49</sup>. This is supported by our findings of genetic differentiation between the northern  
407 Antarctic Peninsula and South Orkney Islands populations.

408           However, the lack of differentiation between specimens from the South Orkney  
409 Islands and specimens from the eastern Weddell Sea means connectivity between these two  
410 regions cannot be discounted based on these data. The existence of migrants or non-breeding  
411 vagrants at the South Orkney Islands would be predicated by a clear and consistent transport  
412 system from the eastern Weddell Sea to the South Orkney Islands microcontinent. Although  
413 fish carried to the shelf slope along trough outflows in the eastern Weddell Sea can come into  
414 contact with the AFS<sup>6</sup>, subsequent transport to the South Orkney Islands microcontinent  
415 remains unclear (Fig., SOI). In addition to the distance along the AFS, fish are exposed to  
416 inflows at the mouths of the Hughes, Ronne (Fig. 1, WS), Jason, and Robertson (Fig. 1, LB)  
417 Troughs that can draw them away from the slope towards the inner shelf. Continued  
418 entrainment in the AFS north of Larsen Bay carries fish around Joinville Island, where the  
419 AACC approaches the AFS (Fig. 1, SOI). Subsequently, the currents separate again, the  
420 AACC forming the southern branch of the Bransfield Gyre<sup>10</sup> (Fig. 1, NAP) and the AFS  
421 moving north along the South Scotia Ridge<sup>9,46,50</sup> (Fig. 1, SOI). However, upon entering the  
422 Hesperides Trough, increased influence by Weddell-Scotia Confluence waters combined with  
423 local bathymetric complexity impede continued identification of the AFS<sup>50</sup>. Thus, the AFS  
424 does not provide a direct pathway to the South Orkney Islands. Alternatively, the Weddell  
425 Front, which forms east of the Joinville Ridge and rounds the Powell Basin to reach the South

426 Orkney Islands microcontinent, may represent a path from the Weddell Sea to the South  
427 Orkney Islands. Future studies will require an interdisciplinary approach to assess the impact  
428 of episodic connectivity on genetic similarity between the South Orkney Islands and the  
429 eastern Weddell Sea. The hydrography between these areas needs to be elaborated in order to  
430 determine the eventual fate of the AFS. Otolith chemistry analyses<sup>51</sup> and dispersal  
431 modelling<sup>52</sup> of fish collected at the South Orkney Islands and the eastern Weddell Sea will be  
432 able to clarify how much the genetic similarity between these regions is due to episodic  
433 connectivity into the local population.

434 Hydrography may also explain the chaotic genetic patchiness observed in the  
435 differentiation patterns between the two Larsen Bay samples and the eastern Weddell Sea and  
436 South Orkney Islands (Table 3). It is important to note that the LB07 and LB11 samples were  
437 collected from slightly different parts of Larsen Bay (Fig. 1, LB). LB07 was collected in the  
438 Larsen B embayment off Scar Inlet, near one of the heads of the Larsen Inlet Trough. The  
439 LB11 samples were collected in the Larsen A embayment, just north of the Seal Nunataks Ice  
440 Shelf, at the head of the Robertson Trough. Since the disintegration of the Larsen A and B  
441 shelves, runoff into the Larsen embayments has been derived from smaller glaciers along the  
442 peninsula that contribute to disparate patterns of freshwater influx between the Larsen A and  
443 B areas<sup>53,54</sup>. Differences in seasonal melting patterns between the two areas are likely to  
444 directly impact coastal buoyancy and connectivity between trough systems in Larsen Bay.  
445 Considering the evidence of gene flow between the eastern Weddell Sea and both the Larsen  
446 Bay and South Orkney Islands, the lack of differentiation between LB11 and SOI11 may be  
447 due to changes in the influx of eastern Weddell Sea migrants into these areas. This is in  
448 contrast to the hypothesis that the observed gene flow results from the direct exchange of  
449 individuals between Larsen Bay and the South Orkney Islands. Changes in recruitment and  
450 may occur in tandem with the influx of eastern Weddell Sea migrants into the respective  
451 Larsen A and Larsen B embayments. This would result in the variations of gene flow  
452 observed between the eastern Weddell Sea, South Orkney Islands, and the LB07 and LB11  
453 sampling locations.

454 The pattern of homogeneity observed among fish across all sampling areas within the  
455 eastern Weddell Sea fails to explain the variation in SL distributions. This suggests  
456 population mixing between local and migrant fish, seen from Atka Bay in the northeast, to  
457 Halley Bay and Coats Land, and finally to the eastern and western sides of the Filchner  
458 Trough in the southeast. Aspects of local hydrography help to explain these observations. In  
459 the southeast Weddell Sea, the AACC and the AFS are functionally equivalent given the  
460 narrowness of the continental shelf in this area<sup>9</sup>. Seasonal and interannual variability in the  
461 AACC in the southeast Weddell Sea<sup>56</sup> may promote and restrict connectivity along the shelf  
462 from Atka Bay to Filchner Trough. Fish that become entrained in the AFS upstream are  
463 introduced to the Weddell Sea east of Atka Bay, as it becomes the southern limb of the  
464 Weddell Gyre<sup>8,57</sup>. Having formed in the Amundsen Sea, the AFS has the potential to connect

465 local trough systems in the Ross Sea and East Antarctica<sup>6,8</sup>. While it remains a more  
466 consistent feature than the AACC, the position and strength of the AFS is nevertheless  
467 sensitive to wind stress forcing on seasonal and interannual time scales in the northwest  
468 Weddell Sea<sup>50,58,59</sup>. Such variations in the intensity of the AFS could explain fluctuations in  
469 the influx of migrants into eastern Weddell Sea populations and provide a general mechanism  
470 for the chaotic genetic patchiness observed among silverfish populations.

471 Subsequent studies analyzing otolith nucleus chemistry in silverfish along the eastern  
472 Weddell Sea will allow us to distinguish between areas more heavily composed of locally  
473 born fish and migrants. Furthermore, enhanced oceanographic data would improve dispersal  
474 modelling, allowing for a more targeted approach in defining connectivity hypotheses.  
475 Contiguous sampling from areas that could contribute migrating fish to the SACCF and the  
476 AFS are needed in order to better define in which ways the various current systems influence  
477 eastern Weddell Sea population mixing. Antarctic silverfish are a pillar of the Southern  
478 Ocean ecosystem<sup>2</sup>. Understanding their population structure and connectivity in the context  
479 of their life history and the impact of hydrography is critical to assessments of Southern  
480 Ocean ecosystem health.

481

## 482 **MATERIALS AND METHODS**

483

### 484 **Sample collection and DNA extraction**

485 A total of 1067 individuals from 19 sampling locations collected by multiple  
486 institutions between 1989 and 2014 were included in the analysis (Fig. 1, Table 1). Of these,  
487 249 individuals collected between 1989 and 1997 from the Ross Sea (RS96, RS97), Halley  
488 Bay (HB89, HB91), and South Shetland Islands (SSI96) were included from a previous study  
489 on population structure using mitochondrial DNA<sup>36</sup>. A further 562 individuals collected  
490 between 2001 and 2012 from Larsen Bay (LB07), Charcot Island (CI10), Marguerite Bay  
491 (MB01, MB02, MB10, MB11), and Joinville Island (JI07, JI10, JI12) were included from a  
492 previous connectivity study focused on the Antarctic Peninsula<sup>19</sup>. The remaining 256  
493 individuals collected in 2011 and 2014 from the South Orkney Islands (SOI11), Larsen Bay  
494 (LB11), Filchner Trough (FT14), Atka Bay (AB14), and Halley Bay (HB14) have not  
495 previously been examined. Table 1 outlines sampling details, including research vessel  
496 information and collection gear.

497 Standard length (SL) data were available from all individuals except from those  
498 collected from RS96, RS97, and HB91. SL data from HB89 and SSI96 represent the length  
499 distribution of fish collected at the sampling stations, but lack identification numbers to  
500 correspond them to the tissue samples collected for genetic analysis. The distribution of SL  
501 was used to identify modes for consideration in the eventual genetics analysis.

502 Muscle tissue or fin clips were preserved in 95-100% ethanol at the time of sampling.  
503 Genomic DNA was extracted from specimens using a standard salting-out procedure<sup>60</sup>.

504 Genomic DNA was extracted from all previously unexamined samples, as well as from tissue  
505 samples remaining from individuals on which the mitochondrial DNA analysis was  
506 performed in Zane *et al.*<sup>36</sup>. Concentration and quality of the extracted DNA (260/280 nm and  
507 260/230 nm) was checked using a NanoDrop UV–Vis spectrophotometer (Thermo Scientific)  
508 prior to PCR amplification. All extracted DNA was of high enough quality to use in  
509 subsequent PCR reactions.

510

### 511 **DNA amplification and microsatellite genotyping**

512 Individuals were genotyped using 16 published EST-linked microsatellites developed  
513 in *Chionodroco hamatus*<sup>61,62</sup>, that had been previously shown to cross-amplify successfully in  
514 *P. antarctica*<sup>19</sup>. The 16 loci were amplified in two multiplex PCR reactions (see Table S1 for  
515 primer sequences and final conditions for all loci). Multiplex PCR reaction volume was 10  
516  $\mu\text{L}$ , containing 1x QIAGEN Multiplex PCR Master mix (HotStartTaq DNA Polymerase,  
517 Multiplex PCR Buffer, dNTP Mix; QIAGEN, Hilden, Germany), 0.2  $\mu\text{M}$  primer mix and 100  
518 ng of genomic DNA. The PCR amplification profile for all loci consisted of: (1) an initial  
519 activation step of 15 min at 95 °C; (2) 30 cycles of denaturation at 94 °C for 30 s, annealing at  
520 57 °C for 90 s, and extension at 72 °C for 60 s; and (3) a final extension of 30 min at 60 °C.

521 PCR products were prepared for microsatellite genotyping and sent to an external  
522 service (BMR Genomics, <http://www.bmr-genomics.com/>), where they were sequenced using  
523 an ABI 3730xl automated sequencer (LIZ 500 as internal size ladder, Applied Biosystems,  
524 Waltham, MA, USA). Microsatellites were analyzed using GeneMarker ver. 2.6  
525 (SoftGenetics). Genotypes of individuals included in the microsatellite analysis published by  
526 Agostini *et al.*<sup>19</sup> were integrated into this analysis. To ensure that the datasets were  
527 comparable, two individual samples from Agostini *et al.*<sup>19</sup> were processed alongside samples  
528 from the present study as positive controls during each amplification and sequencing run.  
529 This allowed the comparison of the raw microsatellite data between the previous and current  
530 study and confirmed that there was no change in microsatellite sizing. Binning was  
531 automated with FlexiBin 2<sup>63</sup> and refined by eye to assure accuracy with the corresponding  
532 binnings established in Agostini *et al.*<sup>19</sup>.

533

### 534 **Data analysis**

535 A suite of programs was used to assess population differentiation and genetic  
536 structuring based on the microsatellite genotypes. Input files were created in the appropriate  
537 software-specific formats using CREATE ver 1.37<sup>64</sup>. Within-sampling location genetic  
538 variability was assessed by calculating observed ( $H_O$ ) and expected ( $H_e$ ) heterozygosity,  
539 number of alleles ( $N_A$ ), and allelic richness ( $A_R$ ) using the R package diveRsity ver. 1.9.89<sup>65</sup>.  
540 Genetic variability was compared between sampling locations using a one-way ANOVA  
541 performed in R<sup>66</sup>. Deviations from Hardy-Weinberg equilibrium were calculated with the R  
542 package diveRsity ver. 1.9.89<sup>65</sup>. The software Micro-Checker 2.2.3 was used to detect the

543 presence of null alleles and scoring errors due to large allele drop-out and stuttering<sup>67</sup>.  
544 Linkage Disequilibrium (LD) probability was tested with GENEPOP online<sup>68</sup>. Significance  
545 levels for multiple comparisons were adjusted using the program SGoF<sup>69</sup>.

546 Detection of loci under selection was carried out using the methods implemented in  
547 LOSITAN ver. 1.0.0<sup>70</sup> and ARLEQUIN 3.5.1.3<sup>71</sup>. Both software generate coalescent  
548 simulations based on observed data and a chosen demographic model of migration to create  
549 the expected distribution of  $F_{ST}$  versus  $H_E$  with neutral markers. Outlier loci are detected  
550 based on the presence of significantly higher or lower  $F_{ST}$  values compared to neutral  
551 expectations. In LOSITAN, 1,000,000 simulations were run under neutral mean  $F_{ST}$ ,  
552 confidence interval of 0.95% and a false discovery rate of 0.01 assuming a Stepwise  
553 Mutation Model (SMM)<sup>19</sup>. In ARLEQUIN, genetic structure was assessed by running 50,000  
554 simulations, simulating 19 groups (corresponding to the number of sampling locations), and  
555 assuming 100 demes per group under the hierarchical island model<sup>72</sup>.

556 The extent to which sampling locations could be clustered into the same group was  
557 assessed using various methods. Discriminant analysis of principal components (DAPC), a  
558 multivariate method in which fish are assigned to known groups, and Principle Coordinate  
559 Analysis (PCoA), a multidimensional scaling method in which the matrix of dissimilarities  
560 was built from  $F_{ST}$  comparisons, were carried out using the R package ADEGENET 2.0.1<sup>73</sup>  
561 and GenALEX 6.501<sup>74,75</sup>, respectively, to provide a visual assessment of differentiation  
562 between sampling locations. Estimation of the number of groups into which genotypes from  
563 the various sampling locations cluster, ignoring a priori information about provenance, was  
564 tested using FLOCK 3.1<sup>76</sup>. FLOCK employs a non Markov Chain Monte Carlo (MCMC)  
565 algorithm that uses an iterative method to divide genotypes into  $k$  clusters. This method has  
566 been shown to allocate clusters more accurately than common Bayesian methods when  
567 population structure is weak<sup>77</sup>.

568 Population differentiation was determined by calculating pairwise genetic distances  
569 represented by  $F_{ST}$ <sup>78</sup> between sampling locations as well as between SL-defined groups.  
570 Hierarchical analysis of molecular variance (AMOVA) was also used to assess population  
571 differentiation. Pairwise genetic differences and AMOVA were calculated in ARLEQUIN  
572 3.5.1.3<sup>71</sup>. Significant differentiation was determined with 10,000 permutation tests. The  
573 significance threshold was adjusted according to SGoF+ correction for multiple tests<sup>69</sup>.

574

### 575 **Data Availability**

576 The datasets generated and analyzed during the current study are available from the  
577 corresponding author on request.

578

### 579 **Acknowledgements**

580 We would like to thank Nils Koschnick (AWI) and Emilio Riginella (University of Padua)  
581 for collecting the 2012 AP and 2014 WS samples during ‘Polarstern’ ANT-XXVIII/4 and

582 ANT-XXIX/9 cruises. This work was supported by the National Program for Antarctic  
 583 Research (PNRA16\_307) to L.Z.; J.A.C. is a PhD student in Evolution, Ecology, and  
 584 Conservation at the University of Padua, with funding from a Cariparo Fellowship for foreign  
 585 students and additional support from an Antarctic Science International (ASI) Bursary, a  
 586 Scientific Committee for Antarctic Research (SCAR) Fellowship, and an Erasmus+ Student  
 587 Traineeship. C.P. acknowledges financial support from the University of Padua  
 588 (BIRD164793/16) and from the European Marie Curie project “Polarexpress” Grant No.  
 589 622320. Funding for J.R.A. was provided by the National Science Foundation (Grant No.  
 590 0741348).

591

### 592 **Author Contributions**

593 C.P., M.W., and R.K. collected the samples; L.Z., J.R.A., and J.A.C. conceived the ideas;  
 594 J.A.C. collected the data, J.A.C., C.P., and L.Z. analyzed the data; C.P., J.R.A., and L.Z.  
 595 contributed to interpretation of results; J.A.C., J.R.A., C.P., and L.Z. wrote the manuscript.  
 596 All authors contributed to the final version of the manuscript.

597

### 598 **Competing Interests**

599 The authors declare that they have no conflict of interest.

600

### 601 **Supplementary Information**

602 Supplementary information accompanies the paper online.

603

### 604 **Figure Legends**

605 **Figure 1** Sampling locations. Yellow arrows approximate the SACCF, Southern Antarctic  
 606 Circumpolar Current Front; Pink arrows approximate the AACC, Antarctic Coastal Current;  
 607 Orange arrows approximate the AFS, Antarctic Slope Front and Current System; and red  
 608 arrows approximate the WF, Weddell Front. Relevant place names and bathymetric features  
 609 are indicated. **Overview.** Map of the Antarctic, showing sampling areas. Sampling stations  
 610 are color-coded by geographic area. Areas of interest in subsequent maps are indicated in  
 611 color-coded squares and ordered by movement along the AFS. Inferred position of the  
 612 SACCF and AFS approximated based on Fig. 7 in Orsi *et al.*<sup>11</sup> and Whitworth *et al.*<sup>8</sup>,  
 613 respectively. **Ross Sea (RS).** Inset shows sampling location details. Position of the AFS is  
 614 approximated based on Ashford *et al.*<sup>6</sup> Fig. 1a. **Weddell Sea (WS).** Insets show sampling  
 615 locations in detail. Red inset shows Atka Bay sampling station. Blue inset shows Halley Bay  
 616 sampling stations. Position of the AACC and AFS approximated are based on Fig. 2b in  
 617 Nicholls *et al.*<sup>56</sup>. **Larsen Bay (LB).** Empty arrows indicate the suggested position of the AFS  
 618 according to Whitworth *et al.*<sup>8</sup>. **Northern Antarctic Peninsula (NAP).** Position of the  
 619 SACCF and AACC are based on Fig. 7 in Orsi *et al.*<sup>11</sup> and Fig. 3 in Thompson *et al.*<sup>46</sup>,  
 620 respectively. Entry of Circumpolar Deep Water from the SACCF into the Bransfield Strait  
 621 through the Boyd Strait is shown according to Savidge and Amft<sup>10</sup>. Yellow SACCF arrows  
 622 and pink AACC arrows within the Bransfield Strait and Trough area represent components of  
 623 the Bransfield Gyre with Bellingshausen influence and Weddell influence respectively, based  
 624 on Fig. 15 in Sangrà *et al.*<sup>55</sup>. **South Orkney Islands (SOI).** Schematic illustration of the

625 circulation drawn from: SACCF (Fig. 7 in Orsi *et al.*<sup>11</sup>), AFS (Whitworth *et al.*<sup>8</sup>, Fig. 6 in  
626 Heywood *et al.*<sup>9</sup>, Fig. 14 in Azaneu *et al.*<sup>50</sup>), AACCC (Fig. 3 in Thompson *et al.*<sup>46</sup>, Fig. 15 in  
627 Sangrà *et al.*<sup>55</sup>), and WF (Fig. 6 in Heywood *et al.*<sup>9</sup>, Fig. 3 in Thompson *et al.*<sup>46</sup>, Fig. 14 in  
628 Azaneu *et al.*<sup>50</sup>). Empty arrows indicate the suggested position of the AFS according to  
629 Azaneu *et al.*<sup>50</sup>. **Western Antarctic Peninsula (WAP)**. Position of the SACCF and AACCC  
630 approximated based on both, Fig. 7 in Orsi *et al.*<sup>11</sup> and Fig. 14 in Moffat *et al.*<sup>7</sup> respectively.  
631 Empty arrows indicate the suggested position of the AACCC according to Moffat *et al.*<sup>7</sup>. Maps  
632 created using the Norwegian Polar Institute's Quantarctica 2.0 package<sup>79</sup> in the software  
633 QGIS version 2.18.9 <http://qgis.osgeo.org><sup>80</sup>.  
634

635 **Figure 2** FLOCK clustering results for *Pleuragramma antarctica* populations. **a** Mean  
636 LLOD scores are ordered by geographic area. **b** Normalized likelihoods, individuals are  
637 ordered by geographic area. ref, reference  $k$  group cluster (user-define  $k = 6$ ). Initial partition  
638 mode by random choice of samples. Number of iterations (re-allocations) per run = 20.  
639 Number of runs per parameter  $k = 50$ . Log likelihood difference (LLOD) threshold = 0  
640 (allocation occurs as soon as there is a highest log-likelihood difference between  
641 populations)<sup>76</sup>. Group acronyms are as in Table 1.  
642

643 **Figure 3** Discriminant analysis of principal components (DAPC) clustering results for  
644 *Pleuragramma antarctica* populations. **a** DAPC run without *a priori* parameters. **b** DAPC  
645 run based on geographic area, acronyms are as in Table 1.  
646

647 **Figure 4** Principal coordinate analysis (PCoA) for *Pleuragramma antarctica* population  
648 samples based on  $F_{ST}$  genetic distance. **a** PCoA of 19 sampling locations. **b** PCoA of six  
649 geographic groups. Sampling location and geographic group acronyms are as in Table 1.  
650  
651  
652  
653  
654  
655  
656  
657  
658  
659  
660  
661  
662  
663  
664  
665



666

**Table 1** *Pleuragramma antarctica* sampling locations between 1989 and 2014 from the six geographic areas analyzed in this study. Collection site, year, acronym, campaign, coordinates, and sample size (*n*) are indicated.

Site	Year	Acronym	Campaign	Coordinates		<i>n</i>
<b>Western Antarctic Peninsula (WAP)</b>						<b>280</b>
Charcot Island (CI)	2010	CI10	NBP 10-02 <sup>a</sup>	-70.117	-76.033	60
Marguerite Bay (MB)	2001	MB01	SO GLOBEC-Cruise 1 <sup>b</sup>	-67.950	-68.350	28
	2002	MB02	SO GLOBEC-Cruise 3 <sup>b</sup>	-68.133	-68.017	49
	2010	MB10	NBP 10-02 <sup>a</sup>	-67.817	-68.150	60
	2011	MB11	LMG Cruise 11-01, Palmer LTER <sup>c</sup>	-67.650	-70.067	83
<b>Northern Antarctic Peninsula (NAP)</b>						<b>250</b>
Joinville Island (JI)	2007	JI07	ANT-XXIII/8 <sup>d</sup>	-62.583	-54.750	34
	2010	JI10	NBP 10-02 <sup>a</sup>	-63.500	-56.667	148
	2012	JI12	ANT-XXVIII/4 <sup>d</sup>	-62.233	-55.300	54
South Shetland Islands (SSI)	1996	SSI96	ANT-XIV/2 <sup>d</sup>	-61.549	-58.205	14
<b>South Orkney Islands (SOI)</b>	2011	SOI11	ANT-XXVII/3 <sup>d</sup>	-61.179	-45.673	<b>47</b>
<b>Larsen Bay (LB)</b>						<b>98</b>
	2007	LB07	ANT-XXIII/8 <sup>d</sup>	-65.500	-61.667	46
	2011	LB11	ANT-XXVII/3 <sup>d</sup>	-64.833	-60.350	52
<b>Weddell Sea (WS)</b>						<b>217</b>
Filchner Trough (FT)	2014	FT14	ANT-XXIX/9 <sup>d</sup>	-76.217	-34.961	50
Halley Bay (HB)	1989	HB89	ANT-VII/4 <sup>d</sup>	-75.155	-27.788	19
	1991	HB91	ANT-IX/3 <sup>d</sup>	-75.250	-25.835	41
	2014	HB14	ANT-XXIX/9 <sup>d</sup>	-75.452	-28.703	82
Atka Bay (AB)	2014	AB14	ANT-XXIX/9 <sup>d</sup>	-70.913	-10.735	25
<b>Ross Sea (RS)</b>						<b>175</b>
Terra Nova Bay	1996	RS96	11th Italian expedition PNRA Italica <sup>e</sup>	-74.810	164.303	91
	1997	RS97	13th Italian expedition PNRA Italica <sup>e</sup>	NA		84

<sup>a</sup> Research vessel (RV) *Nathaniel B. Palmer*. Collection via Multiple Opening and Closing Net, with an Environmental Sensing System (10m2 MOCNESS, MOC-10) outfitted with six 3 mm mesh nets<sup>19,49,81,82</sup>.

<sup>b</sup> Antarctic Research Support Vessel (ARSV) *Laurence M. Gould* as part of the Southern Ocean Global Ocean Ecosystems Dynamics (SO GLOBEC) program. Collection via 10m2 MOCNESS, MOC-10, outfitted with six 3 mm mesh nets<sup>19,49,81,82</sup>.

<sup>c</sup> ARSV *Laurence M. Gould* as part of the Palmer Long-Term Ecological Research (LTER) program. Collection via 2 × 2 m square-frame net with a 700 μm mesh<sup>83</sup>.

<sup>d</sup> RV *Polarstern*, Alfred Wegner Institute for Polar Research (AWI), Bremerhaven, Germany. Collection via commercial benthopelagic trawl, with a cod-end mesh line of 20 mm<sup>36</sup>.

<sup>e</sup> RV *Italica* as part of the National Program of Research in Antarctica (PNRA), Italy. Collection via Hamburg Plankton net with 0.5-1 mm cod-end<sup>36</sup>.

667

668

669

670

671

672

673

674

**Table 2** Summary of genetic variability for *Pleuragramma antarctica* from 19 sampling locations at 15 microsatellite loci. Sample size ( $n$ ), number of alleles ( $N_A$ ), allelic richness ( $A_R$ ), observed heterozygosity ( $H_O$ ), unbiased heterozygosity ( $H_E$ ), and probability of deviation from Hardy-Weinberg equilibrium ( $p_{HWE}$ ) are shown. Allelic richness is calculated based on a minimum sample size of 14 individuals. Standard deviation ( $\pm$  SD) is given in parentheses. Values in red indicate significant HWE deviations after correction for multiple tests as implemented in SGoF+ (threshold for significance with 285 comparisons 0.0137). Sampling location acronyms are as in Table 1.

Sampling location	$n$	$N_A \pm$ SD	$A_R \pm$ SD	$H_O \pm$ SD	$H_E \pm$ SD	$p_{HWE}$
CI10	60	8.40 (5.01)	5.61 (3.13)	0.58 (0.20)	0.62 (0.21)	0.288
MB01	28	7.46 (4.70)	5.54 (3.09)	0.61 (0.27)	0.61 (0.24)	0.766
MB02	49	8.20 (4.27)	5.54 (2.91)	0.62 (0.24)	0.61 (0.23)	0.632
MB10	60	8.86 (5.08)	5.93 (2.94)	0.65 (0.21)	0.64 (0.21)	0.059
MB11	83	9.26 (5.39)	5.75 (3.05)	0.62 (0.22)	0.62 (0.23)	0.773
JI07	34	7.60 (4.74)	5.52 (2.85)	0.63 (0.22)	0.63 (0.21)	0.702
JI10	148	11.00 (5.75)	6.02 (2.85)	0.64 (0.19)	0.65 (0.20)	<b>0.012</b>
JI12	54	8.00 (4.05)	5.45 (2.65)	0.60 (0.22)	0.62 (0.21)	0.044
SSI96	14	5.86 (3.39)	4.98 (2.65)	0.60 (0.22)	0.60 (0.22)	0.077
SOI11	47	7.93 (3.57)	5.59 (2.47)	0.60 (0.19)	0.63 (0.18)	0.080
LB07	46	7.80 (4.31)	5.49 (2.75)	0.61 (0.24)	0.62 (0.22)	<b>0.011</b>
LB11	52	8.53 (4.37)	5.75 (2.92)	0.63 (0.22)	0.63 (0.22)	0.690
FT14	50	8.20 (3.74)	5.70 (2.62)	0.62 (0.21)	0.63 (0.21)	0.909
HB89	19	6.13 (2.61)	5.12 (2.06)	0.62 (0.20)	0.63 (0.19)	0.095
HB91	41	7.93 (4.35)	5.66 (2.81)	0.62 (0.23)	0.63 (0.21)	0.274
HB14	82	9.26 (4.36)	5.69 (2.79)	0.60 (0.19)	0.63 (0.20)	0.037
AB14	25	6.73 (3.12)	5.24 (2.44)	0.64 (0.23)	0.61 (0.22)	0.026
RS96	91	9.80 (4.82)	5.93 (2.94)	0.63 (0.21)	0.64 (0.21)	0.209
RS97	84	9.00 (5.19)	5.73 (2.94)	0.62 (0.20)	0.63 (0.20)	0.913

675

676

677

678

679

680

681

682

683

684

685

686

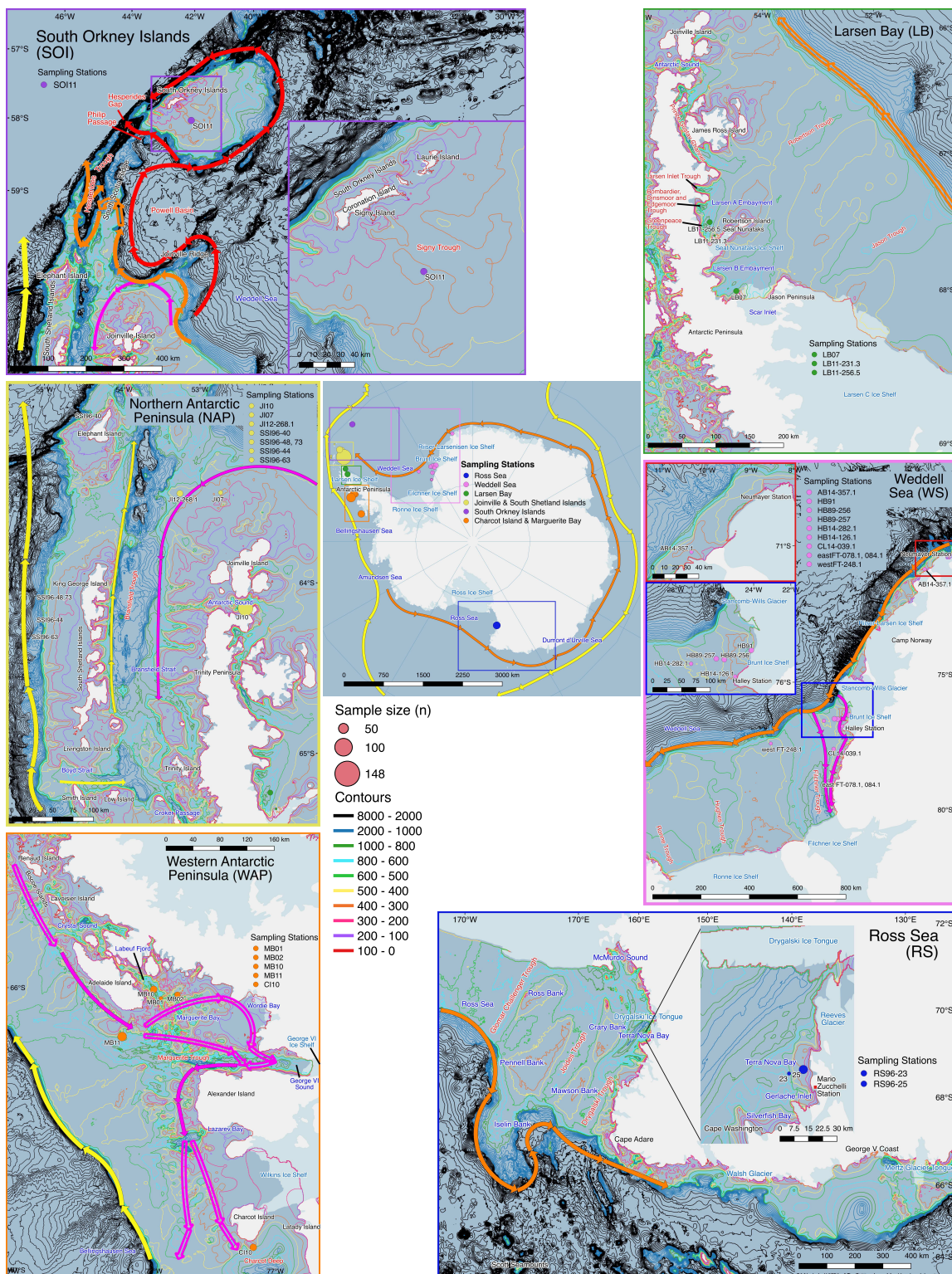
**Table 3** Genetic differentiation among *Pleuragramma antarctica* samples based on microsatellite data. Pairwise  $F_{ST}$  estimates (above the diagonal) and corresponding  $P$ -values (below the diagonal) are shown. Values in red were significant after correction for multiple tests as implemented in SGoF+ (threshold for significance with 171 comparisons 0.0332). Comparisons within the same geographic area are shaded in gray. Numbers in parentheses adjacent to population sample names specify the sample size ( $n$ ). Sampling location acronyms are as in Table 1, colors correspond to geographic area coloring in the map figure. SOI, South Orkney Islands.

	Western Antarctic Peninsula (WAP)					Northern Antarctic Peninsula (NAP)				SOI	Larsen Bay (LB)		Weddell Sea (WS)					Ross Sea (RS)	
	C10 (60)	MB01 (28)	MB02 (49)	MB10 (60)	MB11 (83)	J107 (34)	J110 (148)	J112 (54)	SSI96 (14)	SOI11 (47)	LB07 (46)	LB11 (52)	FT14 (50)	HB89 (19)	HB91 (41)	HB14 (82)	AB14 (25)	RS96 (91)	RS97 (84)
C10	-	-0.0008	-0.0006	0.0007	-0.0008	-0.0033	<b>0.0042</b>	0.0043	-0.0032	<b>0.0100</b>	<b>0.0054</b>	0.0021	0.0002	0.0045	0.0016	0.0001	-0.0012	<b>0.0049</b>	0.0024
MB01	0.6781	-	-0.0008	-0.0022	-0.0016	0.0006	0.0043	0.0047	0.0013	<b>0.0125</b>	0.0057	0.0057	0.0007	0.0010	0.0037	0.0015	0.0008	0.0043	0.0042
MB02	0.6476	0.5735	-	0.0009	0.0008	-0.0014	0.0017	0.0043	-0.0027	<b>0.0100</b>	0.0024	0.0001	0.0008	0.0032	-0.0003	-0.0008	-0.0043	0.0019	<b>0.0039</b>
MB10	0.3761	0.8023	0.2933	-	0.0009	-0.0037	0.0009	0.0037	0.0015	<b>0.0091</b>	0.0027	-0.0005	-0.0000	-0.0030	0.0008	-0.0011	-0.0021	0.0002	0.0010
MB11	0.7148	0.7278	0.2908	0.2391	-	-0.0008	<b>0.0040</b>	<b>0.0043</b>	0.0014	<b>0.0096</b>	<b>0.0094</b>	<b>0.0046</b>	0.0008	0.0019	0.0030	0.0018	-0.0001	<b>0.0041</b>	0.0025
J107	0.9578	0.4125	0.6796	0.9656	0.6136	-	-0.0010	0.0010	-0.0046	<b>0.0059</b>	0.0009	-0.0034	-0.0034	0.0003	0.0002	-0.0027	-0.0053	-0.0018	-0.0026
J110	<b>0.0050</b>	0.0468	0.1351	0.2255	<b>0.0009</b>	0.7206	-	0.0018	-0.0019	0.0031	0.0021	0.0000	-0.0001	-0.0040	0.0007	-0.0004	0.0001	-0.0010	0.0017
J112	0.0376	0.0844	0.0388	0.0389	<b>0.0117</b>	0.3609	0.1218	-	0.0011	0.0013	0.0039	0.0027	-0.0006	0.0023	-0.0015	0.0015	0.0014	0.0020	0.0020
SSI96	0.8883	0.3942	0.7829	0.3009	0.3053	0.8963	0.7773	0.4223	-	0.0013	0.0022	-0.0023	-0.0032	-0.0068	-0.0018	-0.0035	-0.0034	-0.0005	0.0002
SOI11	<b>0.0003</b>	<b>0.0019</b>	<b>0.0004</b>	<b>0.0001</b>	< <b>0.0001</b>	<b>0.0333</b>	0.0398	0.3352	0.4097	-	<b>0.0058</b>	0.0039	0.0003	0.0028	-0.0001	0.0037	0.0049	<b>0.0066</b>	0.0031
LB07	<b>0.0194</b>	0.0552	0.1438	0.0998	< <b>0.0001</b>	0.3566	0.1040	0.0585	0.2782	<b>0.0235</b>	-	0.0020	0.0020	-0.0016	<b>0.0056</b>	0.0004	0.0004	0.0033	0.0033
LB11	0.1878	0.0417	0.4465	0.5802	<b>0.0083</b>	0.9410	0.4981	0.1197	0.7620	0.0630	0.1823	-	-0.0012	0.0066	-0.0012	-0.0008	-0.0035	0.0016	0.0013
FT14	0.5132	0.4165	0.3355	0.4850	0.3013	0.9320	0.5431	0.6490	0.8470	0.4840	0.1973	0.7401	-	-0.0012	-0.0012	-0.0015	-0.0037	-0.0009	-0.0013
HB89	0.2861	0.4788	0.2574	0.7111	0.3197	0.4860	0.8371	0.3928	0.8850	0.3797	0.6357	0.1285	0.6179	-	0.0021	-0.0025	0.0016	-0.0048	0.0003
HB91	0.2813	0.1429	0.5330	0.3281	0.0726	0.4670	0.3548	0.7993	0.7201	0.5527	<b>0.0251</b>	0.7284	0.7284	0.3960	-	-0.0006	-0.0031	0.0015	0.0007
HB14	0.5533	0.3417	0.7140	0.8004	0.1089	0.9379	0.7097	0.2525	0.9270	0.0534	0.4498	0.7405	0.8699	0.7597	0.6806	-	-0.0051	0.0011	-0.0009
AB14	0.6856	0.3856	0.9274	0.7509	0.4464	0.9520	0.4831	0.3312	0.7616	0.0891	0.4093	0.9015	0.9162	0.3727	0.8489	0.9932	-	0.0011	-0.0004
RS96	<b>0.0047</b>	0.0512	0.1306	0.4294	<b>0.0026</b>	0.8272	0.9078	0.1130	0.5626	<b>0.0001</b>	0.0391	0.1572	0.7323	0.8800	0.2032	0.2109	0.3073	-	0.0024
RS97	0.0939	0.0758	<b>0.0274</b>	0.2540	0.0365	0.9262	0.0674	0.1339	0.4861	0.0740	0.0520	0.2238	0.8167	0.5103	0.3830	0.8084	0.5485	0.0398	-

**Table 4** Genetic differentiation among *Pleuragramma antarctica* samples, pooling sampling locations from common geographic areas. Pairwise  $F_{ST}$  estimates (above the diagonal) and corresponding  $P$ -values (below the diagonal) are shown. Values in red were significant after correction for multiple tests as implemented in SGoF+ (threshold for significance with 15 comparisons 0.0142). Numbers in parentheses adjacent to group names indicate the sample size ( $n$ ). Group acronyms are as in Table 1, colors correspond to geographic area coloring in the map figure.

	WAP (280)	NAP (257)	SOI (47)	LB (98)	WS (210)	RS (175)
WAP	-	<b>0.0039</b>	<b>0.0153</b>	<b>0.0041</b>	<b>0.0034</b>	<b>0.0059</b>
NAP	< <b>0.0001</b>	-	<b>0.0039</b>	0.0005	0.0001	0.0001
SOI	< <b>0.0001</b>	<b>0.0079</b>	-	<b>0.0056</b>	0.0038	<b>0.0049</b>
LB	< <b>0.0001</b>	0.2865	<b>0.0033</b>	-	0.0007	0.0017
WS	< <b>0.0001</b>	0.4538	0.0143	0.2067	-	0.0001
RS	< <b>0.0001</b>	0.4597	<b>0.0029</b>	0.0312	0.4492	-

Figure 1



687  
688  
689  
690  
691

Figure 2

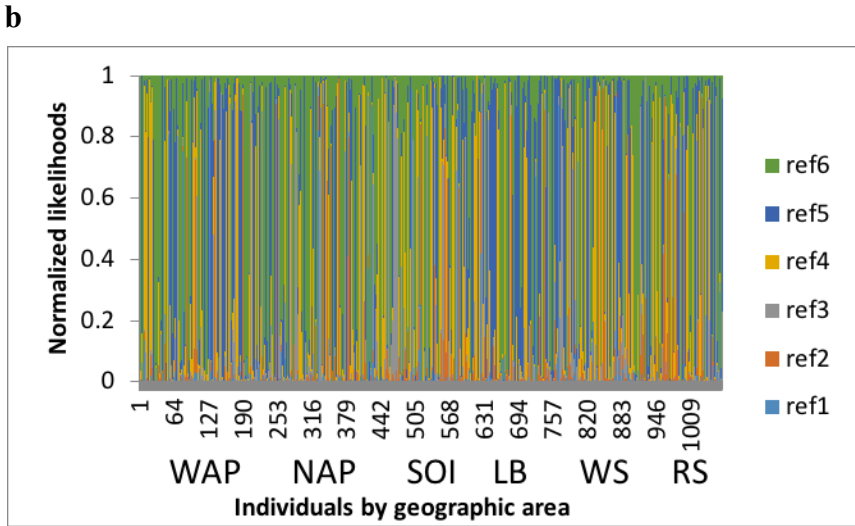
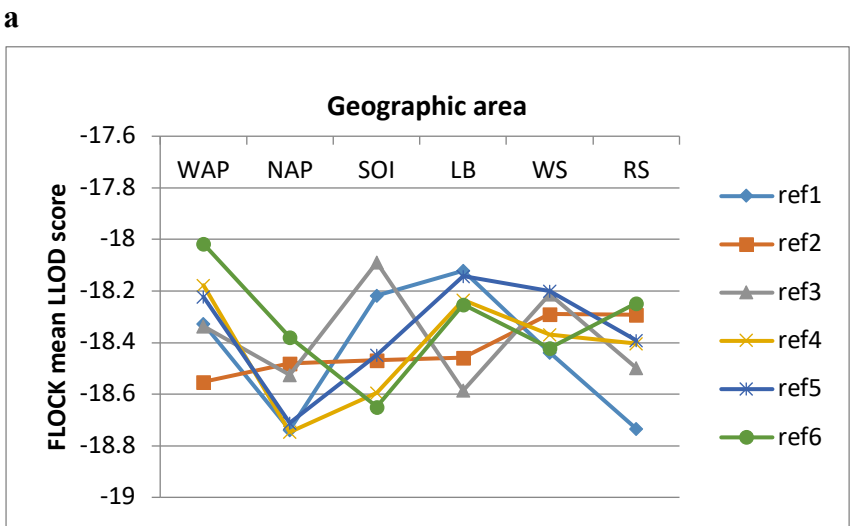
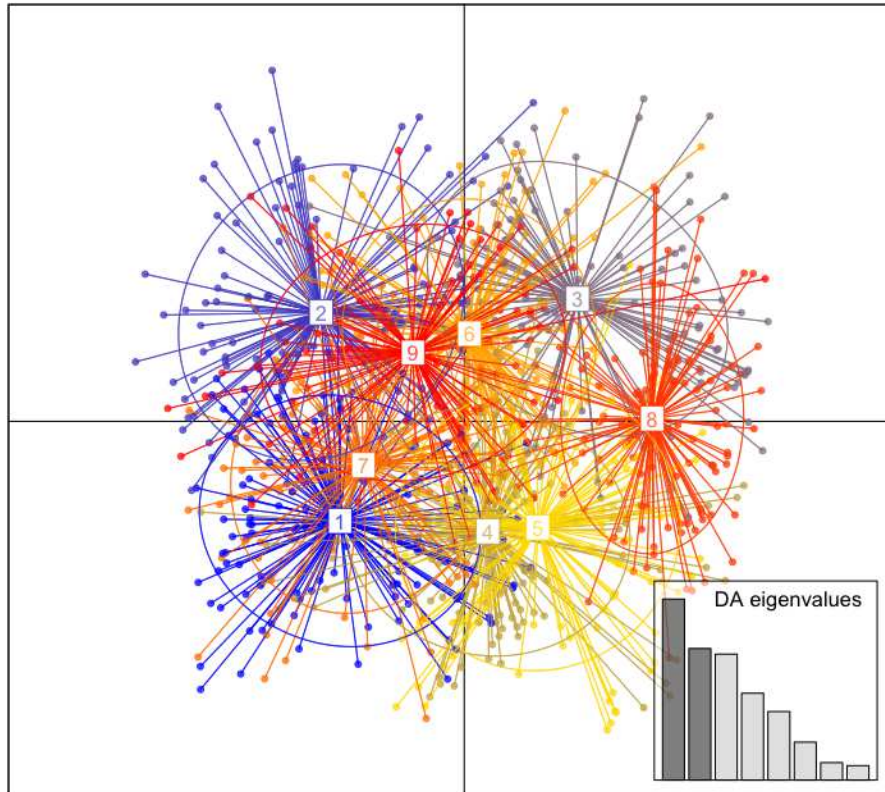


Figure 3

a



b

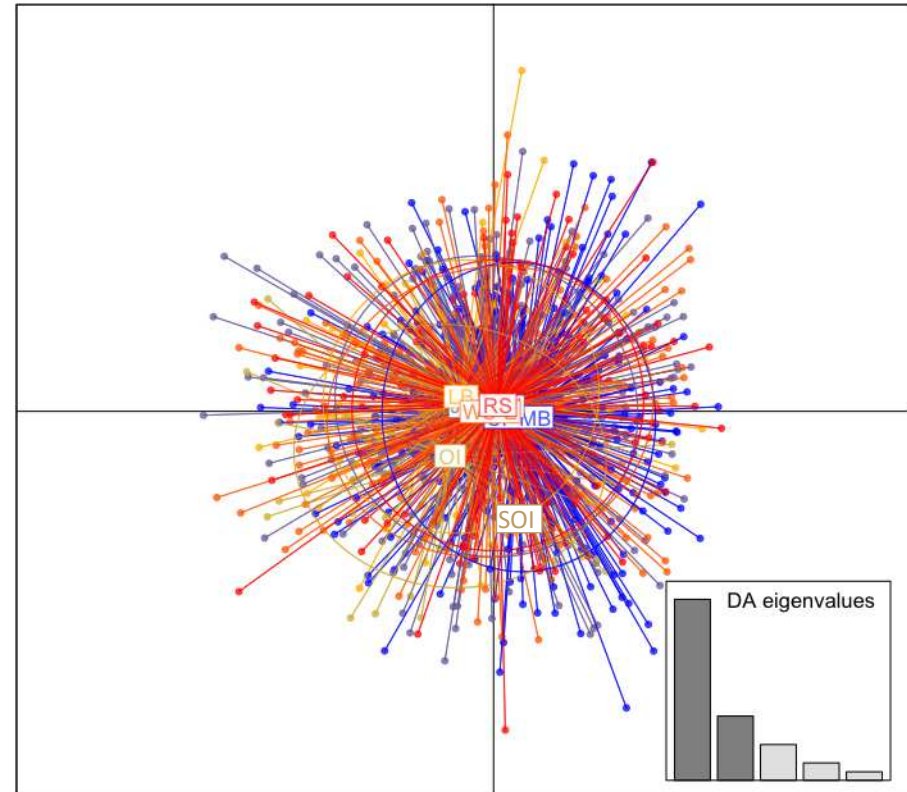
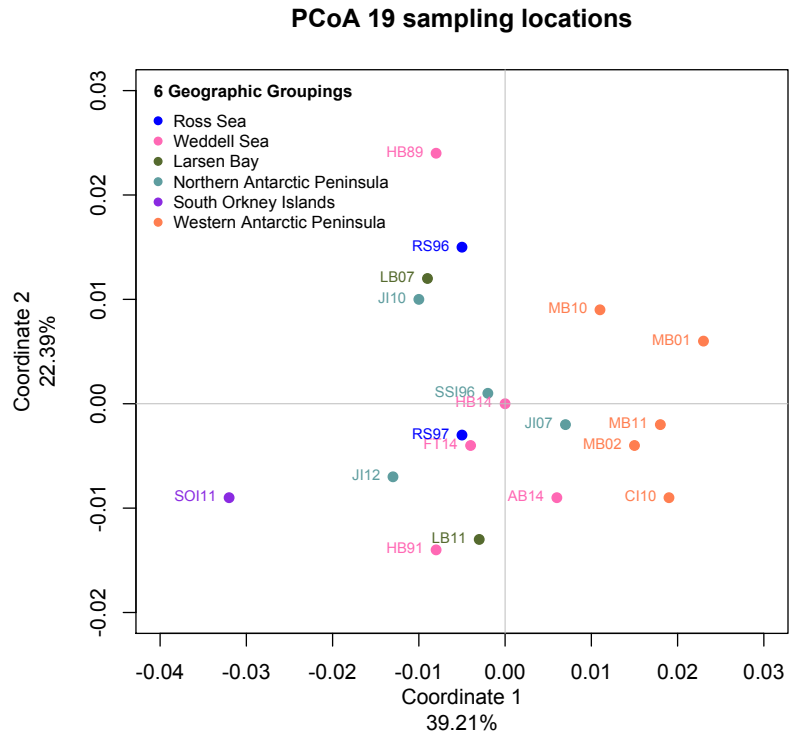
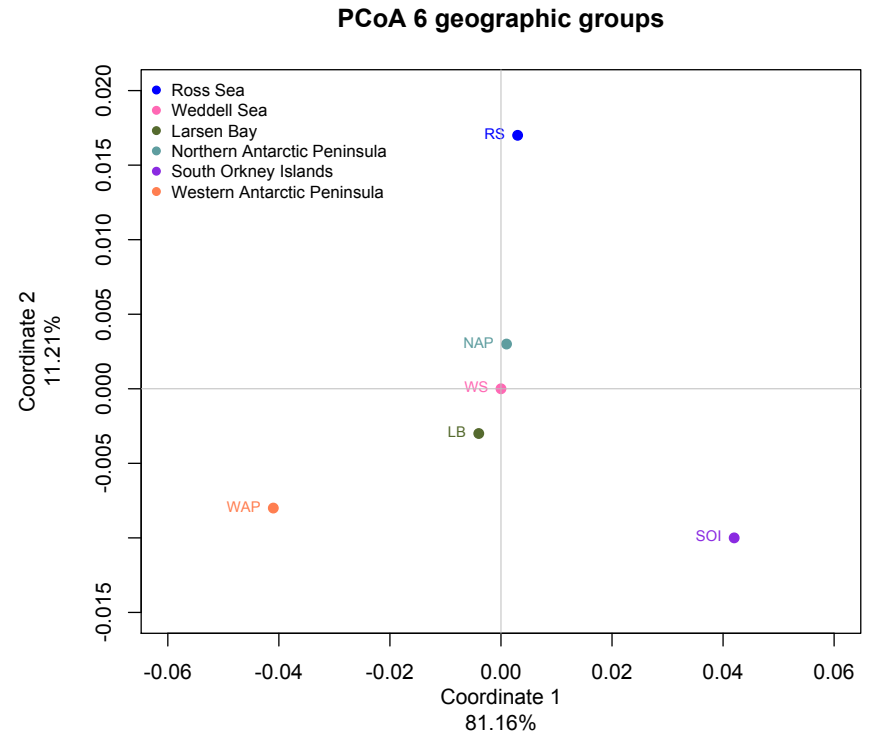


Figure 4

a



b





692 **References**

- 693 1 Duhamel, G. *et al.* in *Biogeographic Atlas of the Southern Ocean*. (eds De Broyer C.  
694 *et al.*) Ch. 7, 328-362 (Scientific Committee on Antarctic Research, 2014).
- 695 2 Koubbi, P. *et al.* in *The Antarctic Silverfish: a Keystone Species in a Changing*  
696 *Ecosystem* (eds Marino Vacchi, Eva Pisano, & Laura Ghigliotti) 287-305 (Springer  
697 International Publishing, 2017).
- 698 3 La Mesa, M. & Eastman, J. T. Antarctic silverfish: Life strategies of a key species in  
699 the high-Antarctic ecosystem. *Fish and Fisheries* **13**, 241-266 (2012).
- 700 4 Vacchi, M. *et al.* A nursery area for the Antarctic silverfish *Pleuragramma*  
701 *antarcticum* at Terra Nova Bay (Ross Sea): First estimate of distribution and  
702 abundance of eggs and larvae under the seasonal sea-ice. *Polar Biology* **35**, 1573-  
703 1585, doi:10.1007/s00300-012-1199-y (2012).
- 704 5 Wöhrmann, A. P. A., Hagen, W. & Kunzmann, A. Adaptations of the Antarctic  
705 silverfish *Pleuragramma antarcticum* (Pisces: Nototheniidae) to pelagic life in high-  
706 Antarctic waters. *Marine Ecology Progress Series* **151**, 205-218 (1997).
- 707 6 Ashford, J., Zane, L., Torres, J. J., La Mesa, M. & Simms, A. R. in *The Antarctic*  
708 *Silverfish: a Keystone Species in a Changing Ecosystem* (eds Marino Vacchi, Eva  
709 Pisano, & Laura Ghigliotti) 193-234 (Springer International Publishing, 2017).
- 710 7 Moffat, C., Beardsley, R. C., Owens, B. & van Lipzig, N. A first description of the  
711 Antarctic Peninsula Coastal Current. *Deep Sea Research Part II: Topical Studies in*  
712 *Oceanography* **55**, 277-293, doi:10.1016/j.dsr2.2007.10.003 (2008).
- 713 8 Whitworth, T., Orsi, A. H., Kim, S. J., Nowlin, W. D. & Locarnini, R. A. in *Ocean, Ice,*  
714 *and Atmosphere: Interactions at the Antarctic Continental Margin* 1-27 (American  
715 Geophysical Union, 1998).
- 716 9 Heywood, K. J., Naveira Garabato, A. C., Stevens, D. P. & Muench, R. D. On the fate  
717 of the Antarctic Slope Front and the origin of the Weddell Front. *Journal of*  
718 *Geophysical Research: Oceans* **109**, C06021, doi:10.1029/2003JC002053 (2004).
- 719 10 Savidge, D. K. & Amft, J. A. Circulation on the West Antarctic Peninsula derived from  
720 6 years of shipboard ADCP transects. *Deep-Sea Research Part I: Oceanographic*  
721 *Research Papers* **56**, 1633-1655, doi:10.1016/j.dsr.2009.05.011 (2009).
- 722 11 Orsi, A. H., Whitworth Iii, T. & Nowlin Jr, W. D. On the meridional extent and fronts  
723 of the Antarctic Circumpolar Current. *Deep-Sea Research Part I* **42**, 641-673,  
724 doi:10.1016/0967-0637(95)00021-W (1995).
- 725 12 La Mesa, M. *et al.* Influence of environmental conditions on spatial distribution and  
726 abundance of early life stages of antarctic silverfish, *Pleuragramma antarcticum*  
727 (Nototheniidae), in the Ross Sea. *Antarctic Science* **22**, 243-254,  
728 doi:10.1017/S0954102009990721 (2010).
- 729 13 Guidetti, P., Ghigliotti, L. & Vacchi, M. Insights into spatial distribution patterns of  
730 early stages of the Antarctic silverfish, *Pleuragramma antarctica*, in the platelet ice  
731 of Terra Nova Bay, Antarctica. *Polar Biology* **38**, 333-342, doi:doi: 10.1007/s00300-  
732 014-1589-4 (2014).
- 733 14 Lancraft, T. M., Reisenbichler, K. R., Robison, B. H., Hopkins, T. L. & Torres, J. J. A krill-  
734 dominated micronekton and macrozooplankton community in Croker Passage,  
735 Antarctica with an estimate of fish predation. *Deep-Sea Research Part II: Topical*  
736 *Studies in Oceanography* **51**, 2247-2260, doi:10.1016/j.dsr2.2004.07.004 (2004).

- 737 15 Giraldo, C. *et al.* Lipid dynamics and trophic patterns in *Pleuragramma antarctica* life  
738 stages. *Antarctic Science* **27**, 429-438, doi:10.1017/S0954102015000036 (2015).
- 739 16 Eastman, J. T. *Pleuragramma antarcticum* (Pisces, Nototheniidae) as food for other  
740 fishes in McMurdo Sound, Antarctica. *Polar Biology* **4**, 155-160,  
741 doi:10.1007/BF00263878 (1985).
- 742 17 La Mesa, M., Eastman, J. T. & Vacchi, M. The role of notothenioid fish in the food  
743 web of the Ross Sea shelf waters: A review. *Polar Biology* **27**, 321-338,  
744 doi:10.1007/s00300-004-0599-z (2004).
- 745 18 Kellermann, A. Food and feeding ecology of postlarval and juvenile *Pleuragramma*  
746 *antarcticum* (Pisces; Notothenioidei) in the seasonal pack ice zone off the Antarctic  
747 peninsula. *Polar Biology* **7**, 307-315, doi:10.1007/BF00443949 (1987).
- 748 19 Agostini, C. *et al.* Genetic differentiation in the ice-dependent fish *Pleuragramma*  
749 *antarctica* along the Antarctic Peninsula. *Journal of Biogeography* **42**, 1103-1113,  
750 doi:10.1111/jbi.12497 (2015).
- 751 20 Brooks, C. M. *et al.* Early life history connectivity of Antarctic silverfish  
752 (*Pleuragramma antarctica*) in the Ross Sea. *Fisheries Oceanography* **27**, 1-14,  
753 doi:10.1111/fog.12251 (2018).
- 754 21 Daniels, R. A. & Lipps, J. H. Distribution and Ecology of Fishes of the Antarctic  
755 Peninsula. *Journal of Biogeography* **9**, 1-9, doi:10.2307/2844726 (1982).
- 756 22 Hubold, G. Spatial distribution of *Pleuragramma antarcticum* (Pisces: Nototheniidae)  
757 near the Filchner- and Larsen ice shelves (Weddell sea/antarctica). *Polar Biology* **3**,  
758 231-236, doi:10.1007/BF00292628 (1984).
- 759 23 Kellermann, A. Geographical distribution and abundance of postlarval and juvenile  
760 *Pleuragramma antarcticum* (Pisces, Notothenioidei) off the Antarctic Peninsula.  
761 *Polar Biology* **6**, 111-119, doi:10.1007/BF00258262 (1986).
- 762 24 Vacchi, M., La Mesa, M., Dalu, M. & Macdonald, J. Early life stages in the life cycle of  
763 Antarctic silverfish, *Pleuragramma antarcticum* in Terra Nova Bay, Ross Sea.  
764 *Antarctic Science* **16**, 299-305, doi:10.1017/S0954102004002135 (2004).
- 765 25 Koubbi, P. *et al.* Spatial distribution and inter-annual variations in the size frequency  
766 distribution and abundances of *Pleuragramma antarcticum* larvae in the Dumont  
767 d'Urville Sea from 2004 to 2010. *Polar Science* **5**, 225-238,  
768 doi:10.1016/j.polar.2011.02.003 (2011).
- 769 26 La Mesa, M., Piñones, A., Catalano, B. & Ashford, J. Predicting early life connectivity  
770 of Antarctic silverfish, an important forage species along the Antarctic Peninsula.  
771 *Fisheries Oceanography* **24**, 150-161, doi:10.1111/fog.12096 (2015).
- 772 27 Lowe, W. H. & Allendorf, F. W. What can genetics tell us about population  
773 connectivity? *Molecular ecology* **19**, 3038-3051, doi:10.1111/j.1365-  
774 294X.2010.04688.x (2010).
- 775 28 Matschiner, M., Hanel, R. & Salzburger, W. Gene flow by larval dispersal in the  
776 Antarctic notothenioid fish *Gobionotothen gibberifrons*. *Molecular ecology* **18**, 2574-  
777 2587, doi:10.1111/j.1365-294X.2009.04220.x (2009).
- 778 29 Papetti, C. *et al.* Population genetic structure and gene flow patterns between  
779 populations of the Antarctic icefish *Chionodraco rastrospinosus*. *Journal of*  
780 *Biogeography* **39**, 1361-1372, doi:10.1111/j.1365-2699.2011.02682.x (2012).
- 781 30 Damerau, M., Matschiner, M., Salzburger, W. & Hanel, R. Comparative population  
782 genetics of seven notothenioid fish species reveals high levels of gene flow along

- 783 ocean currents in the southern Scotia Arc, Antarctica. *Polar Biology* **35**, 1073-1086,  
784 doi:10.1007/s00300-012-1155-x (2012).
- 785 31 Parker, R. W., Paige, K. N. & DeVries, A. L. Genetic variation among populations of  
786 the Antarctic toothfish: Evolutionary insights and implications for conservation. *Polar*  
787 *Biology* **25**, 256-261, doi:10.1007/s00300-001-0333-z (2002).
- 788 32 Kuhn, K. L. & Gaffney, P. M. Population subdivision in the Antarctic toothfish  
789 (*Dissostichus mawsoni*) revealed by mitochondrial and nuclear single nucleotide  
790 polymorphisms (SNPs). *Antarctic Science* **20**, 327-338,  
791 doi:10.1017/S0954102008000965 (2008).
- 792 33 Patarnello, T., Marcato, S., Zane, L., Varotto, V. & Bargelloni, L. Phylogeography of  
793 the Chionodraco genus (Perciformes, Channichthyidae) in the Southern Ocean.  
794 *Molecular Phylogenetics and Evolution* **28**, 420-429, doi:10.1016/S1055-  
795 7903(03)00124-6 (2003).
- 796 34 Papetti, C., Susana, E., Patarnello, T. & Zane, L. Spatial and temporal boundaries to  
797 gene flow between *Chaenocephalus aceratus* populations at South Orkney and  
798 South Shetlands. *Marine Ecology Progress Series* **376**, 269-281,  
799 doi:10.3354/meps07831 (2009).
- 800 35 Damerau, M., Matschiner, M., Salzburger, W. & Hanel, R. Population divergences  
801 despite long pelagic larval stages: lessons from crocodile icefishes (Channichthyidae).  
802 *Molecular ecology* **23**, 284-299, doi:10.1111/mec.12612 (2014).
- 803 36 Zane, L. *et al.* Demographic history and population structure of the Antarctic  
804 silverfish *Pleuragramma antarcticum*. *Molecular ecology* **15**, 4499-4511,  
805 doi:10.1111/j.1365-294X.2006.03105.x (2006).
- 806 37 Johnson, M. S. & Black, R. Chaotic genetic patchiness in an intertidal limpet,  
807 *Siphonaria* sp. *Marine Biology* **70**, 157-164, doi:10.1007/BF00397680 (1982).
- 808 38 Efremenko, V. N. Atlas of fish larvae of the Southern Ocean. *Cybiurn* **7**, 1-74 (1983).
- 809 39 La Mesa, M., Riginella, E., Mazzoldi, C. & Ashford, J. Reproductive resilience of ice-  
810 dependent Antarctic silverfish in a rapidly changing system along the Western  
811 Antarctic Peninsula. *Marine Ecology* **36**, 235-245, doi:10.1111/maec.12140 (2015).
- 812 40 Cuéllar-Pinzón, J., Presa, P., Hawkins, S. J. & Pita, A. Genetic markers in marine  
813 fisheries: Types, tasks and trends. *Fisheries Research* **173**, Part 3, 194-205,  
814 doi:10.1016/j.fishres.2015.10.019 (2016).
- 815 41 Emslie, S. D., Fraser, W., Smith, R. C. & Walker, W. Abandoned penguin colonies and  
816 environmental change in the Palmer Station area, Anvers Island, Antarctic Peninsula.  
817 *Antarctic Science* **10**, 257-268 (1998).
- 818 42 Goethel, D., Quinn, T. & Cadrin, S. *Incorporating Spatial Structure in Stock*  
819 *Assessment: Movement Modeling in Marine Fish Population Dynamics*. Vol. 19  
820 (2011).
- 821 43 Hawkins, S. J. *et al.* Fisheries stocks from an ecological perspective: Disentangling  
822 ecological connectivity from genetic interchange. *Fisheries Research* **179**, 333-341,  
823 doi:<https://doi.org/10.1016/j.fishres.2016.01.015> (2016).
- 824 44 Fuentes-Pardo, A. P. & Ruzzante, D. E. Whole-genome sequencing approaches for  
825 conservation biology: Advantages, limitations and practical recommendations.  
826 *Molecular ecology*, doi:10.1111/mec.14264 (2017).
- 827 45 Moteki, M., Koubbi, P., Pruvost, P., Tavernier, E. & Hulley, P.-A. Spatial distribution of  
828 pelagic fish off Adélie and George V Land, East Antarctica in the austral summer  
829 2008. *Polar Science* **5**, 211-224, doi:10.1016/j.polar.2011.04.001 (2011).

- 830 46 Thompson, A. F., Heywood, K. J., Thorpe, S. E., Renner, A. H. H. & Traslviña, A. Surface  
831 Circulation at the Tip of the Antarctic Peninsula from Drifters. *Journal of Physical*  
832 *Oceanography* **39**, 3-26, doi:10.1175/2008JPO3995.1 (2009).
- 833 47 Orsi, A. H., Nowlin, W. D. & Whitworth, T. On the circulation and stratification of the  
834 Weddell Gyre. *Deep Sea Research Part I: Oceanographic Research Papers* **40**, 169-  
835 203, doi:10.1016/0967-0637(93)90060-G (1993).
- 836 48 Dickens, W. A. *et al.* A new bathymetric compilation for the South Orkney Islands  
837 region, Antarctic Peninsula (49°-39°W to 64°-59°S): Insights into the glacial  
838 development of the continental shelf. *Geochemistry, Geophysics, Geosystems* **15**,  
839 2494-2514, doi:10.1002/2014GC005323 (2014).
- 840 49 Ferguson, J. W. *Population structure and connectivity of an important pelagic forage*  
841 *fish in the Antarctic ecosystem, *Pleuragramma antarcticum*, in relation to large scale*  
842 *circulation.*, (2012).
- 843 50 Azaneu, M., Heywood, K. J., Queste, B. Y. & Thompson, A. F. Variability of the  
844 Antarctic Slope Current System in the Northwestern Weddell Sea. *Journal of Physical*  
845 *Oceanography* **47**, 2977-2997, doi:10.1175/JPO-D-17-0030.1 (2017).
- 846 51 Ashford, J. *et al.* Does large-scale ocean circulation structure life history connectivity  
847 in antarctic toothfish (*Dissostichus mawsoni*)? *Canadian Journal of Fisheries and*  
848 *Aquatic Sciences* **69**, 1903-1919, doi:10.1139/f2012-111 (2012).
- 849 52 Young, E. F. *et al.* Oceanography and life history predict contrasting genetic  
850 population structure in two Antarctic fish species. *Evolutionary Applications* **8**, 486-  
851 509, doi:10.1111/eva.12259 (2015).
- 852 53 Seehaus, T., Marinsek, S., Helm, V., Skvarca, P. & Braun, M. Changes in ice dynamics,  
853 elevation and mass discharge of Dinsmoor-Bombardier-Edgeworth glacier system,  
854 Antarctic Peninsula. *Earth and Planetary Science Letters* **427**, 125-135,  
855 doi:10.1016/j.epsl.2015.06.047 (2015).
- 856 54 Wuite, J. *et al.* Evolution of surface velocities and ice discharge of Larsen B outlet  
857 glaciers from 1995 to 2013. *The Cryosphere* **9**, 957-969, doi:10.5194/tc-9-957-2015  
858 (2015).
- 859 55 Sangrà, P. *et al.* The Bransfield current system. *Deep-Sea Research Part I:*  
860 *Oceanographic Research Papers* **58**, 390-402, doi:10.1016/j.dsr.2011.01.011 (2011).
- 861 56 Nicholls, K. W., Østerhus, S., Makinson, K., Gammelsrød, T. & Fahrbach, E. Ice-ocean  
862 processes over the continental shelf of the southern Weddell Sea, Antarctica: A  
863 review. *Reviews of Geophysics* **47**, RG3003, doi:10.1029/2007RG000250 (2009).
- 864 57 Schröder, M. & Fahrbach, E. On the structure and the transport of the eastern  
865 Weddell Gyre. *Deep-Sea Research Part II: Topical Studies in Oceanography* **46**, 501-  
866 527, doi:10.1016/S0967-0645(98)00112-X (1999).
- 867 58 Meijers, A. J. S. *et al.* Wind-driven export of Weddell Sea slope water. *Journal of*  
868 *Geophysical Research: Oceans* **121**, 7530-7546, doi:10.1002/2016JC011757 (2016).
- 869 59 Youngs, M. K., Thompson, A. F., Flexas, M. M. & Heywood, K. J. Weddell Sea Export  
870 Pathways from Surface Drifters. *Journal of Physical Oceanography* **45**, 1068-1085,  
871 doi:10.1175/JPO-D-14-0103.1 (2015).
- 872 60 Patwary, M. U., Kenchington, E. L., Bird, C. J. & Zouros, E. The use of random  
873 amplified polymorphic DNA markers in genetic studies of the sea scallop *Placopecten*  
874 *magellanicus* (Gmelin, 1791). *Journal of Shellfish Research* **13**, 547-553 (1994).
- 875 61 Molecular Ecology Resources Primer Development Consortium *et al.* Permanent  
876 genetic resources added to Molecular Ecology Resources Database 1 October 2010-

- 877 30 November 2010. *Molecular ecology resources* **11**, 418-421, doi:10.1111/j.1755-  
878 0998.2010.02970.x (2011).
- 879 62 Agostini, C. *et al.* Permanent genetic resources added to molecular ecology  
880 resources database 1 April 2013-31 May 2013. *Molecular ecology resources* **13**, 966-  
881 968, doi:10.1111/1755-0998.12140 (2013).
- 882 63 Amos, W. *et al.* Automated binning of microsatellite alleles: Problems and solutions.  
883 *Molecular Ecology Notes* **7**, 10-14, doi:10.1111/j.1471-8286.2006.01560.x (2007).
- 884 64 Coombs, J. A., Letcher, B. H. & Nislow, K. H. create: a software to create input files  
885 from diploid genotypic data for 52 genetic software programs. *Molecular ecology*  
886 *resources* **8**, 578-580, doi:10.1111/j.1471-8286.2007.02036.x (2008).
- 887 65 Keenan, K., McGinnity, P., Cross, T. F., Crozier, W. W. & Prodöhl, P. A. DiveRsity: An R  
888 package for the estimation and exploration of population genetics parameters and  
889 their associated errors. *Methods in Ecology and Evolution* **4**, 782-788,  
890 doi:10.1111/2041-210X.12067 (2013).
- 891 66 R: A language and environment for statistical computing. (R Foundation for  
892 Statistical Computing, Vienna, Austria, 2016).
- 893 67 Van Oosterhout, C., Hutchinson, W. F., Wills, D. P. M. & Shipley, P. MICRO-CHECKER:  
894 Software for identifying and correcting genotyping errors in microsatellite data.  
895 *Molecular Ecology Notes* **4**, 535-538, doi:10.1111/j.1471-8286.2004.00684.x (2004).
- 896 68 Rousset, F. GENEPOP'007: A complete re-implementation of the GENEPOP software  
897 for Windows and Linux. *Molecular ecology resources* **8**, 103-106, doi:10.1111/j.1471-  
898 8286.2007.01931.x (2008).
- 899 69 Carvajal-Rodriguez, A. & de Uña-Alvarez, J. Assessing Significance in High-Throughput  
900 Experiments by Sequential Goodness of Fit and q-Value Estimation. *PloS one* **6**,  
901 e24700, doi:10.1371/journal.pone.0024700 (2011).
- 902 70 Antao, T., Lopes, A., Lopes, R. J., Beja-Pereira, A. & Luikart, G. LOSITAN: A workbench  
903 to detect molecular adaptation based on a Fst-outlier method. *BMC Bioinformatics*  
904 **9**, 323, doi:10.1186/1471-2105-9-323 (2008).
- 905 71 Excoffier, L. & Lischer, H. E. L. Arlequin suite ver 3.5: a new series of programs to  
906 perform population genetics analyses under Linux and Windows. *Molecular ecology*  
907 *resources* **10**, 564-567, doi:10.1111/j.1755-0998.2010.02847.x (2010).
- 908 72 Excoffier, L., Hofer, T. & Foll, M. Detecting loci under selection in a hierarchically  
909 structured population. *Heredity* **103**, 285-298, doi:10.1038/hdy.2009.74 (2009).
- 910 73 Jombart, T. ADEGENET: A R package for the multivariate analysis of genetic markers.  
911 *Bioinformatics* **24**, 1403-1405, doi:10.1093/bioinformatics/btn129 (2008).
- 912 74 Peakall, R. O. D. & Smouse, P. E. genalex 6: genetic analysis in Excel. Population  
913 genetic software for teaching and research. *Molecular Ecology Notes* **6**, 288-295,  
914 doi:10.1111/j.1471-8286.2005.01155.x (2006).
- 915 75 Peakall, R. & Smouse, P. E. GenALEX 6.5: Genetic analysis in Excel. Population genetic  
916 software for teaching and research-an update. *Bioinformatics* **28**, 2537-2539,  
917 doi:10.1093/bioinformatics/bts460 (2012).
- 918 76 Duchesne, P. & Turgeon, J. FLOCK: a method for quick mapping of admixture without  
919 source samples. *Molecular ecology resources* **9**, 1333-1344, doi:10.1111/j.1755-  
920 0998.2009.02571.x (2009).
- 921 77 Duchesne, P. & Turgeon, J. FLOCK provides reliable solutions to the "number of  
922 populations" problem. *Journal of Heredity* **103**, 734-743, doi:10.1093/jhered/ess038  
923 (2012).

- 924 78 Weir, B. S. & Cockerham, C. C. Estimating F-Statistics for the Analysis of Population  
925 Structure. *Evolution* **38**, 1358-1370, doi:10.2307/2408641 (1984).
- 926 79 Matsuoka, K., Skoglund, A. & Roth, G. (Norwegian Polar Institute, 2018).
- 927 80 QGIS Geographic Information System. Open Source Geospatial Foundation Project.  
928 (2018).
- 929 81 Donnelly, J. & Torres, J. J. Pelagic fishes in the Marguerite Bay region of the West  
930 Antarctic Peninsula continental shelf. *Deep-Sea Research Part II: Topical Studies in*  
931 *Oceanography* **55**, 523-539, doi:10.1016/j.dsr2.2007.11.015 (2008).
- 932 82 Ferguson, J. *et al.* Connectivity and population structure in *Pleuragramma*  
933 *antarcticum*. *CCAMLR Scientific Papers Working Group on Fish Stock Assessment WG-*  
934 **FSA-11/19** (2011).
- 935 83 Ruck, K. E., Steinberg, D. K. & Canuel, E. A. Regional differences in quality of krill and  
936 fish as prey along the Western Antarctic Peninsula. *Marine Ecology Progress Series*  
937 **509**, 39-55, doi:10.3354/meps10868 (2014).
- 938

Supplementary Information **Caccavo *et al.* 2018**

1 **Supplementary Information** Along-shelf connectivity and circumpolar gene flow in Antarctic silverfish (*Pleuragramma antarctica*)

2  
3 Jilda Alicia Caccavo<sup>1\*</sup>, Chiara Papetti<sup>1,2</sup>, Maj Wetjen<sup>3</sup>, Rainer Knust<sup>4</sup>, Julian R. Ashford<sup>5</sup>, Lorenzo Zane<sup>1,2</sup>

4  
5 <sup>1</sup> Department of Biology, University of Padua, Via G. Colombo 3, Padua 35121, Italy.

6 <sup>2</sup> Consorzio Nazionale Interuniversitario per le Scienze del Mare (CoNISMa), Piazzale Flaminio 9, Rome 00196, Italy.

7 <sup>3</sup> Institute for Environmental Sciences, University of Koblenz-Landau, Fortstraße 7, Landau 76829, Germany.

8 <sup>4</sup> Helmholtz Center for Polar and Marine Research, Alfred Wegener Institute, Am Alten Hafen 26, Bremerhaven 27568, Germany.

9 <sup>5</sup> Department of Ocean, Earth and Atmospheric Sciences, Center for Quantitative Fisheries Ecology, Old Dominion University, 800 West 46<sup>th</sup>  
10 Street, Norfolk, VA 23508, United States.

11

12 **Corresponding author**

13 \* Jilda Alicia Caccavo, [ergo@jildacaccavo.com](mailto:ergo@jildacaccavo.com), ORCID: 0000-0002-8172-7855

14

15

16

17

18

19

20

21

22

23



**Table S1** Primer sequences and amplification conditions used to amplify 16 EST-linked microsatellite loci in *Pleuragramma antarctica*. Locus names, repeat motifs, primer pair sequences, fluorescent dye of forward primer, size range of fragments in base pairs, annealing temperature for single-locus amplification, and the respective multiplex reaction set are shown (adapted from Agostini et al.<sup>1</sup>).

Locus	Motif	Primer sequences (5' - 3')	Dye	Size range	T <sup>a</sup> (°C)	Locus set for multiplexing
Ch10105 <sup>b</sup>	(CTG) <sub>12</sub>	F: TGC CTT GGT TAG GAT TAA ACG T R: AGA AGT GCT CCA TCA AGT CCA	6-FAM	96 - 131	57	1
Ch10441 <sup>b</sup>	(CA) <sub>10</sub>	F: GTC CTT ACC TGG CAG TGC AGA R: GCA CAT CAG TCC AAA ATC GGT G	PET	110 - 162	60	2
Ch10857 <sup>b</sup>	(CA) <sub>9</sub>	F: GCT TAA ATC ACC ATG TGC CCA R: TGG ACA TGA ATG TAC CAA AAC G	6-FAM	161 - 195	57	1
Ch11230 <sup>b</sup>	(GA) <sub>7</sub>	F: ATC ACA CAG CTG ACT GGG GCT R: TGA GAC TCG TCC GCG AAT GGA	NED	90 - 116	60	2
Ch11483 <sup>b</sup>	(TAA) <sub>7</sub>	F: ATC AAA CTG AAC AGC CTG TGT R: TGG AGA ACA GGA ATG GAC AGA	NED	124 - 168	57	2
Ch126 <sup>c</sup>	(AAT) <sub>7</sub>	F: CGG TTT TTA TGC ATG TTG CCA R: ACT GCT CAT TCA CAC TGG TTC	NED	264 - 282	56	1
Ch13222 <sup>b</sup>	(TTG) <sub>6</sub>	F: GTC CCA TGG TGA CTG ATA GGT R: ACG AGT CAA TGT AAC CGG AAG	PET	82 - 98	57	1
Ch17977 <sup>b</sup>	(GAT) <sub>8</sub>	F: TTG ACT GAC AGC TTG GGT GCA R: GAA TGA GCC ATG TTG AGC CC	6-FAM	162 - 234	57	2
Ch18085 <sup>b</sup>	(TGA) <sub>6</sub>	F: TTT AGG GGT GGC ACA TTG GAC R: ACA AAC CTT CTC CTT GTC TTC T	VIC	98 - 137	57	1
Ch19846 <sup>b</sup>	(GT) <sub>14</sub>	F: CGA CCT TTG AGA AAG GCG GCA R: CGA CGT GTA TCA CAA GGG TCA	6-FAM	116 - 141	60	2
Ch24332 <sup>b</sup>	(GCA) <sub>8</sub>	F: ATC GGT TGT CGT CCT CCA CAC R: GGC TGT TTC TGG ATC AGC GGT	6-FAM	67 - 96	60	2
Ch25478 <sup>b</sup>	(AC) <sub>8</sub>	F: ACA GTG TTG TCT TGG AGA GGT R: GGA GAG AAG TAC ATG AGG AGG A	PET	143 - 175	57	2
Ch2931 <sup>b</sup>	(TCT) <sub>8</sub> t-(TTC) <sub>6</sub>	F: GGG CTT TCA GGA GCA TCG GGA R: ACT TGA ACC TGA CGT GGC AAC	VIC	79 - 132	60	2
Ch4796 <sup>b</sup>	(GAT) <sub>8</sub>	F: ACA ATG GTT GGT GAG AGC TCC R: TGA GTT AAG CAG AAC AAG TGC	VIC	156 - 208	57	2
Ch520 <sup>b</sup>	(TC) <sub>7</sub>	F: GGA ACA ACT TGA GCC AAG ACA R: CCA TAA AAG TGC ATC ATC GCT	6-FAM	259 - 273	57	1
Ch623 <sup>c</sup>	(AAC) <sub>7</sub>	F: GCT GTT TGA TTC CCT CGT GAG G R: AAA AGT GGT CCT CCG CTG CAG T	PET	174 - 295	62	1

<sup>a</sup> Reported annealing temperature refers to single-locus PCR. Loci were amplified together in two multiplex reactions. Multiplex PCR reaction volume was 10 µL, containing 1x QIAGEN Multiplex PCR Master mix (HotStartTaq DNA Polymerase, Multiplex PCR Buffer, dNTP Mix; QIAGEN, Hilden, Germany), 0.2 µM primer mix and 100 ng of genomic DNA. The PCR amplification profile for all loci consisted of: (1) an initial activation step of 15 min at 95 °C; (2) 30 cycles of denaturation at 94 °C for 30 s, annealing at 57 °C for 90 s and extension at 72 °C for 60 s; and (3) a final extension of 30 min at 60 °C.

<sup>b</sup> Molecular Ecology Resources Primer Development Consortium et al.<sup>2</sup>

<sup>c</sup> Molecular Ecology Resources Primer Development Consortium et al.<sup>3</sup>

**Table S2** Genetic variability of *Pleurogramma antarctica* for each locus across all nineteen sampling locations. Sample size ( $n$ ), number of alleles ( $N_A$ ), % of total observed alleles per locus per sampling location, allelic richness based on a minimum sample size of 14 individuals ( $A_R$ ), observed heterozygosity ( $H_O$ ), unbiased heterozygosity ( $H_E$ ) and probability of deviation from Hardy-Weinberg equilibrium ( $pHWE$ ) are shown. Values in bold indicate significant HWE deviations after correction for multiple tests as implemented in SGoF+<sup>4</sup> (threshold for significance with 304 comparisons 0.008). Sampling location acronyms are as in Table 1.

Locus	CI10								MB01						MB02						
	$n$	$N_A$	%	$A_R$	$H_O$	$H_E$	$pHWE$	$n$	$N_A$	%	$A_R$	$H_O$	$H_E$	$pHWE$	$n$	$N_A$	%	$A_R$	$H_O$	$H_E$	$pHWE$
<b>Ch126</b>	60	3	42.86	2.21	0.45	0.51	0.300	28	3	42.86	2.38	0.46	0.51	0.711	49	4	57.14	3.00	0.59	0.55	0.763
<b>Ch520</b>	60	4	50.00	3.09	0.33	0.38	0.488	28	4	50.00	3.38	0.39	0.51	0.020	49	5	62.50	3.70	0.47	0.48	0.754
<b>Ch623</b>	60	23	69.70	14.35	0.92	0.94	<b>0.000</b>	28	20	60.61	12.75	0.96	0.92	0.219	49	20	60.61	12.82	0.90	0.92	0.975
<b>Ch10105</b>	60	6	66.67	3.54	0.30	0.31	0.146	28	3	33.33	1.86	0.07	0.07	1.000	49	5	55.56	2.89	0.24	0.24	0.182
<b>Ch10857</b>	60	9	52.94	6.34	0.68	0.69	0.903	28	9	52.94	6.03	0.54	0.66	0.091	49	7	41.18	5.59	0.57	0.67	0.702
<b>Ch13222</b>	60	3	50.00	2.26	0.17	0.16	1.000	28	2	33.33	1.94	0.18	0.16	1.000	49	4	66.67	1.75	0.06	0.06	1.000
<b>Ch18085</b>	60	10	71.43	7.29	0.83	0.83	0.852	28	9	64.29	6.98	0.86	0.82	0.790	49	9	64.29	7.02	0.86	0.83	0.998
<b>Ch2931</b>	60	10	58.82	6.96	0.73	0.83	0.891	28	10	58.82	7.55	0.86	0.82	0.165	49	11	64.71	7.09	0.84	0.82	0.370
<b>Ch4796</b>	60	13	72.22	9.07	0.75	0.87	<b>0.002</b>	28	12	66.67	9.71	0.96	0.88	0.985	49	14	77.78	10.09	0.94	0.89	0.793
<b>Ch10441</b>	60	9	39.13	5.36	0.65	0.65	0.643	28	10	43.48	7.17	0.86	0.76	0.535	49	9	39.13	6.00	0.61	0.68	0.524
<b>Ch11230</b>	60	7	50.00	4.90	0.77	0.72	0.744	28	5	35.71	4.69	0.71	0.71	0.996	49	7	50.00	5.00	0.78	0.72	1.000
<b>Ch11483</b>	60	10	66.67	5.43	0.47	0.56	0.675	28	9	60.00	6.26	0.57	0.64	0.409	49	9	60.00	4.67	0.45	0.46	0.096
<b>Ch17977</b>	60	8	53.33	5.08	0.58	0.63	0.722	28	4	26.67	3.60	0.57	0.56	0.955	49	7	46.67	4.60	0.65	0.62	0.509
<b>Ch19846</b>	60	8	66.67	6.26	0.70	0.78	0.690	28	8	66.67	6.56	0.86	0.78	0.996	49	8	66.67	6.52	0.86	0.80	0.941
<b>Ch24332</b>	60	6	60.00	4.02	0.60	0.62	0.096	28	5	50.00	3.92	0.57	0.60	0.320	49	5	50.00	3.70	0.73	0.62	0.184
<b>Ch25478</b>	60	4	25.00	2.96	0.57	0.56	0.422	28	4	25.00	3.04	0.46	0.56	0.036	49	6	37.50	3.69	0.61	0.63	0.341
<b>Overall</b>	60	133	55.97	5.57	0.59	0.63	0.025	28	117	48.15	5.49	0.62	0.62	0.443	49	130	56.28	5.51	0.64	0.62	0.938

Locus	MB10								MB11								JI07							
	<i>n</i>	<i>N<sub>A</sub></i>	%	<i>A<sub>R</sub></i>	<i>H<sub>O</sub></i>	<i>H<sub>E</sub></i>	<i>pHWE</i>	<i>n</i>	<i>N<sub>A</sub></i>	%	<i>A<sub>R</sub></i>	<i>H<sub>O</sub></i>	<i>H<sub>E</sub></i>	<i>pHWE</i>	<i>n</i>	<i>N<sub>A</sub></i>	%	<i>A<sub>R</sub></i>	<i>H<sub>O</sub></i>	<i>H<sub>E</sub></i>	<i>pHWE</i>			
Ch126	60	4	57.14	2.40	0.43	0.52	0.205	83	3	42.86	2.77	0.58	0.55	0.661	34	5	71.43	3.22	0.56	0.54	1.000			
Ch520	60	5	62.50	4.07	0.62	0.56	0.855	83	5	62.50	3.58	0.45	0.40	0.712	34	3	37.50	2.95	0.50	0.41	0.362			
Ch623	60	24	72.73	13.71	0.93	0.93	0.038	83	25	75.76	13.58	0.89	0.93	0.012	34	22	66.67	13.01	0.97	0.92	0.106			
Ch10105	60	4	44.44	2.88	0.22	0.21	0.594	83	5	55.56	3.16	0.25	0.23	0.680	34	4	44.44	2.99	0.24	0.22	1.000			
Ch10857	60	11	64.71	6.36	0.75	0.73	0.121	83	10	58.82	6.32	0.73	0.71	0.937	34	7	41.18	5.29	0.76	0.74	0.716			
Ch13222	60	4	66.67	2.40	0.25	0.22	1.000	83	3	50.00	1.94	0.10	0.10	<b>0.000</b>	34	3	50.00	2.31	0.21	0.23	1.000			
Ch18085	60	10	71.43	7.21	0.83	0.83	0.171	83	11	78.57	7.05	0.87	0.82	0.959	34	10	71.43	7.47	0.76	0.82	0.715			
Ch2931	60	10	58.82	7.52	0.83	0.81	0.998	83	10	58.82	6.91	0.73	0.81	0.279	34	10	58.82	7.61	0.71	0.84	0.333			
Ch4796	60	13	72.22	9.37	0.82	0.88	0.996	83	14	77.78	10.72	0.93	0.90	1.000	34	11	61.11	9.11	1.00	0.88	1.000			
Ch10441	60	11	47.83	7.20	0.73	0.71	0.436	83	12	52.17	6.09	0.69	0.68	0.989	34	9	39.13	5.85	0.74	0.66	0.289			
Ch11230	60	8	57.14	5.68	0.68	0.76	0.986	83	6	42.86	4.64	0.80	0.73	0.603	34	7	50.00	5.71	0.88	0.76	0.547			
Ch11483	60	8	53.33	5.20	0.65	0.57	0.597	83	8	53.33	4.26	0.55	0.56	0.461	34	5	33.33	3.77	0.59	0.48	0.606			
Ch17977	60	9	60.00	5.13	0.62	0.66	<b>0.000</b>	83	10	66.67	4.85	0.58	0.58	0.013	34	7	46.67	5.73	0.68	0.69	0.828			
Ch19846	60	8	66.67	6.45	0.87	0.80	0.216	83	8	66.67	6.04	0.71	0.78	0.618	34	7	58.33	5.72	0.76	0.77	0.385			
Ch24332	60	6	60.00	4.64	0.60	0.65	0.934	83	7	70.00	4.55	0.69	0.63	0.914	34	4	40.00	3.79	0.62	0.64	0.800			
Ch25478	60	6	37.50	4.43	0.68	0.64	0.018	83	8	50.00	4.45	0.64	0.63	0.686	34	7	43.75	4.12	0.47	0.61	0.019			
Overall	60	141	59.57	5.92	0.66	0.65	0.017	83	145	60.15	5.68	0.64	0.63	0.076	34	121	50.86	5.54	0.65	0.64	0.791			

Locus	JI10							JI12							SSI96						
	<i>n</i>	<i>N<sub>A</sub></i>	%	<i>A<sub>R</sub></i>	<i>H<sub>O</sub></i>	<i>H<sub>E</sub></i>	<i>pHWE</i>	<i>n</i>	<i>N<sub>A</sub></i>	%	<i>A<sub>R</sub></i>	<i>H<sub>O</sub></i>	<i>H<sub>E</sub></i>	<i>pHWE</i>	<i>n</i>	<i>N<sub>A</sub></i>	%	<i>A<sub>R</sub></i>	<i>H<sub>O</sub></i>	<i>H<sub>E</sub></i>	<i>pHWE</i>
<b>Ch126</b>	148	6	85.71	3.08	0.63	0.55	0.384	54	5	71.43	3.00	0.50	0.54	1.000	14	2	28.57	2.00	0.57	0.49	0.620
<b>Ch520</b>	148	8	100.00	4.15	0.57	0.58	0.713	54	6	75.00	3.87	0.44	0.51	0.210	14	5	62.50	4.15	0.50	0.42	1.000
<b>Ch623</b>	148	28	84.85	13.77	0.91	0.94	0.574	54	20	60.61	12.56	0.80	0.92	0.092	14	15	45.45	11.59	0.86	0.91	<b>0.000</b>
<b>Ch10105</b>	148	6	66.67	3.72	0.32	0.37	0.074	54	5	55.56	3.35	0.20	0.25	0.359	14	3	33.33	2.66	0.36	0.30	1.000
<b>Ch10857</b>	148	12	70.59	6.60	0.70	0.74	0.858	54	11	64.71	6.33	0.74	0.71	0.090	14	5	29.41	4.59	0.64	0.69	0.170
<b>Ch13222</b>	148	4	66.67	2.26	0.16	0.17	0.718	54	3	50.00	2.10	0.15	0.14	1.000	14	3	50.00	2.29	0.14	0.14	1.000
<b>Ch18085</b>	148	12	85.71	7.69	0.84	0.85	0.931	54	8	57.14	6.78	0.85	0.81	0.507	14	6	42.86	5.74	0.71	0.80	0.879
<b>Ch2931</b>	148	10	58.82	7.02	0.78	0.81	0.297	54	8	47.06	6.19	0.67	0.82	0.999	14	7	41.18	6.39	0.79	0.82	0.475
<b>Ch4796</b>	148	14	77.78	9.56	0.82	0.89	0.491	54	12	66.67	8.86	0.98	0.87	0.991	14	11	61.11	8.89	0.93	0.86	0.009
<b>Ch10441</b>	148	17	73.91	6.54	0.67	0.70	<b>0.000</b>	54	7	30.43	5.13	0.67	0.66	0.910	14	6	26.09	5.48	0.64	0.72	0.136
<b>Ch11230</b>	148	9	64.29	5.23	0.74	0.74	0.860	54	7	50.00	5.18	0.69	0.70	0.222	14	5	35.71	4.59	0.57	0.73	0.842
<b>Ch11483</b>	148	12	80.00	5.06	0.55	0.58	<b>0.000</b>	54	8	53.33	4.43	0.54	0.57	0.739	14	5	33.33	3.80	0.29	0.37	0.082
<b>Ch17977</b>	148	9	60.00	5.20	0.60	0.63	0.035	54	8	53.33	5.52	0.63	0.63	0.308	14	4	26.67	3.53	0.64	0.56	0.663
<b>Ch19846</b>	148	10	83.33	6.36	0.80	0.79	0.250	54	8	66.67	6.50	0.78	0.79	0.386	14	8	66.67	7.07	0.86	0.83	0.811
<b>Ch24332</b>	148	8	80.00	4.87	0.62	0.65	0.842	54	6	60.00	3.80	0.57	0.59	0.013	14	5	50.00	3.97	0.71	0.62	<b>0.006</b>
<b>Ch25478</b>	148	9	56.25	4.45	0.67	0.63	0.267	54	5	31.25	3.39	0.56	0.59	0.023	14	3	18.75	2.65	0.50	0.53	0.594
<b>Overall</b>	148	174	74.66	5.97	0.65	0.66	<b>0.001</b>	54	127	55.82	5.44	0.61	0.63	0.146	14	93	40.73	4.96	0.61	0.61	<b>0.006</b>

Locus	SOI11								LB07								LB11							
	<i>n</i>	<i>N<sub>A</sub></i>	%	<i>A<sub>R</sub></i>	<i>H<sub>O</sub></i>	<i>H<sub>E</sub></i>	<i>pHWE</i>	<i>n</i>	<i>N<sub>A</sub></i>	%	<i>A<sub>R</sub></i>	<i>H<sub>O</sub></i>	<i>H<sub>E</sub></i>	<i>pHWE</i>	<i>n</i>	<i>N<sub>A</sub></i>	%	<i>A<sub>R</sub></i>	<i>H<sub>O</sub></i>	<i>H<sub>E</sub></i>	<i>pHWE</i>			
Ch126	47	3	42.86	2.24	0.40	0.50	0.140	46	3	42.86	2.72	0.65	0.49	0.152	52	3	42.86	2.57	0.60	0.52	0.879			
Ch520	47	6	75.00	4.54	0.51	0.60	0.108	46	5	62.50	3.96	0.50	0.60	0.328	52	7	87.50	4.52	0.58	0.57	0.948			
Ch623	47	18	54.55	12.21	0.91	0.92	1.000	46	20	60.61	12.82	0.87	0.93	0.997	52	21	63.64	13.57	0.88	0.93	1.000			
Ch10105	47	6	66.67	3.93	0.36	0.35	0.329	46	4	44.44	2.66	0.17	0.18	<b>0.001</b>	52	5	55.56	2.88	0.23	0.21	1.000			
Ch10857	47	9	52.94	6.25	0.72	0.66	0.938	46	9	52.94	5.74	0.54	0.63	0.816	52	10	58.82	6.23	0.73	0.74	0.713			
Ch13222	47	3	50.00	2.24	0.19	0.21	1.000	46	3	50.00	1.86	0.04	0.12	<b>0.001</b>	52	2	33.33	1.91	0.15	0.14	1.000			
Ch18085	47	8	57.14	6.59	0.91	0.80	0.997	46	8	57.14	6.69	0.83	0.82	0.861	52	9	64.29	7.20	0.88	0.82	0.869			
Ch2931	47	9	52.94	6.75	0.70	0.82	0.444	46	11	64.71	7.75	0.78	0.83	0.939	52	9	52.94	6.96	0.77	0.83	0.172			
Ch4796	47	12	66.67	8.74	0.79	0.87	0.902	46	10	55.56	7.88	0.91	0.86	0.921	52	12	66.67	9.13	0.92	0.88	1.000			
Ch10441	47	7	30.43	4.88	0.49	0.56	0.111	46	11	47.83	6.74	0.70	0.70	0.142	52	10	43.48	6.07	0.58	0.63	0.046			
Ch11230	47	6	42.86	4.79	0.64	0.68	0.847	46	6	42.86	5.12	0.70	0.74	0.781	52	7	50.00	5.19	0.73	0.72	0.105			
Ch11483	47	7	46.67	4.85	0.60	0.55	0.764	46	7	46.67	4.63	0.61	0.55	0.597	52	7	46.67	4.49	0.48	0.50	<b>0.001</b>			
Ch17977	47	8	53.33	5.58	0.60	0.59	0.728	46	6	40.00	4.38	0.54	0.57	0.982	52	8	53.33	4.82	0.67	0.64	0.996			
Ch19846	47	7	58.33	5.79	0.66	0.73	0.744	46	9	75.00	6.46	0.83	0.78	0.587	52	10	83.33	7.11	0.88	0.82	0.852			
Ch24332	47	8	80.00	4.81	0.64	0.67	0.757	46	6	60.00	4.35	0.57	0.65	0.579	52	8	80.00	4.97	0.60	0.69	0.455			
Ch25478	47	8	50.00	4.50	0.55	0.64	<b>0.000</b>	46	5	31.25	3.79	0.67	0.59	0.784	52	7	43.75	3.82	0.50	0.59	<b>0.005</b>			
Overall	47	125	55.02	5.54	0.61	0.63	0.213	46	123	52.15	5.47	0.62	0.63	0.114	52	135	57.89	5.71	0.64	0.64	0.106			

Locus	FT14								HB89								HB91							
	<i>n</i>	<i>N<sub>A</sub></i>	%	<i>A<sub>R</sub></i>	<i>H<sub>O</sub></i>	<i>H<sub>E</sub></i>	<i>pHWE</i>	<i>n</i>	<i>N<sub>A</sub></i>	%	<i>A<sub>R</sub></i>	<i>H<sub>O</sub></i>	<i>H<sub>E</sub></i>	<i>pHWE</i>	<i>n</i>	<i>N<sub>A</sub></i>	%	<i>A<sub>R</sub></i>	<i>H<sub>O</sub></i>	<i>H<sub>E</sub></i>	<i>pHWE</i>			
Ch126	50	4	57.14	3.07	0.50	0.56	1.000	19	2	28.57	2.00	0.53	0.49	1.000	41	3	42.86	2.49	0.51	0.51	1.000			
Ch520	50	5	62.50	3.79	0.56	0.49	0.791	19	4	50.00	3.91	0.63	0.60	0.228	41	7	87.50	4.67	0.51	0.57	<b>0.000</b>			
Ch623	50	17	51.52	12.04	0.96	0.92	0.025	19	11	33.33	8.73	0.74	0.85	0.516	41	21	63.64	13.07	0.98	0.93	0.569			
Ch10105	50	4	44.44	2.69	0.18	0.17	1.000	19	4	44.44	3.69	0.47	0.46	0.545	41	5	55.56	3.21	0.27	0.28	0.364			
Ch10857	50	8	47.06	5.62	0.58	0.70	0.389	19	6	35.29	5.32	0.74	0.65	0.487	41	8	47.06	6.51	0.78	0.75	0.773			
Ch13222	50	2	33.33	1.99	0.30	0.26	0.046	19	3	50.00	2.36	0.16	0.15	1.000	41	4	66.67	2.45	0.15	0.14	1.000			
Ch18085	50	10	71.43	7.23	0.72	0.83	0.121	19	9	64.29	7.46	0.89	0.83	0.534	41	7	50.00	6.59	0.78	0.82	0.999			
Ch2931	50	11	64.71	7.55	0.80	0.83	0.553	19	8	47.06	7.06	0.63	0.82	0.574	41	9	52.94	6.72	0.63	0.81	0.249			
Ch4796	50	13	72.22	9.41	0.96	0.88	0.999	19	9	50.00	7.77	0.84	0.86	1.000	41	13	72.22	9.69	0.98	0.88	1.000			
Ch10441	50	8	34.78	5.72	0.62	0.64	0.855	19	8	34.78	6.19	0.84	0.73	0.102	41	7	30.43	5.15	0.46	0.62	<b>0.000</b>			
Ch11230	50	6	42.86	4.86	0.64	0.70	0.811	19	6	42.86	5.11	0.63	0.71	0.884	41	7	50.00	5.55	0.71	0.73	0.698			
Ch11483	50	8	53.33	5.34	0.52	0.54	0.772	19	6	40.00	4.42	0.47	0.58	<b>0.000</b>	41	6	40.00	4.06	0.56	0.54	0.543			
Ch17977	50	8	53.33	5.08	0.58	0.59	0.082	19	4	26.67	3.70	0.58	0.54	0.690	41	6	40.00	4.47	0.56	0.63	0.419			
Ch19846	50	9	75.00	6.60	0.74	0.81	0.999	19	8	66.67	6.63	0.89	0.80	0.075	41	10	83.33	7.17	0.80	0.81	0.996			
Ch24332	50	8	80.00	4.91	0.68	0.65	1.000	19	4	40.00	3.52	0.42	0.63	0.011	41	6	60.00	4.31	0.76	0.64	0.666			
Ch25478	50	8	50.00	4.53	0.66	0.62	0.975	19	6	37.50	4.13	0.47	0.55	1.000	41	7	43.75	4.47	0.68	0.64	0.542			
Overall	50	129	55.85	5.65	0.62	0.64	0.689	19	98	43.22	5.12	0.62	0.64	0.039	41	126	55.37	5.66	0.63	0.64	0.037			

Locus	HB14								AB14								RS96							
	<i>n</i>	<i>N<sub>A</sub></i>	%	<i>A<sub>R</sub></i>	<i>H<sub>O</sub></i>	<i>H<sub>E</sub></i>	<i>pHWE</i>	<i>n</i>	<i>N<sub>A</sub></i>	%	<i>A<sub>R</sub></i>	<i>H<sub>O</sub></i>	<i>H<sub>E</sub></i>	<i>pHWE</i>	<i>n</i>	<i>N<sub>A</sub></i>	%	<i>A<sub>R</sub></i>	<i>H<sub>O</sub></i>	<i>H<sub>E</sub></i>	<i>pHWE</i>			
Ch126	82	5	71.43	2.81	0.57	0.53	0.017	25	3	42.86	2.84	0.60	0.55	1.000	91	3	42.86	2.62	0.55	0.52	0.331			
Ch520	82	7	87.50	4.23	0.57	0.54	0.391	25	5	62.50	3.76	0.48	0.47	<b>0.000</b>	91	7	87.50	4.04	0.58	0.52	0.069			
Ch623	82	21	63.64	12.94	0.87	0.93	0.946	25	15	45.45	11.64	0.96	0.91	1.000	91	23	69.70	13.70	0.88	0.93	0.988			
Ch10105	82	4	44.44	3.18	0.27	0.27	0.159	25	4	44.44	2.33	0.12	0.12	1.000	91	5	55.56	3.27	0.25	0.26	0.600			
Ch10857	82	8	47.06	5.38	0.57	0.69	0.931	25	8	47.06	6.06	0.76	0.73	0.480	91	11	64.71	6.70	0.71	0.76	0.625			
Ch13222	82	4	66.67	2.50	0.20	0.20	1.000	25	2	33.33	1.96	0.16	0.21	0.335	91	3	50.00	2.20	0.16	0.18	0.203			
Ch18085	82	9	64.29	7.30	0.83	0.83	0.996	25	7	50.00	6.24	0.84	0.81	0.997	91	11	78.57	7.69	0.89	0.84	1.000			
Ch2931	82	12	70.59	6.92	0.73	0.81	0.795	25	9	52.94	7.06	0.80	0.83	0.008	91	12	70.59	6.85	0.68	0.79	0.630			
Ch4796	82	15	83.33	9.70	0.89	0.88	0.166	25	10	55.56	7.67	0.88	0.85	<b>0.000</b>	91	14	77.78	9.73	0.91	0.89	1.000			
Ch10441	82	10	43.48	5.54	0.48	0.64	0.010	25	7	30.43	5.48	0.68	0.60	0.973	91	11	47.83	6.12	0.67	0.71	0.827			
Ch11230	82	8	57.14	5.14	0.67	0.72	0.978	25	6	42.86	4.59	0.68	0.70	<b>0.004</b>	91	7	50.00	4.79	0.70	0.68	0.831			
Ch11483	82	10	66.67	4.60	0.54	0.54	0.543	25	6	40.00	4.71	0.68	0.58	0.308	91	9	60.00	4.82	0.55	0.55	0.966			
Ch17977	82	7	46.67	4.71	0.62	0.61	0.777	25	7	46.67	5.08	0.76	0.63	0.021	91	9	60.00	5.22	0.62	0.62	0.940			
Ch19846	82	10	83.33	7.23	0.78	0.82	0.477	25	7	58.33	6.13	0.68	0.79	0.088	91	10	83.33	6.88	0.87	0.80	0.997			
Ch24332	82	8	80.00	4.72	0.60	0.65	0.315	25	5	50.00	3.57	0.64	0.57	0.422	91	10	100.00	4.87	0.64	0.67	0.564			
Ch25478	82	9	56.25	3.70	0.50	0.58	0.208	25	6	37.50	4.21	0.68	0.62	<b>0.005</b>	91	9	56.25	4.37	0.63	0.61	0.970			
Overall	82	147	64.53	5.66	0.61	0.64	0.288	25	107	46.25	5.21	0.65	0.62	<b>0.000</b>	91	154	65.92	5.87	0.64	0.65	0.993			

Locus	<i>n</i>	<i>N<sub>A</sub></i>	%	RS97			<i>pHWE</i>
				<i>A<sub>R</sub></i>	<i>H<sub>O</sub></i>	<i>H<sub>E</sub></i>	
Ch126	84	3	42.86	2.60	0.54	0.53	1.000
Ch520	84	6	75.00	3.88	0.42	0.48	0.393
Ch623	84	24	72.73	13.54	0.93	0.93	0.786
Ch10105	84	4	44.44	3.12	0.26	0.25	0.759
Ch10857	84	10	58.82	6.29	0.73	0.76	0.065
Ch13222	84	3	50.00	2.27	0.23	0.23	0.311
Ch18085	84	10	71.43	7.83	0.86	0.83	1.000
Ch2931	84	9	52.94	6.44	0.68	0.79	0.883
Ch4796	84	15	83.33	9.44	0.83	0.87	0.398
Ch10441	84	10	43.48	6.04	0.60	0.64	0.517
Ch11230	84	8	57.14	4.72	0.71	0.68	<b>0.002</b>
Ch11483	84	8	53.33	4.19	0.55	0.51	0.740
Ch17977	84	8	53.33	5.09	0.57	0.62	0.377
Ch19846	84	10	83.33	6.88	0.82	0.80	0.870
Ch24332	84	7	70.00	4.35	0.68	0.64	1.000
Ch25478	84	8	50.00	4.01	0.60	0.60	0.111
Overall	84	143	60.13	5.67	0.62	0.64	0.386

25  
26  
27  
28  
29  
30  
31  
32  
33  
34  
35



36

**Table S3** Analysis of Molecular Variance (AMOVA) among 19 populations of *P. antarctica*, among six groups based on geographic origin, and among individuals within populations. Global results for fixation indices  $F_{ST}$ ,  $F_{SC}$ , and  $F_{CT}$  reported in upper table, results by locus reported in lower table.

Source of variation	df	Proportion of variation	P-value	Fixation Indices	
Among groups	5	0.16	0.00218 ± 0.00050	$F_{ST}$	0.00161
Among populations within groups	13	0.00	0.63050 ± 0.00429	$F_{SC}$	0.00002
Among individuals within populations	2115	99.84	0.00644 ± 0.00087	$F_{CT}$	0.00159

Locus	$F_{SC}$	P-value	$F_{ST}$	P-value	$F_{SC}$	P-value
Ch126	0.00222	0.21436	0.00322	0.11287	0.00100	0.31168
Ch520	0.00272	0.14782	0.00583	0.01525	0.00311	0.16238
Ch623	-0.00118	0.93178	-0.00083	0.93248	0.00035	0.18139
Ch10105	0.00264	0.16455	0.00529	0.02604	0.00266	0.18634
Ch10857	0.00030	0.50772	0.00173	0.24465	0.00143	0.14436
Ch13222	0.00253	0.21772	0.00267	0.19158	0.00014	0.44020
Ch18085	-0.00079	0.67248	-0.00131	0.81139	-0.00051	0.79634
Ch2931	0.00256	0.18356	0.00231	0.16030	-0.00025	0.57743
Ch4796	-0.00143	0.84980	-0.00073	0.78752	0.00070	0.38485
Ch10441	0.00197	0.24109	0.00197	0.19099	0.00000	0.42762
Ch11483	0.00111	0.32614	-0.00120	0.65604	-0.00231	0.99822
Ch17977	-0.00251	0.87376	-0.00239	0.93010	0.00012	0.46446
Ch19846	-0.00047	0.61356	0.01231	0.00000	0.01277	0.00059
Ch24332	-0.00156	0.71347	-0.00190	0.84584	-0.00034	0.64149
Ch25478	-0.00297	0.87149	0.00042	0.50792	0.00339	0.01970

37

38

39

40

41

42

43

44

45

46

47

**Table S4** Genetic differentiation among *Pleuragramma antarctica* samples including small and large size clusters from Joinville Island 2010. Pairwise  $F_{ST}$  estimates (above the diagonal) and corresponding  $P$ -values (below the diagonal) are shown; bold values indicate uncorrected probability below 0.05, asterisks indicate significant values after correction for multiple tests as implemented in SGoF+<sup>4</sup>. Values shaded in light gray indicate gains of significance compared to the original analysis<sup>1</sup>. Values shaded in dark gray indicate losses of significance compared to the original analysis. Numbers in parentheses adjacent to group names indicate sample size ( $n$ ). Sampling location acronyms are as in Table 1. JI10S, Joinville Island 2010 small cluster; JI10L, Joinville Island 2010 large cluster.

	C10 (60)	MB01 (28)	MB02 (49)	MB10 (60)	MB11 (83)	J107 (34)	J10S (68)	J10L (72)	J12 (54)	SS196 (14)	SO11 (47)	LB07 (46)	LB11 (52)	FT14 (50)	HB89 (19)	HB91 (41)	HB14 (82)	AB14 (25)	RS96 (91)	RS97 (84)
<b>C10</b>	-	-0.0008	-0.0002	0.0007	-0.0008	-0.0033	0.0061	0.0048	0.0043	-0.0044	0.0100	0.0054	0.0021	0.0002	0.0067	0.0016	0.0001	-0.0012	0.0049	0.0024
<b>MB01</b>	0.6810	-	-0.0004	-0.0022	-0.0016	0.0006	0.0070	0.0043	0.0047	0.0016	-0.0125	0.0057	0.0057	0.0007	0.0051	0.0037	0.0015	0.0008	0.0043	0.0042
<b>MB02</b>	0.5787	0.5126	-	0.0015	0.0010	-0.0013	0.0041	0.0016	0.0039	-0.0041	0.0103	0.0021	0.0006	0.0010	0.0062	0.0004	-0.0003	-0.0036	0.0023	0.0043
<b>MB10</b>	0.3758	0.7993	0.2069	-	0.0009	-0.0037	0.0032	0.0006	0.0037	-0.0012	0.0091	0.0027	-0.0005	-0.0000	0.0047	0.0008	-0.0011	-0.0021	0.0002	0.0010
<b>MB11</b>	0.7213	0.7356	0.2443	0.2427	-	-0.0008	0.0061	0.0047	0.0043	0.0012	0.0096	0.0094	0.0046	0.0008	0.0060	0.0030	0.0018	-0.0001	0.0041	0.0025
<b>J107</b>	0.9567	0.4147	0.6655	0.9617	0.6194	-	0.0031	-0.0032	0.0010	-0.0084	0.0059	0.0009	-0.0034	-0.0034	0.0054	0.0002	-0.0027	-0.0053	-0.0018	-0.0026
<b>J10S</b>	<b>0.0041*</b>	<b>0.0156*</b>	<b>0.0284*</b>	<b>0.0399*</b>	<b>0.0005*</b>	0.1056	-	0.0040	0.0034	0.0013	0.0045	0.0055	0.0037	0.0019	-0.0004	0.0005	0.0021	0.0038	0.0001	0.0044
<b>J10L</b>	<b>0.0096*</b>	0.0691	0.1819	0.3252	<b>0.0020*</b>	0.9572	<b>0.0098*</b>	-	0.0024	-0.0042	0.0042	0.0003	-0.0018	0.0002	0.0049	0.0032	-0.0008	-0.0018	-0.0000	0.0019
<b>J12</b>	<b>0.0358*</b>	0.0902	0.0527	<b>0.0388*</b>	<b>0.0115*</b>	0.3543	0.0514	0.1143	-	0.0020	0.0013	0.0039	0.0027	-0.0006	0.0053	-0.0015	0.0015	0.0014	0.0020	0.0020
<b>SS196</b>	0.8949	0.3972	0.8144	0.5788	0.3643	0.9734	0.4086	0.8656	0.3729	-	0.0010	0.0012	-0.0057	-0.0062	0.0034	-0.0018	-0.0050	-0.0072	-0.0016	-0.0016
<b>SO11</b>	<b>0.0006*</b>	<b>0.0016*</b>	<b>0.0009*</b>	<b>0.0006*</b>	<b>0.0001*</b>	<b>0.0383</b>	<b>0.0265*</b>	<b>0.0312*</b>	0.3132	0.4789	-	0.0058	0.0039	0.0003	0.0066	-0.0001	0.0037	0.0049	0.0066	0.0031
<b>LB07</b>	<b>0.0188*</b>	0.0518	0.1708	0.0958	<b>0.0001*</b>	0.3593	<b>0.0095</b>	0.4401	0.0598	0.4017	<b>0.0212*</b>	-	0.0020	0.0020	0.0047	0.0056	0.0004	0.0004	0.0033	0.0033
<b>LB11</b>	0.1806	<b>0.0453</b>	0.3619	0.5866	<b>0.0088*</b>	0.9430	<b>0.0361*</b>	0.8908	0.1145	0.9241	0.0650	0.1872	-	-0.0012	0.0098	-0.0012	-0.0008	-0.0035	0.0016	0.0013
<b>FT14</b>	0.5172	0.4127	0.3118	0.4773	0.2877	0.9348	0.1716	0.4705	0.6511	0.9403	0.4792	0.1909	0.7452	-	0.0044	-0.0012	-0.0015	-0.0037	-0.0009	-0.0013
<b>HB89</b>	0.0826	0.1752	0.0647	0.1036	0.0501	0.1201	0.5773	0.1046	0.1347	0.3473	0.0970	0.1393	<b>0.014*</b>	0.1607	-	0.0047	0.0024	0.0066	0.0017	0.0057
<b>HB91</b>	0.2849	0.1499	0.4115	0.3282	0.0648	0.4695	0.4343	0.0736	0.7977	0.6767	0.5613	<b>0.0245*</b>	0.7272	0.7308	0.1513	-	-0.0006	-0.0031	0.0015	0.0007
<b>HB14</b>	0.5501	0.3427	0.6011	0.8075	0.1110	0.9388	0.1104	0.7651	0.2477	0.9273	0.0570	0.4541	0.7321	0.8674	0.3111	0.6730	-	-0.0051	0.0011	-0.0009
<b>AB14</b>	0.6987	0.3851	0.8802	0.7514	0.4561	0.9474	0.1031	0.7432	0.3292	0.9054	0.0926	0.4136	0.9021	0.9088	0.0950	0.8464	0.9948	-	0.0011	-0.0004
<b>RS96</b>	<b>0.0038*</b>	0.0557	0.0871	0.4265	<b>0.0021*</b>	0.8266	0.4733	0.5089	0.1134	0.6513	<b>0.0019*</b>	<b>0.0387*</b>	0.1593	0.7272	0.3082	0.2056	0.2117	0.3128	-	0.0024
<b>RS97</b>	0.0946	0.0675	<b>0.0183*</b>	0.2533	<b>0.0392*</b>	0.9226	<b>0.0061*</b>	0.1035	0.1422	0.6717	0.0702	0.0508	0.2248	0.8198	0.0698	0.3866	0.8077	0.5514	<b>0.0391*</b>	-

**Table S5** Genetic differentiation among *Pleuragramma antarctica* sampling locations from the eastern Weddell Sea. Pairwise  $F_{ST}$  estimates (above the diagonal) and corresponding  $P$ -values (below the diagonal) are shown. Numbers in parentheses adjacent to group names indicate sample size ( $n$ ). FT, Filchner Trough; CL, Coats Land; HB, Halley Bay; AB, Atka Bay.

	<b>west FT (23)</b>	<b>east FT (27)</b>	<b>CL (29)</b>	<b>HB (52)</b>	<b>AB (25)</b>
<b>west FT</b>	-	0.0027	-0.0053	-0.0019	-0.0019
<b>east FT</b>	0.2798	-	-0.0015	0.0007	-0.0039
<b>CL</b>	0.9602	0.7372	-	-0.0028	-0.0060
<b>HB</b>	0.7556	0.4143	0.9051	-	-0.0062
<b>AB</b>	0.6489	0.8309	0.9830	0.9954	-

59  
60  
61  
62  
63  
64  
65  
66  
67  
68  
69  
70  
71  
72  
73  
74  
75  
76  
77

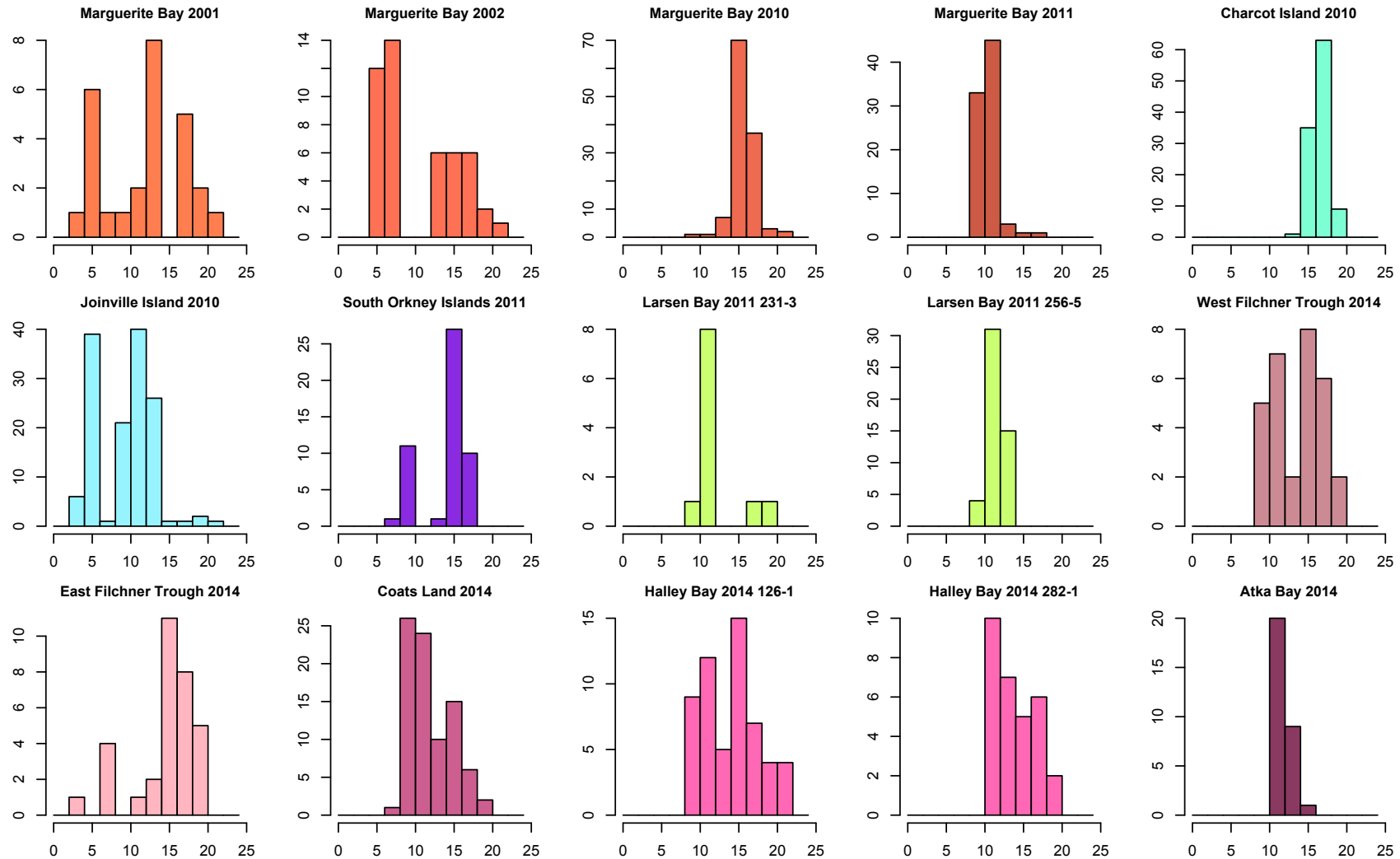


**Figure S1** Standard length (SL) distributions of *Pleuragramma antarctica* around the Antarctic Peninsula and Weddell Sea. Sampling locations and collection years are specified above the graphs. When several collections were performed within the same year and area, sampling stations are listed after the collection year. Frequency indicated on the y-axis and SL in cm indicated on the x-axis.

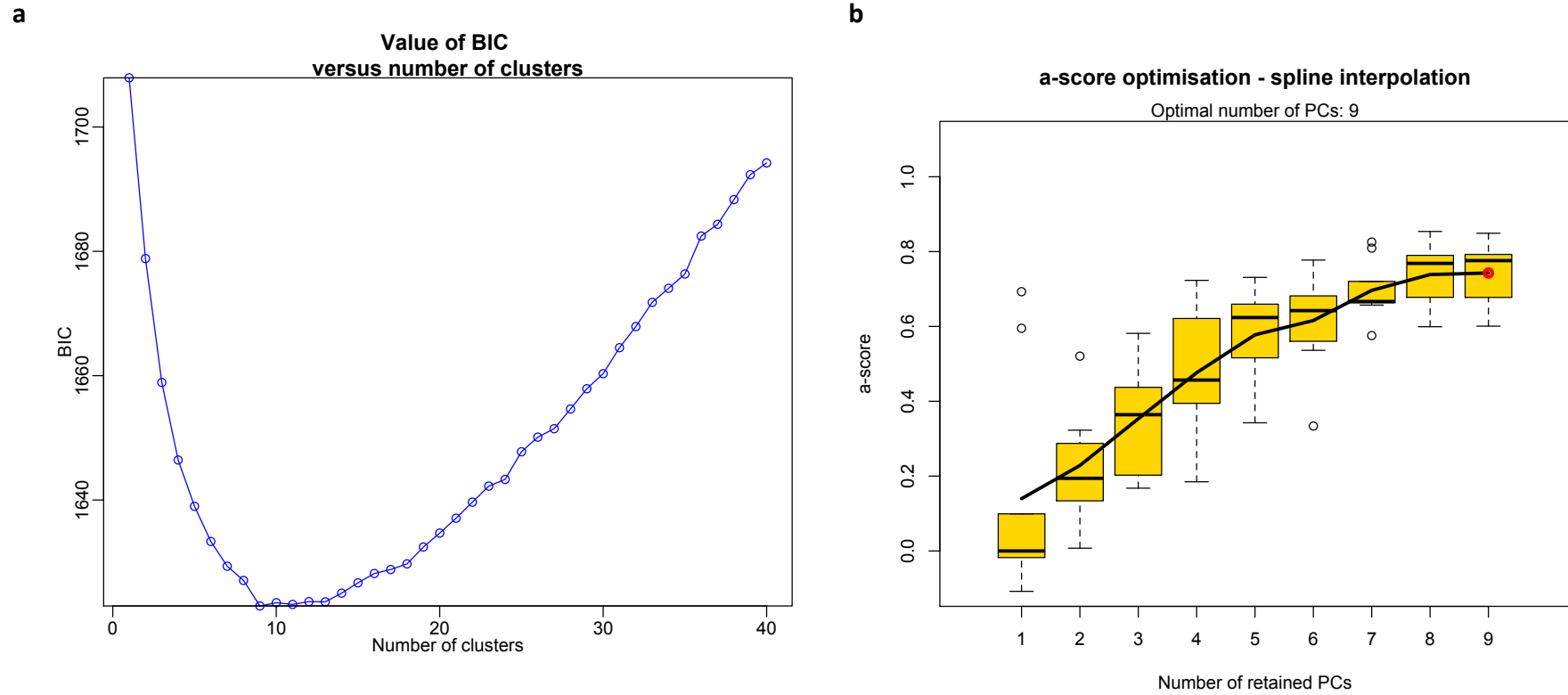


**Figure S2** Discriminant analysis of principal components (DAPC) analysis criteria. **a** Bayesian Information Criterion (BIC) plotted for increasing numbers of clusters, indicating the optimal number of clusters at  $k = 9$ . **b** Plot of a-score optimization based on the *adegenet* R package function *optim.a.score*, used to quantify the trade-off between discrimination power and over-fitting by calculating the difference between the proportion of observed and random discrimination, indicating the optimal number of principal components (PCs) to retain is nine<sup>5</sup>.

78  
79  
80  
81  
82

**Table S2** Genetic variability of *Pleurogramma antarctica* for each locus across all nineteen sampling locations. Sample size ( $n$ ), number of alleles ( $N_A$ ), % of total observed alleles per locus per sampling location, allelic richness based on a minimum sample size of 14 individuals ( $A_R$ ), observed heterozygosity ( $H_O$ ), unbiased heterozygosity ( $H_E$ ) and probability of deviation from Hardy-Weinberg equilibrium ( $pHWE$ ) are shown. Values in bold indicate significant HWE deviations after correction for multiple tests as implemented in SGoF+<sup>4</sup> (threshold for significance with 304 comparisons 0.008). Sampling location acronyms are as in Table 1.

Locus	C110								MB01						MB02						
	$n$	$N_A$	%	$A_R$	$H_O$	$H_E$	$pHWE$	$n$	$N_A$	%	$A_R$	$H_O$	$H_E$	$pHWE$	$n$	$N_A$	%	$A_R$	$H_O$	$H_E$	$pHWE$
<b>Ch126</b>	60	3	42.86	2.21	0.45	0.51	0.300	28	3	42.86	2.38	0.46	0.51	0.711	49	4	57.14	3.00	0.59	0.55	0.763
<b>Ch520</b>	60	4	50.00	3.09	0.33	0.38	0.488	28	4	50.00	3.38	0.39	0.51	0.020	49	5	62.50	3.70	0.47	0.48	0.754
<b>Ch623</b>	60	23	69.70	14.35	0.92	0.94	<b>0.000</b>	28	20	60.61	12.75	0.96	0.92	0.219	49	20	60.61	12.82	0.90	0.92	0.975
<b>Ch10105</b>	60	6	66.67	3.54	0.30	0.31	0.146	28	3	33.33	1.86	0.07	0.07	1.000	49	5	55.56	2.89	0.24	0.24	0.182
<b>Ch10857</b>	60	9	52.94	6.34	0.68	0.69	0.903	28	9	52.94	6.03	0.54	0.66	0.091	49	7	41.18	5.59	0.57	0.67	0.702
<b>Ch13222</b>	60	3	50.00	2.26	0.17	0.16	1.000	28	2	33.33	1.94	0.18	0.16	1.000	49	4	66.67	1.75	0.06	0.06	1.000
<b>Ch18085</b>	60	10	71.43	7.29	0.83	0.83	0.852	28	9	64.29	6.98	0.86	0.82	0.790	49	9	64.29	7.02	0.86	0.83	0.998
<b>Ch2931</b>	60	10	58.82	6.96	0.73	0.83	0.891	28	10	58.82	7.55	0.86	0.82	0.165	49	11	64.71	7.09	0.84	0.82	0.370
<b>Ch4796</b>	60	13	72.22	9.07	0.75	0.87	<b>0.002</b>	28	12	66.67	9.71	0.96	0.88	0.985	49	14	77.78	10.09	0.94	0.89	0.793
<b>Ch10441</b>	60	9	39.13	5.36	0.65	0.65	0.643	28	10	43.48	7.17	0.86	0.76	0.535	49	9	39.13	6.00	0.61	0.68	0.524
<b>Ch11230</b>	60	7	50.00	4.90	0.77	0.72	0.744	28	5	35.71	4.69	0.71	0.71	0.996	49	7	50.00	5.00	0.78	0.72	1.000
<b>Ch11483</b>	60	10	66.67	5.43	0.47	0.56	0.675	28	9	60.00	6.26	0.57	0.64	0.409	49	9	60.00	4.67	0.45	0.46	0.096
<b>Ch17977</b>	60	8	53.33	5.08	0.58	0.63	0.722	28	4	26.67	3.60	0.57	0.56	0.955	49	7	46.67	4.60	0.65	0.62	0.509
<b>Ch19846</b>	60	8	66.67	6.26	0.70	0.78	0.690	28	8	66.67	6.56	0.86	0.78	0.996	49	8	66.67	6.52	0.86	0.80	0.941
<b>Ch24332</b>	60	6	60.00	4.02	0.60	0.62	0.096	28	5	50.00	3.92	0.57	0.60	0.320	49	5	50.00	3.70	0.73	0.62	0.184
<b>Ch25478</b>	60	4	25.00	2.96	0.57	0.56	0.422	28	4	25.00	3.04	0.46	0.56	0.036	49	6	37.50	3.69	0.61	0.63	0.341
<b>Overall</b>	60	133	55.97	5.57	0.59	0.63	0.025	28	117	48.15	5.49	0.62	0.62	0.443	49	130	56.28	5.51	0.64	0.62	0.938

Locus	MB10								MB11								JI07							
	<i>n</i>	<i>N<sub>A</sub></i>	%	<i>A<sub>R</sub></i>	<i>H<sub>O</sub></i>	<i>H<sub>E</sub></i>	<i>pHWE</i>	<i>n</i>	<i>N<sub>A</sub></i>	%	<i>A<sub>R</sub></i>	<i>H<sub>O</sub></i>	<i>H<sub>E</sub></i>	<i>pHWE</i>	<i>n</i>	<i>N<sub>A</sub></i>	%	<i>A<sub>R</sub></i>	<i>H<sub>O</sub></i>	<i>H<sub>E</sub></i>	<i>pHWE</i>			
Ch126	60	4	57.14	2.40	0.43	0.52	0.205	83	3	42.86	2.77	0.58	0.55	0.661	34	5	71.43	3.22	0.56	0.54	1.000			
Ch520	60	5	62.50	4.07	0.62	0.56	0.855	83	5	62.50	3.58	0.45	0.40	0.712	34	3	37.50	2.95	0.50	0.41	0.362			
Ch623	60	24	72.73	13.71	0.93	0.93	0.038	83	25	75.76	13.58	0.89	0.93	0.012	34	22	66.67	13.01	0.97	0.92	0.106			
Ch10105	60	4	44.44	2.88	0.22	0.21	0.594	83	5	55.56	3.16	0.25	0.23	0.680	34	4	44.44	2.99	0.24	0.22	1.000			
Ch10857	60	11	64.71	6.36	0.75	0.73	0.121	83	10	58.82	6.32	0.73	0.71	0.937	34	7	41.18	5.29	0.76	0.74	0.716			
Ch13222	60	4	66.67	2.40	0.25	0.22	1.000	83	3	50.00	1.94	0.10	0.10	<b>0.000</b>	34	3	50.00	2.31	0.21	0.23	1.000			
Ch18085	60	10	71.43	7.21	0.83	0.83	0.171	83	11	78.57	7.05	0.87	0.82	0.959	34	10	71.43	7.47	0.76	0.82	0.715			
Ch2931	60	10	58.82	7.52	0.83	0.81	0.998	83	10	58.82	6.91	0.73	0.81	0.279	34	10	58.82	7.61	0.71	0.84	0.333			
Ch4796	60	13	72.22	9.37	0.82	0.88	0.996	83	14	77.78	10.72	0.93	0.90	1.000	34	11	61.11	9.11	1.00	0.88	1.000			
Ch10441	60	11	47.83	7.20	0.73	0.71	0.436	83	12	52.17	6.09	0.69	0.68	0.989	34	9	39.13	5.85	0.74	0.66	0.289			
Ch11230	60	8	57.14	5.68	0.68	0.76	0.986	83	6	42.86	4.64	0.80	0.73	0.603	34	7	50.00	5.71	0.88	0.76	0.547			
Ch11483	60	8	53.33	5.20	0.65	0.57	0.597	83	8	53.33	4.26	0.55	0.56	0.461	34	5	33.33	3.77	0.59	0.48	0.606			
Ch17977	60	9	60.00	5.13	0.62	0.66	<b>0.000</b>	83	10	66.67	4.85	0.58	0.58	0.013	34	7	46.67	5.73	0.68	0.69	0.828			
Ch19846	60	8	66.67	6.45	0.87	0.80	0.216	83	8	66.67	6.04	0.71	0.78	0.618	34	7	58.33	5.72	0.76	0.77	0.385			
Ch24332	60	6	60.00	4.64	0.60	0.65	0.934	83	7	70.00	4.55	0.69	0.63	0.914	34	4	40.00	3.79	0.62	0.64	0.800			
Ch25478	60	6	37.50	4.43	0.68	0.64	0.018	83	8	50.00	4.45	0.64	0.63	0.686	34	7	43.75	4.12	0.47	0.61	0.019			
Overall	60	141	59.57	5.92	0.66	0.65	0.017	83	145	60.15	5.68	0.64	0.63	0.076	34	121	50.86	5.54	0.65	0.64	0.791			

Locus	JI10							JI12							SSI96						
	<i>n</i>	<i>N<sub>A</sub></i>	%	<i>A<sub>R</sub></i>	<i>H<sub>O</sub></i>	<i>H<sub>E</sub></i>	<i>pHWE</i>	<i>n</i>	<i>N<sub>A</sub></i>	%	<i>A<sub>R</sub></i>	<i>H<sub>O</sub></i>	<i>H<sub>E</sub></i>	<i>pHWE</i>	<i>n</i>	<i>N<sub>A</sub></i>	%	<i>A<sub>R</sub></i>	<i>H<sub>O</sub></i>	<i>H<sub>E</sub></i>	<i>pHWE</i>
Ch126	148	6	85.71	3.08	0.63	0.55	0.384	54	5	71.43	3.00	0.50	0.54	1.000	14	2	28.57	2.00	0.57	0.49	0.620
Ch520	148	8	100.00	4.15	0.57	0.58	0.713	54	6	75.00	3.87	0.44	0.51	0.210	14	5	62.50	4.15	0.50	0.42	1.000
Ch623	148	28	84.85	13.77	0.91	0.94	0.574	54	20	60.61	12.56	0.80	0.92	0.092	14	15	45.45	11.59	0.86	0.91	<b>0.000</b>
Ch10105	148	6	66.67	3.72	0.32	0.37	0.074	54	5	55.56	3.35	0.20	0.25	0.359	14	3	33.33	2.66	0.36	0.30	1.000
Ch10857	148	12	70.59	6.60	0.70	0.74	0.858	54	11	64.71	6.33	0.74	0.71	0.090	14	5	29.41	4.59	0.64	0.69	0.170
Ch13222	148	4	66.67	2.26	0.16	0.17	0.718	54	3	50.00	2.10	0.15	0.14	1.000	14	3	50.00	2.29	0.14	0.14	1.000
Ch18085	148	12	85.71	7.69	0.84	0.85	0.931	54	8	57.14	6.78	0.85	0.81	0.507	14	6	42.86	5.74	0.71	0.80	0.879
Ch2931	148	10	58.82	7.02	0.78	0.81	0.297	54	8	47.06	6.19	0.67	0.82	0.999	14	7	41.18	6.39	0.79	0.82	0.475
Ch4796	148	14	77.78	9.56	0.82	0.89	0.491	54	12	66.67	8.86	0.98	0.87	0.991	14	11	61.11	8.89	0.93	0.86	0.009
Ch10441	148	17	73.91	6.54	0.67	0.70	<b>0.000</b>	54	7	30.43	5.13	0.67	0.66	0.910	14	6	26.09	5.48	0.64	0.72	0.136
Ch11230	148	9	64.29	5.23	0.74	0.74	0.860	54	7	50.00	5.18	0.69	0.70	0.222	14	5	35.71	4.59	0.57	0.73	0.842
Ch11483	148	12	80.00	5.06	0.55	0.58	<b>0.000</b>	54	8	53.33	4.43	0.54	0.57	0.739	14	5	33.33	3.80	0.29	0.37	0.082
Ch17977	148	9	60.00	5.20	0.60	0.63	0.035	54	8	53.33	5.52	0.63	0.63	0.308	14	4	26.67	3.53	0.64	0.56	0.663
Ch19846	148	10	83.33	6.36	0.80	0.79	0.250	54	8	66.67	6.50	0.78	0.79	0.386	14	8	66.67	7.07	0.86	0.83	0.811
Ch24332	148	8	80.00	4.87	0.62	0.65	0.842	54	6	60.00	3.80	0.57	0.59	0.013	14	5	50.00	3.97	0.71	0.62	<b>0.006</b>
Ch25478	148	9	56.25	4.45	0.67	0.63	0.267	54	5	31.25	3.39	0.56	0.59	0.023	14	3	18.75	2.65	0.50	0.53	0.594
Overall	148	174	74.66	5.97	0.65	0.66	<b>0.001</b>	54	127	55.82	5.44	0.61	0.63	0.146	14	93	40.73	4.96	0.61	0.61	<b>0.006</b>



Locus	SOI11								LB07								LB11							
	<i>n</i>	<i>N<sub>A</sub></i>	%	<i>A<sub>R</sub></i>	<i>H<sub>O</sub></i>	<i>H<sub>E</sub></i>	<i>pHWE</i>	<i>n</i>	<i>N<sub>A</sub></i>	%	<i>A<sub>R</sub></i>	<i>H<sub>O</sub></i>	<i>H<sub>E</sub></i>	<i>pHWE</i>	<i>n</i>	<i>N<sub>A</sub></i>	%	<i>A<sub>R</sub></i>	<i>H<sub>O</sub></i>	<i>H<sub>E</sub></i>	<i>pHWE</i>			
Ch126	47	3	42.86	2.24	0.40	0.50	0.140	46	3	42.86	2.72	0.65	0.49	0.152	52	3	42.86	2.57	0.60	0.52	0.879			
Ch520	47	6	75.00	4.54	0.51	0.60	0.108	46	5	62.50	3.96	0.50	0.60	0.328	52	7	87.50	4.52	0.58	0.57	0.948			
Ch623	47	18	54.55	12.21	0.91	0.92	1.000	46	20	60.61	12.82	0.87	0.93	0.997	52	21	63.64	13.57	0.88	0.93	1.000			
Ch10105	47	6	66.67	3.93	0.36	0.35	0.329	46	4	44.44	2.66	0.17	0.18	<b>0.001</b>	52	5	55.56	2.88	0.23	0.21	1.000			
Ch10857	47	9	52.94	6.25	0.72	0.66	0.938	46	9	52.94	5.74	0.54	0.63	0.816	52	10	58.82	6.23	0.73	0.74	0.713			
Ch13222	47	3	50.00	2.24	0.19	0.21	1.000	46	3	50.00	1.86	0.04	0.12	<b>0.001</b>	52	2	33.33	1.91	0.15	0.14	1.000			
Ch18085	47	8	57.14	6.59	0.91	0.80	0.997	46	8	57.14	6.69	0.83	0.82	0.861	52	9	64.29	7.20	0.88	0.82	0.869			
Ch2931	47	9	52.94	6.75	0.70	0.82	0.444	46	11	64.71	7.75	0.78	0.83	0.939	52	9	52.94	6.96	0.77	0.83	0.172			
Ch4796	47	12	66.67	8.74	0.79	0.87	0.902	46	10	55.56	7.88	0.91	0.86	0.921	52	12	66.67	9.13	0.92	0.88	1.000			
Ch10441	47	7	30.43	4.88	0.49	0.56	0.111	46	11	47.83	6.74	0.70	0.70	0.142	52	10	43.48	6.07	0.58	0.63	0.046			
Ch11230	47	6	42.86	4.79	0.64	0.68	0.847	46	6	42.86	5.12	0.70	0.74	0.781	52	7	50.00	5.19	0.73	0.72	0.105			
Ch11483	47	7	46.67	4.85	0.60	0.55	0.764	46	7	46.67	4.63	0.61	0.55	0.597	52	7	46.67	4.49	0.48	0.50	<b>0.001</b>			
Ch17977	47	8	53.33	5.58	0.60	0.59	0.728	46	6	40.00	4.38	0.54	0.57	0.982	52	8	53.33	4.82	0.67	0.64	0.996			
Ch19846	47	7	58.33	5.79	0.66	0.73	0.744	46	9	75.00	6.46	0.83	0.78	0.587	52	10	83.33	7.11	0.88	0.82	0.852			
Ch24332	47	8	80.00	4.81	0.64	0.67	0.757	46	6	60.00	4.35	0.57	0.65	0.579	52	8	80.00	4.97	0.60	0.69	0.455			
Ch25478	47	8	50.00	4.50	0.55	0.64	<b>0.000</b>	46	5	31.25	3.79	0.67	0.59	0.784	52	7	43.75	3.82	0.50	0.59	<b>0.005</b>			
Overall	47	125	55.02	5.54	0.61	0.63	0.213	46	123	52.15	5.47	0.62	0.63	0.114	52	135	57.89	5.71	0.64	0.64	0.106			

Locus	FT14								HB89						HB91						
	<i>n</i>	<i>N<sub>A</sub></i>	%	<i>A<sub>R</sub></i>	<i>H<sub>O</sub></i>	<i>H<sub>E</sub></i>	<i>pHWE</i>	<i>n</i>	<i>N<sub>A</sub></i>	%	<i>A<sub>R</sub></i>	<i>H<sub>O</sub></i>	<i>H<sub>E</sub></i>	<i>pHWE</i>	<i>n</i>	<i>N<sub>A</sub></i>	%	<i>A<sub>R</sub></i>	<i>H<sub>O</sub></i>	<i>H<sub>E</sub></i>	<i>pHWE</i>
Ch126	50	4	57.14	3.07	0.50	0.56	1.000	19	2	28.57	2.00	0.53	0.49	1.000	41	3	42.86	2.49	0.51	0.51	1.000
Ch520	50	5	62.50	3.79	0.56	0.49	0.791	19	4	50.00	3.91	0.63	0.60	0.228	41	7	87.50	4.67	0.51	0.57	<b>0.000</b>
Ch623	50	17	51.52	12.04	0.96	0.92	0.025	19	11	33.33	8.73	0.74	0.85	0.516	41	21	63.64	13.07	0.98	0.93	0.569
Ch10105	50	4	44.44	2.69	0.18	0.17	1.000	19	4	44.44	3.69	0.47	0.46	0.545	41	5	55.56	3.21	0.27	0.28	0.364
Ch10857	50	8	47.06	5.62	0.58	0.70	0.389	19	6	35.29	5.32	0.74	0.65	0.487	41	8	47.06	6.51	0.78	0.75	0.773
Ch13222	50	2	33.33	1.99	0.30	0.26	0.046	19	3	50.00	2.36	0.16	0.15	1.000	41	4	66.67	2.45	0.15	0.14	1.000
Ch18085	50	10	71.43	7.23	0.72	0.83	0.121	19	9	64.29	7.46	0.89	0.83	0.534	41	7	50.00	6.59	0.78	0.82	0.999
Ch2931	50	11	64.71	7.55	0.80	0.83	0.553	19	8	47.06	7.06	0.63	0.82	0.574	41	9	52.94	6.72	0.63	0.81	0.249
Ch4796	50	13	72.22	9.41	0.96	0.88	0.999	19	9	50.00	7.77	0.84	0.86	1.000	41	13	72.22	9.69	0.98	0.88	1.000
Ch10441	50	8	34.78	5.72	0.62	0.64	0.855	19	8	34.78	6.19	0.84	0.73	0.102	41	7	30.43	5.15	0.46	0.62	<b>0.000</b>
Ch11230	50	6	42.86	4.86	0.64	0.70	0.811	19	6	42.86	5.11	0.63	0.71	0.884	41	7	50.00	5.55	0.71	0.73	0.698
Ch11483	50	8	53.33	5.34	0.52	0.54	0.772	19	6	40.00	4.42	0.47	0.58	<b>0.000</b>	41	6	40.00	4.06	0.56	0.54	0.543
Ch17977	50	8	53.33	5.08	0.58	0.59	0.082	19	4	26.67	3.70	0.58	0.54	0.690	41	6	40.00	4.47	0.56	0.63	0.419
Ch19846	50	9	75.00	6.60	0.74	0.81	0.999	19	8	66.67	6.63	0.89	0.80	0.075	41	10	83.33	7.17	0.80	0.81	0.996
Ch24332	50	8	80.00	4.91	0.68	0.65	1.000	19	4	40.00	3.52	0.42	0.63	0.011	41	6	60.00	4.31	0.76	0.64	0.666
Ch25478	50	8	50.00	4.53	0.66	0.62	0.975	19	6	37.50	4.13	0.47	0.55	1.000	41	7	43.75	4.47	0.68	0.64	0.542
Overall	50	129	55.85	5.65	0.62	0.64	0.689	19	98	43.22	5.12	0.62	0.64	0.039	41	126	55.37	5.66	0.63	0.64	0.037

Locus	HB14								AB14								RS96							
	<i>n</i>	<i>N<sub>A</sub></i>	%	<i>A<sub>R</sub></i>	<i>H<sub>O</sub></i>	<i>H<sub>E</sub></i>	<i>pHWE</i>	<i>n</i>	<i>N<sub>A</sub></i>	%	<i>A<sub>R</sub></i>	<i>H<sub>O</sub></i>	<i>H<sub>E</sub></i>	<i>pHWE</i>	<i>n</i>	<i>N<sub>A</sub></i>	%	<i>A<sub>R</sub></i>	<i>H<sub>O</sub></i>	<i>H<sub>E</sub></i>	<i>pHWE</i>			
Ch126	82	5	71.43	2.81	0.57	0.53	0.017	25	3	42.86	2.84	0.60	0.55	1.000	91	3	42.86	2.62	0.55	0.52	0.331			
Ch520	82	7	87.50	4.23	0.57	0.54	0.391	25	5	62.50	3.76	0.48	0.47	<b>0.000</b>	91	7	87.50	4.04	0.58	0.52	0.069			
Ch623	82	21	63.64	12.94	0.87	0.93	0.946	25	15	45.45	11.64	0.96	0.91	1.000	91	23	69.70	13.70	0.88	0.93	0.988			
Ch10105	82	4	44.44	3.18	0.27	0.27	0.159	25	4	44.44	2.33	0.12	0.12	1.000	91	5	55.56	3.27	0.25	0.26	0.600			
Ch10857	82	8	47.06	5.38	0.57	0.69	0.931	25	8	47.06	6.06	0.76	0.73	0.480	91	11	64.71	6.70	0.71	0.76	0.625			
Ch13222	82	4	66.67	2.50	0.20	0.20	1.000	25	2	33.33	1.96	0.16	0.21	0.335	91	3	50.00	2.20	0.16	0.18	0.203			
Ch18085	82	9	64.29	7.30	0.83	0.83	0.996	25	7	50.00	6.24	0.84	0.81	0.997	91	11	78.57	7.69	0.89	0.84	1.000			
Ch2931	82	12	70.59	6.92	0.73	0.81	0.795	25	9	52.94	7.06	0.80	0.83	0.008	91	12	70.59	6.85	0.68	0.79	0.630			
Ch4796	82	15	83.33	9.70	0.89	0.88	0.166	25	10	55.56	7.67	0.88	0.85	<b>0.000</b>	91	14	77.78	9.73	0.91	0.89	1.000			
Ch10441	82	10	43.48	5.54	0.48	0.64	0.010	25	7	30.43	5.48	0.68	0.60	0.973	91	11	47.83	6.12	0.67	0.71	0.827			
Ch11230	82	8	57.14	5.14	0.67	0.72	0.978	25	6	42.86	4.59	0.68	0.70	<b>0.004</b>	91	7	50.00	4.79	0.70	0.68	0.831			
Ch11483	82	10	66.67	4.60	0.54	0.54	0.543	25	6	40.00	4.71	0.68	0.58	0.308	91	9	60.00	4.82	0.55	0.55	0.966			
Ch17977	82	7	46.67	4.71	0.62	0.61	0.777	25	7	46.67	5.08	0.76	0.63	0.021	91	9	60.00	5.22	0.62	0.62	0.940			
Ch19846	82	10	83.33	7.23	0.78	0.82	0.477	25	7	58.33	6.13	0.68	0.79	0.088	91	10	83.33	6.88	0.87	0.80	0.997			
Ch24332	82	8	80.00	4.72	0.60	0.65	0.315	25	5	50.00	3.57	0.64	0.57	0.422	91	10	100.00	4.87	0.64	0.67	0.564			
Ch25478	82	9	56.25	3.70	0.50	0.58	0.208	25	6	37.50	4.21	0.68	0.62	<b>0.005</b>	91	9	56.25	4.37	0.63	0.61	0.970			
Overall	82	147	64.53	5.66	0.61	0.64	0.288	25	107	46.25	5.21	0.65	0.62	<b>0.000</b>	91	154	65.92	5.87	0.64	0.65	0.993			

Locus	<i>n</i>	<i>N<sub>A</sub></i>	%	RS97			<i>pHWE</i>
				<i>A<sub>R</sub></i>	<i>H<sub>O</sub></i>	<i>H<sub>E</sub></i>	
Ch126	84	3	42.86	2.60	0.54	0.53	1.000
Ch520	84	6	75.00	3.88	0.42	0.48	0.393
Ch623	84	24	72.73	13.54	0.93	0.93	0.786
Ch10105	84	4	44.44	3.12	0.26	0.25	0.759
Ch10857	84	10	58.82	6.29	0.73	0.76	0.065
Ch13222	84	3	50.00	2.27	0.23	0.23	0.311
Ch18085	84	10	71.43	7.83	0.86	0.83	1.000
Ch2931	84	9	52.94	6.44	0.68	0.79	0.883
Ch4796	84	15	83.33	9.44	0.83	0.87	0.398
Ch10441	84	10	43.48	6.04	0.60	0.64	0.517
Ch11230	84	8	57.14	4.72	0.71	0.68	<b>0.002</b>
Ch11483	84	8	53.33	4.19	0.55	0.51	0.740
Ch17977	84	8	53.33	5.09	0.57	0.62	0.377
Ch19846	84	10	83.33	6.88	0.82	0.80	0.870
Ch24332	84	7	70.00	4.35	0.68	0.64	1.000
Ch25478	84	8	50.00	4.01	0.60	0.60	0.111
Overall	84	143	60.13	5.67	0.62	0.64	0.386

25  
26  
27  
28  
29  
30  
31  
32  
33  
34  
35

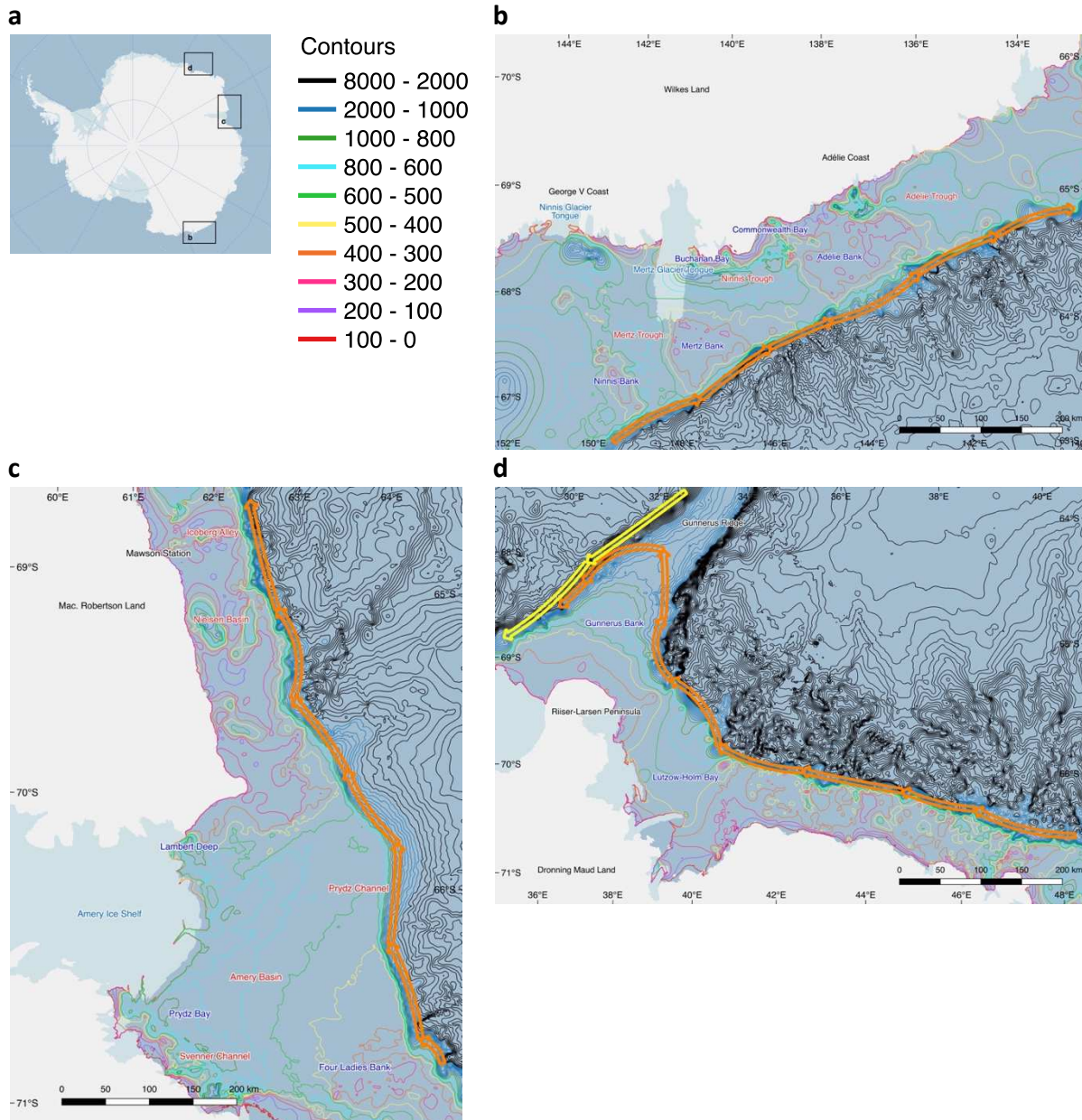


**Figure S3** East Antarctica. Yellow arrows approximate the SACCF, Southern Antarctic Circumpolar Current Front; Orange arrows approximate the AFS, Antarctic Slope Front and Current System. Empty arrows indicate suggested positions according to Fig.7 in Orsi *et al.*<sup>6</sup> and Whitworth *et al.*<sup>7</sup> for the SAACF and AFS, respectively. Relevant place names and bathymetric features are specified. **a** Map of the Antarctic. Areas of interest in subsequent maps are indicated in squares and ordered by movement along the AFS. **b** George V and Adélie Coasts. **c** Prydz Bay north to Iceberg Alley. **d** Lützwow Bay. Maps created using the Norwegian Polar Institute’s Quantarctica 2.0 package<sup>8</sup> in the software QGIS version 2.18.9 <http://qgis.osgeo.org><sup>9</sup>.

84 **References**

85

- 86 1 Agostini, C. *et al.* Genetic differentiation in the ice-dependent fish *Pleuragramma antarctica* along the Antarctic Peninsula. *Journal*  
87 *of Biogeography* **42**, 1103-1113, doi:10.1111/jbi.12497 (2015).
- 88 2 Molecular Ecology Resources Primer Development Consortium *et al.* Permanent genetic resources added to Molecular Ecology  
89 Resources Database 1 October 2010-30 November 2010. *Molecular ecology resources* **11**, 418-421, doi:10.1111/j.1755-  
90 0998.2010.02970.x (2011).
- 91 3 Molecular Ecology Resources Primer Development Consortium *et al.* Permanent genetic resources added to molecular ecology  
92 resources database 1 April 2013-31 May 2013. *Molecular ecology resources* **13**, 966-968, doi:10.1111/1755-0998.12140 (2013).
- 93 4 Carvajal-Rodriguez, A. & de Uña-Alvarez, J. Assessing Significance in High-Throughput Experiments by Sequential Goodness of Fit  
94 and q-Value Estimation. *PloS one* **6**, e24700, doi:10.1371/journal.pone.0024700 (2011).
- 95 5 Jombart, T. Adegenet: A R package for the multivariate analysis of genetic markers. *Bioinformatics* **24**, 1403-1405,  
96 doi:10.1093/bioinformatics/btn129 (2008).
- 97 6 Orsi, A. H., Whitworth Iii, T. & Nowlin Jr, W. D. On the meridional extent and fronts of the Antarctic Circumpolar Current. *Deep-Sea*  
98 *Research Part I* **42**, 641-673, doi:10.1016/0967-0637(95)00021-W (1995).
- 99 7 Whitworth, T., Orsi, A. H., Kim, S. J., Nowlin, W. D. & Locarnini, R. A. in *Ocean, Ice, and Atmosphere: Interactions at the Antarctic*  
100 *Continental Margin* 1-27 (American Geophysical Union, 1998).
- 101 8 Matsuoka, K., Skoglund, A. & Roth, G. (Norwegian Polar Institute, 2018).
- 102 9 QGIS Geographic Information System. Open Source Geospatial Foundation Project. (2018).

103

104

105

106

107

108

109

110

# Chapter 4

## Population structure and connectivity of Antarctic silverfish in the Weddell Sea using otolith chemistry

Published as:

**Caccavo JA**, Ashford J, Ryan S, Papetti C, Schröder M, Zane L (2018) Spatially-based population structure and life history connectivity of the Antarctic silverfish along the southern Weddell Sea shelf. *In preparation*.

1 *Draft preparation for submission to MEPS ([Author Guidelines](#))*

2

3

**TITLE**

4 Spatially-based population structure and life history connectivity of the Antarctic silverfish

5 along the southern Weddell Sea shelf.

6

7

**RUNNING PAGE HEAD**

8 Connectivity of silverfish in the Weddell

9

10 Jilda Alicia Caccavo<sup>1\*</sup>, Julian R. Ashford<sup>2</sup>, Svenja Ryan<sup>3</sup>, Chiara Papetti<sup>1,4</sup>, Michael

11 Schröder, Lorenzo Zane<sup>1,4</sup>

12

13 <sup>1</sup> Department of Biology, University of Padua, Padua 35121, Italy.

14 <sup>2</sup> Department of Ocean, Earth and Atmospheric Sciences, Center for Quantitative Fisheries

15 Ecology, Old Dominion University, Norfolk, VA 23508, United States.

16 <sup>3</sup> Helmholtz Center for Polar and Marine Research, Alfred Wegener Institute, Am Alten

17 Hafen 26, Bremerhaven 27568, Germany.

18 <sup>4</sup> Consorzio Nazionale Interuniversitario per le Scienze del Mare (CoNISMa), Rome 00196,

19 Italy.

20

21 **Corresponding author**

22 \* Jilda Alicia Caccavo, [ergo@jildacaccavo.com](mailto:ergo@jildacaccavo.com), ORCID: 0000-0002-8172-7855

23



24 **ABSTRACT**

25 A multidisciplinary approach was employed to examine a physical-biological population  
26 hypothesis for a critical forage species, the Antarctic silverfish (*Pleuragramma antarctica*).  
27 Microsatellite markers previously showed homogeneity in allele frequencies along the  
28 Antarctic Slope Front (ASF) and the associated Antarctic Slope Front Current (ASC)  
29 westward from the Ross Sea to the northern tip of the Antarctic Peninsula. Furthermore,  
30 spatially recurring length modes suggested episodic connectivity. In this paper, as part of a  
31 recent hydrographic survey of the Filchner Trough system in the southern Weddell Sea,  
32 otolith nucleus chemistry, which provides a record of environmental exposure during early  
33 life, was used to test between scenarios concerning silverfish population connectivity.  
34 Despite strong gene flow observed from Atka Bay to west of the Filchner Trough, significant  
35 population structuring was observed using otolith chemistry, in the same samples as used for  
36 the genetic study. Mg-Ca<sup>-1</sup> and Sr-Ca<sup>-1</sup> differentiated large and small length modes,  
37 suggestive of disparate origins for the two size groups, and Mg-Ca<sup>-1</sup> showed significant  
38 contrasts between Atka Bay, Halley Bay and Filchner Trough. Self-recruitment shaped by  
39 circulation associated with the Filchner Trough, fluctuations in mixing between immigrant  
40 and locally-recruited fish and feeding opportunities between inflowing Modified Warm Deep  
41 Water (MWDW) and outflowing Ice Shelf Water (ISW), help explain structuring revealed by  
42 otolith chemistry, length, abundance and biomass data, as well as gene flow along the AFS.  
43 The results illustrate how comparisons between multi-disciplinary techniques based on  
44 integrated sampling designs that incorporate hydrography can enhance understanding of  
45 population structure and connectivity around the Southern Ocean.

46

47 **KEY WORDS**

48 Physical-biological interactions, Filchner Trough, population differentiation, life history  
49 connectivity, trough circulation, Modified Warm Deep Water (MWDW), Ice-Shelf Water  
50 (ISW), otolith chemistry

51

## 52 INTRODUCTION

### 53 *Life history and along-shelf connectivity*

54 Antarctic silverfish have a circumpolar distribution and, as an important forage  
55 species, perform a critical role connecting higher and lower trophic levels in Southern Ocean  
56 shelf ecosystems (Duhamel et al. 2014, Koubbi et al. 2017). Despite lacking a swim bladder,  
57 silverfish are pelagic throughout their life history, including a cryopelagic egg and early  
58 larval phase, maintaining neutral buoyancy by sequestration of lipids in adipocytes (Eastman  
59 1985, La Mesa & Eastman 2012). Similar to related benthic notothenioids, Antarctic  
60 silverfish are inactive, remaining suspended in the water column to feed (Wöhrmann et al.  
61 1997). These life history and behavior characteristics accentuate silverfish interactions with  
62 current and front systems that potentially play a key role in maintaining connectivity between  
63 areas along the Antarctic continental shelf (Ashford et al. 2017).

64 Early development of silverfish in the platelet ice layer beneath coastal fast ice (e.g.  
65 Vacchi et al. 2004) is followed by advection of larvae over the shelf, and descent into deeper  
66 waters as juveniles and adults (La Mesa et al. 2010, Guidetti et al. 2014). Mature silverfish  
67 inhabit depths from 400 – 700 m (La Mesa & Eastman 2012), and exhibit a diurnal vertical  
68 migration (Lancraft et al. 2004). Life history structured by circulation associated with glacial  
69 trough systems has been hypothesized (Ashford et al. 2017) for areas where early life stages  
70 of silverfish have been found around the Antarctic (Ghigliotti et al. 2017), including the Ross  
71 Sea (Guglielmo et al. 1998), Antarctic Peninsula (Kellermann 1986), Dumont d’Urville Sea

72 (Koubbi et al. 2011) and Weddell Sea (Hubold 1984). In this physical-biological hypothesis,  
73 fish entrained in the trough circulation are carried offshore towards the continental shelf  
74 break, and mixing with inflowing water masses carries a proportion back inshore. Fish  
75 reaching the continental shelf-break become exposed to currents along the continental slope,  
76 which transport them to trough systems downstream (Ashford et al. 2017). Brooks et al.  
77 (2018) examined the cross-shelf component of the hypothesis by comparing samples caught  
78 along the outflow and inflow of the Drygalski Trough in the Ross Sea, and found evidence  
79 supporting a unified population spatially constrained by cryopelagic incubation under fast ice  
80 at the head of the trough. Along the shelf, low levels of heterogeneity have been shown using  
81 mitochondrial DNA (Zane et al. 2006) and microsatellite markers (Caccavo et al. 2018).  
82 Comparing multiple areas around the Antarctic, Caccavo et al. (2018) tested the along-shelf  
83 component of the physical-biological hypothesis, finding evidence of strong circumpolar  
84 gene flow. Regions where levels of gene flow were reduced corresponded to discontinuities  
85 in the large-scale circulation.

86         Three major hydrographic features account for most of the transport around the  
87 Antarctic Margin. The Antarctic Slope Front (ASF) and associated Antarctic Slope Front  
88 Current (ASC)(Orsi et al. 1995, Whitworth et al. 1998) separate warm, saline oceanic water  
89 masses from colder, fresher shelf waters, and play an important role regionally in mediating  
90 the transport of warm water onto the shelf. The ASC is first identifiable in the western  
91 Amundsen Sea, from where it flows westward along the slope of the Ross Sea, East  
92 Antarctica and the Weddell Sea (Orsi et al. 1995). In the western Weddell Sea, it rounds the  
93 tip of the Antarctic Peninsula off Joinville Island, before entering the Hesperides Trough  
94 (Azaneu et al. 2017). Analyzing silverfish from shelf areas along the ASF and ASC, Caccavo  
95 et al. (2018) found no significant differences in allele frequencies from the Ross Sea to

96 Joinville Island. By contrast, along the South Scotia Ridge east of the Hesperides Trough,  
97 fish over the South Orkney shelf differentiated from those along the ASF.

98         The second major hydrographic feature is the Antarctic Circumpolar Current (ACC),  
99 which remains offshore for the majority of its circumpolar extent but approaches the  
100 continental slope of the eastern Amundsen Sea. From there it flows eastward and north along  
101 the Bellingshausen Sea and Antarctic Peninsula, before once again moving seaward off the  
102 South Shetland Islands (Orsi et al. 1995, Savidge & Amft 2009). Caccavo et al. (2018) found  
103 a distinct pattern of differentiation in microsatellite markers between fish sampled along the  
104 western Antarctic Peninsula and those caught along the AFS.

105         Close to the continent, the Antarctic Coastal Current (AACC) transports fresh shelf  
106 waters, occupying the upper part of the water column. Freshwater input from precipitation,  
107 run-off, sea-ice and glacial melt influence its presence and strength, which varies spatially,  
108 seasonally and between years (Moffat et al. 2008, Dutrieux et al. 2014). The AACC merges  
109 with the ASF around Joinville Island at the northern tip of the Antarctic Peninsula before  
110 separating to continue along the Trinity Peninsula (Thompson et al. 2009). There, it forms the  
111 southern boundary of the Bransfield Gyre (Savidge & Amft 2009), which carries water past  
112 the South Shetland Islands, and Caccavo et al. (2018) found evidence of high levels of gene  
113 flow between fish sampled along the ASF and the South Shetland Islands.

114         The AACC also merges with the ASF along the narrow shelf in the eastern Weddell  
115 Sea, where westward flow is forced by prevailing easterly winds. Freshening in autumn  
116 shoreward of the ASF off the Riiser-Larsen Ice Shelf near Camp Norway (Fig. 1), coincides  
117 with increased wind speeds and the arrival of the previous summer's melt from sea-ice off  
118 the Fimbul Ice Shelf upstream (Graham et al. 2013). Where the shelf widens west of the  
119 Stancomb-Wills Ice Stream, flow along the shelf-break splits and one branch follows the

120 400-450m isobath in Halley Bay south past the Brunt Ice Shelf, to form a thick layer of cold  
121 relatively fresh water over the shelf at 76°S and at 77°S (Nicholls et al. 2009). A coastal  
122 current is also found carrying relatively fresh Eastern Shelf Water (ESW) southward from  
123 near the Brunt Ice Shelf and along the eastern shelf adjoining the Filchner Trough (Fig.  
124 1)(Nicholls et al. 2009). Recently hatched larvae indicated spawning associated with Camp  
125 Norway and Filchner Troughs (Hubold 1984, Ashford et al. 2017), suggestive of separate,  
126 coherent populations, yet Caccavo et al. (2018) found no genetic differentiation and evidence  
127 of strong gene flow between Atka Bay upstream of Camp Norway, Halley Bay off the Brunt  
128 Ice Shelf, and areas around Filchner Trough.

129         A second water mass present is Modified Warm Deep Water (MWDW) transported  
130 across the shelf-break along the eastern flank of the Filchner Trough (Nicholls et al. 2009).  
131 MWDW is formed as a result of mixing between intermediate Warm Deep Water (WDW)  
132 carried along the slope in the AFS and a layer of Winter Water (WW) above. WDW is a  
133 derivative of Circumpolar Deep Water (CDW) that is very nutrient rich but poor in oxygen.  
134 The CDW is transported within the ACC, and inflow of WDW occurs at the eastern boundary  
135 of the Weddell Gyre (Ryan et al. 2016). Intrusions of MWDW are found over the shelf off  
136 Camp Norway during winter (Graham et al. 2013). During summer, weaker wind forcing  
137 causes relaxation of the slope front, promoting inflow of warm water across the Filchner  
138 Trough sill (Ryan et al. 2017). The MWDW follows the eastern flank of the Filchner Trough  
139 over its eastern shelf offshore of the coastal current, providing a second, deeper pathway  
140 connecting flow along the slope to the inner shelf (Fig. 1)(Ryan et al. 2017). Nearby, above  
141 the eastern slope of the Filchner Trough, Ice Shelf Water (ISW), emerging from the Filchner  
142 Ice Shelf cavity, is transported northward and exits the trough across the sill to contribute to

143 deep water formation in the Weddell Sea. In winter, southward flow of MWDW ceases, and  
144 the ISW in the trough extends on to the adjacent eastern shelf (Ryan et al. 2017).

145 ***Testing population structure along the southern Weddell Sea shelf***

146 Several studies implicate connectivity between Antarctic silverfish populations via  
147 current and front systems. In the Ross Sea, Brooks et al. (2018), as well as noting that fish  
148 reaching the shelf front become exposed to along-shelf connectivity, suggested that larvae  
149 found in the Bay of Whales may have been spawned by fish transported from the eastern  
150 Amundsen Sea along the AACC. Caccavo et al. (2018) found, in addition to regional  
151 connectivity along the ASF, evidence indicating recent influx of silverfish along the inflow of  
152 Marguerite Trough. This was consistent with an earlier review by Kellermann (1996), who  
153 suggested that fish spawned in the Bellingshausen Sea were transported over the western  
154 Antarctic Peninsula shelf via slope transport in the ACC. Genetics data also indicated  
155 connectivity via the AACC between silverfish found in Marguerite Bay and Charcot Island  
156 (Agostini et al. 2015), which was further supported by reproductive data (La Mesa et al.  
157 2015b), otolith chemistry (Ferguson 2012), community spatial distributions (Parker et al.  
158 2015), and particle simulations based on a circulation model for the southwestern Antarctic  
159 Peninsula shelf (Piñones et al. 2011). Additionally, particle simulations combined with  
160 otolith age data suggested that larvae sampled off Joinville Island were spawned in Larsen  
161 Bay in the western Weddell Sea, and were subsequently transported around the northern  
162 Antarctic Peninsula and into the Bransfield Gyre via the AACC (La Mesa et al. 2015a).

163 In the Weddell Sea, White and Piatkowski (1993) noted that dense larval distributions  
164 found over the shelf slope east of the Filchner Trough mouth were consistent with an earlier  
165 hypothesis of westward dispersal by surface currents (Hubold 1984). Much of the evidence  
166 for the role of hydrography in connectivity between silverfish populations derives from

167 indirect observation using monodisciplinary approaches (Hubold 1984, Kellermann 1986,  
168 Kellermann 1996, Agostini et al. 2015, Brooks et al. 2018, Caccavo et al. 2018). Yet  
169 multidisciplinary studies can allow cross-corroboration and comparison between  
170 complementary techniques (Begg et al. 1999), while understanding of the physical context  
171 can help directly address the role of physical-biological interactions in structuring silverfish  
172 populations (Ashford et al. 2017, Davis et al. 2017, Brooks et al. 2018). Connectivity  
173 hypotheses between neighboring populations, in which the interplay between local  
174 hydrographic features and life history is important, can be tested (Ashford et al. 2017). In this  
175 context, although high levels of gene flow were consistent with dispersal from shelf areas  
176 near Atka Bay and Camp Norway predicted by White and Piatkowski (1993), length  
177 distributions in older stages vary considerably around the Antarctic (Ferguson 2012, Caccavo  
178 et al. 2018), indicative of spatial structuring. Given that all life stages of silverfish are pelagic  
179 and are thus continuously exposed to cross-shelf and along-slope current features, the level of  
180 exchange of individuals between otherwise demographically distinct populations would  
181 homogenize any existing genetic differentiation between areas (Palsbøll et al. 2007, Lowe &  
182 Allendorf 2010).

183         The integration of multiple fisheries population techniques allows for synergies that  
184 ultimately strengthen the understanding of population structure and demography (Welch et al.  
185 2015). Such approaches can be highly flexible, with selection of techniques and sampling  
186 designs targeted to test precise spatial predictions from physical-biological hypotheses (La  
187 Mesa et al. 2015a, Ashford et al. 2017, Brooks et al. 2018). Analysis of trace element  
188 deposition in fish otoliths has been shown to successfully resolve population structure in  
189 marine species based on distinct otolith nucleus chemistry indicative of disparate  
190 environmental exposure in early life (Campana 1999, Thorrold & Swearer 2009). While

191 allele frequency distributions highlight population processes on a multi-generational  
192 timescale and length distributions can indicate spatial structuring at the time of sampling,  
193 otolith chemistry reflects environmental exposure over an individual's life history. Otolith  
194 chemistry therefore has the potential to resolve population structure where gene flow  
195 homogenizes genetic differences, and throw light on the mechanisms explaining spatial  
196 length distributions and genetic connectivity (Ashford et al. 2006, Taillebois et al. 2017).

197 Otolith edge chemistry reflects environmental conditions directly prior to capture.  
198 Spatial discrimination has been tested between sampling areas around the maritime Antarctic  
199 and southern South America (Ashford et al. 2005), across frontal systems within the ACC  
200 (Ashford et al. 2007), and along the continental slope off the Ross Sea (Ashford et al. 2012).  
201 By contrast, otolith nucleus chemistry records environmental exposure during early life, and  
202 has successfully tested population hypotheses in multiple notothenioid species: Patagonian  
203 toothfish (*Dissostichus eleginoides*) (Ashford et al. 2006), Scotia Sea icefish  
204 (*Chaenocephalus aceratus*) (Ashford et al. 2010), Antarctic toothfish (*Dissostichus mawsoni*)  
205 (Ashford et al. 2012), as well as Antarctic silverfish (Ferguson 2012).

206 In this study, we therefore examined the physical-biological hypothesis of Ashford et  
207 al. (2017) using otolith nucleus chemistry from the same fish analyzed by Caccavo et al.  
208 (2018) caught along the southern continental margin of the Weddell Sea between Atka Bay  
209 and Filchner Trough. Variation in length distributions was characterized by strong modes that  
210 recurred spatially, and Caccavo et al. (2018) suggested these may reflect episodic  
211 connectivity via the ASF predicted by Ashford et al. (2017). Accordingly, material from  
212 otolith nuclei was compared between fish collected in Atka Bay, Halley Bay and along  
213 Filchner Trough, to test between three scenarios: 1) the existence of one homogeneous  
214 population with a shared spawning ground upstream, 2) the presence of discrete, independent



215 populations associated with spatially separated trough systems, and 3) episodic connectivity  
216 associated with the ASF and AACC between areas along the southern Weddell shelf.  
217 Whereas similar nucleus chemistry would support the null hypothesis of shared early life  
218 history among southern Weddell Sea fish, significant differences would be consistent with  
219 distinct populations along the continental shelf from Atka Bay to Filchner Trough.  
220 Differences between modes that were nevertheless similar across areas would suggest  
221 influxes of fish from more than one spawning ground along the shelf.

222

## 223 **METHODS**

### 224 *Field sampling*

225 Antarctic silverfish were collected in the southern Weddell Sea from January –  
226 February 2014 during the research cruise PS82 (ANT-XXIX/9) by the RV *Polarstern*,  
227 investigating the Filchner Outflow System. A Seabird 911+ CTD (Conductivity-  
228 Temperature-Depth), measuring salinity, temperature and pressure, and attached to a carousel  
229 with 24 water bottles, was deployed to investigate the physical environment in the region  
230 around the Filchner Trough, including the course of the coastal current and MWDW flowing  
231 towards the Filchner Ice Shelf (Knust & Schröder, 2014) . A total of 142 CTD profiles were  
232 obtained along oceanographic transects across and along the continental slope and shelf  
233 break, and across the eastern shelf adjoining the trough (Fig. 1). The distribution of bottom  
234 water masses over the slope and continental shelf were reported by Schröder et al. (2014).  
235 The CTD section at 76°S was described by Ryan et al. (2017), including seasonal evolution  
236 based on data retrieved from three moorings.

237 Integrated with the physical measurements, silverfish were sampled from stations  
238 around the Filchner Trough including the adjoining eastern shelf. All sampling was

239 undertaken during the day when fish were near the bottom during their diurnal migration  
240 (Fig. 1, Table 1), using a commercial benthic trawl with a cod-end mesh line of 20 mm.  
241 Standard length (SL) was measured for all individuals, and biomass, abundance and size  
242 distribution determined for each haul. Catches were randomly sub-sampled for tissue and  
243 otoliths for subsequent analyses. For comparison, samples were also collected in Atka Bay  
244 and off Camp Norway, with corresponding CTD data.

#### 245 *Laboratory procedures*

246 Biomass and abundance indices were reported by Wetjen et al. (2014a) and Wetjen et  
247 al. (2014b) and genetic analyses were undertaken and reported by Caccavo et al. (2018).  
248 Length distributions showed two recurrent modes, of immature fish at approximately 10 cm  
249 and mature fish at approximately 15 cm SL. For the otolith chemistry, however, the length  
250 modes were not uniformly distributed between sampling areas, precluding a cross-wise  
251 experimental design with area and length group as factors. Instead, five stations were selected  
252 along the shelf in relation to the position of the AACCC, the AFS, and inflows over the shelf-  
253 break: in Atka Bay; across the eastern shelf adjoining Filchner Trough corresponding to three  
254 CTD sections across Halley Bay, at 76°S and at 77°S; and near the shelf-break corresponding  
255 to a section across the western shelf downstream of the trough mouth (Table 2, Fig. 1). All  
256 fish in a given sampling area were pooled if only one mode was present; if the distribution  
257 was bimodal, a cut-off was set at 13 cm and fish were pooled into groups of large and small  
258 individuals. This resulted in eight groups from each of which 25 fish were randomly sub-  
259 sampled to form experimental treatments. In Halley Bay, both large and small groups at  
260 Station 126 were supplemented by randomly selected fish from nearby at Station 129.  
261 Similarly, six fish from Station 84 supplemented those sampled at 77°S from Station 78,  
262 resulting in eight treatments: Atka Bay (AB), Halley Bay small mode (HB-S) and large mode

263 (HB-L), Coats Land small (CL-S) and large (CL-L), East Filchner Trough (EF), West  
264 Filchner Trough small (WF-S) and large (WF-L) (Table 2).

265 One randomly selected otolith from each fish was used for elemental analysis.  
266 Otoliths were prepared using a standard protocol developed at the Center for Quantitative  
267 Fisheries Ecology at Old Dominion University (Ashford et al. 2012). They were initially  
268 cleaned using glass probes and rinsed in Milli-Q water. Any remaining surface contamination  
269 was removed by 5 minutes incubation in 20% Ultra-Pure hydrogen peroxide, followed by  
270 rinsing in Milli-Q water. Otoliths were then mounted onto slides using crystal bond, and  
271 ground from the anterior side using a Crystal Master 8 Machine with 3M film to reveal a  
272 transverse surface just above the primordium. In a clean room, mounted otoliths were given a  
273 final polish by hand using 3M film, and once again rinsed with Milli-Q water and allowed to  
274 dry. Otoliths were removed from the polishing slide and mounted on petrographic slides in a  
275 random blocks design, with slide as the blocking factor. In this way, all eight treatments were  
276 represented on each petrographic slide, and the slides were then rinsed and sonicated  
277 individually for 5 minutes in Milli-Q water, before placement under a laminar-flow hood to  
278 dry.

279 Minor and trace elements were measured using a Finnegan Mat Element 2 double-  
280 focusing sector-field Inductively Coupled Plasma Mass Spectrometer (ICP-MS) located in  
281 the Plasma Mass Spectrometry Facility at Woods Hole Oceanographic Institution (WHOI).  
282 Samples were introduced into the ICP in an automated sequence (Chen et al. 2000) in which  
283 otolith material ablated with a 193 nm laser ablation system was combined with HNO<sub>3</sub>  
284 aerosol introduced by a microflow nebulizer. The subsequent mixture was then carried to the  
285 ICP torch. For quality control, we used a calcium carbonate reference produced by the United  
286 States Geological Survey (Microanalytics Carbonate Standard, MACS-3), for which

287 elemental fractionation, mass-load, and matrix effects have been shown to be small for  
288 lithophile elements, especially when used with 193 nm laser ablation (Jochum et al. 2012).  
289 In the same way as the samples, MACS-3 material was ablated and introduced into the spray  
290 chamber as an aerosol; HNO<sub>3</sub> aerosol alone was also introduced into the spray chamber by  
291 the nebulizer as blanks. The randomized blocked design controlled for operational variability  
292 in the instrument. Blank and reference readings of count rate (count s<sup>-1</sup>) were taken before  
293 and after each block, and every four otoliths within blocks. Otoliths were analyzed for <sup>48</sup>Ca,  
294 <sup>25</sup>Mg, <sup>55</sup>Mn, <sup>88</sup>Sr and <sup>138</sup>Ba and reported as ratios to <sup>48</sup>Ca. Background counts were subtracted  
295 from otolith counts by interpolating between the readings taken before and after every four  
296 otoliths, and the corrected otolith counts were then converted to element:Ca (Me·Ca<sup>-1</sup>) ratios  
297 using the standards. To measure ratios indicative of conditions to which fish were exposed  
298 during early life, a grid raster type 150 μm x 200 μm was placed over the otolith nucleus  
299 corresponding to the first summer of growth, and the area was ablated using a 20 μm  
300 diameter laser beam at a frequency of 10 Hz and a power of 60%, traveling over the raster at  
301 6 μm s<sup>-1</sup>. Background levels of Ba increased over the course of the analyses; however, the  
302 randomized blocks design guarded against any resulting biases.

### 303 *Statistical analysis*

304 The ratio data were checked for multivariate outliers by plotting squared Mahalanobis  
305 distances of the residuals ( $D^2_i$ ) against the corresponding quantiles ( $Q-Q$  plot) of the  $\chi^2$   
306 distribution (Khatree & Naik 1999), and none were identified. Data for Mg·Ca<sup>-1</sup> and Ba·Ca<sup>-1</sup>  
307 were found not to conform to multivariate normality based on tests using Mardia's  
308 multivariate skewness and kurtosis measures ( $\alpha = 0.05$ ) and  $Q-Q$  plots of squared  
309 Mahalanobis distances ( $d^2_i$ ); variance-covariance matrices were not equal according to  
310 Bartlett's modification ( $\alpha = 0.10$ ). Univariate power transformations (Ashford et al. 2007)

311 succeeded in stabilizing the variances, the transformed data conforming to multivariate  
312 normality with equal variance-covariance matrices. The data transformations were  $y^{0.01}$  for  
313  $\text{Mg}\cdot\text{Ca}^{-1}$ , and  $y^{-1}$  for  $\text{Ba}\cdot\text{Ca}^{-1}$ ; no transformation was required for  $\text{Sr}\cdot\text{Ca}^{-1}$ .

314         Once transformed data fulfilled assumptions, we tested between population  
315 hypotheses using multivariate analysis of variance (MANOVA). Contrasts were constructed  
316 between (i) Atka Bay and Halley Bay; (ii) Filchner Trough and Halley Bay; and (iii) large  
317 and small modes in the length distributions for areas with both modes in Halley Bay and  
318 Filchner Trough. Equal variance-covariance ratios allowed for the calculation of canonical  
319 discriminant variates for graphic illustration (Khattree & Naik 2000). Univariate models were  
320 used to examine the influence of each  $\text{Me}\cdot\text{Ca}^{-1}$ ; as  $\text{Mn}\cdot\text{Ca}^{-1}$  values were less than detection  
321 limits and showed no differences, they were dropped from the analyses. Evaluating  
322 differences between treatments further, we also used Student-Newman-Keuls (SNK) and  
323 Scheffé tests for pairwise comparisons in an ordered array of treatment means based on  
324 experimentwise error rates.

325

## 326 **RESULTS**

### 327 *Physical data: Topography and hydrography*

328         Generally, the Filchner Trough was filled with dense ISW and intrusions of MWDW  
329 were observed to the east and west of the Filchner sill (Fig. 2)(Schröder et al. 2014). Further  
330 south, the bottom layer was occupied by ISW along the eastern flank of the trough and the  
331 adjoining shelf, and ESW closer to shore. The bottom layer at stations deeper along the  
332 continental slope was occupied by Weddell Sea Deep Water (WSDW)(Schröder et al. 2014).  
333 The section at  $76^{\circ}\text{S}$  showed a layer of ISW reaching onto the eastern shelf in January 2014,

334 with a trace of MWDW at mid-depth from a southward flowing intrusion along the eastern  
335 flank of the trough (Fig. 3)(Ryan et al. 2017).

336 Examining the CTD profiles (Fig. 4) for stations selected for otolith chemistry, the  
337 bottom trawl sample from Atka Bay was taken from a depth of 351 m along the narrow shelf  
338 characteristic of the eastern Weddell Sea, where the AACC merges with the AFS. The  
339 corresponding CTD data showed the presence of fresh ESW throughout the whole water  
340 column, resembling a typical summer profile with a warm, fresh surface layer. No intrusions  
341 of MWDW were observed (Fig. 4).

342 At the stations east of the Filchner Trough, salinities were generally higher (Fig. 4). In  
343 Halley Bay, a more saline water column was observed, but no evidence of MWDW (Fig. 4).  
344 Increased temperature in the surface layer, and no associated reduction in salinity suggested  
345 sampling located in the summer polynya, caused by off-shore winds pushing the ice away  
346 from the coast. The depth profile corresponding to station 129 was similar. At 76°S off Coats  
347 Land along the transect described by Ryan et al. (2017)(Fig. 3), the CTD data was taken near  
348 the eastern edge of the southward flowing MWDW incursion. In the bottom layer, where the  
349 sample of silverfish was taken at a depth of 450 m, a small decrease in temperature and  
350 increase in salinity suggested proximity to the ISW layer reaching over the shelf from the  
351 flank of the Filchner Trough (Fig. 4). In the surface layer, decreased salinity and increased  
352 temperature indicated some continuing effects from melting sea ice (Fig. 4). At 77°S,  
353 temperature and salinity indicated continuing meltwater in the surface layer, and a solid layer  
354 of ESW to 360 m over the eastern shelf (Fig. 4). However, fish were sampled further offshore  
355 and deeper, along the 450 m and 700 m bottom contours, exposed to ISW flowing north  
356 along the eastern flank of the trough (Fig. 4).

357 At the station west of the Filchner Trough mouth, warm, salty water characterized by  
358 a reduction in oxygen indicated MWDW occupying the bottom layer (WF in Fig. 4), part of  
359 the western incursion described by (Schröder et al. 2014), facilitated by lifting of the  
360 isopycnals due to the dense Filchner outflow (Nicholls et al. 2009). Some freshening near the  
361 surface, without an associated increase in temperature, showed the influence of sea ice  
362 melting.

### 363 ***Biological data: Spatial length distributions and nucleus chemistry***

364 Stations where silverfish were most abundant coincided with the distribution of  
365 MWDW in the bottom layer. High abundance indices were associated with regions where  
366 MWDW intrusions were observed over the shelf east (Fig. 5, Stations 166, 306, 282, 129) of  
367 the trough mouth, in the trough mouth (Station 188) and over the shelf west (Station 248) of  
368 the trough mouth (Wetjen et al. 2014a). By comparison, abundance indices were much lower  
369 further south over the eastern shelf, and along the shelf-break at stations 331, 316, 11, 175,  
370 201 and 249.

371 Moreover, abundance and biomass indices showed evidence of spatial decoupling  
372 related to differences in the distribution of fish from the large and small modes in the length  
373 distribution (Fig. 6). Mature large-mode fish were found throughout the region around the  
374 Filchner Trough, including hauls along the section at 77°S and the northeastern part of Halley  
375 Bay, but not further east where only three fish were caught off Camp Norway and immature  
376 fish were found in Atka Bay. The intrusion of MWDW along the eastern shelf was  
377 associated with small-mode fish at stations 282, 296, 126 and 39. However, small-mode fish  
378 were not caught in hauls along the 77°S section or in northeastern Halley Bay.

379 Compared to the genetic analysis, in which no spatial differences in gene frequencies  
380 were found (Caccavo et al. 2018), the chemistry in the otolith nuclei showed significant

381 differentiation (multivariate ANOVA Pillai's trace;  $F = 3.36$ ,  $df = 21$ ,  $p < 0.0001$ ; Table 3a),  
382 discounting the null hypothesis of a single population with a shared spawning area upstream.  
383 All MANOVA contrasts were significant using an experiment-wise alpha level of  $\alpha =$   
384  $0.0166$ , indicative of population structuring along the southern Weddell Sea continental shelf.  
385 Strong contrast between large and small length modes (Pillai's trace;  $F = 6.18$ ,  $df = 3$ ,  $p =$   
386  $0.0005$ ) was consistent with separate origins for immature and mature fish. Differences  
387 between Atka Bay and Halley Bay (multivariate ANOVA Pillai's trace;  $F = 11.94$ ;  $df = 3$ ,  $p$   
388  $< 0.0001$ ), and Halley Bay and Filchner Trough (Pillai's trace;  $F = 4.66$ ,  $df = 3$ ,  $p = 0.0038$ )  
389 suggested further population structuring. Along the first canonical variable (Fig. 7), the  
390 distribution of variates reflected the differences between large and small mode fish, and  
391 between Atka Bay and Halley Bay. Along the second variable, there was some indication of  
392 sub-grouping in small mode fish in southern Halley Bay and off Coats Land.

393         Examining univariate data for adults, differences in otolith nucleus chemistry between  
394 areas were primarily due to  $Mg \cdot Ca^{-1}$  (Table 3b), which showed strong differences for all three  
395 contrasts.  $Sr \cdot Ca^{-1}$  showed a significant difference between large and small mode fish, but not  
396 between Atka Bay, Halley Bay and Filchner Trough.  $Ba \cdot Ca^{-1}$  showed no significant  
397 differences for any of the contrasts. The Scheffé test for  $Mg \cdot Ca^{-1}$  indicated ordering: Atka  
398 Bay differed significantly from large fish in southern Halley Bay and the southern Filchner  
399 Trough, but was similar to small fish west of the Filchner Trough and at the  $76^{\circ}S$  section.  
400  $Sr \cdot Ca^{-1}$  showed no significant differences, but treatments were ordered according to mode,  
401 with Atka Bay most similar to small fish at  $76^{\circ}S$ , Halley Bay and west of Filchner Trough.  
402 Similarly, ordering by  $Ba \cdot Ca^{-1}$  showed small fish at  $76^{\circ}S$  to be most similar to small fish in  
403 Halley Bay and Atka Bay. Overall, these results suggest that immature fish in Atka Bay had  
404 similar environmental exposure during early life as small-mode fish in Halley Bay and



405 Filchner Trough, consistent with episodic connectivity, but their early life exposure differed  
406 from large-mode fish. Including large-mode fish from Halley Bay can help explain the  
407 difference in the contrast with Atka Bay; nevertheless, the difference between Halley Bay  
408 and Filchner Trough suggested further population structuring linked to water mass properties  
409 and circulation over the southern Weddell Sea continental shelf.

410

## 411 **DISCUSSION**

### 412 *Population structure and connectivity in the southern Weddell Sea*

413 Our results illustrate the utility of multidisciplinary approaches (Begg et al. 1999) for  
414 addressing population structure in Antarctic fish. Even though Caccavo et al. (2018) found  
415 high levels of gene flow, the chemistry in otolith nuclei indicated significant population  
416 structuring along the south Weddell Sea continental shelf, discounting the null hypothesis of  
417 a single population of shared provenance. Mediated by physiological processes like growth  
418 that are associated with changes in water properties in the Southern Ocean (Ashford et al.  
419 2005, Ashford et al. 2006),  $\text{Mg}\cdot\text{Ca}^{-1}$  and  $\text{Sr}\cdot\text{Ca}^{-1}$  differentiated large and small length modes,  
420 suggesting separate origins and a role for connectivity as well as local self-recruitment in  
421 structuring length distributions. Inter-annual variability may explain some of the difference  
422 between modes; nevertheless, even after accounting for mode,  $\text{Mg}\cdot\text{Ca}^{-1}$  showed differences  
423 between Halley Bay and Filchner Trough, consistent with spatially-based structuring along  
424 the eastern shelf.

425 Integrating the sources of information, similarities in chemistry and length  
426 distributions indicated that fish from Atka Bay had the same origin as small mode fish in  
427 Halley Bay and Filchner Trough, implicating along-shelf connectivity in determining spatial

428 distributions and gene flow. White and Piatkowski (1993) found evidence that larvae  
429 dispersed along the continental shelf; and our results suggest that the ASF facilitated  
430 connectivity in immature fish as well, in deeper water following ontogenetic movement to  
431 depth. Thus, abundance indices, biomass indices, and length all showed strong spatial  
432 association with MWDW along the shelf break and intruding along the eastern flank of  
433 Filchner Trough. Notably however, the small mode was not found in northeastern Halley  
434 Bay, where water from the eastern continental shelf flows inshore along the 400m isobath  
435 (Nicholls et al. 2009).

436         Large-mode fish showed a different spatial distribution, occurring in northeastern  
437 Halley Bay and all samples around Filchner Trough. They accounted for high abundance  
438 indices associated with the incursion of MWDW east of the Filchner sill. They were also  
439 found in association with small-mode fish close to the interface between ISW and MWDW  
440 along the Filchner Trough and western shelf-break. Provenance from areas upstream would  
441 be consistent with the dense aggregations of larvae found by Hubold (1984) off Camp  
442 Norway and the evidence supporting dispersal reported by White and Piatkowski (1993). In  
443 this scenario, larval dispersal supplies northeastern Halley Bay, mediated by juvenile  
444 movement from the upper water column to deeper, slow-flowing ESW off the Brunt Ice  
445 Shelf. Feeding opportunities reinforce local retention of older stages where nutrient-rich  
446 MWDW enters the continental shelf. Young stages continuing in the coastal current, or older  
447 stages following flow in deeper ESW, penetrate further south along the eastern shelf  
448 accounting for the lower abundance indices encountered there during sampling.

449         Nevertheless, the scenario lacks corroborating evidence of similar large-mode fish in  
450 Atka Bay or Camp Norway Trough. This absence also argues against supply from areas  
451 further upstream: the narrow shelf in this region is characterized by strong wind-driven

452 surface flow toward the coast (Graham et al. 2013) that brings water from the AFS over the  
453 shelf, and hence any larvae entrained within it. Sampling effects may be responsible: only  
454 one sample was taken in Atka Bay and off Camp Norway, and further sampling may have  
455 revealed adult fish. However, Hubold (1984) also found considerable numbers of larvae over  
456 the southern Filchner Trough and suggested that the local wind field and circulation  
457 structured early life history, connectivity and retention as far north as the ASF. Large  
458 aggregations of larvae were also found during the same cruise as our sampling (Fig. 9)(Auel  
459 et al. 2014) suggesting a competing scenario, in which a local population supplies adult  
460 distributions over the adjoining shelf. In the following section, we build on Hubold's original  
461 insights, integrating recent knowledge available on the physical system in the Filchner  
462 Trough, and outlining how physical-biological interactions with circulation and water  
463 structure might help underpin dispersal and retention in a local population.

#### 464 ***Physical-biological interactions and life history closure over the Filchner Trough***

465 In this scenario, a discrete, self-recruiting population is structured by the trough  
466 circulation (Ashford et al. 2017), constrained by cryopelagic early stages under sea-ice near  
467 the head of the trough. Considerable consistency in silverfish reproductive timing and  
468 behavior (La Mesa et al. 2015b) suggests hatching in December and early January as  
469 elsewhere, under sea-ice near the Filchner Ice Shelf. Larvae disperse northward in the trough  
470 circulation in a similar manner to the Drygalski Trough (Brooks et al. 2018), consistent with  
471 the distributions found by Hubold (1984) and Auel et al. (2014)(Fig. 9). ISW fills the trough  
472 and northward flow occurs year-round along the trough flank from under the ice shelf. As a  
473 result, spawning in the vicinity of the ice shelf exposes adults to this flow during late winter  
474 and early summer. Movement northward is consistent with exclusively large-mode fish  
475 sampled in ISW at 77°S at 700 m during this study, compared to sharply decreasing numbers

476 at shallower depths over the adjoining shelf. At 76°S, however, ISW reaches onto the shelf  
477 during winter and summer (Ryan et al. 2017), and in this study, fish were found at 450 m  
478 near the ISW interface but not further inshore at 250 m. Moreover, MWDW from the  
479 continental slope intrudes south at mid-depth during Phase 1 in the scheme presented by  
480 Ryan et al. (2017), potentially exposing fish to southward flow during their diurnal  
481 movement. During Phase 2 in autumn (mid-March to July), the MWDW intrusion reaches the  
482 bottom and flow in the benthic layer is strongly southward. In Phase 3, the inflow stops, and  
483 the remaining MWDW likely mixes away into the water column due to strong surface forcing  
484 during winter. Slow, westward flow occurs in a narrow band off the eastern shelf, providing a  
485 pathway for adults returning to spawning areas near the head of the trough.

486         Nevertheless, the strong northward flow of ISW that occurs throughout the year along  
487 the flank of the trough, crosses the sill to contribute to deep water formation. Consequently,  
488 older fish remaining in ISW are exposed to water that connects to the continental slope,  
489 accounting for large-mode fish sampled at the trough mouth and downstream associated with  
490 the ASF. The outflow also provides a return pathway to the continental slope for fish  
491 transferring from the MWDW intrusions. Physical effects, due to trough configuration,  
492 meanders and mixing between water masses, potentially interact with biological ones, like  
493 diurnal migration through the water column and feeding opportunities along the boundary  
494 between the two water masses, to determine rates of transfer between the trough outflow and  
495 inflow. Those reaching inflowing water over the edge of the adjoining shelf are retained in  
496 the population, whereas those remaining over the trough flank eventually encounter the AFS  
497 and are advected westward along the continental slope as part of the ASC.

498         Less clear in this scenario is how larvae in the surface layer reach the eastern shelf. In  
499 the Ross Sea, the Drygalski Trough runs parallel with the coast, so that offshore winds  
500 generate flows that can enhance mixing across the trough as well as cross-shelf advection

501 (Brooks et al. 2018). Near Coulman Island, a potentially important area for larval transfer to  
502 the trough inflow (Brooks et al. 2018) is characterized by proximity of the coast on the  
503 western side of the trough, a reverse slope, and curvature in the trough configuration. In the  
504 Filchner Trough, the coast lies parallel on its eastern side, and winds at Halley Station are  
505 predominantly southwestward. As a result, Ekman flows may facilitate advection over the  
506 eastern shelf. The configuration of the trough may also play a role, shoaling along the reverse  
507 slope coinciding with a shift in orientation from northeast-southwest near the ice shelf to  
508 north-south near the shelf-break.

509         Moreover, Filchner Trough is characterized by outflow along the eastern flank  
510 (Darelius et al. 2014, Ryan et al. 2017), and the coastal polynya is narrow, often with  
511 proximity of the ice edge to the eastern shelf during summer (Fig. 9b, Fig. 9c). Meltwater  
512 from sea-ice is an important source of iron to the euphotic zone (McGillicuddy et al. 2015),  
513 and interactions between the outflow, ice edge and wind field are likely to influence larval  
514 growth and survival (Brooks et al. 2018). Thus, when conditions do not coincide at the right  
515 time, mortality may be large; or large numbers of larvae are advected to the slope front, as  
516 indicated by Hubold (1984), where they are lost to the system. By contrast, much larger  
517 proportions retained when conditions coincide may form dominant year classes consistent  
518 with the length distributions found by Hubold and Tomo (1989) and in this study.

#### 519 ***Examining physical-biological hypotheses using a multidisciplinary approach.***

520         Multidisciplinary approaches can promote synergies that ultimately strengthen the  
521 understanding of population structure and demography (Welch et al. 2015). Immigration of  
522 young stages into Filchner Trough along the coastal current, or older stages along intrusions  
523 of MWDW from the AFS, can help explain strong gene flow along East Antarctica into the  
524 Weddell Sea (Caccavo et al. 2018). Export of larvae along the ASF, or older fish in ISW

525 across the Filchner sill, are consistent with genetic homogeneity in shelf areas downstream  
526 along the ASF. Variability in length distributions on small spatial scales and over time can  
527 help explain changes in allele frequencies representative of chaotic genetic patchiness,  
528 previously found in silverfish (Zane et al. 2006, Agostini et al. 2015) and more generally  
529 attributed to inter-annual variations in recruitment and dispersal (Johnson & Black 1982).  
530 Our results suggest that variability in provenance with length, as indicated by the otolith  
531 chemistry, may also play a role.

532         Such comparisons between techniques can yield further insights. High levels of gene  
533 flow argue that a hypothesis of a discrete population in Filchner Trough remains incomplete:  
534 in a discrete population, self-recruitment and mortality exclusively determine abundance, and  
535 there is no migration to support gene flow. Moreover, inconsistent with random mixing in a  
536 single population, otolith chemistry indicated structure along the adjoining eastern shelf with  
537 Halley Bay, even when length distributions were taken into account. Additionally, small  
538 numbers of larvae along the shelf-break east of the Filchner Trough and in Halley Bay (Fig.  
539 9)(Auel et al. 2014) supported continuing larval connectivity in the upper water column along  
540 the slope, and the possibility of localized spawning in Halley Bay. Taken together, these  
541 results suggest that migrants, at different life stages and following multiple pathways, may  
542 join one or more local populations along the southern Weddell Sea continental shelf.  
543 Associated with the circulation in the Filchner Trough, abundances are determined by  
544 immigration and emigration as well as self-recruitment and mortality.

545         Length distributions indicate that these vital rates vary considerably over time, and  
546 the hydrography can help to explain the variation. The four phases defined by Ryan et al.  
547 (2017) described circulation patterns in the southern Weddell Sea following MWDW influx  
548 onto the shelf during summer and autumn; surface freezing temperatures and the

549 development of a weakly stratified water column cause a subsequent shift in circulation  
550 patterns during winter. However, points of transition between the predominant phases are  
551 often characterized by variable flow (October being the month with the highest observed  
552 variability in this respect), and seasonal variations in water mass thickness and penetration  
553 are likely to contribute to variability in the strength and direction of the circulation between  
554 years. While a consistent feature along the Weddell Sea continental slope, the ASF is  
555 sensitive to wind stress forcing on seasonal and inter-annual time scales (Youngs et al. 2015,  
556 Meijers et al. 2016, Azaneu et al. 2017), and the AACC also shows increased current speed in  
557 response (Daae et al. 2018). Moorings at 76°S have suggested considerable inter-annual  
558 variation in the amount of MWDW and the distance it penetrates onto the shelf (Ryan et al.  
559 2017). As a result, physical-biological interactions with the annual life cycle are likely to  
560 generate considerable variation in the composition of year classes.

561         Mixing between immigrants and locally-recruited fish can explain the structuring  
562 found in the otolith chemistry, varying in relation to position between the ice shelf, Halley  
563 Bay, and the shelf-break. The hydrographic regime, in addition to generally low adult  
564 abundances compared to the slope regions, argue that relatively few mature fish contribute  
565 disproportionately to spawning along the southern shelf. The high levels of abundance and  
566 biomass observed at stations along the slope (Fig. 5) associated with MWDW may represent  
567 attraction to feeding opportunities, and relatively few adults subsequently return to spawning  
568 areas at the trough head. Instead, physical-biological interactions with the slope current may  
569 result in entrainment and advection downstream.

570         Further research can address these questions and estimate the relative importance of  
571 self-recruitment, mortality and migration rates in determining silverfish abundance and  
572 distribution. Our results illustrate how multi-disciplinary approaches can offer important

573 advantages when used to test spatial predictions based on physical-biological population  
574 hypotheses. As previously demonstrated by Brooks et al. (2018) in the Ross Sea, sampling  
575 targeted by water mass is critical in characterizing distributions in relation to hydrographic  
576 variability in the southern Weddell Sea. Downstream, similar sampling will be crucial to  
577 understand how much the southern Weddell Sea contributes to silverfish aggregations in  
578 Larsen Bay and around the tip of the Antarctic Peninsula. Caccavo et al. (2018) have already  
579 shown no significant genetic differentiation between fish from the Weddell Sea, Larsen Bay,  
580 and the northern Antarctic Peninsula. Otolith chemistry can test whether this genetic  
581 panmixia is representative of a single population supplying these areas, or smaller coherent  
582 populations structured by the local circulation. A similar approach along East Antarctica can  
583 throw light on the physical-biological interactions supporting gene flow along the AFS from  
584 the Ross Sea. In this way, multi-disciplinary techniques, integrated in sampling designs that  
585 incorporate hydrography, can help strengthen our understanding of population structure along  
586 the shelf and the spatial scales on which connectivity occurs around the Southern Ocean.

587

#### 588 **ABBREVIATIONS**

589	AB	Atka Bay
590	AACC	Antarctic Coastal Current
591	ACC	Antarctic Circumpolar Current
592	ASF	Antarctic Slope Front
593	ASC	Antarctic Slope Front Current
594	CL	Coats Land
595	EF	East Filchner Trough



596	HB	Halley Bay
597	ESW	Eastern Shelf Water
598	ICP-MS	Inductively Coupled Plasma Mass Spectrometer
599	ISW	Ice Shelf Water
600	MANOVA	multivariate analysis of variance
601	MWDW	Modified Warm Deep Water
602	SL	Standard length
603	SNK	Student-Newman-Keuls test
604	WDW	Warm Deep Water
605	WF	West Filchner Trough
606	WHOI	Woods Hole Oceanographic Institution
607	WSDW	Weddell Sea Deep Water
608	WW	Winter Water
609		
610		
611		
612		
613		
614		
615		
616		

617 **Tables**

**Table 1** Biological sampling details for *Pleuragramma antarctica*. Sampling area, station, date of collection, coordinates and depth are indicated for all benthic trawl stations. Biomass, abundance and standard length (mean, standard deviation, range) are indicated for stations where fish were found.

Sampling area	Sampling station	Date	Latitude	Longitude	Depth (m)	Biomass (g)	Abundance (n)	Standard length (cm)		
								mean	± S.D.	range
Atka Bay (AB)										
	357-1	17/02/14	-70.913	-10.735	354.0	914.0	30	11.8	1.1	(10.2 - 15.0)
Riiser-Larsen										
	341-1	14/02/14	-72.799	-19.495	739.7	47.0	3	12.6	1.9	(10.8 - 14.5)
Halley Bay (HB)										
slope	331-1	12/02/14	-74.590	-26.887	762.7	1284.0	28	16.6	2.7	(10.0 - 21.5)
	316-1	10/02/14	-74.660	-28.763	769.0	116.0	3	15.8	3.1	(14.0 - 19.3)
	011-1	03/01/14	-74.705	-29.900	406.2	0.0	0	NA	NA	NA
	175-1	25/01/14	-74.491	-30.977	530.5	0.0	0	NA	NA	NA
shelf	166-1	24/01/14	-74.907	-26.688	306.0	66500.0	–	15.4	2.2	(11.9 - 20.2)
	018-1	04/01/14	-75.201	-27.543	391.2	2948.0	165	–	–	–
	306-1	09/02/14	-75.116	-28.750	421.7	48000.0	–	13.9	2.0	(9.5 - 17.5)
	282-1	07/02/14	-75.000	-29.494	411.2	20552.0	–	13.7	2.8	(10.2 - 20.0)
coast	129-1	20/01/14	-75.358	-27.743	371.7	24000.0	–	16.8	3.1	(9.6 - 22.8)
	126-1	19/01/14	-75.504	-27.467	281.5	4489.0	189	14.1	3.6	(9.0 - 21.5)
	296-1	08/02/14	-75.534	-28.714	396.0	3500.0	–	14.4	2.8	(9.2 - 19.3)
Coats Land (CL)										
	039-1	07/01/14	-76.097	-30.312	453.0	1897.0	118	12.0	2.6	(8.0 - 18.5)
	053-1	08/01/14	-76.322	-29.141	261.0	0.0	0	NA	NA	NA
East Filchner Trough (EF)										
	078-1	12/01/14	-77.032	-33.588	699.5	1350.0	–	15.0	3.7	(3.4 - 19.0)
	084-1	13/01/14	-77.013	-33.698	435.2	473.0	15	13.6	5.2	(7.0 - 20.0)
	088-1	14/01/14	-76.966	-32.945	265.2	0.0	0	NA	NA	NA
West Filchner Trough (WF)										
	188-1	26/01/14	-74.657	-33.762	592.2	758.0	49	–	–	–
	201-1	27/01/14	-74.571	-36.428	427.7	0.0	0	NA	NA	NA
	249-1	03/02/14	-74.544	-37.379	377.5	0.0	0	NA	NA	NA
	248-1	03/02/14	-74.608	-37.598	391.0	15050.0	873	14.0	2.9	(9.5 - 19.0)
	244-1	02/02/14	-74.816	-39.704	415.5	0.0	0	NA	NA	NA
							– no data	Abundance/Biomass		high
										low
										absent

**Table 2** *Pleuragramma antarctica* treatment group details. Sampling area, station, acronym, sample size (n) and standard length (mean, standard deviation, range) are indicated for all samples used in the otolith analysis.

Sampling area	Sampling station	Treatment group acronym	n	Standard length (cm)		
				mean	± S.D.	range
Atka Bay (AB)	357-1	AB	25	11.7	1.1	(10.2 - 15.0)
Halley Bay (HB)	129-1	HB-small (HB-S)	4	11.8	0.5	(11.0 - 12.0)
		HB-large (HB-L)	1	17.0	NA	NA
Coats Land (CL)	126-1	HB-small (HB-S)	21	10.4	1.0	(9.0 - 12.5)
		HB-large (HB-L)	24	15.8	2.1	(13.5 - 21.5)
	039-1	CL-small (CL-S)	25	10.2	0.9	(9.0 - 12.5)
		CL-large (CL-L)	25	15.1	1.4	(13.2 - 18.5)
East Filchner Trough (EF)	078-1	EF	19	15.9	2.1	(10.5 - 19.0)
	084-1	EF	6	16.8	2.7	(12.5 - 20.0)
West Filchner Trough (WF)	248-1	WF-small (WF-S)	25	10.7	0.9	(9.0 - 12.0)
		WF-large (WF-L)	25	15.7	1.7	(13.0 - 19.0)

620

621

622

623

624

625

**Table 3** Results of multivariate (a) and univariate (b) analyses of variance (MANOVA, ANOVA) for otolith nuclei of *Pleuragramma antarctica*, F- and *p*-values shown. ANOVA testing for difference in concentrations of Mg·Ca<sup>-1</sup>, Ba·Ca<sup>-1</sup>; and Sr·Ca<sup>-1</sup>. Asterisks (\*) indicate significance at experiment-wide  $\alpha = 0.0166$ .

(a) MANOVA

<b>Pillai's Trace</b>	<b>F-value</b>	<b><i>p</i>-value</b>
H <sub>0</sub> : No treatment effect	3.36	<0.0001*
C <sub>1</sub> : Atka Bay and Halley Bay	11.94	<0.0001*
C <sub>2</sub> : Halley Bay and Filchner Trough	4.66	0.0038*
C <sub>3</sub> : Small (< 13 cm) and Large (≥ 13 cm)	6.18	0.0005*

(b) ANOVA

<b>Contrast</b>	<b>F-value</b>			<b><i>p</i>-value</b>		
	<b>Mg · Ca<sup>-1</sup></b>	<b>Sr · Ca<sup>-1</sup></b>	<b>Ba · Ca<sup>-1</sup></b>	<b>Mg · Ca<sup>-1</sup></b>	<b>Sr · Ca<sup>-1</sup></b>	<b>Ba · Ca<sup>-1</sup></b>
Atka Bay and Halley Bay	32.73	2.22	0.03	<0.0001*	0.1380	0.8610
Halley Bay and Filchner Trough	9.90	0.26	0.99	0.0020*	0.6090	0.3220
Small (< 13 cm) and Large (≥ 13 cm)	8.94	11.03	2.54	0.0032*	0.0010*	0.1130

626

627

## 628 Figures

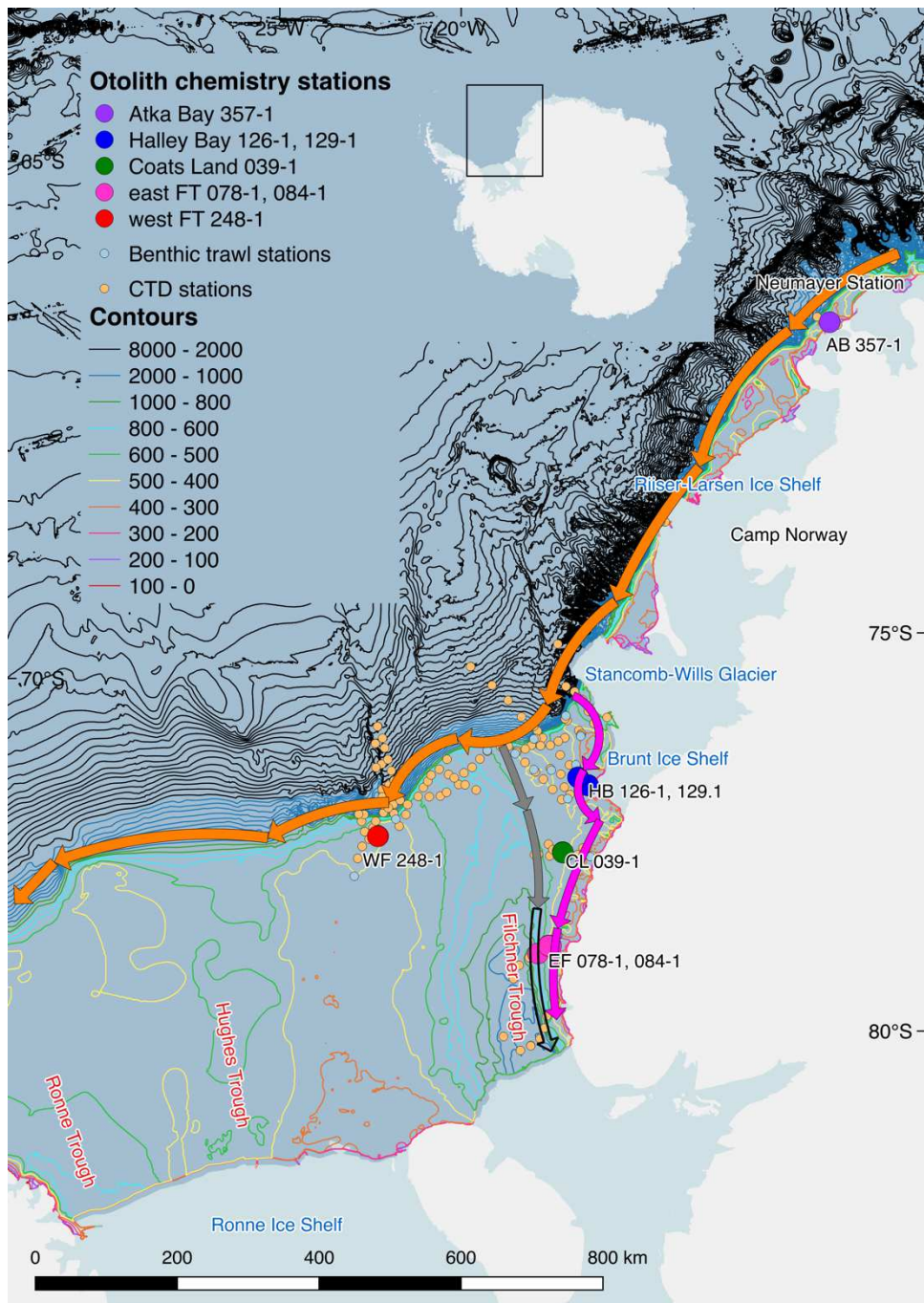


**Figure 1** Sampling locations. Orange arrows approximate the ASC, Antarctic Slope Front Current; Pink arrows approximate the coastal current; current positions based on Fig. 2b in Nicholls et al. (2009). Gray arrows approximate the intrusion of MWDW along the eastern side of the Filchner Trough based on Fig. 1 in Ryan et al. (2017), with the southernmost empty arrow indicating the maximum reach of MWDW. Relevant place names and bathymetric features are indicated. Station acronyms are as in Table 1. Map created using the Norwegian Polar Institute's Quantarctica 2.0 package (Matsuoka et al. 2018) in the software QGIS version 2.18.9 <http://qgis.osgeo.org> (QGIS Development Team 2018).

629

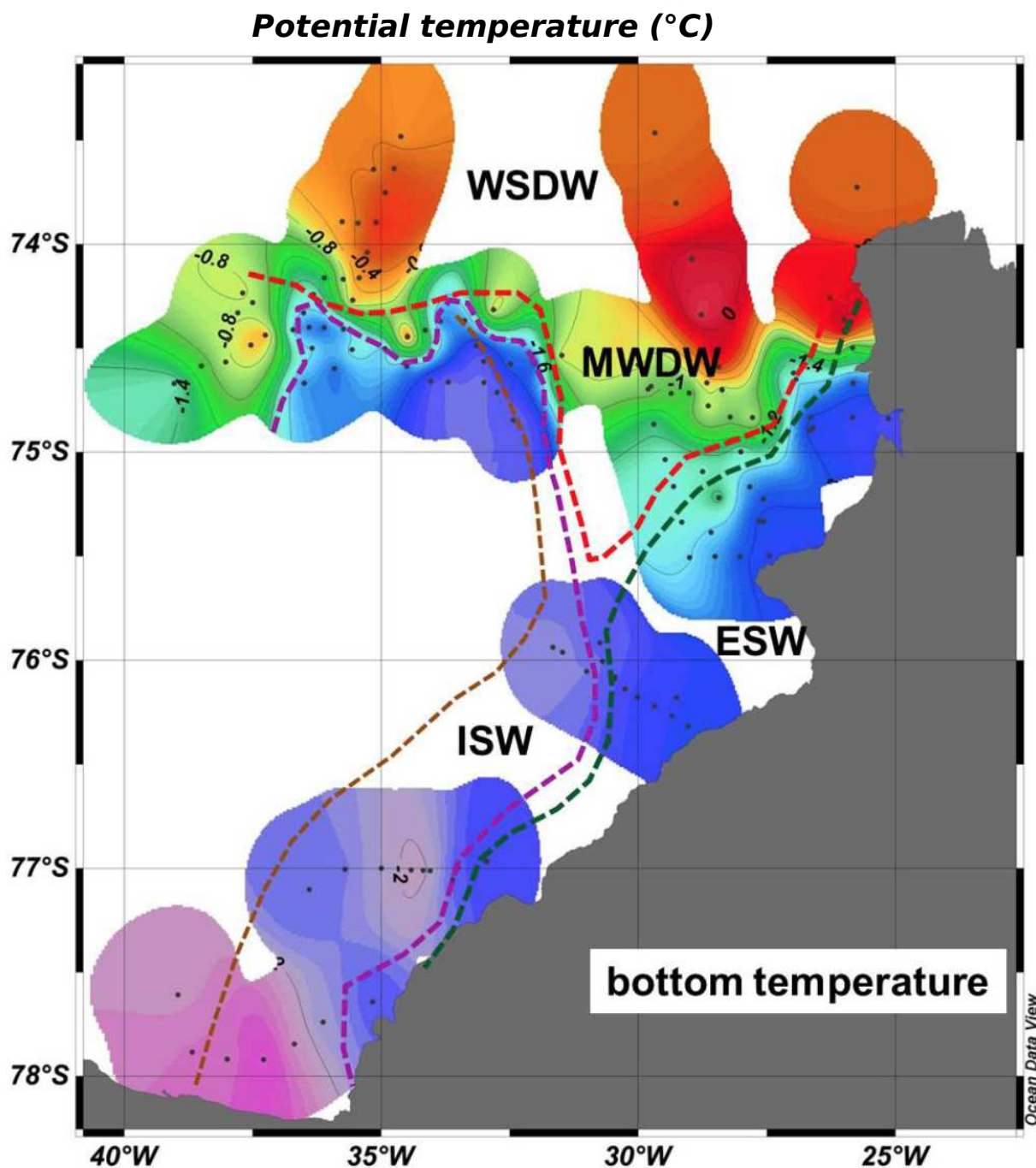


**Figure 2** Southern Weddell Sea predominant water masses. Reproduced from Schröder et al. (2014) Fig. 3.2.1.9a. ESW, Eastern Shelf Water; ISW, Ice Shelf Water; MWDW, Modified Weddell Deep Water; WSDW, Weddell Sea Deep Water.

630

631

632

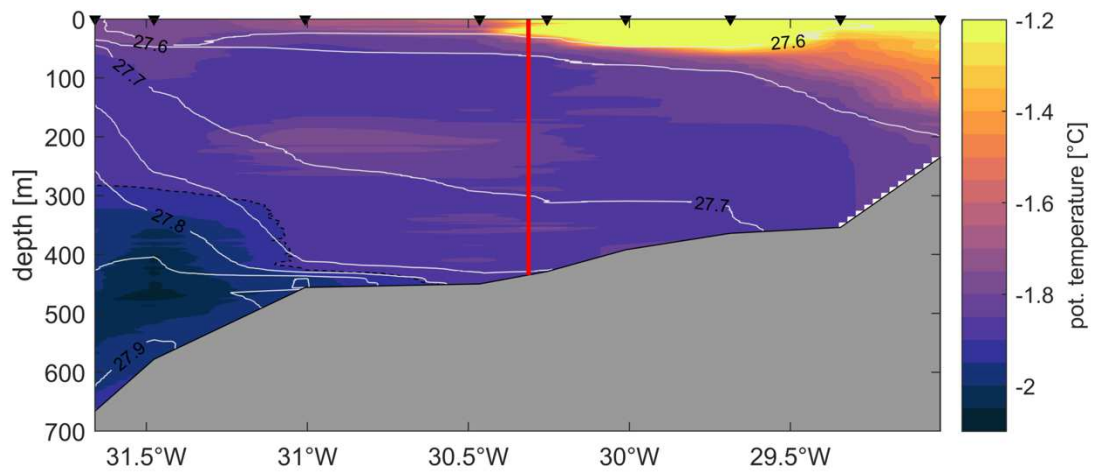


**Figure 3** Potential temperature section along 76°S obtained during the 2014 research cruise PS82 by the RV *Polarstern*. The red vertical line indicates the location of station 39 from the present study. White isolines are potential density lines referenced to the surface. The black dashed line indicates the  $-1.9^{\circ}\text{C}$  isotherm to visualize the Ice Shelf Water (ISW) layer ( $\theta < -1.9^{\circ}\text{C}$ ).

633

634

635

636

637

638

639

640

641

642



643

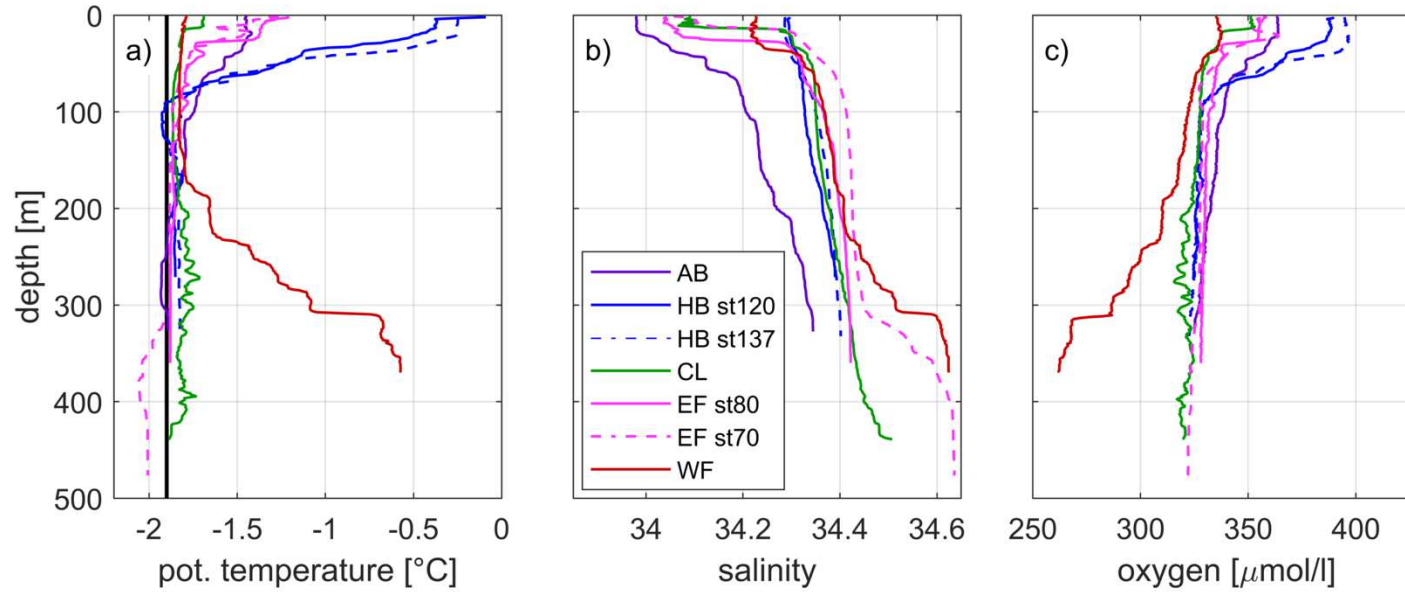


**Figure 4** CTD profiles showing (a) Potential temperature, (b) salinity and (c) dissolved oxygen. Plots correspond to data from Atka Bay (purple), Halley Bay (blue, CTD station 120 solid line, CTD station 137 dashed line), Coats Land (green), east Filchner Trough (pink, CTD station 80 solid line, CTD station 70 dashed line), west Filchner Trough (red). Treatment group acronyms are as in Table 1.

644

645

646

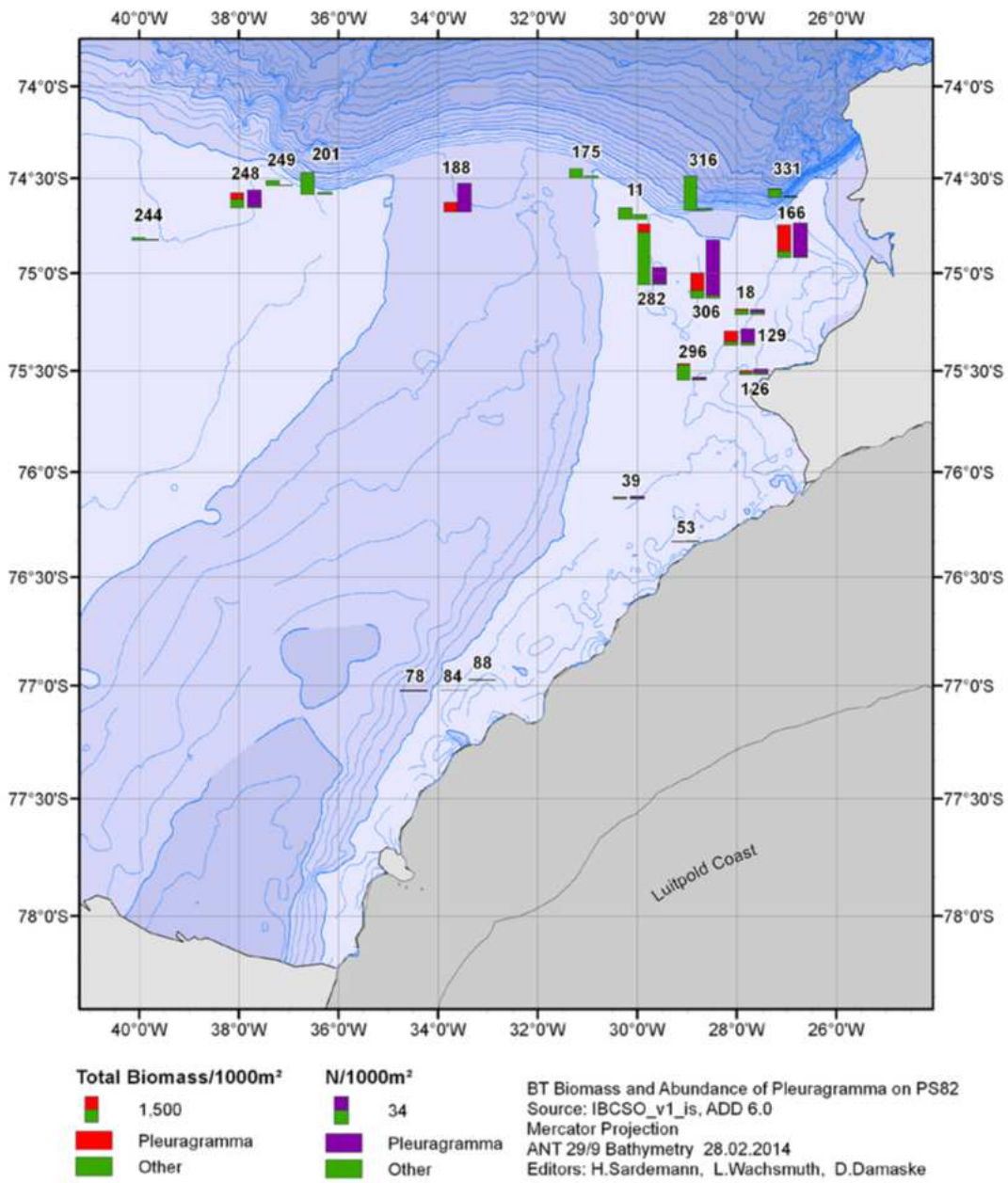


**Figure 5** *Pleuragramma antarctica* abundance and biomass in the southern Weddell Sea. Reproduced from Wetjen et al. (2014a) Fig. 3.3.4.2.1.

647

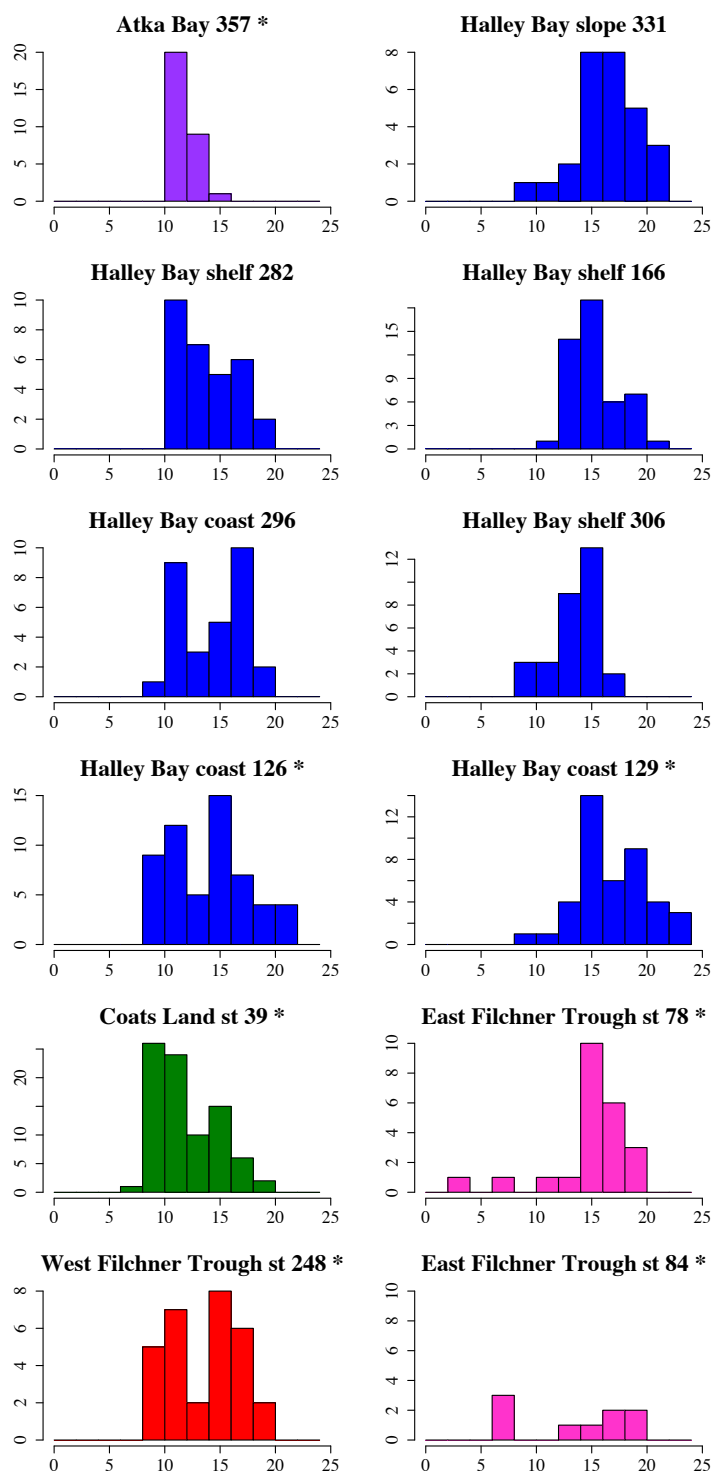


**Figure 6** Standard length (SL) distributions of *Pleuragramma antarctica* in the Weddell Sea. Sampling locations stations are specified above the graphs. Frequency indicated on the y-axis and SL in cm indicated on the x-axis. Asterisks (\*) indicate stations sub-sampled for otolith chemistry. Left column highlights bimodal stations, right column highlights unimodal stations. Station, st.

648

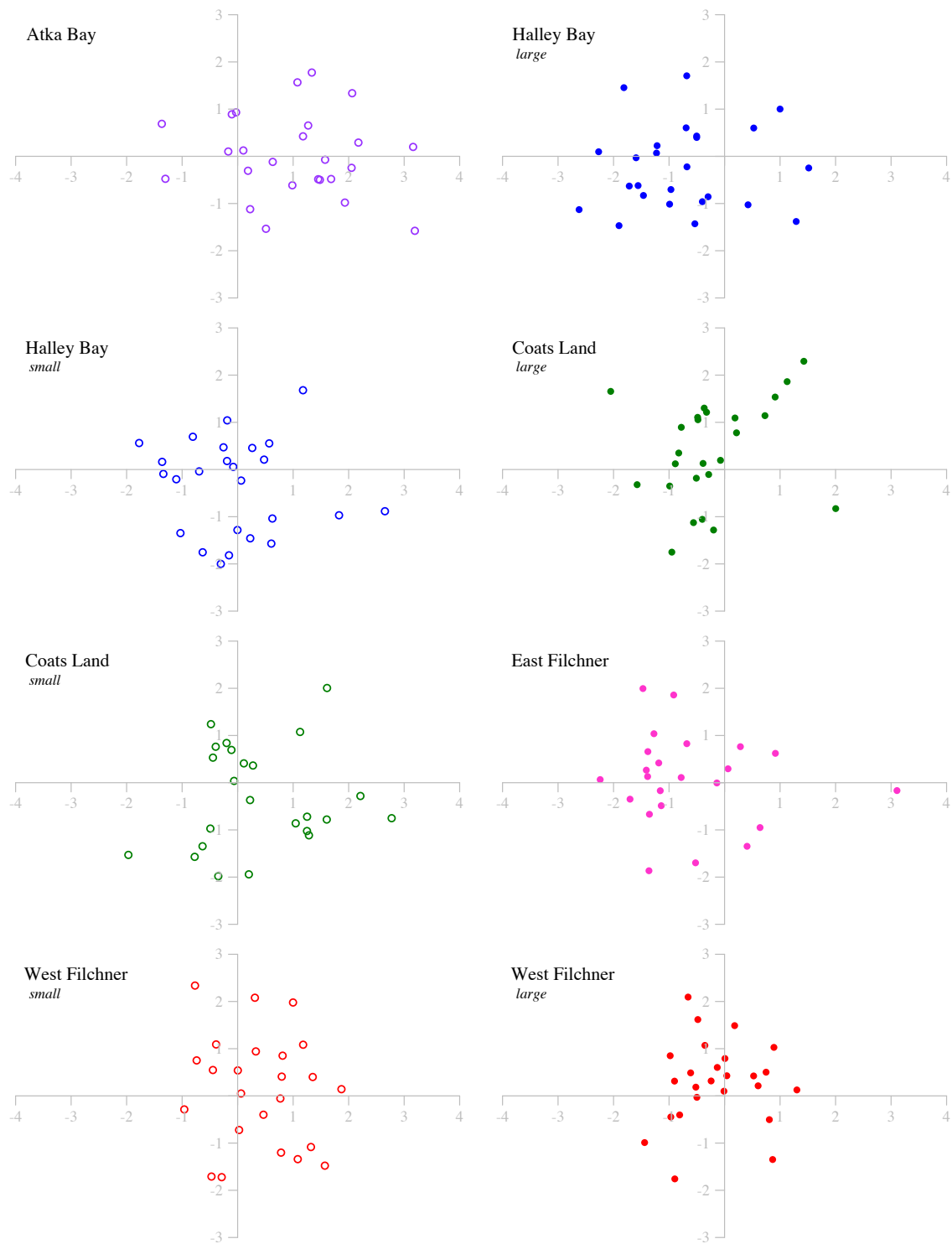


**Figure 7** Relationships between *Pleuragramma antarctica* from the different treatment groups using canonical discriminant variates based on otolith nucleus chemistry. Open circles represent treatment groups composed of small fish, filled circles indicate treatment groups consisting of large fish.

649

650

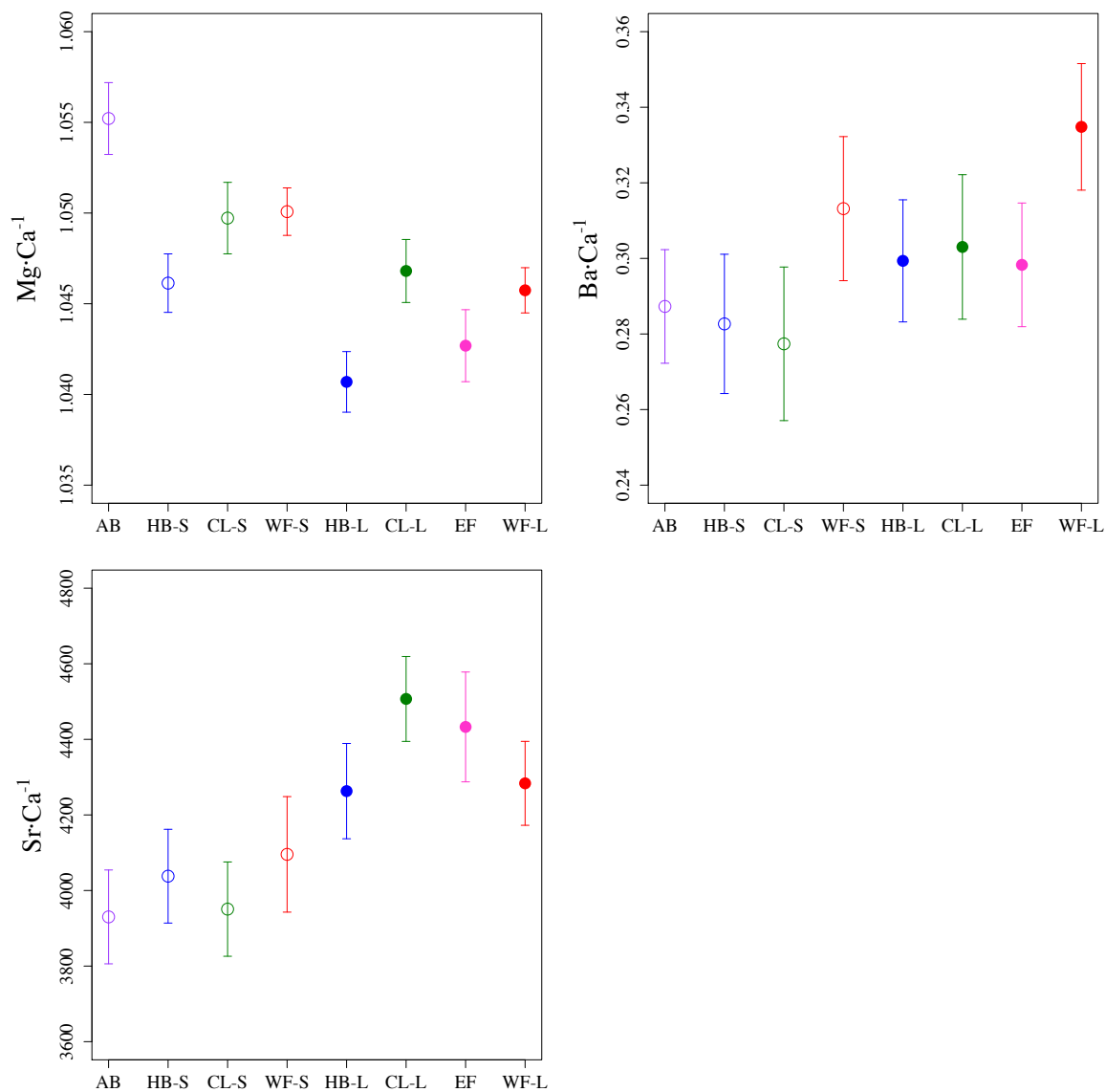
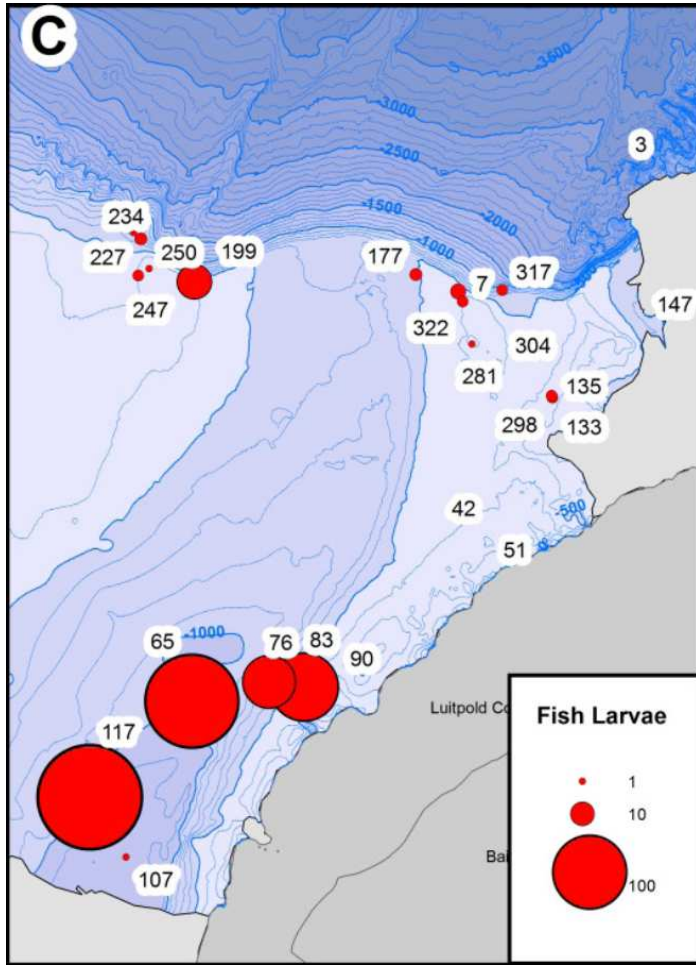


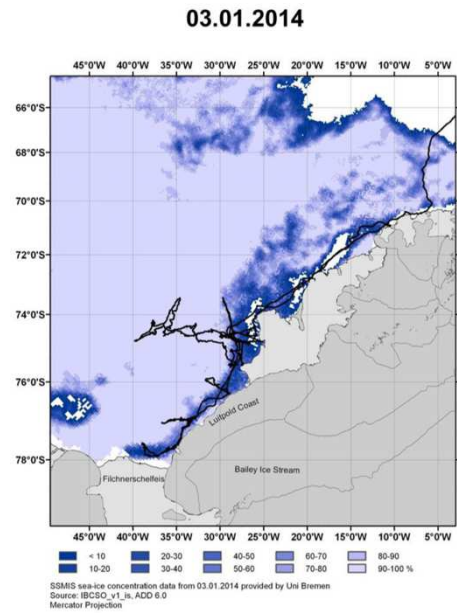
**Figure 8** Mean concentrations of Mg·Ca<sup>-1</sup>, Ba·Ca<sup>-1</sup>; and Sr·Ca<sup>-1</sup> of *Pleuragramma antarctica*, following transformation from  $\mu\text{mol}\cdot\text{mol}^{-1}$  using  $y^{0.01}$  for Mg·Ca<sup>-1</sup> and  $y^{-1}$  for Ba·Ca<sup>-1</sup>; no transformation for Sr·Ca<sup>-1</sup>. Bars indicate standard error. Open and filled circles represent treatment groups composed of small and large fish respectively. Treatment group acronyms are as in Table 1.

651

(a)



(b)



(c)

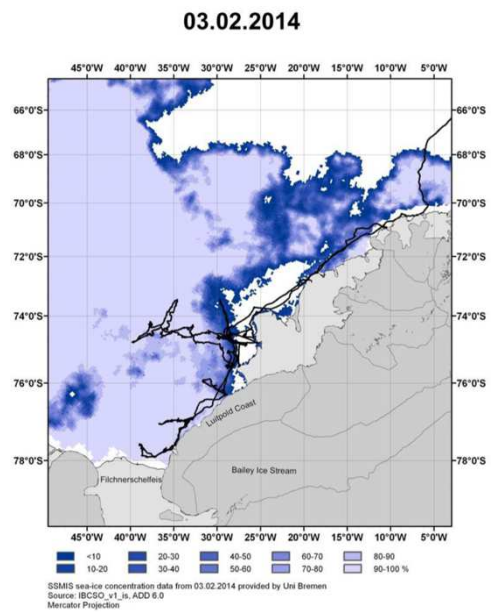


**Figure 9** Maps of the southeastern Weddell Sea showing (a) the total number of fish larvae per catch (of which ca. 90% were *Pleuragramma antarctica*), reproduced from Fig. 3.3.1.1c from Auel et al. (2014); and sea ice cover in January (b) and February (c) of 2014, reproduced from Fig. 1.2 from Knust & Schröder, 2014.

652

653

654 **ACKNOWLEDGEMENTS**

655 We would like to thank Nils Koschnick (AWI) and Emilio Riginella (University of Padua)  
 656 for their help in collecting samples onboard the RV *Polarstern*. This work was supported by  
 657 the National Program for Antarctic Research (PNRA16\_307) to L.Z.; J.A.C. is a PhD student  
 658 in Evolution, Ecology and Conservation at the University of Padua, with funding from a  
 659 Cariparo Fellowship for foreign students and additional support from an Antarctic Science  
 660 International (ASI) Bursary, a Scientific Committee for Antarctic Research (SCAR)  
 661 Fellowship and an Erasmus+ Student Traineeship. C.P. acknowledges financial support from  
 662 the University of Padua (BIRD164793/16) and from the European Marie Curie project  
 663 “Polarexpress” Grant No. 622320. Funding for J.R.A. was provided by the National Science  
 664 Foundation (Grant No. 0741348).

665

666 **LITERATURE CITED**

- 667 Agostini C, Patarnello T, Ashford JR, Torres JJ, Zane L, Papetti C (2015) Genetic  
 668 differentiation in the ice-dependent fish *Pleuragramma antarctica* along the  
 669 Antarctic Peninsula. *Journal of Biogeography* 42:1103-1113
- 670 Ashford J, Dinniman M, Brooks C, Andrews AH, Hofmann E, Cailliet G, Jones C, Ramanna N  
 671 (2012) Does large-scale ocean circulation structure life history connectivity in  
 672 antarctic toothfish (*Dissostichus mawsoni*)? *Canadian Journal of Fisheries and*  
 673 *Aquatic Sciences* 69:1903-1919
- 674 Ashford J, la Mesa M, Fach BA, Jones C, Everson I (2010) Testing early life connectivity using  
 675 otolith chemistry and particle-tracking simulations. *Canadian Journal of Fisheries and*  
 676 *Aquatic Sciences* 67:1303-1315
- 677 Ashford J, Zane L, Torres JJ, La Mesa M, Simms AR (2017) Population Structure and Life  
 678 History Connectivity of Antarctic Silverfish (*Pleuragramma antarctica*) in the  
 679 Southern Ocean Ecosystem. In: Vacchi M, Pisano E, Ghigliotti L (eds) *The Antarctic*  
 680 *Silverfish: a Keystone Species in a Changing Ecosystem*. Springer International  
 681 Publishing, Cham
- 682 Ashford JR, Arkhipkin AI, Jones CM (2006) Can the chemistry of otolith nuclei determine  
 683 population structure of Patagonian toothfish *Dissostichus eleginoides*? *Journal of fish*  
 684 *biology* 69:708-721
- 685 Ashford JR, Arkhipkin AI, Jones CM (2007) Otolith chemistry reflects frontal systems in the  
 686 Antarctic Circumpolar Current. *Marine Ecology Progress Series* 351:249-260

- 687 Ashford JR, Jones CM, Hofmann E, Everson I, Moreno C, Duhamel G, Williams R (2005) Can  
688 otolith elemental signatures record the capture site of Patagonian toothfish  
689 (*Dissostichus eleginoides*), a fully marine fish in the Southern Ocean? Canadian  
690 Journal of Fisheries and Aquatic Sciences 62:2832-2840
- 691 Auel H, Dürschlag J, Dieter J, Ksionzek K, Kohlbach D, Lange B, Vortkamp M, Flores H, Graeve  
692 M, Koch B (2014) Biological and biogeochemical processes in sea ice and the pelagic  
693 realm. In: Knust R, Schröder A (eds) The expedition PS82 of the Research Vessel  
694 Polarstern to the southern Weddell Sea in 2013/2014, Book 680. Ber Polarforsch  
695 Meeresforsch
- 696 Azaneu M, Heywood KJ, Queste BY, Thompson AF (2017) Variability of the Antarctic Slope  
697 Current System in the Northwestern Weddell Sea. Journal of Physical Oceanography  
698 47:2977-2997
- 699 Begg GA, Friedland KD, Pearce JB (1999) Stock identification and its role in stock assessment  
700 and fisheries management: An overview. Fisheries Research 43:1-8
- 701 Brooks CM, Caccavo JA, Ashford J, Dunbar R, Goetz K, La Mesa M, Zane L (2018) Early life  
702 history connectivity of Antarctic silverfish (*Pleuragramma antarctica*) in the Ross  
703 Sea. Fisheries Oceanography 27:1-14
- 704 Caccavo JA, Papetti C, Wetjen M, Knust R, Ashford JR, Zane L (2018) Along-shelf connectivity  
705 and circumpolar gene flow in Antarctic silverfish (*Pleuragramma antarctica*).  
706 Scientific Reports: *Accepted*
- 707 Campana SE (1999) Chemistry and composition of fish otoliths: Pathways, mechanisms and  
708 applications. Marine Ecology Progress Series 188:263-297
- 709 Chen Z, Canil D, Longerich HP (2000) Automated in situ trace element analysis of silicate  
710 materials by laser ablation inductively coupled plasma mass spectrometry. Fresenius'  
711 Journal of Analytical Chemistry 368:73-78
- 712 Daae K, Darelus E, Fer I, Østerhus S, Ryan S (2018) Wind Stress Mediated Variability of the  
713 Filchner Trough Overflow, Weddell Sea. Journal of Geophysical Research: Oceans  
714 123:3186-3203
- 715 Darelus E, Makinson K, Daae K, Fer I, Holland PR, Nicholls KW (2014) Hydrography and  
716 circulation in the Filchner Depression, Weddell Sea, Antarctica. Journal of  
717 Geophysical Research: Oceans 119:5797-5814
- 718 Davis LB, Hofmann EE, Klinck JM, Piñones A, Dinniman MS (2017) Distributions of krill and  
719 Antarctic silverfish and correlations with environmental variables in the western  
720 Ross Sea, Antarctica. Marine Ecology Progress Series 584:45-65
- 721 Duhamel G, Hulley P-A, Causse R, Koubbi P, Vacchi M, Pruvost P, Vigetta S, Irisson J-O,  
722 Mormède S, Belchier M, Dettai A, Detrich HW, Gutt J, Jones CD, Koch K-H, Lopez  
723 Abellan LJ, Van de Putte AP (2014) Biogeographic patterns of fish. In: De Broyer C.,  
724 Koubbi P., Griffiths H.J., Raymond B., d' UdAC, Van De Putte A, Danis B, David B,  
725 Grant S, Gutt J, Held C, Hosie G, Huettmann F, Post A, Ropert-Coudert Y (eds)  
726 Biogeographic Atlas of the Southern Ocean. Scientific Committee on Antarctic  
727 Research, Cambridge
- 728 Dutrieux P, De Rydt J, Jenkins A, Holland PR, Ha HK, Lee SH, Steig EJ, Ding Q, Abrahamsen EP,  
729 Schröder M (2014) Strong Sensitivity of Pine Island Ice-Shelf Melting to Climatic  
730 Variability. Science 343:174



- 731 Eastman JT (1985) The evolution of neutrally buoyant notothenioid fishes: their  
732 specializations and potential interactions in the Antarctic marine food web. Antarctic  
733 nutrient cycles and food webs:430-436
- 734 Ferguson JW (2012) Population structure and connectivity of an important pelagic forage  
735 fish in the Antarctic ecosystem, *Pleuragramma antarcticum*, in relation to large scale  
736 circulation. MS Thesis, Old Dominion University, Norfolk, VA.
- 737 Ghigliotti L, Ferrando S, Carlig E, Di Blasi D, Gallus L, Pisano E, Hanchet S, Vacchi M (2017)  
738 Reproductive features of the Antarctic silverfish (*Pleuragramma antarctica*) from the  
739 western Ross Sea. Polar Biology 40:199-211
- 740 Graham JA, Heywood KJ, Chavanne CP, Holland PR (2013) Seasonal variability of water  
741 masses and transport on the Antarctic continental shelf and slope in the  
742 southeastern Weddell Sea. Journal of Geophysical Research: Oceans 118:2201-2214
- 743 Guglielmo L, Granata A, Greco S (1998) Distribution and abundance of postlarval and  
744 juvenile *Pleuragramma antarcticum* (Pisces, Nototheniidae) off Terra Nova Bay (Ross  
745 Sea, Antarctica). Polar Biology 19:37-51
- 746 Guidetti P, Ghigliotti L, Vacchi M (2014) Insights into spatial distribution patterns of early  
747 stages of the Antarctic silverfish, *Pleuragramma antarctica*, in the platelet ice of  
748 Terra Nova Bay, Antarctica. Polar Biology 38:333-342
- 749 Hubold G (1984) Spatial distribution of *Pleuragramma antarcticum* (Pisces: Nototheniidae)  
750 near the Filchner- and Larsen ice shelves (Weddell sea/antarctica). Polar Biology  
751 3:231-236
- 752 Hubold G, Tomo AP (1989) Age and growth of Antarctic Silverfish *Pleuragramma*  
753 *antarcticum* Boulenger, 1902, from the southern Weddell Sea and Antarctic  
754 Peninsula. Polar Biology 9:205-212
- 755 Jochum KP, Scholz D, Stoll B, Weis U, Wilson SA, Yang Q, Schwalb A, Börner N, Jacob DE,  
756 Andreae MO (2012) Accurate trace element analysis of speleothems and biogenic  
757 calcium carbonates by LA-ICP-MS. Chemical Geology 318-319:31-44
- 758 Johnson MS, Black R (1982) Chaotic genetic patchiness in an intertidal limpet, *Siphonaria* sp.  
759 Marine Biology 70:157-164
- 760 Kellermann A (1986) Geographical distribution and abundance of postlarval and juvenile  
761 *Pleuragramma antarcticum* (Pisces, Notothenioidei) off the Antarctic Peninsula.  
762 Polar Biology 6:111-119
- 763 Kellermann AK (1996) Midwater Fish Ecology. In: Ross RM, Hofmann EE, Quetin LB (eds)  
764 Foundations for Ecological Research West of the Antarctic Peninsula, Book 70.  
765 American Geophysical Union, Washington
- 766 Khatree R, Naik DN (1999) Applied Multivariate Statistics with SAS Software. SAS Publishing
- 767 Khatree R, Naik DN (2000) Multivariate Data Reduction and Discrimination with SAS  
768 Software. SAS Publishing
- 769 Knust R SM (2014) The expedition PS82 of the Research Vessel Polarstern to the southern  
770 Weddell Sea in 2013/14. Ber Polarforsch Meeresforsch, Book 680
- 771 Koubbi P, Grant S, Ramm D, Vacchi M, Ghigliotti L, Pisano E (2017) Conservation and  
772 Management of Antarctic Silverfish *Pleuragramma antarctica* Populations and  
773 Habitats. In: Vacchi M, Pisano E, Ghigliotti L (eds) The Antarctic Silverfish: a Keystone  
774 Species in a Changing Ecosystem. Springer International Publishing, Cham
- 775 Koubbi P, O'Brien C, Loots C, Giraldo C, Smith M, Tavernier E, Vacchi M, Vallet C, Chevallier J,  
776 Moteki M (2011) Spatial distribution and inter-annual variations in the size

- 777 frequency distribution and abundances of *Pleuragramma antarcticum* larvae in the  
778 Dumont d'Urville Sea from 2004 to 2010. *Polar Science* 5:225-238
- 779 La Mesa M, Catalano B, Russo A, Greco S, Vacchi M, Azzali M (2010) Influence of  
780 environmental conditions on spatial distribution and abundance of early life stages  
781 of antarctic silverfish, *Pleuragramma antarcticum* (Nototheniidae), in the Ross Sea.  
782 *Antarctic Science* 22:243-254
- 783 La Mesa M, Eastman JT (2012) Antarctic silverfish: Life strategies of a key species in the  
784 high-Antarctic ecosystem. *Fish and Fisheries* 13:241-266
- 785 La Mesa M, Piñones A, Catalano B, Ashford J (2015a) Predicting early life connectivity of  
786 Antarctic silverfish, an important forage species along the Antarctic Peninsula.  
787 *Fisheries Oceanography* 24:150-161
- 788 La Mesa M, Riginella E, Mazzoldi C, Ashford J (2015b) Reproductive resilience of ice-  
789 dependent Antarctic silverfish in a rapidly changing system along the Western  
790 Antarctic Peninsula. *Marine Ecology* 36:235-245
- 791 Lancraft TM, Reisenbichler KR, Robison BH, Hopkins TL, Torres JJ (2004) A krill-dominated  
792 micronekton and macrozooplankton community in Croker Passage, Antarctica with  
793 an estimate of fish predation. *Deep-Sea Research Part II: Topical Studies in*  
794 *Oceanography* 51:2247-2260
- 795 Lowe WH, Allendorf FW (2010) What can genetics tell us about population connectivity?  
796 *Molecular ecology* 19:3038-3051
- 797 Matsuoka K, Skoglund A, Roth G (2018) Quantarctica [Data set]. Norwegian Polar Institute
- 798 McGillicuddy DJ, Sedwick PN, Dinniman MS, Arrigo KR, Bibby TS, Greenan BJW, Hofmann EE,  
799 Klinck JM, Smith WO, Mack SL, Marsay CM, Sohst BM, Dijken GL (2015) Iron supply  
800 and demand in an Antarctic shelf ecosystem. *Geophysical Research Letters* 42:8088-  
801 8097
- 802 Meijers AJS, Meredith MP, Abrahamsen EP, Morales Maqueda MA, Jones DC, Naveira  
803 Garabato AC (2016) Wind-driven export of Weddell Sea slope water. *Journal of*  
804 *Geophysical Research: Oceans* 121:7530-7546
- 805 Moffat C, Beardsley RC, Owens B, van Lipzig N (2008) A first description of the Antarctic  
806 Peninsula Coastal Current. *Deep Sea Research Part II: Topical Studies in*  
807 *Oceanography* 55:277-293
- 808 Nicholls KW, Østerhus S, Makinson K, Gammelsrød T, Fahrbach E (2009) Ice-ocean processes  
809 over the continental shelf of the southern Weddell Sea, Antarctica: A review.  
810 *Reviews of Geophysics* 47:RG3003
- 811 Orsi AH, Whitworth Iii T, Nowlin Jr WD (1995) On the meridional extent and fronts of the  
812 Antarctic Circumpolar Current. *Deep-Sea Research Part I* 42:641-673
- 813 Palsbøll PJ, Bérubé M, Allendorf FW (2007) Identification of management units using  
814 population genetic data. *Trends in Ecology & Evolution* 22:11-16
- 815 Piñones A, Hofmann EE, Dinniman MS, Klinck JM (2011) Lagrangian simulation of transport  
816 pathways and residence times along the western Antarctic Peninsula. *Deep-Sea*  
817 *Research Part II: Topical Studies in Oceanography* 58:1524-1539
- 818 QGIS Development Team (2018) QGIS Geographic Information System. Open Source  
819 Geospatial Foundation Project.
- 820 Ryan S, Hattermann T, Darelus E, Schröder M (2017) Seasonal cycle of hydrography on the  
821 eastern shelf of the Filchner Trough, Weddell Sea, Antarctica. *Journal of Geophysical*  
822 *Research: Oceans* 122:6437-6453

- 823 Savidge DK, Amft JA (2009) Circulation on the West Antarctic Peninsula derived from 6 years  
824 of shipboard ADCP transects. Deep-Sea Research Part I: Oceanographic Research  
825 Papers 56:1633-1655
- 826 Schröder M, Wisotzki A, Ryan S, Huneke W, Semper S, Osterhus S, Schwegmann S, Castellani  
827 G (2014) Observations of the hydrographic conditions and water mass compositions  
828 at the Filchner Sill and in the Filchner Trough. In: Knust R, Schröder A (eds) The  
829 expedition PS82 of the Research Vessel Polarstern to the southern Weddell Sea in  
830 2013/2014, Book 680. Ber Polarforsch Meeresforsch
- 831 Taillebois L, Barton DP, Crook DA, Saunders T, Taylor J, Hearnden M, Saunders RJ, Newman  
832 SJ, Travers MJ, Welch DJ, Greig A, Dudgeon C, Maher S, Ovenden JR (2017) Strong  
833 population structure deduced from genetics, otolith chemistry and parasite  
834 abundances explains vulnerability to localized fishery collapse in a large Sciaenid fish,  
835 *Protonibea diacanthus*. Evolutionary Applications
- 836 Thompson AF, Heywood KJ, Thorpe SE, Renner AHH, Trasviña A (2009) Surface Circulation at  
837 the Tip of the Antarctic Peninsula from Drifters. Journal of Physical Oceanography  
838 39:3-26
- 839 Thorrold SR, Swearer SE (2009) Otolith Chemistry. In: Green BS, Mapstone BD, Carlos G,  
840 Begg GA (eds) Tropical Fish Otoliths: Information for Assessment, Management and  
841 Ecology. Springer Netherlands, Dordrecht
- 842 Vacchi M, La Mesa M, Dalu M, Macdonald J (2004) Early life stages in the life cycle of  
843 Antarctic silverfish, *Pleuragramma antarcticum* in Terra Nova Bay, Ross Sea.  
844 Antarctic Science 16:299-305
- 845 Welch DJ, Newman SJ, Buckworth RC, Ovenden JR, Broderick D, Lester RJG, Gribble NA,  
846 Ballagh AC, Charters RA, Stapley J, Street R, Garrett RN, Begg GA (2015) Integrating  
847 different approaches in the definition of biological stocks: A northern Australian  
848 multi-jurisdictional fisheries example using grey mackerel, *Scomberomorus*  
849 *semifasciatus*. Marine Policy 55:73-80
- 850 Wetjen M, Wätjen K, Knust R (2014a) The role of the Antarctic silverfish *Pleuragramma*  
851 *antarcticum* in the Antarctic waters. In: Knust R, Schröder A (eds) The expedition  
852 PS82 of the Research Vessel Polarstern to the southern Weddell Sea in 2013/2014,  
853 Book 680. Ber Polarforsch Meeresforsch
- 854 Wetjen M, Wätjen K, Papetti C, Babbucci M, Riginella E, Koschnick N, Knust R, Sandersfeld T  
855 (2014b) Fish communities, distribution and production. In: Knust R, Schröder A (eds)  
856 The expedition PS82 of the Research Vessel Polarstern to the southern Weddell Sea  
857 in 2013/2014, Book 680. Ber Polarforsch Meeresforsch
- 858 White MG, Piatkowski U (1993) Abundance, horizontal and vertical distribution of fish in  
859 eastern Weddell Sea micronekton. Polar Biology 13:41-53
- 860 Whitworth T, Orsi AH, Kim SJ, Nowlin WD, Locarnini RA (1998) Water Masses and Mixing  
861 Near the Antarctic Slope Front. Ocean, Ice, and Atmosphere: Interactions at the  
862 Antarctic Continental Margin. American Geophysical Union
- 863 Wöhrmann APA, Hagen W, Kunzmann A (1997) Adaptations of the Antarctic silverfish  
864 *Pleuragramma antarcticum* (Pisces: Nototheniidae) to pelagic life in high-Antarctic  
865 waters. Marine Ecology Progress Series 151:205-218
- 866 Youngs MK, Thompson AF, Flexas MM, Heywood KJ (2015) Weddell Sea Export Pathways  
867 from Surface Drifters. Journal of Physical Oceanography 45:1068-1085

868 Zane L, Marcato S, Bargelloni L, Bortolotto E, Papetti C, Simonato M, Varotto V, Patarnello T  
869 (2006) Demographic history and population structure of the Antarctic silverfish  
870 *Pleuragramma antarcticum*. *Molecular ecology* 15:4499-4511  
871

# **Chapter 5**

Discussion and conclusion

## Discussion and conclusion

The previous three chapters have made strides in addressing many of the questions laid out at the onset of both the present thesis, and the Antarctic silverfish life history hypothesis.

Brooks et al. (2018) addressed the question of population connectivity through the lens of the Ross Sea, using life history data in conjunction with hydrographic and sea ice data to reconstruct the role of trough circulation in structuring early life stages of silverfish. Evidence was also found for a novel nursery ground in the Bay of Whales, where previously it had been thought that only Terra Nova Bay supported a silverfish nursery in the Ross Sea (Guglielmo et al. 1998). Open questions remain regarding the extent to which the Bay of Whales represents a true nursery ground, especially in terms of how retention and self-recruitment could sustain a coherent population in the area. The use of mitochondrial DNA sequencing to confirm that the newly hatched larvae found in the Bay of Whales were indeed Antarctic silverfish was an essential piece of evidence in support of the potential nursery ground. The mechanisms by which adults may have arrived to the Bay of Whales to spawn presents intriguing hypotheses regarding connectivity between the Ross Sea and other parts of the Southern Ocean.

Caccavo et al. (2018a) explored this very regional connectivity alluded to in the close of Brooks et al. (2018) using a microsatellite-based analysis to test hypotheses regarding population connectivity in a hydrographic framework. There were several hurdles to be overcome in this endeavor. The first was how to build upon the previous investigations of silverfish population connectivity (Zane et al. 2006, Agostini et al. 2015), better integrating the hydrographic context laid out in the recently described life history hypothesis (Ashford et al. 2017a). The second was how to detect genetic differentiation in a species and clade for that matter where high levels of gene flow and population homogeneity is the norm (Zane et al. 2006, Matschiner et al. 2009, Damerou et al. 2012, Agostini et al. 2015). These challenges were overcome in part by updating the analysis methods used in the previous silverfish investigations. Statistical methods designed to work with allele frequencies from species experiencing high levels of gene flow were employed, including the optimization of test statistics and alternative clustering methods.

Two significant results came from the Caccavo et al. (2018a) study. The first was that populations along the Antarctic Slope Front and Current System (AFS) all experienced high levels of gene flow between them, emphasizing the importance of large-scale slope circulation in facilitating regional and circumpolar connectivity. The second result was the observation of genetically differentiated populations outside the reach of the AFS. Evidence was corroborated for significant genetic differentiation of the western Antarctic Peninsula population, first observed in Agostini et al. (2015), as well as shown for the first time in the population at the South Orkney Islands. These results provide both a mechanism and a

framework in which to consider the previous findings regarding silverfish population structure, while also facilitating the creation of well-designed hypotheses to further define the role of slope currents in circumpolar connectivity, as well as the interplay between regional and circumpolar hydrography.

A first example of such a follow-up to Caccavo et al. (2018a) can be seen in Caccavo et al. (2018b), which set out to test connectivity between trough systems in the Weddell Sea. Working on a similar regional scale to the Brooks et al. (2018) investigation, Caccavo et al. (2018b) used otolith chemistry to compare provenance between areas in the Weddell Sea between which no genetic differentiation had been observed in Caccavo et al. (2018a). Variable distributions of dominant cohorts combined with suggestions of trough-based population structuring and westward dispersal from earlier studies (Hubold 1984, White & Piatkowski 1993) made the Weddell Sea the ideal region from the earlier silverfish genetics work on which to focus multiple techniques of population description.

Using ratios of trace element deposition in the otolith nucleus as a proxy for early environmental exposure (Ashford et al. 2006), Caccavo et al. (2018b) found evidence for population structuring despite a lack of genetic differentiation between the same sampling areas. The integration of CTD data to identify the varying influence of water masses in different areas allowed for a more nuanced view of the circulation underlying the observed structuring in the southern Weddell Sea. Intrusions of Warm Deep Water (WDW) carried in the AFS along the slope mix with colder continental shelf waters and become Modified Warm Deep Water (MWDW). Biomass and abundance indices, as well the smaller cohort all exhibited a strong spatial association with MWDW, supporting evidence of westward connectivity of early life stages proposed by White and Piatkowski (1993), though our results point to a deeper transport pathway associated with ontogenic movement to depth. In contrast, the large cohort of silverfish were linked to deeper, colder shelf waters inshore, associated with the Antarctic Coastal Current (AACC), likely responsible for their distribution moving south from Halley Bay to the head of Filchner Trough. Outflow of Ice Shelf Water (ISW) in the Filchner Trough is likely responsible for the transport of older life stages towards the shelf edge, where exposure to the slope current facilitates connectivity with populations outside the Filchner system, and explains abundances of larger length modes found closer to the trough mouth.

Despite the fact that Antarctic silverfish were collected only during the summer season, data from moorings in the area have allowed a picture of hydrography shifts throughout the year to take shape (Ryan et al. 2017). Distinct phases of predominant flows with a strong seasonal association, as well as variations in wind and meltwater which contribute to interannual variability in flow strengths, explain the observation of dominant year classes, likely due to variation in levels of dispersal and retention. Hydrography-driven control of dominant cohorts

was also observed in the Ross Sea in Brooks et al. (2018), and is thus likely a feature of silverfish life history connectivity.

Such interannual variability would explain the observation of chaotic genetic patchiness in the genetics results, in which genetic differentiation varied between years. While such patchiness was not observed in the Weddell Sea, this may be due to the inability of the genetics to detect such variations in population structure. The constant low-level exchange of individuals between local populations would homogenize any genetic differentiation, despite the significant impact on the population structure of fluctuating exchange levels due to variations in hydrography and ensuing dispersal and retention. Subsequent work in the Weddell Sea will involve analysis of the otolith edge chemistry signatures that are representative of environmental conditions to which fish were exposed immediately prior to capture (Ashford et al. 2005). While the analysis of otolith nucleus chemistry clearly shows population structuring based on significantly different early life environmental exposure in the region, otolith edge chemistry data will strengthen the supposition of water mass occupation derived from CTD measurements at the time of capture (Ashford et al. 2005). Furthermore, the impact of diet cannot be discounted (and will be explored further in Appendix 1), as magnesium was the trace element most responsible for the observed differences between groups, and changes in magnesium deposition in otoliths have been associated with diet (Loewen et al. 2016).

The integration of multidisciplinary techniques, life history traits, genetics, hydrography and otolith chemistry, has provided tangible evidence in support of the Antarctic silverfish life history hypothesis, as well as emphasizing the importance of large-scale circulation in maintaining connectivity between local and circumpolar populations. The use of multi-scale inquiries to contextualize regional findings, and the reciprocal value of regional investigations to describe mechanisms of connectivity emphasize the importance of distributing research focus across scales to address questions of population structure.

Several black boxes remain. The extent to which life stage and distant from the coast may have influenced heterogeneity found between sampling locations remains to be seen. Differences between mature and immature adults were difficult to ascertain from the present samples given the paucity of associated length data overall, the unimodal quality of most of the length distributions, and the lack of genetic differentiation found between size groups when the data were available. The results from the Discriminant Analysis of Principle Components (DAPC), while not indicating any clusters based on geographic provenance, did reveal evidence for nine clusters of unknown relevance. While these nine clusters may have arisen due to historical extinction and recolonization events related to glacial periods which structured past populations of silverfish (Ashford et al. 2017b), it remains an intriguing possibility that they were ontogenically derived.



Due to the lack of samples from East Antarctica, the role of the AFS in connecting Ross Sea fish to the Weddell Sea and Antarctic Peninsula remains speculative. Large distributions of silverfish have been found across the continental shelf in East Antarctica (La Mesa & Eastman 2012), as well as in association with trough systems off Wilkes Land (Moteki et al. 2011), which supports the hypothesis that other trough systems along East Antarctica provide suitable habitats for silverfish populations (Ashford et al. 2017b). Furthermore, sampling along the Amundsen and the Bellingshausen Seas will be critical to parsing the influence on local populations of the Antarctic Circumpolar Current (ACC) once it reaches the slope and travels north along the Antarctic Peninsula (Orsi et al. 1995) from that of the AFS which forms in the Amundsen Sea (Whitworth et al. 1998). Kellermann (1996) hypothesized the slope pathway between the Bellingshausen and the western Antarctic Peninsula. An inshore pathway also exists however, as was discussed in Brooks et al. (2018), suggesting that distributions of older fish in the Amundsen Sea (Donnelly et al. 2004) may be transported via the AACC (Orsi & Wiederwohl 2009) to the eastern Ross Sea.

Finally, it is of critical importance to remember that despite the static connotations of a term like structure, population structure is anything but. Connectivity is dynamic, and evidence from genetics, otolith chemistry, and distributions all suggest that population structure is not static. Thus the importance of regular sampling to assess how connectivity is changing over time is essential to forming a dynamic picture of population structure that is truly relevant to silverfish life history.

Some of the greatest harbingers of change in the Southern Ocean ecosystem derive from regions where little is known about silverfish population structure, i.e. the Amundsen Sea, where the Pine Island Glacier is experiencing some of the most dramatic area losses in the Antarctic (Dutrieux et al. 2014), and East Antarctica, where a recent catastrophic Adélie penguin die-off attributed to abnormal sea ice extent and weather conditions (Slezak 2017) has increased pressure to create a Marine Protected Area in the East Antarctic sector (The Pew Charitable Trusts 2017). Silverfish from these areas likely have a critical influence on downstream populations, and yet, variable ocean conditions due to a changing climate make it difficult to predict how connectivity will be impacted. It is uncertain whether increased variability in levels of gene flow that until now have maintained genetically diverse populations will cross a threshold after which adverse impacts of population isolation, bottlenecks and inbreeding will be inevitable (Jones et al. 2007).

Antarctic silverfish are a pillar of the Southern Ocean ecosystem. Understanding their population structure and connectivity in the context of their life history and the impact of hydrography is critical to assessments of Southern Ocean ecosystem health. Building on the synergies of multidisciplinary techniques to create a nuanced and dynamic picture of population structure in a hypothesis-testing framework is the best way to move forward in the study of this keystone species.

## References

- Agostini C, Patarnello T, Ashford JR, Torres JJ, Zane L, Papetti C (2015) Genetic differentiation in the ice-dependent fish *Pleuragramma antarctica* along the Antarctic Peninsula. *Journal of Biogeography* 42:1103-1113
- Ashford J, Dinniman M, Brooks C (2017a) Physical–biological interactions influencing large toothfish over the Ross Sea shelf. *Antarctic Science*:1-8
- Ashford J, Zane L, Torres JJ, La Mesa M, Simms AR (2017b) Population Structure and Life History Connectivity of Antarctic Silverfish (*Pleuragramma antarctica*) in the Southern Ocean Ecosystem. In: Vacchi M, Pisano E, Ghigliotti L (eds) *The Antarctic Silverfish: a Keystone Species in a Changing Ecosystem*. Springer International Publishing, Cham
- Ashford JR, Arkhipkin AI, Jones CM (2006) Can the chemistry of otolith nuclei determine population structure of Patagonian toothfish *Dissostichus eleginoides*? *Journal of fish biology* 69:708-721
- Ashford JR, Jones CM, Hofmann E, Everson I, Moreno C, Duhamel G, Williams R (2005) Can otolith elemental signatures record the capture site of Patagonian toothfish (*Dissostichus eleginoides*), a fully marine fish in the Southern Ocean? *Canadian Journal of Fisheries and Aquatic Sciences* 62:2832-2840
- Brooks CM, Caccavo JA, Ashford J, Dunbar R, Goetz K, La Mesa M, Zane L (2018) Early life history connectivity of Antarctic silverfish (*Pleuragramma antarctica*) in the Ross Sea. *Fisheries Oceanography* 27:1-14
- Caccavo JA, Ashford JR, Ryan S, Papetti C, Schröder A, Zane L (2018b) Spatially-based population structure and life history connectivity of the Antarctic silverfish (*Pleuragramma antarctica*) along the southern Weddell Sea shelf. *Marine Ecology Progress Series: In preparation*
- Caccavo JA, Papetti C, Wetjen M, Knust R, Ashford JR, Zane L (2018a) Along-shelf connectivity and circumpolar gene flow in Antarctic silverfish (*Pleuragramma antarctica*). *Scientific Reports: Accepted*
- Damerau M, Matschiner M, Salzburger W, Hanel R (2012) Comparative population genetics of seven notothenioid fish species reveals high levels of gene flow along ocean currents in the southern Scotia Arc, Antarctica. *Polar Biology* 35:1073-1086
- Donnelly J, Torres JJ, Sutton TT, Simoniello C (2004) Fishes of the eastern Ross Sea, Antarctica. *Polar Biology* 27:637-650
- Dutrieux P, De Rydt J, Jenkins A, Holland PR, Ha HK, Lee SH, Steig EJ, Ding Q, Abrahamsen EP, Schröder M (2014) Strong Sensitivity of Pine Island Ice-Shelf Melting to Climatic Variability. *Science* 343:174
- Guglielmo L, Granata A, Greco S (1998) Distribution and abundance of postlarval and juvenile *Pleuragramma antarcticum* (Pisces, Nototheniidae) off Terra Nova Bay (Ross Sea, Antarctica). *Polar Biology* 19:37-51
- Hubold G (1984) Spatial distribution of *Pleuragramma antarcticum* (Pisces: Nototheniidae) near the Filchner- and Larsen ice shelves (Weddell sea/antarctica). *Polar Biology* 3:231-236
- Jones GP, Srinivasan M, Almany GR (2007) Population connectivity and conservation of marine biodiversity. *Oceanography* 20:100-111

- Kellermann AK (1996) Midwater Fish Ecology. In: Ross RM, Hofmann EE, Quetin LB (eds) Foundations for Ecological Research West of the Antarctic Peninsula, Book 70. American Geophysical Union, Washington
- La Mesa M, Eastman JT (2012) Antarctic silverfish: Life strategies of a key species in the high-Antarctic ecosystem. *Fish and Fisheries* 13:241-266
- Loewen TN, Carriere B, Reist JD, Halden NM, Anderson WG (2016) Review: Linking physiology and biomineralization processes to ecological inferences on the life history of fishes. *Comparative Biochemistry and Physiology -Part A : Molecular and Integrative Physiology* 202:123-140
- Matschiner M, Hanel R, Salzburger W (2009) Gene flow by larval dispersal in the Antarctic notothenioid fish *Gobionotothen gibberifrons*. *Molecular ecology* 18:2574-2587
- Moteki M, Koubbi P, Pruvost P, Tavernier E, Hulley P-A (2011) Spatial distribution of pelagic fish off Adélie and George V Land, East Antarctica in the austral summer 2008. *Polar Science* 5:211-224
- Orsi AH, Whitworth Iii T, Nowlin Jr WD (1995) On the meridional extent and fronts of the Antarctic Circumpolar Current. *Deep-Sea Research Part I* 42:641-673
- Orsi AH, Wiederwohl CL (2009) A recount of Ross Sea waters. *Deep-Sea Research Part II: Topical Studies in Oceanography* 56:778-795
- Ryan S, Hattermann T, Darelius E, Schröder M (2017) Seasonal cycle of hydrography on the eastern shelf of the Filchner Trough, Weddell Sea, Antarctica. *Journal of Geophysical Research: Oceans* 122:6437-6453
- Slezak M (2017) Penguin disaster as only two chicks survive from colony of 40,000 *The Guardian*
- The Pew Charitable Trusts (2017) A Network of Marine Protected Areas in the Southern Ocean.
- White MG, Piatkowski U (1993) Abundance, horizontal and vertical distribution of fish in eastern Weddell Sea micronekton. *Polar Biology* 13:41-53
- Whitworth T, Orsi AH, Kim SJ, Nowlin WD, Locarnini RA (1998) Water Masses and Mixing Near the Antarctic Slope Front. *Ocean, Ice, and Atmosphere: Interactions at the Antarctic Continental Margin*. American Geophysical Union
- Zane L, Marcato S, Bargelloni L, Bortolotto E, Papetti C, Simonato M, Varotto V, Patarnello T (2006) Demographic history and population structure of the Antarctic silverfish *Pleuragramma antarcticum*. *Molecular ecology* 15:4499-4511



# Appendix 1

Trophic ecology in the Antarctic silverfish (*Pleuragramma antarctica*)

## Appendix 1 - Trophic ecology in the Antarctic silverfish (*Pleuragramma antarctica*)

### Background and aims

#### Trophic ecology in Antarctic silverfish: state of the art

Antarctic silverfish (*Pleuragramma antarctica*) are a keystone species in the Southern Ocean, providing an essential link between trophic levels (Duhamel et al. 2014, Koubbi et al. 2017). In line with their changing niche occupation as they develop from larvae to juveniles and adults, silverfish also experience ontogenic shifts in prey consumption (Kellermann 1987, Giraldo et al. 2011). The diet of Antarctic silverfish has been studied using stable isotopes and fatty acid analysis on fish from the western Ross Sea (Granata et al. 2009, Pinkerton et al. 2013), Dumont d'Urville Sea (Giraldo et al. 2011, Giraldo et al. 2015), as well as earlier work on stomach contents analysis in the Antarctic Peninsula (Kellermann 1987) and the eastern Weddell Sea (Hubold 1985). Together, these studies suggest that Antarctic silverfish are generalist feeders adapted to feeding on a wide range of zooplankton species depending on life stage, location, and availability (Granata et al. 2009). While research has focused on characterizing silverfish diet and describing ontogenic changes, no studies have taken into account the impact of local hydrography on dietary shifts.

#### Evidence for interplay between hydrography and diet

Pelagic throughout all of their life history, with an energy-efficient foraging strategy, Antarctic silverfish population structure is heavily impacted by hydrography and bathymetry (Ashford et al. 2017, Caccavo et al. 2018a). Considering the role of water mass dynamics in the distribution and availability of Antarctic silverfish prey species, prey consumption is likely to vary depending on the local hydrographic environment. Water mass fronts with rapid velocity shear have been shown to correspond with zones of high productivity (Moffat et al. 2008), supporting the hypothesis that prey-seeking behavior contributes to population structuring in silverfish by facilitating entrainment into water masses that promote connectivity between neighboring and distant populations (Ashford et al. 2017).

#### Fatty acid (FA) analysis to describe diet

In keeping with the old adage “you are what you eat”, the fatty acid (FA) composition of lipids in marine organisms can be analyzed in order to elucidate the contribution of various prey items to the diet of an individual (Falk-Petersen et al. 1987, Dalsgaard et al. 2003). This is due to the fact that FAs are able to be transferred through the food chain unchanged as they are

incorporated into higher trophic levels, leaving a signature of FA contribution from prey consumed (Dalsgaard et al. 2003). Thus, by analyzing the FA signature of various potential prey species and comparing these with the FA signatures of silverfish, prey contribution can be assessed.

## **Extended Summary**

### The effect of hydrography on diet composition in Antarctic silverfish in the eastern Weddell Sea

To date, the only research looking at diet of Antarctic silverfish in the Weddell Sea used stomach contents analysis (Hubold 1985), which only provides a temporal snapshot of diet patterns, an especially poor indicator of diet in a generalist species (Cortés 1997). While euphausiids were the most consistent prey species found in the stomachs of silverfish adults in the southeast Weddell Sea (Hubold 1985), FA analysis of fish from Dumont d'Urville found this to be the case only in juveniles, while adult diets were primarily composed of copepods (Giraldo et al. 2015). The use of a more comprehensive technique such as FA analysis is thus needed in the Weddell Sea in order to resolve this discrepancy regarding regional diet variation. Furthermore, in addition to characterizing diet patterns in the Weddell Sea, knowledge of the local hydrography in the area and its potential impacts on population structuring affords the unique opportunity to investigate silverfish diet in the Weddell Sea in a hydrographic context.

The Filchner Trough is known to be an important bathymetric feature in the southeast Weddell Sea, and large distributions of Antarctic silverfish larvae and adults found in its vicinity support the hypothesis that this trough system maintains a coherent population of silverfish (Hubold 1984, Knust R 2014). Modified Warm Deep Water (MWDW) carried by the Antarctic Slope Front and Current System (AFS) has been shown to penetrate the continental shelf at the Filchner Trough, where it flows south along the flank towards the Filchner Ice Shelf (Ryan et al. 2017). In contrast, the southern part of the Filchner Trough is characterized by colder, saltier Ice Shelf Water (ISW), which flows north towards the shelf break, where it contributes to deep water formation in the Weddell Sea (Ryan et al. 2017). East of the Filchner Trough along at Halley Bay and north to where the continental shelf narrows at Atka Bay, Eastern Shelf Water (ESW) is prevalent, another form of cold, salty Winter Water (WW) fed by runoff (Nicholls et al. 2009). While otolith chemistry has indicated that fish at Halley Bay and Filchner Trough have separate origins suggesting that they represent two separate populations (Caccavo et al. unpublished data), lack of genetic differentiation between the two areas insinuates a basal level of connectivity to support gene flow (Caccavo et al. 2018a).

Connectivity between the two areas is likely to be supported by the Antarctic Coastal Current (AACC), which moves in a southeasterly direction along the continental shelf inshore (Graham et al. 2013). Thus, fish from Halley Bay may be advected southeast towards the head of the Filchner Trough, where entrainment in the outflow of ISW away from the coast brings them into contact with MWDW.

While entrainment into these various water masses may simply be stochastic and derive from passive exposure, to what extent could prey availability encourage fish to aggregate towards MWDW? A first step in answering this question is to investigate differences in diet between fish in ESW in Halley Bay, and fish in MWDW west of Filchner Trough.

To this end, Antarctic silverfish from west Filchner Trough and within Halley Bay (Fig. 1), in addition to 13 potential prey species (see Table 1 for details) collected at nearby stations during the same sampling expedition (RV *Polarstern*, PS82 ANT-XXIX/9), were processed for FA analysis as in Giraldo et al. (2015)(Table 1, 2). Correspondence analysis was used to determine the extent to which FA composition distinguished between sampling areas. Preliminary results indicate that the FA signature of polar lipids clearly distinguishes adults from west Filchner Trough, while also demonstrating the expected ontogenic separation between juvenile and adult fish (Fig. 2). The ongoing analysis being carried in together with collaborators at the Laboratoire d'Océanographie de Villefranche-sur-Mer (France) will reveal which plankton species are responsible for contributing to this differentiation in FA signature between Filchner and Halley fish.

While the present study is preliminary in scope, it successfully rejected the null hypothesis of diet homogeneity between fish inhabiting MWDW in the Filchner Trough and fish residing in ESW in Halley Bay. A larger sample size to better grasp the variability of diet within trough and shelf areas, as well as the replication of such an analysis in other trough systems along the Southern Ocean continental shelf ecosystem will allow for greater insights into the relationship between prey-seeking behavior and hydrography in the framework of population structuring in Antarctic silverfish.



## Figures and Tables

**Table 1** Fish and plankton sampling for FA analysis by sampling station. Red text refers to stations in the west Filchner Trough, all other stations located in Halley Bay.

Taxon	Stations																			Total
	003	007	018	124	129	135	147	155	234	247	248	250	281	282	298	304	306	317	322	
<b><i>Pleuragramma antarctica</i></b>																				
Juveniles	--	--	--	--	--	--	--	1	1	--	--	1	--	--	--	--	--	--	1	4
Adults	--	--	5	--	3	--	--	--	--	--	5	--	--	3	--	--	3	--	--	19
																			<b>Total</b>	<b>23</b>
<b>Potential prey</b>																				
<i>Calanus propinquus</i>	--	--	--	--	--	--	--	1	2	--	--	--	--	--	--	--	--	1	--	4
<i>Clione sp.</i>	--	--	--	--	--	--	--	2	2	--	--	--	--	--	--	--	--	1	--	5
<i>Diphyes antarctica</i>	1	--	--	1	--	1	--	1	2	--	--	--	1	--	1	1	--	1	--	10
<i>Epimeria sp.</i>	--	--	--	--	--	--	--	--	2	1	--	--	1	--	1	--	--	--	--	5
<i>Euphausia crystallophias</i>	--	--	--	--	--	--	--	--	--	--	--	--	--	--	--	1	--	--	--	1
<i>Eusirus sp.</i>	--	--	--	--	--	--	--	--	--	--	--	--	--	--	1	--	--	--	--	1
<i>Hyperia sp.</i>	--	--	--	--	--	--	--	--	1	--	--	--	--	--	1	--	--	--	--	2
<i>Hyperoche sp.</i>	--	--	--	--	--	--	--	1	2	--	--	--	--	--	--	--	--	--	--	3
<i>Megacalanus sp.</i>	--	--	--	--	--	--	--	2	2	--	--	--	--	--	--	--	--	--	--	4
<i>Paraeuchaeta antarctica</i>	--	--	--	--	--	--	--	2	1	--	--	--	--	--	--	--	--	1	--	4
<i>Pseudochormene rossi</i>	--	2	--	1	--	--	1	--	1	--	--	--	1	--	1	--	--	--	--	7
<i>Sagitta sp.</i>	--	--	--	1	--	--	--	5	4	--	--	1	--	--	--	--	--	1	--	12
<i>Themisto gaudichaudii</i>	--	--	--	--	--	--	--	--	--	--	--	--	--	--	1	--	--	1	--	2
																			<b>Total</b>	<b>60</b>

**Table 2** Fish and plankton station list indicating collection date and coordinates (**a**), and list of sample IDs of adults (**b**) and juveniles (**c**) used in FA analysis. Red text refers to stations in the west Filchner Trough, all other stations located in Halley Bay. TG, triglyceride fraction; PL, phospholipid fraction.

<b>a</b>				<b>b</b>	
<b>Station List</b>				<b>Lipid Sample IDs</b>	
Station	Date	Latitude	Longitude	Station	ID
3	2-Jan-14	-73.747	-25.77		
7	3-Jan-14	-74.728	-29.809		018-1 PL7
18	4-Jan-14	-75.201	-27.543		018-1 TG7
124	19-Jan-14	-75.497	-27.432	18	018-2 PL15
129	20-Jan-14	-75.358	-27.743		018-2 TG15
135	20-Jan-14	-75.319	-27.613		018-3 PL19
147	21-Jan-14	-74.822	-25.213		018-3 TG19
155	22-Jan-14	-74.566	-28.301		129-1 PL5
234	1-Feb-14	-74.276	-37.858	129	129-1 TG5
247	3-Feb-14	-74.558	-37.749		129-2 PL13
248	3-Feb-14	-74.606	-37.615		129-2 TG13
250	3-Feb-14	-74.512	-37.473		248-1 PL1
281	7-Feb-14	-74.997	-29.58		248-1 TG1
282	7-Feb-14	-75	-29.494	248	248-2 PL2
298	8-Feb-14	-75.559	-28.718		248-2 TG2
304	9-Feb-14	-75.084	-28.734		248-4 PL3
306	9-Feb-14	-75.116	-28.75		248-4 TG3
317	10-Feb-14	-74.652	-28.845		248-5 PL4
322	11-Feb-14	-74.661	-29.918		248-5 TG4
					282-1 PL6
				282	282-1 TG6
					282-2 PL14
					282-2 TG14
					306-1 PL8
				306	306-1 TG8
					306-2 PL16
					306-2 TG16
					306-3 PL20
					306-3 TG20
<b>c</b>					
<b>Lipid Sample IDs</b>					
Station	ID				
<b>Juveniles</b>					
155	0958 PL12				
	0958 TG12				
234	1205 PL11				
	1205 TG11				
250	1356 PL9				
	1356 TG9				
322	1411 PL10				
	1411 TG10				

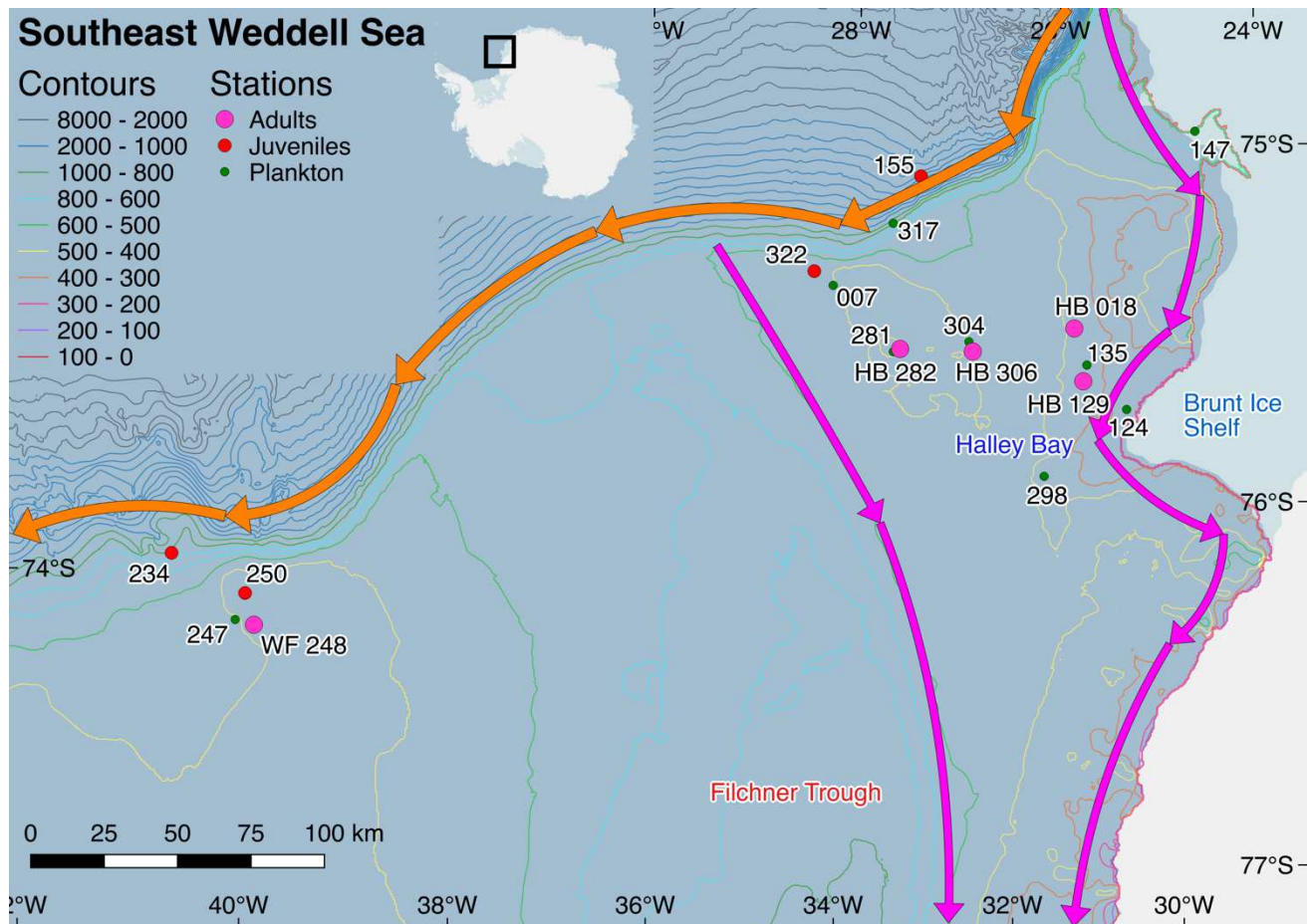


**Figure 1** Sampling locations. Orange arrows approximate the AFS, Antarctic Slope Front and Current System; Pink arrows approximate the AACC, Antarctic Coastal Current; current positions based on Fig 2b in Nicholls et al. (2009). Relevant place names and bathymetric features are indicated. Station numbers are as in Table 1 and 2; WF, west Filchner Trough; HB, Halley Bay. Map created using the Norwegian Polar Institute's Quantarctica 2.0 package (Matsuoka et al. 2018) in the software QGIS version 2.18.9 <http://qgis.osgeo.org> (QGIS Development Team 2018).

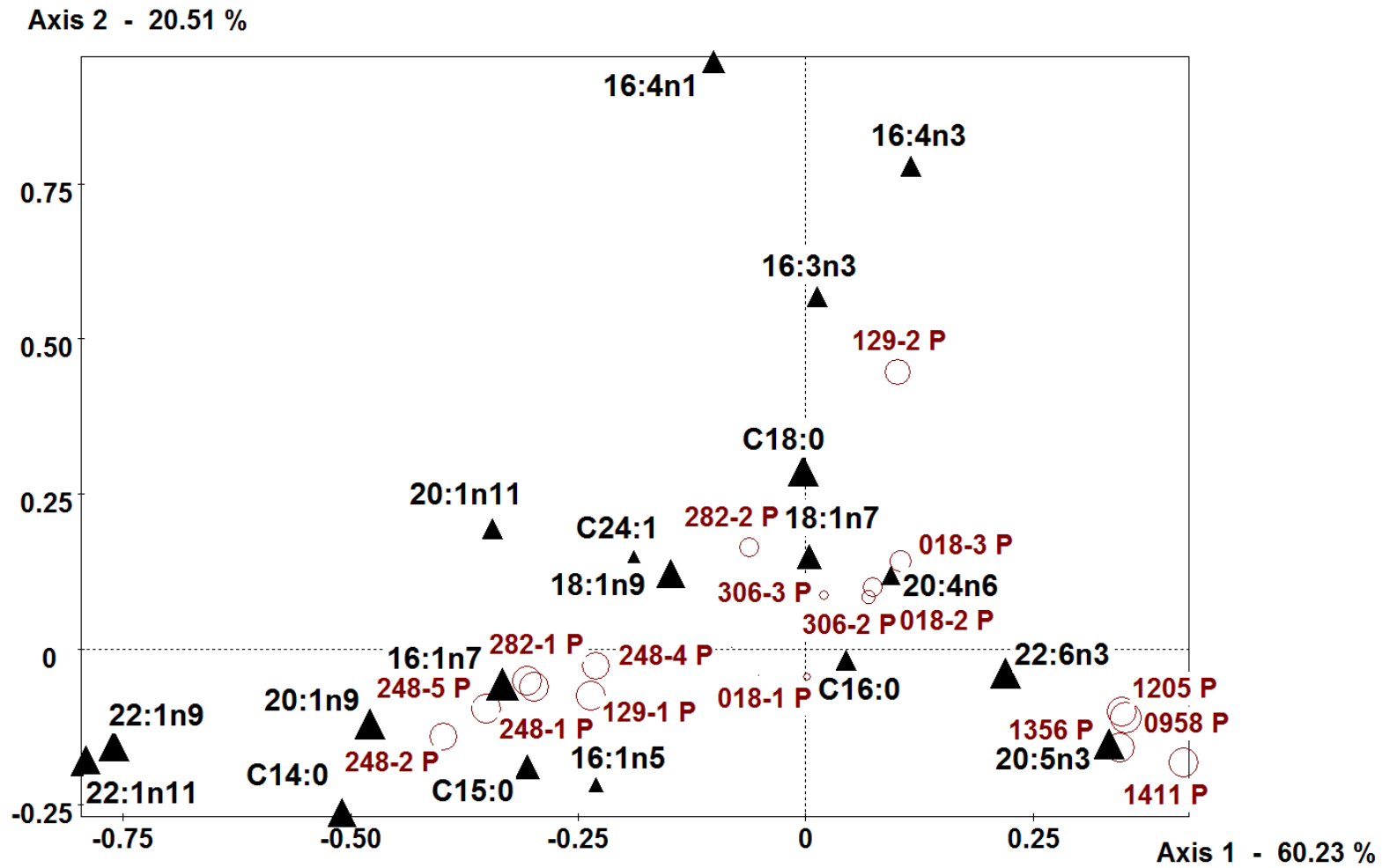


**Figure 2** Correspondence analysis of FA signature of polar lipids in *Pleuragramma antarctica*. FA descriptors represented by black triangles, red circles correspond to individual fish (see Table 3 for sample IDs).

## References

- Ashford J, Zane L, Torres JJ, La Mesa M, Simms AR (2017) Population Structure and Life History Connectivity of Antarctic Silverfish (*Pleuragramma antarctica*) in the Southern Ocean Ecosystem. In: Vacchi M, Pisano E, Ghigliotti L (eds) The Antarctic Silverfish: a Keystone Species in a Changing Ecosystem. Springer International Publishing, Cham
- Caccavo JA, Papetti C, Wetjen M, Knust R, Ashford JR, Zane L (2018a) Along-shelf connectivity and circumpolar gene flow in Antarctic silverfish (*Pleuragramma antarctica*). *Scientific Reports: Accepted*
- Cortés E (1997) A critical review of methods of studying fish feeding based on analysis of stomach contents: application to elasmobranch fishes. *Canadian Journal of Fisheries and Aquatic Sciences* 54:726-738
- Dalsgaard J, St John M, Kattner G, Müller-Navarra D, Hagen W (2003) Fatty acid trophic markers in the pelagic marine environment. *Adv Mar Biol* 46:225-340
- Duhamel G, Hulley P-A, Causse R, Koubbi P, Vacchi M, Pruvost P, Vigetta S, Irisson J-O, Mormède S, Belchier M, Dettai A, Detrich HW, Gutt J, Jones CD, Koch K-H, Lopez Abellan LJ, Van de Putte AP (2014) Biogeographic patterns of fish. In: De Broyer C., Koubbi P., Griffiths H.J., Raymond B., d' UdAC, Van De Putte A, Danis B, David B, Grant S, Gutt J, Held C, Hosie G, Huettmann F, Post A, Ropert-Coudert Y (eds) *Biogeographic Atlas of the Southern Ocean*. Scientific Committee on Antarctic Research, Cambridge
- Falk-Petersen S, Sargent JR, Tande KS (1987) Lipid composition of zooplankton in relation to the sub-arctic food web. *Polar Biology* 8:115-120
- Giraldo C, Cherel Y, Vallet C, Mayzaud P, Tavernier E, Moteki M, Hosie G, Koubbi P (2011) Ontogenic changes in the feeding ecology of the early life stages of the Antarctic silverfish (*Pleuragramma antarcticum*) documented by stable isotopes and diet analysis in the Dumont d'Urville Sea (East Antarctica). *Polar Science* 5:252-263
- Giraldo C, Mayzaud P, Tavernier E, Boutoute M, Penot F, Koubbi P (2015) Lipid dynamics and trophic patterns in *Pleuragramma antarctica* life stages. *Antarctic Science* 27:429-438
- Graham JA, Heywood KJ, Chavanne CP, Holland PR (2013) Seasonal variability of water masses and transport on the Antarctic continental shelf and slope in the southeastern Weddell Sea. *Journal of Geophysical Research: Oceans* 118:2201-2214
- Granata A, Zagami G, Vacchi M, Guglielmo L (2009) Summer and spring trophic niche of larval and juvenile *Pleuragramma antarcticum* in the Western Ross Sea, Antarctica. *Polar Biology* 32:369-382
- Hubold G (1984) Spatial distribution of *Pleuragramma antarcticum* (Pisces: Nototheniidae) near the Filchner- and Larsen ice shelves (Weddell sea/antarctica). *Polar Biology* 3:231-236
- Hubold G (1985) Stomach contents of the Antarctic Silverfish *Pleuragramma antarcticum* from the southern and eastern Weddell Sea (Antarctica). *Polar Biology* 5:43-48

- Kellermann A (1987) Food and feeding ecology of postlarval and juvenile *Pleuragramma antarcticum* (Pisces; Notothenioidei) in the seasonal pack ice zone off the Antarctic peninsula. *Polar Biology* 7:307-315
- Knust R SM (2014) The expedition PS82 of the Research Vessel Polarstern to the southern Weddell Sea in 2013/14. *Ber Polarforsch Meeresforsch, Book 680*
- Koubbi P, Grant S, Ramm D, Vacchi M, Ghigliotti L, Pisano E (2017) Conservation and Management of Antarctic Silverfish *Pleuragramma antarctica* Populations and Habitats. In: Vacchi M, Pisano E, Ghigliotti L (eds) *The Antarctic Silverfish: a Keystone Species in a Changing Ecosystem*. Springer International Publishing, Cham
- Matsuoka K, Skoglund A, Roth G (2018) Quantarctica [Data set]. Norwegian Polar Institute
- Moffat C, Beardsley RC, Owens B, van Lipzig N (2008) A first description of the Antarctic Peninsula Coastal Current. *Deep Sea Research Part II: Topical Studies in Oceanography* 55:277-293
- Nicholls KW, Østerhus S, Makinson K, Gammelsrød T, Fahrbach E (2009) Ice-ocean processes over the continental shelf of the southern Weddell Sea, Antarctica: A review. *Reviews of Geophysics* 47:RG3003
- Pinkerton MH, Forman J, Bury SJ, Brown J, Horn P, O'Driscoll RL (2013) Diet and trophic niche of Antarctic silverfish *Pleuragramma antarcticum* in the Ross Sea, Antarctica. *Journal of fish biology* 82:141-164
- QGIS Development Team (2018) QGIS Geographic Information System. Open Source Geospatial Foundation Project.
- Ryan S, Hattermann T, Darelius E, Schröder M (2017) Seasonal cycle of hydrography on the eastern shelf of the Filchner Trough, Weddell Sea, Antarctica. *Journal of Geophysical Research: Oceans* 122:6437-6453

## Appendix 2

### Using population genetics to assess the population structure and connectivity of the striped venus *Chamelea gallina*

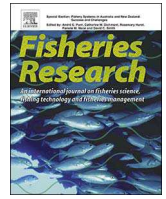
Published as:

Papetti C, Schiavon L, Milan M, Lucassen M, **Caccavo JA**, Paterno M, Boscari E, Marino IAM, Congiu L, Zane L (2018) Genetic variability of the striped venus *Chamelea gallina* in the northern Adriatic Sea. Fisheries Research 201:68-78. doi: 10.1016/j.fishres.2018.01.006.



Contents lists available at ScienceDirect

Fisheries Research

journal homepage: [www.elsevier.com/locate/fishres](http://www.elsevier.com/locate/fishres)

## Genetic variability of the striped venus *Chamelea gallina* in the northern Adriatic Sea



Chiara Papetti<sup>a,d,\*</sup>, Luca Schiavon<sup>a,1</sup>, Massimo Milan<sup>b</sup>, Magnus Lucassen<sup>c</sup>,  
Jilda Alicia Caccavo<sup>a,d</sup>, Marta Paterno<sup>a,d</sup>, Elisa Boscari<sup>a,d</sup>, Ilaria Anna Maria Marino<sup>a,d</sup>,  
Leonardo Congiu<sup>a,d</sup>, Lorenzo Zane<sup>a,d</sup>

<sup>a</sup> Department of Biology, University of Padova, 35121 Padova, Italy

<sup>b</sup> Department of Comparative Biomedicine and Food Science, University of Padova, 35020 Legnaro, Italy

<sup>c</sup> Alfred Wegener Institute Helmholtz Centre for Polar and Marine Research, D-27570 Bremerhaven, Germany

<sup>d</sup> Consorzio Nazionale Interuniversitario per le Scienze del Mare (CoNISMa), 00196 Roma, Italy

### ARTICLE INFO

Handled by J. Viñas

#### Keywords:

Microsatellite  
Clam fishery  
Bivalvia  
Adriatic Sea  
Effective population size  
Gene flow

### ABSTRACT

*Chamelea gallina* is a valuable commercial species in the Mediterranean Sea. The strong fishing pressure on *C. gallina* in the northern and central Adriatic Sea has paralleled a clear-cut decrease in clam population density and the occurrence of several irregular mortality events. Despite the commercial interest in this species, nothing is known about its genetic sub-structuring at the geographic and/or temporal scale, nor its levels of genetic variability. Analyzing microsatellite genotypes for samples collected in the Adriatic Sea, we detected large geographic genetic homogeneity with gene flow guided by broad scale circulation in the north-south direction. Our results also indicate weak genetic differentiation among size classes at the local and temporal scale. These small genetic differences might be determined by variability of local circulation and reproductive success, partial overlapping generations and high larval mortality rates as suggested by our estimates of the effective number of breeders. In fact, global effective population size estimates over multiple generations are medium-high, but a low number of breeders are responsible for the small clams size class recruitment. Notwithstanding, it was not possible to detect signatures of bottleneck. Future efforts in fishery management should aim to maintain genetic diversity – essential to the long-term sustainability of the resource – and limit effective population size fluctuations while considering the need to improve water quality to avoid mass mortality events.

### 1. Introduction

Bivalves represent important economic resources for fisheries and aquaculture and play a key role in coastal ecosystems where they typically face multiple stresses due to the variability of environmental conditions. Fishing pressure can decrease genetic variation through bottlenecks and interfere with genetic connectivity among populations (Hutchings and Reynolds, 2004; Munguía-Vega et al., 2015).

In this study, we examine the case of the clam *Chamelea gallina* (Fig. 1a), which is distributed throughout the Mediterranean, the Black Sea (Moschino and Marin, 2006), along the Portuguese coast and in a few sites of the Northern Atlantic (Baceljau and Gofas, 1994; Eggleton et al., 2007). This endobenthic clam lives in wild banks on sandy or sandy/muddy seabeds 1000–4000 m off the coastline (Casali, 1984). *C. gallina* is gonochoric and reaches sexual maturity between the first and

second year of life, when the shell length attains 12 mm (Casali, 1984; Froglija, 1989). Its spawning period is long, occurring in two intervals between April and October (Morello et al., 2005b), and is largely influenced by environmental conditions, which may anticipate or delay gamete emission (Froglija, 1975; Romanelli et al., 2009). Larvae are pelagic for 15–30 days before settling into the seabed (Froglija, 1975; Romanelli et al., 2009).

The strong fishing pressure on *C. gallina* in the sandy coastal bottoms (3–12 m depth) of the northern and central Adriatic Sea has existed for over 30 years, escalating progressively since the 1970s and reaching an apex when the species became of extreme economic importance in the early 1980s (Froglija, 1989; Morello et al., 2005a,b). After the first high fishing yields, the landings soon started declining to one sixth of the output recorded 25–30 years prior, despite various measures adopted to limit the fishing effort (cuts in landings allowed,

\* Corresponding author at: Department of Biology, University of Padova, via G. Colombo, 3, 35121 Padova, Italy.

E-mail address: [chiara.papetti@unipd.it](mailto:chiara.papetti@unipd.it) (C. Papetti).

<sup>1</sup> These authors equally contributed to this study.



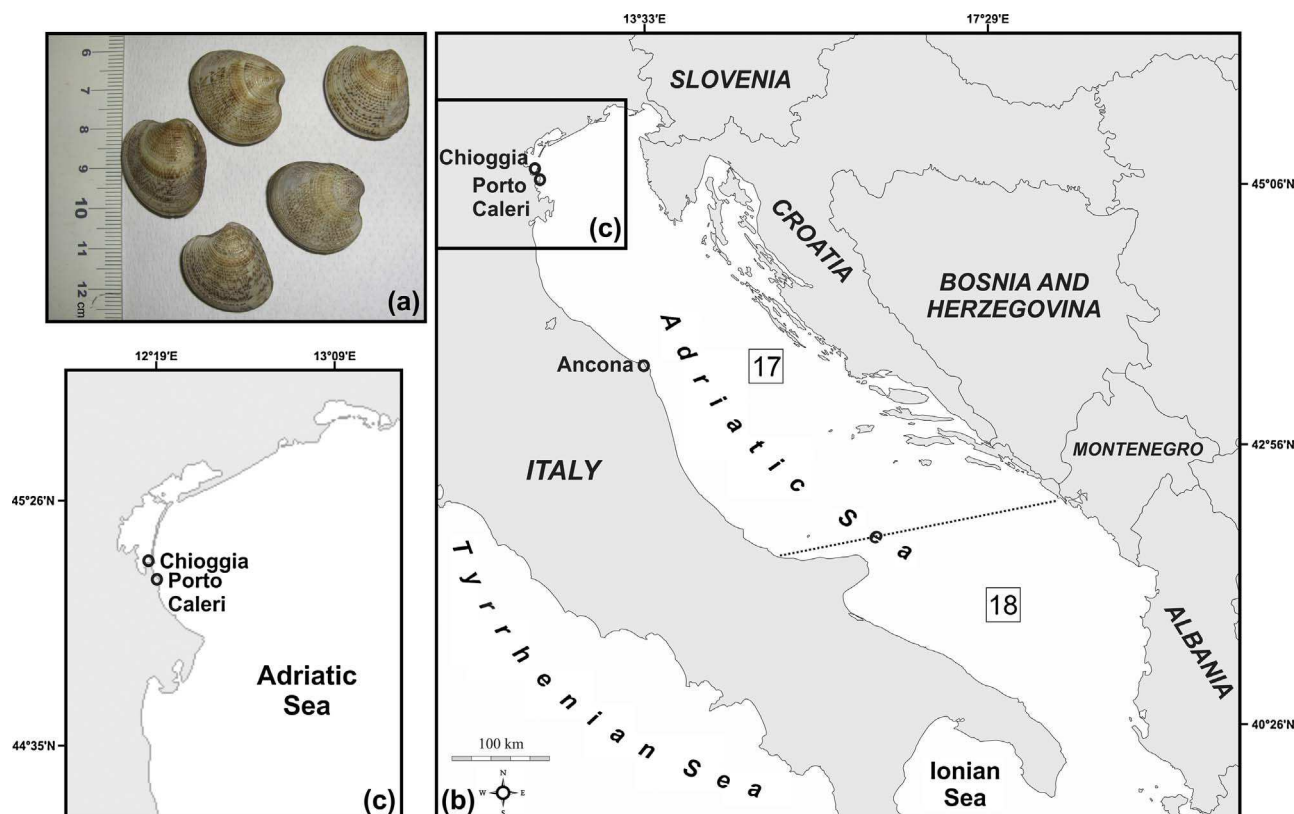


Fig. 1. *Chamelea gallina* sampling area. In a) specimens of *C. gallina* collected in Chioggia in 2009 (photograph taken by the authors), b) three sampling localities in the central-northern Adriatic Sea and in detail c) the two sampling localities off the Venice lagoon (Chioggia and Porto Caleri). All collection sites belong to the Geographical Subarea 17 (GSA 17 for the northern–central Adriatic; General Fisheries Commission for the Mediterranean, [www.gfcm.org](http://www.gfcm.org)). Straight-line geographic distance between Porto Caleri and Chioggia is less than 10 km. Mean distance between Chioggia/Porto Caleri and Ancona is less than 200 km.

fleet reduction, creation of local fishermen consortia). Lately, the decline in *C. gallina* biomass has also been aggravated by the occurrence of several irregular mortality events in the Adriatic Sea (Gizzi et al., 2016; Milan et al., 2016).

One of the main goals of fishery management of *C. gallina* should be to ensure sufficient reproductive potential in a stock to allow for sustainable exploitation. This would help to preserve not only standing genetic diversity, but also the evolutionary potential of the species over long-time scales. So far, despite the commercial interest in this species, nothing is known about *C. gallina* genetic sub-structuring at the geographic and/or temporal scale, nor its levels of genetic variability.

In light of these premises, our study was designed with a specific focus on the northern-central Adriatic Sea, to improve our knowledge about *C. gallina* for future efficient management plans. The main aim of this study was to determine the genetic sub-structuring of *C. gallina* in three intensively exploited sites (Porto Caleri, Chioggia and Ancona) of the northern-central Adriatic Sea and the connectivity among sites in terms of relative gene flow. Notably, besides the geographic scale, we have also considered whether temporal differences occur among size classes within each location by comparing small clams (likely immature and resulting from the most recent reproductive season) and big clams (presumably representing the pool of parental cohorts).

We also searched for potential effects of long-term fishing pressure and mortality events in *C. gallina* by determining the contemporary effective population size  $N_e$ , indicative of the species potential to maintain genetic variability (Frankham, 1995) and by assessing whether populations experience signatures of recent bottleneck.

## 2. Materials and methods

### 2.1. Biological sample collection and handling

*Chamelea gallina* (Fig. 1a) samples were collected between October 2009 and December 2010 from Chioggia, Porto Caleri and Ancona (between 0.3 and 3 miles off the coast, Table 1, Fig. 1b and c) by commercial fishermen. Sampling location coordinates and samples related data are shown in Table 1.

Specimens were immediately placed in ice after fishing and sorting. Clams were cold-transported within three hours from collection to the laboratory where they were stored at  $-80^{\circ}\text{C}$  to preserve genomic DNA until subsequent analysis.

### 2.2. Size class definition

To check for temporal variability of genetic structure and assess whether the parental pools have a different genetic composition from offspring in the same geographic location, we separated individuals that likely resulted from the most recent reproductive season (the small size class) from potential parental cohorts (the big size class). For each sampling event, we collected two random samples of individuals with the length of the left shell (maximum distance on the anterior-posterior axis) smaller and larger than 12 mm. Owing to lack of information about the age vs. size and growth rates of *C. gallina* in the northern Adriatic Sea, the threshold between the two groups was set at 12 mm according to literature (Casali, 1984; Frogliola, 1989, MG Marin personal communication). Sampling occurred by hydraulic dredge and this method does not give access to very small clams (below 5 mm, MG Marin personal communication, see Section 4.1 Caveats in the Discussion). The length of the left shell was measured for all genotyped clams

**Table 1**

*Chamelea gallina* sampling, genetic diversity and relatedness. List of samples used for this study and their locations of origin (including coordinates). Also indicated are the collection months and year, the approximate size class subdivision based on length of the anterior-posterior axis of the left shell (in mm), the sample acronym, the number of clams within each sample, allelic richness ( $A_R$ ), the observed and expected heterozygosity ( $H_o$  and  $H_e$ ), the average within sample relatedness (r-values) values obtained for each sample and the corresponding probabilities (p-values) of being obtained by chance when compared to a random distribution of relatedness values.

Location	Coordinates	Month	Year	Size class	Sample acronym	Shell size range	N	$A_R^d$	$H_o^e$	$H_e^f$	r-values	p-values
Porto Caleri	45° 06.214' N 12° 20.660' E	October <sup>g</sup>	2009	small <sup>b</sup>	PtoCA09_small	8.2–10.2	25	6.1	0.53	0.58	0.085082	0.849
		October	2009	big <sup>c</sup>	PtoCA09_big	12.8–15.0	23	5.52	0.43	0.57	0.102129	0.624
		October, November <sup>h</sup>	2010	small	PtoCA10_small	7.2–11.7	23	4.79	0.39	0.51	0.112261	0.444
		October, November	2010	big	PtoCA10_big	13.1–27.4	25	4.56	0.33	0.47	0.203289	0.024
Chioggia	45° 10.590' N 12° 19.670' E	October	2009	small	CH09_small	7.5–8.8	25	5.24	0.47	0.56	0.104825	0.563
		October, December	2009	big	CH09_big	14.5–19.3	24	5.01	0.37	0.53	0.126278	0.254
		November	2010	small	CH10_small	7.0–10.6	25	5.46	0.43	0.54	0.097195	0.687
		October, November	2010	big	CH10_big	15.5–18.8	24	5.15	0.48	0.54	0.108259	0.504
Ancona	n.a. <sup>a</sup>	June	2010	big	AN10_big	22.8–27.0	45	5.51	0.42	0.56	0.127173	0.199
Total	–	–	–	–	–	–	239					

<sup>a</sup> Specific coordinates of sampling activity off Ancona are not available.

<sup>b</sup> Clams smaller than 12 mm (length of anterior-posterior axis of left shell) are likely the result of the last reproductive season.

<sup>c</sup> Clams larger than 12 mm (length of anterior-posterior axis of left shell) are the potential pool of parental cohorts.

<sup>d</sup> Allelic richness was calculated as the mean across loci.

<sup>e</sup> Observed heterozygosity was calculated as mean across loci.

<sup>f</sup> Expected heterozygosity was calculated as mean across loci.

<sup>g</sup> Samples obtained in a single fishing trip.

<sup>h</sup> Samples obtained from two fishing trips occurred in the indicated months and pooled.

to the nearest 0.1 mm using a caliper (Table 1 and Figs. S1a and b in Supplementary Material).

### 2.3. Marker amplification and genotyping

Genomic DNA was extracted from 239 clams following Patwary et al. (1994). Microsatellite loci used in this study are EST-linked markers and were described by Coppe et al. (2012) (Table S1 in Supplementary Material). Initially, 12 loci were amplified in multiplex in a GeneAmp PCR System 9700 thermal cycler (Applied Biosystems). Final amplification conditions for all 12 loci are reported in Table S1 in Supplementary Material. Amplified fragments were screened using an ABI 3130 XL automatic capillary sequencer [Applied Biosystems; service provided by BMR Genomics, <http://bmr-genomics.com>, LIZ 500 (50–500 bp) as internal size ladder, Applied Biosystems] and analyzed using GeneMarker ver. 2.2 (SoftGenetics). Two authors carried out genotype calling independently. Binning was automated with the software FlexiBin ver. 2 (Amos et al., 2007) and refined by eye. All samples with unsuccessful PCR and ~10% of all clams were re-amplified and re-run to ensure repeatability of allele scoring and to check for genotyping artefacts (O'Leary et al., 2013). We discarded all specimens that could not be assigned to a multi-locus genotype at a minimum of eight loci. Locus 41630, originally considered as monomorphic in a small sample of 12 specimens (Coppe et al., 2012), displayed new alleles, previously unscored. Locus 20467 presented several null genotypes even after replicated PCRs. This locus was removed from the final dataset that included 11 markers. For the remaining 11 loci, Micro-Checker ver. 2.2.3 (van Oosterhout et al., 2004) was used to identify possible genotyping errors due to stuttering, large allele dropout, and null alleles (10,000 randomizations). To verify if null alleles could affect results, their frequencies were estimated with the correction algorithm of van Oosterhout et al. (2004) implemented in Micro-Checker ver. 2.2.3. The software adjusts the number of homozygote genotypes in each size class to reflect the estimated frequency of null alleles and the 'real' numbers of homozygotes. A new dataset for each locus was hence obtained by considering the adjusted genotypes. The two datasets (original and corrected) were then used to calculate single locus estimates of HWE probability and inbreeding index ( $F_{IS}$ ; see next section). Results obtained from the original and corrected datasets were compared to assess the extent of bias due to null alleles. However, since genotypes adjusted by Micro-Checker ver. 2.2.3 are ordered by allele size such that the row

numbers did not correspond to the original sample numbers, none of the subsequent multi-locus analyses were performed with the adjusted dataset. All input files for downstream population genetics analyses were produced with CREATE ver. 1.37 (Coombs et al., 2008) or by hand by the authors.

### 2.4. Genetic diversity, inbreeding, tests for selection and relatedness

Mean number of alleles, allelic richness, percentage of total alleles observed per locus per sample, observed and expected heterozygosity, HWE test and  $F_{IS}$  values were obtained by the R package diveRsim ver. 1.9.90 (Keenan et al., 2013) (R ver. 3.3.2, 95% confidence intervals – 95% CI – obtained using a bootstrap method with 10,000 replicates).

Linkage disequilibrium (LD) probability test was performed with the software Genepop on the web (Fisher's exact test, nominal significant threshold  $\alpha = 0.05$ , Raymond and Rousset, 1995; Rousset, 2008).

Loci potentially under selection were identified using LOSITAN ver. 1.0.0 (Antao et al., 2008). The program considers markers that show significantly higher or lower  $F_{ST}$  values compared with neutral expectations as outlier loci. These markers are suggested as putatively subject to natural selection (Antao et al., 2008; Beaumont and Nichols, 1996). In our analysis, 1,000,000 simulations were run assuming a Stepwise Mutation Model (SMM) following Agostini et al. (2013). We adjusted the p-value for all multiple comparisons obtained in this study as implemented in the program SGoF+ (Carvajal-Rodríguez and de Uña-Alvarez, 2011).

We used the R package related ver. 1.0 (Pew et al., 2015; Wang, 2011) to test if the relatedness within each *C. gallina* sample was higher than expected by chance (Frasier, 2008). We followed the authors instructions to choose the most suitable method across five moment estimators (Li et al., 1993; Lynch and Ritland, 1999; Queller and Goodnight, 1989; Ritland, 1996; Wang, 2002) and two likelihood-based estimators (the dyadic likelihood estimator – dyadml, Milligan, 2003; and the triadic likelihood estimator – trioml, Wang, 2007). We calculated the average within-group relatedness and the associated p-values by comparing them with a distribution of expected values (generated by randomly shuffling individuals between category groups for 1000 permutations and keeping size constant, with the function *grouprel*). If the observed mean relatedness was greater than that of the permuted data ( $P > 0.95$ ), then the null hypothesis, that the mean within-category relatedness is random, was rejected (Schneider et al., 2016).

## 2.5. Power test, population differentiation, and gene flow network

Owing to the small genetic distance estimates obtained in this study (see Section 3. Results), we assessed the power of our loci and samples sizes to evaluate the magnitude of true differences that may have gone unnoticed. Hence, we applied the Fisher's and Chi-square tests by using POWSIM ver. 4.1 (Ryman and Palm, 2006).  $F_{ST}$  in POWSIM refers to Nei's  $G_{ST}$  modified to be independent of the number of subpopulations (Nei, 1987; Nei and Kumar, 2000; Ryman and Palm, 2006) and therefore we referred to our  $G_{ST}$  estimates to identify which genetic distance thresholds to test (see Section 3. Results). To assess the statistical power of our 11 markers to detect  $F_{ST}$  ( $G_{ST}$ ) values  $\leq 0.01$ , we used observed sample sizes and allele frequencies taken from our 9 samples and 1000 replicates. Following the POWSIM manual, we tested several combinations of  $N_e$  (100–3000) and generations (1–60) to account for the variability in  $N_e$  estimation.

To estimate the extent of bias possibly introduced by the presence of null alleles, pairwise unbiased  $F_{ST}$  (Weir, 1996) were calculated using the software FreeNA (Chapuis and Estoup, 2007) with and without null alleles correction. The software estimates null allele frequencies for each locus and population, implementing the so-called excluding null allele (ENA) correction to provide accurate estimation of  $F_{ST}$  in the presence of null alleles (Dempster et al., 1977; Weir, 1996). 95% CIs for  $F_{ST}$  values were obtained using 10,000 bootstrap iterations, with and without ENA algorithm and visually compared for overlap. Significance was assumed when zero was not present in the 95% CI (Whitlock and Schluter, 2009).

$F_{ST}$  (Weir and Cockerham, 1984),  $D_{JOST}$  (Jost, 2008),  $G_{ST}$  (Nei and Chesser, 1983) and  $G'_{ST}$  (Hedrick, 2005) estimates and their associated 95% CIs were calculated with the R package *diveRsim* ver. 1.9.90 (with 10,000 bootstrap replicates among loci). Significance was assumed when zero was not present in the 95% CI (Whitlock and Schluter, 2009). We evaluated which of the differentiation estimators was most suitable for population genetic inference of *C. gallina* by applying the *corplot* function implemented by *diveRsim* ver. 1.9.90.

Each estimator is differently sensitive to evolutionary, demographic and ecological processes affecting populations.  $D_{JOST}$  best reflects historical events and is more sensitive to differences in mutation rates among loci.  $F_{ST}$  and  $G_{ST}$  (and  $G'_{ST}$  as standardized  $G_{ST}$  over the maximum expected  $G_{ST}$ ) are best suited to track contemporary processes and thus more sensitive to recent demographic events, changes in effective population size and migration rates (Raeymaekers et al., 2012).

The relative direction of gene flow among samples was estimated using the *divMigrate* function from the R package *diveRsim* ver 1.9.90 (Keenan et al., 2013), using  $D_{JOST}$ ,  $G_{ST}$  and  $N_m$  as measures of genetic distance (Sundqvist et al., 2016). We considered only samples collected in 2010 to assess contemporary gene flow at the same time scale. To avoid bias due to sample size, we pooled small and big clams from each location. To test whether migration between pools of samples collected in 2010 was asymmetrical (significantly higher in one direction than the other), 95% confidence intervals were calculated from 100,000 bootstrap iterations.

## 2.6. Contemporary effective population size and demographic history

To test the hypothesis that fishing pressure could have triggered a decrease in effective population size ( $N_e$ ) in *C. gallina*, we estimated  $N_e$  using different methods to assess robustness and concordance of results. Contemporary estimates of effective population size were calculated by NeEstimator ver. 2 (Do et al., 2014). Two approaches were used, the first to calculate single-sample  $N_e$  (with two single-sample methods: the molecular coancestry method  $C_n$ , Nomura, 2008; and the linkage disequilibrium LD, Waples and Do, 2008); and the second, the standard temporal method, to obtain  $N_e$  from temporally replicated samples and size classes (Waples, 1989), with three different options (Jorde and Ryman, 2007; Nei and Tajima, 1981; Pollak, 1983). Low-frequency

alleles (with frequency  $< 0.05$ ) were eliminated when estimating  $N_e$  with the linkage disequilibrium method (Waples and Do, 2008) to avoid bias due to small samples sizes (Waples and Do, 2010). Low frequency alleles were retained by the coancestry method, as they have not been shown to introduce bias with this method (Do et al., 2014).

In this study, the LD method was applied to single-samples to obtain estimates of the per-generation  $N_e$  and to pools of samples (all samples and geographic and temporal pools) to estimate the multi-generation  $N_e$ . Geographically and temporally pooled samples were also used to test for the effect of sample size. Nomura (2008) indicates that the application of the coancestry method to a sample of juveniles (small clams in our case) gives an estimate of 'the effective number of breeders' (from now referred to as  $N_b$ ). This method has been applied to small clams samples only.

For temporal methods, big clams of each sampling site were assigned to generation 0 in that they likely represent a mix of parental cohorts of the newborns (small clams). Consequently, small clams were considered as generation 1. We assumed that small clams collected in 2010 were born during the last reproductive season from big clams sampled in 2010 (generation 0). Although the size of first reproduction has never been estimated for *C. gallina* in the Adriatic Sea, Casali (1984) and Froggia (1989) suggest that sexual maturity is reached when the shell attains a length of at least 12 mm. To avoid increasing bias by including overlapping generations due to multiple reproductive events occurring during the spawning season (between April and October, Milan et al., 2016; Morello et al., 2005a,b), we did not test pooled samples but only compared 2009 big clams to 2009 small clams, 2010 big clams to 2010 small clams and 2009 big clams to 2010 small clams within each location. Temporal methods estimate the harmonic average  $N_e$  over the generations in the sampling interval. When the samples are separated by one generation, as we assumed for our samples, these methods estimate the effective number of breeders ( $N_b$ , Wang, 2016).

To assess whether a recent severe demographic bottleneck caused by fishing occurred and affected the current genetic diversity or not, we used two approaches. We first applied the Wilcoxon signed-rank test in the software Bottleneck ver. 1.2.02 (Cornuet and Luikart, 1996; Piry et al., 1999) as this test is robust for the effects of both small samples sizes ( $< 30$ ) and a small number of loci ( $< 20$ ) (Piry et al., 1999). The analyses were conducted using a 70% SMM and 30% Infinite Allele Model (IAM) in the Two Phase Model (TPM) (Di Rienzo et al., 1994), and a TPM variance of 12, as recommended for microsatellites (Jensen et al., 2013; Piry et al., 1999) with 10,000 replications. The software searches for an excess of heterozygotes based on the observed allele frequencies, as a sign that rare alleles were lost faster than heterozygosity (Luikart and Cornuet, 1998; Munguía-Vega et al., 2015). Second, to test if a significant reduction in the ratio of the number of alleles lost by drift to the range in allele sizes has occurred (Garza and Williamson, 2001; Munguía-Vega et al., 2015), we calculated M values of Garza and Williamson (M-ratio test, Garza and Williamson, 2001) for all samples and loci with Arlequin 3.5.1.3, modified index after Excoffier et al. (2005, the adjustment avoids a division by zero when a gene sample is fixed for a single allele – monomorphic locus). Critical significance values ( $M_c$ ), were calculated using the software Critical\_M (Assis et al., 2013; Garza and Williamson, 2001). These calculations were made using different combinations of the requested parameters (sample size  $N$ , pre-bottleneck  $\Theta = 4N_e\mu$ , mean size of non-stepwise mutations  $\Delta_g$ , and % larger mutations  $p_s$ ), which are known to influence the  $M_c$  results (Assis et al., 2013; Busch et al., 2007). Since no information on several of these parameters is available for *C. gallina* in the sampled areas, we followed the manual instructions and the  $M_c$  values for each site were calculated for samples size of 25 (45 for Ancona) imposing two possible values of pre-bottleneck  $N_e$  ( $\Theta = 2$  and 6), one value for the mean size of non-stepwise mutations ( $\Delta_g = 3.5$ ) and the one-step model percentage (90 and 80%, % larger mutations  $p_s = 0.9$  and 0.8; Table S12b in Supplementary Material, Assis et al., 2013). Observed M-ratios below  $M_c$  indicate a bottleneck (Assis et al., 2013;

**Table 2** *Chamelea gallina* D<sub>joST</sub> and G<sub>sr</sub> estimates of pairwise genetic distance between samples and corresponding 95% confidence intervals (95% CI). The table reports the genetic distances calculated with the R package *diversity* ver. 1.9.90 (Keenan et al., 2013). Below the diagonal is the genetic distance D<sub>joST</sub> (in brackets) with corresponding 95% CI (in brackets) and above the diagonal is the genetic distance G<sub>sr</sub> (Hedrick, 2005) with corresponding 95% CI (in brackets). Genetic distances in bold indicate significantly different sample pairs (where the 95% CI does not contain the zero).

Samples	PtoCA09_small	PtoCA09_big	PtoCA10_small	PtoCA10_big	CH09_small	CH09_big	CH10_small	CH10_big	ANI0_big
PtoCA09_small		0.0175 [-0.0021, 0.0406]	0.0161 [-0.0058, 0.0419]	<b>0.032 [0.0072, 0.0622]</b>	0.0122 [-0.0065, 0.0354]	0.0263 [-0.0109, 0.0816]	0.0034 [-0.0086, 0.0153]	0.013 [-0.0046, 0.0315]	0.0141 [-0.0003, 0.0324]
PtoCA09_big	0.0052 [-0.0028, 0.0278]		0.0117 [-0.0001, 0.0241]	<b>0.0287 [0.005, 0.0528]</b>	0.0173 [-0.0015, 0.0398]	0.034 [-0.0082, 0.091]	<b>0.0162 [0.0027, 0.0291]</b>	0.000 [-0.0155, 0.0156]	-0.0026 [-0.0157, 0.015]
PtoCA10_small	0.0037 [-0.0026, 0.0242]	0.0037 [-0.001, 0.0138]		0.0188 [-0.0096, 0.0523]	0.0172 [-0.0123, 0.0679]	0.064 [-0.0108, 0.064]	0.0019 [-0.0127, 0.0159]	0.0205 [-0.0017, 0.0452]	0.0123 [-0.0026, 0.0284]
PtoCA10_big	0.0103 [-0.0028, 0.0334]	0.0098 [-0.0019, 0.0279]	0.0024 [-0.003, 0.0153]		0.0089 [-0.0113, 0.0321]	0.002 [-0.0112, 0.013]	0.0228 [-0.0008, 0.0564]	0.0261 [-0.0017, 0.0607]	0.0227 [-0.0011, 0.0526]
CH09_small	0.0003 [-0.0036, 0.0082]	0.0057 [-0.0019, 0.0224]	0.0016 [-0.0071, 0.0171]	0.001 [-0.0031, 0.0093]		0.0069 [-0.0201, 0.043]	0.0199 [-0.0034, 0.0484]	<b>0.0237 [0.0021, 0.0471]</b>	<b>0.0172 [0.0004, 0.0359]</b>
CH09_big	0.0032 [-0.0035, 0.022]	0.0034 [-0.0018, 0.0191]	0.0042 [-0.0041, 0.0297]	0.0009 [-0.0037, 0.0097]	0.000 [-0.0119, 0.0075]		0.0198 [-0.0104, 0.0672]	0.016 [-0.0022, 0.0372]	0.0153 [-0.0021, 0.0356]
CH10_small	0.000 [-0.0036, 0.0032]	0.0048 [-0.0019, 0.0181]	0.0003 [-0.0046, 0.0105]	0.0017 [-0.003, 0.0132]	0.000 [-0.0097, 0.0126]	0.000 [-0.0097, 0.0124]		0.005 [-0.0083, 0.0221]	0.0108 [-0.0013, 0.0242]
CH10_big	0.0009 [-0.0017, 0.0101]	-0.0007 [-0.0096, 0.0017]	0.0039 [-0.0017, 0.0191]	0.0051 [-0.0031, 0.0192]	0.000 [-0.0099, 0.0167]	0.0005 [-0.0025, 0.0097]	0.000 [-0.0052, 0.0039]		0.0043 [-0.0108, 0.0199]
ANI0_big	0.004 [-0.0012, 0.0148]	0.000 [-0.0057, 0.0029]	0.0002 [-0.0022, 0.0066]	0.0056 [-0.0029, 0.0227]	0.0032 [-0.0012, 0.0135]	0.0045 [-0.0014, 0.0182]	0.0019 [-0.0009, 0.0082]	-0.0003 [-0.0069, 0.0027]	

Garza and Williamson, 2001). The lowest value obtained (0.62, Table S12b in Supplementary Material) was used as the conservative threshold for bottleneck evaluation.

### 3. Results

#### 3.1. Genetic diversity, inbreeding, tests for selection and relatedness

High polymorphism was found for *Chamelea gallina* with the number of alleles ranging from 2 to 23 and mean allelic richness of 5.260, (Standard Deviation SD ± 0.455) as well as observed heterozygosity (0.427 ± 0.060) and expected heterozygosity (0.540 ± 0.033) considering all samples and 11 loci (Table 1 reports samples acronyms and a synthesis of basic statistics, Tables S2 and S3 in Supplementary Material report detailed genetic diversity parameters and allelic frequencies). Exact tests for LD yielded no significant values for all loci combinations (data not reported). A significant departure from Hardy-Weinberg Equilibrium (HWE) was observed for 38 out of 99 samples (after SGoF+, Carvajal-Rodríguez and de Uña-Alvarez, 2011, correction for multiple tests, Table S4 in Supplementary Material) and particularly affecting Locus 1243 with all samples in Hardy-Weinberg Disequilibrium (HWD). HWD was due to heterozygote deficiency in most cases, suggesting two alternative explanations, not reciprocally excluding: the presence of technical artefacts, such as non-amplifying alleles (null alleles), or the influence of biological factors (Dharmarajan et al., 2013; Waples, 2015).

The software Micro-Checker ver. 2.2.3 (van Oosterhout et al., 2004) indicated the presence of null alleles for all HWD samples. Because of the correction with Micro-Checker ver. 2.2.3, 9 out of 38 comparisons originally deviating from HWE were no longer significant (HWE p-values for the original and corrected datasets are shown in Table S4 in Supplementary Material).

The 36.36% of inbreeding index (F<sub>IS</sub>) estimates were positive for the original dataset (including their 95% CI) and 8.08% remained higher than zero, although lower than the original, when applying the Micro-Checker ver. 2.2.3 adjustment (Table S5 in Supplementary Material).

None of the 11 microsatellites was identified as an outlier by LOSITAN (Antao et al., 2008) (Table S6 and Fig. S2 in Supplementary Material).

Related (Pew et al., 2015; Wang, 2011) simulations suggested trioml (triadic likelihood estimator, estimates ranging from 0 to 1, Wang, 2007) as the most appropriate estimator with the highest correlation coefficient (0.811714, correlation coefficients for all seven estimators are reported in Table S7a in Supplementary Material). In general, this method was demonstrated to be more accurate than other methods (either moment or likelihood methods) as it incorporates correction for genotyping errors, considers inbreeding and uses a third individual as a control in estimating the relatedness of a dyad (Wang, 2007). Results reported in Table 1 were obtained with trioml method only. However, relatedness values and corresponding p-values for all estimators are reported in Table S7b and c in Supplementary Material. The average relatedness for the whole dataset was 0.118499. All single within-group relatedness estimates ranged between 0.085082 (PtoCA09\_small) and 0.203289 (PtoCA10\_big, Table 1). None of the samples differed from random expectations after SGoF+ correction although PtoCA10\_big was associated with a p-value < 0.05 (P = 0.024, Table 1).

#### 3.2. Power test, population differentiation, and gene flow network

A power analysis indicated our set of 11 microsatellites had a 100% chance (both Fisher's and Chi square method) to detect F<sub>ST</sub> values as small as 0.01 considering observed allelic frequencies and sample sizes at various combinations of N<sub>e</sub> (100–3000) and generations (2–60, Table S8 in Supplementary Material). For lower F<sub>ST</sub> values and average N<sub>e</sub> of 1000, the power was 98.40 and 99.70% (F<sub>ST</sub> = 0.005, Fisher's and Chi square method), 66.90 and 73.90% (F<sub>ST</sub> = 0.0025, Fisher's and Chi

square method, Table S8 in Supplementary Material for all  $N_e$  and generations tested). These values are in the range of the  $G'_{ST}$  (and  $G_{ST}$ ) obtained in our analysis (see below and Tables 2 and S10 in Supplementary Material). However, when  $F_{ST}$  (Nei's  $G_{ST}$ ) values fall below 0.001, the power of our markers also decreases to 23.30 and 22.30% ( $F_{ST} = 0.001$ , Fisher's and Chi square method, Table S8 in Supplementary Material). Hence, our dataset enables us to detect differences associated with  $F_{ST}$  (Nei's  $G_{ST}$ ) higher than 0.001. In this study, all significant comparisons obtained for the  $G'_{ST}$  and the  $G_{ST}$  estimates range between 0.0162 and 0.032 and between 0.0045 and 0.0097 respectively, and only three comparisons for  $G'_{ST}$  and 8 for  $G_{ST}$  fall below the 0.002 threshold (Tables 2 and S10 in Supplementary Material).

Mean  $F_{ST}$  estimates obtained with FreeNA – with and without ENA correction – showed slight differences due to an increase in  $F_{ST}$  distances when accounting for null alleles in most cases but with overlapping 95% CIs (Fig. S3 in Supplementary Material). Since the application of correction for null alleles has been demonstrated to produce an overestimation of the  $F_{ST}$  values in the case of significant population differentiation, only genetic distances obtained from the original dataset were considered in this study, without applying subsequent correction (Aglieri et al., 2014; Chapuis and Estoup, 2007). Hence, all subsequent differentiation analyses were conducted on the original dataset.

The analyses carried out with *diveR*sity provided different estimations of genetic distances for each estimator used. The estimator comparison obtained with the *diveR*sity function *corplot* showed a nearly negative/neutral correlation between  $F_{ST}$  (Weir and Cockerham, 1984) and the allele numbers as well as between  $G_{ST}$  (Nei and Chesser, 1983) and the allele numbers. A positive correlation between  $D_{JOST}$  (Jost, 2008),  $G'_{ST}$  (Hedrick, 2005) and the allele number suggests that these estimators are less biased by mutation (and therefore by the high number of low frequency alleles) and therefore more likely to estimate demographic processes (Keenan et al., 2013) (Fig. 2). Henceforth, we have used only these two estimators ( $D_{JOST}$ ,  $G'_{ST}$ ) considering that  $D_{JOST}$  best reflects historical events (Raeymaekers et al., 2012), while  $G'_{ST}$  is best suited to track contemporary processes, recent demographic events and changes in effective population size (Raeymaekers et al., 2012). For completeness,  $F_{ST}$  and  $G_{ST}$  estimates are reported in Table S10 in Supplementary Material.

The global multi-locus  $D_{JOST}$  was low and the 95% CI contained zero, thus the value was not considered significant ( $D_{JOST} = 0.0052$ , 95% CI [-0.0007, 0.0142]). All  $D_{JOST}$  pairwise comparisons were not significant and ranged from -0.0007 (big clams from Porto Caleri 2009 vs. big clams from Chioggia 2010) to 0.0103 (small clams from Porto Caleri 2009 vs. small clams Porto Caleri 2010; Table 2).

$G'_{ST}$  estimates, slightly higher than those of  $D_{JOST}$ , revealed a weak but significant differentiation ( $G'_{ST} = 0.0179$ , 95% CI [0.0053, 0.032]). Five comparisons were significantly different when considering  $G'_{ST}$  estimates (Table 2) and we observed that small clams collected in 2009 were generally different from big clams collected in 2010 (Table 2).

The directional relative migration networks for three estimators ( $D_{JOST}$ ,  $G_{ST}$ ,  $N_m$ ) as obtained by *divMigrate* depicted relative migration rates (above 0.5) among three pools of samples collected in 2010 (Fig. 3a–c) with a main gene flow direction occurring southwards. The estimated gene flow from Porto Caleri to Ancona was higher (1) than the reverse in all analyses, although it was only significantly asymmetrical in the  $N_m$  analysis (Fig. 3c) and no further significant asymmetries were detected in the analyses. Nonetheless, the Porto Caleri-Chioggia direction also exhibited a relatively higher gene flow than the opposite direction for all estimators (Fig. 3a–c). Chioggia and Ancona have a relatively similar gene flow in both directions with the  $G_{ST}$ ,  $N_m$  estimators (Fig. 3b and c), but not with  $D_{JOST}$  (Fig. 3a).

### 3.3. Contemporary effective population size and demographic history

Global estimated  $N_e$  based on LD method for a single pool of 239 clams is 1994.9 (95% CI [452.6,  $\infty$ ]) and indicates the estimated  $N_e$  for the whole pool of an unspecified number of generations (Table S11a in Supplementary Material).  $N_e$  estimates (LD method) for geographic pools were close to the global values in Chioggia ( $N_e = 2197.3$ , 95% CI [220.0,  $\infty$ ]), but lower in Porto Caleri ( $N_e = 830.8$ , 95% CI [180.3,  $\infty$ ]) and Ancona ( $N_e = 73.4$ , 95% CI [39.4, 246.8]), Table S11a in Supplementary Material).  $N_e$  values for 2009 and 2010 (Porto Caleri and Chioggia pooled) are small but both with the upper CI limit equal to infinity ( $N_e = 304.7$ , 95% CI [126.0,  $\infty$ ] in 2009 and  $N_e = 344.9$ , 95% CI [134.6,  $\infty$ ] in 2010, Table S11a in Supplementary Material).

$N_e$  estimates (LD method) obtained for single-samples (Table S11b in Supplementary Material) varied between 26.4 (Porto Caleri big clams

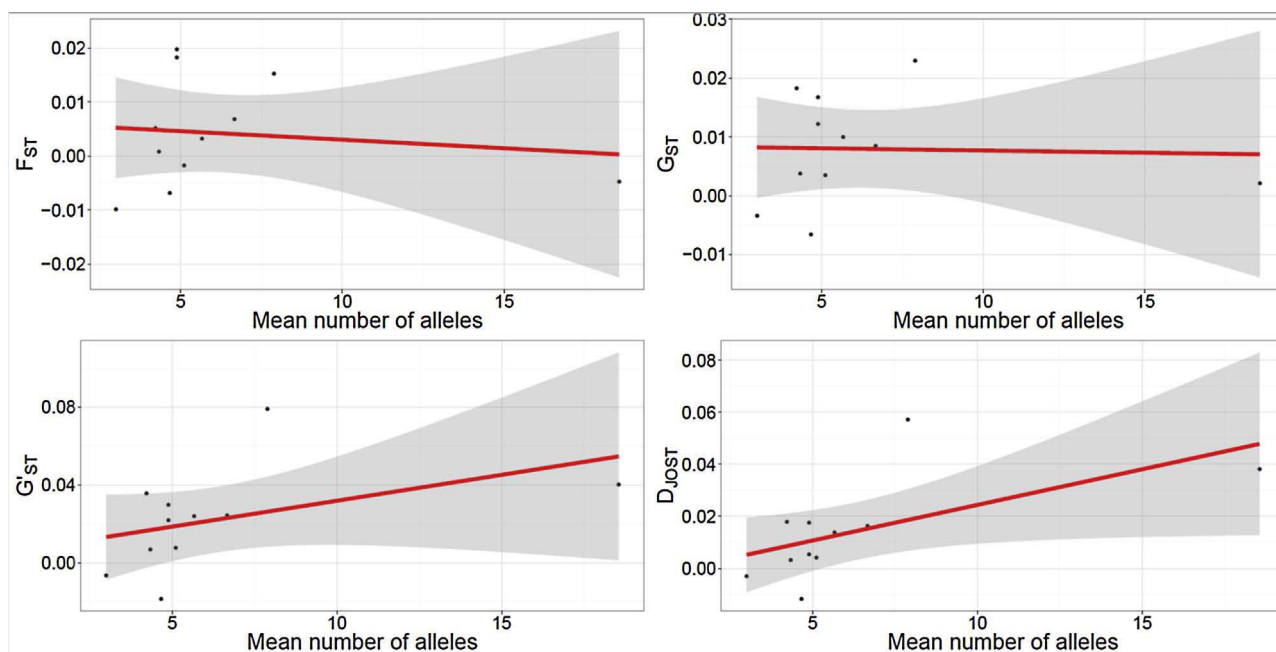
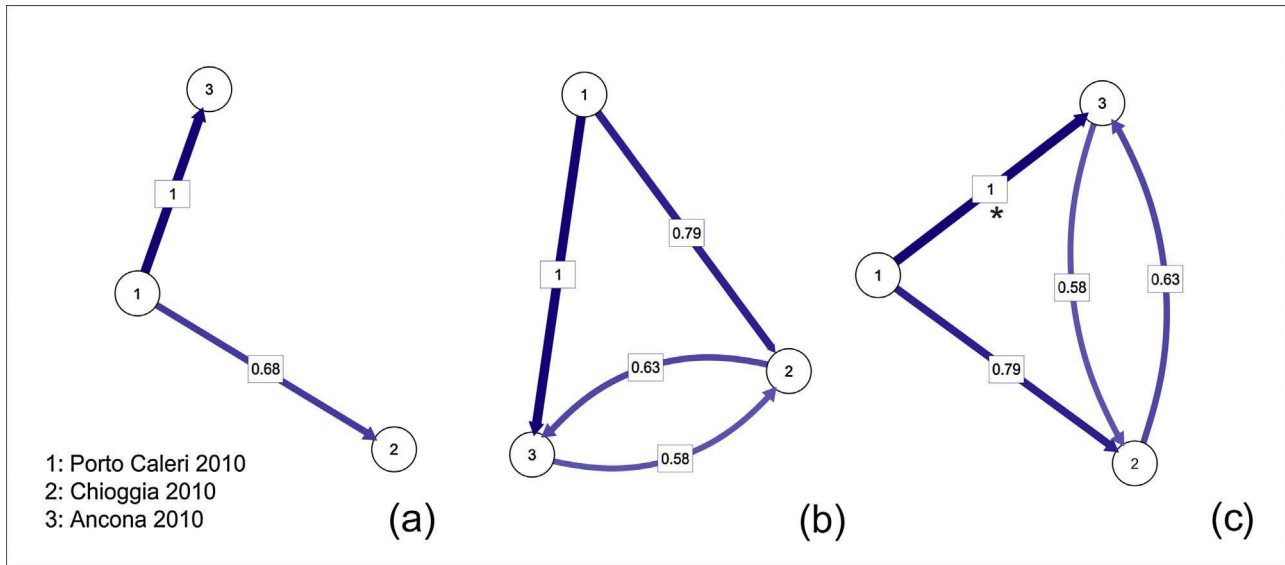


Fig. 2. Relationship between  $F_{ST}$ ,  $G_{ST}$ ,  $G'_{ST}$ ,  $D_{JOST}$  and the mean number of alleles per locus (polymorphism). Correlations calculated with *diveR*sity ver. 1.9.90 (Keenan et al., 2013). The lines represent the line of best fit.



**Fig. 3.** Directional relative migration (gene flow) networks connecting pools of samples collected in 2010. Relative values were calculated by *divMigrate* (with *diveRsity* ver. 1.9.90, Keenan et al., 2013). (a) Illustrates the calculated migration values based on  $D_{JOST}$ , (b) on  $G_{ST}$  estimates and (c) on  $N_m$ . Arrows indicate the direction of gene flow, and numbers show relative migration coefficient. Values found to be asymmetric are indicated by darker and thicker arrows and the filter threshold for the asymmetric values was set to 0.5. Gene flow values statistically higher than the others in the shown direction are indicated with \*.

2010) and 1295.4 (Chioggia small clams 2010). For several estimates based on the LD method, the corresponding CI intervals were very wide, with an upper limit of infinity in most cases (Tables S11a–b in Supplementary Material). This is frequently due to sampling error or small sample size (see Section 4.1 Caveats in Discussion, Hare et al., 2011; Waples and Do, 2010). In two cases (big clams from Porto Caleri 2010 and Ancona 2010, Table S11b in Supplementary Material) this possibility is clearly excluded by an upper 95% CI of 101.3 and 246.8, respectively. Moreover, for all LD estimates, the lower 95% CI limits are very small (range 12.9–151.8 in Table S11b in Supplementary Material) and indicate the lowest possible  $N_e$  values.

In general, estimates of parental  $N_e$  ( $N_b$ ) obtained for small clams samples with the coancestry method Cn (Nomura, 2008) were orders of magnitude lower than those obtained with the LD method. Despite the small number of markers and sample size,  $N_b$  estimates obtained with the Cn method have finite 95% CI limits in most, but not all, cases. In three out of four cases, we obtained definite 95% CI with Cn method for small clams. These estimates indicate that effective breeders are less than 283.6 (Tables S11b in Supplementary Material).

A small number of breeders were consistently obtained by temporal methods. As mentioned in the materials and methods, effective population sizes estimated using temporal replicates likely separated by one generation correspond to parental  $N_e$  (i.e.  $N_b$ ; Table S11c in Supplementary Material). Temporal values range from 17.5 to 326.2. In this case, only 8 out of 18 estimates have finite CI limits. All 95% CI obtained by Jorde and Ryman's (2007) approach excluded an effective number of breeders higher than 481.8, (Table S11c in Supplementary Material).

Considering that HWD could bias  $N_e$  estimates (Hare et al., 2011), we have attempted to estimate  $N_e$  also by including only loci that were in HWE for at least 5 samples. Results were not conclusive and more estimates than in previous tests resulted in infinite 95% CIs or infinite point estimates, with some  $N_e$  values being negative (data not shown).

The M-ratio test indicated signs of bottleneck for all samples at several but not all loci (Tables S12a and b in Supplementary Material). The Wilcoxon test indicated that no significant heterozygosity excess exists across loci therefore providing no signs of bottleneck (Table S13 in Supplementary Material).

#### 4. Discussion

This study investigated for the first time the genetic population structure of the commercially important bivalve *Chamelea gallina* in a highly-exploited region of the northern-central Adriatic Sea. We genotyped species-specific nuclear markers for small and big clams collected in 2009 and 2010. Our results indicate strong connectivity among geographic areas with a main southward gene flow direction, and genetic differences, though weak, among big clams (considered as mature adults) and small clams (considered offspring from the most recent reproductive season) at local geographic scale. Despite the fishing pressure, no clear signs of bottleneck were identified from our analyses and  $N_e$  estimates over a multiple-generation scale are medium to high though a low number of breeders are responsible for recruitment of the small size classes.

##### 4.1. Caveats

Before discussing the results in detail, we raise four caveats. First, we have used an approximate method to separate clams likely resulting from the most recent reproductive season and their potential parental cohorts. The sampling gear has also hindered the collection of very small clams (~below 5 mm). The limitations of this approach imply that we have had limited access to individuals born at the end of the reproductive season (very small clams ~5 mm or less) and instead likely accessed clams born at the beginning and during the mid-reproductive season. This approach may have led to a simplified population genetic structure (as big clams are presumably a pool of cohorts and very small clams were not accessible) and has not allowed for the assessment of the degree of overlapping among generations of clams. However, available information about growth rates and age vs. size in *C. gallina* is scant and much more intensive sampling would be required to accurately measure these parameters.

Second, some of the samples and loci analyzed in this study were affected by HWD. These departures from Hardy-Weinberg equilibrium can reflect analytical artefacts, real biological phenomena or both. Among the artefacts, one likely explanation for a deficit in heterozygotes is the presence of null alleles. Microsatellite null alleles are commonly encountered in studies involving mollusks (Addison and Hart, 2005). This is usually ascribed to high variability in the flanking

regions and elevated effective population size. We cannot completely rule out null alleles as cause for HWD in our markers, but we argue that if null alleles represented the exclusive factor accounting for HWD in our dataset, they should have heavily affected  $F_{IS}$  comparative tests and the correction applied with Micro-Checker should have mitigated disequilibrium for all cases. On the other hand, it has been shown that the influence of null alleles in studies of population genetics might be marginal compared to other factors such as the number of loci and strength of population differentiation (Carlsson, 2008; Dharmarajan et al., 2013). Samples in HWD are commonly included in mollusk's population differentiation tests (e.g. the pink abalone *Haliotis corrugata*, Munguía-Vega et al., 2015). In our specific case, we consider that some real biological phenomena might contribute, together with null alleles, to the excess of homozygosity. Heterozygote deficiencies in molecular markers have been widely reported for wild bivalves partially due to high larval mortality owing to inbreeding depression and leading to high variability at the single locus level (Plough and Hedgecock, 2011). Inbreeding has been indicated among possible drivers of Hardy-Weinberg disequilibrium also for other marine invertebrate species with large scale dispersal potential such as the jellyfish *Pelagia noctiluca* (Aglieri et al., 2014). We excluded the possibility that the microsatellites used were under selection with LOSITAN analysis. We consider that mixing of differentiated pools of different geographic origin (e.g. Wahlund effect, Wahlund, 1928) is less likely in species such as *C. gallina* with a high potential for homogenization due to larval dispersal, but we cannot rule out the presence of mixed pools of clams resulting from the same reproductive season but different pulses of gametes emissions (at least two emission peaks during the spawning season, Milan et al., 2016; Morello et al., 2005a,b). The extent to which these departures from HWE have affected downstream analyses was evaluated by running FreeNA, which showed that higher  $F_{ST}$  values caused by accounting for null alleles, indicative of increased genetic distances, nonetheless had overlapping 95% CIs.

Third, our samples sizes are small and results possibly prone to sample bias. Nonetheless, a power test showed that allelic frequency variability at our 11 loci and the sample size available can detect significant differences corresponding to  $F_{ST}$  as small as 0.01 and 0.005 ( $F_{ST}$  as Nei's  $G_{ST}$ ) with 100% power and in the case of  $F_{ST} = 0.0025$  with 66% power ( $N_e = 1000$ , Fisher's test, Table S8 in Supplementary Material). Thus, at lower levels of genetic distance ( $F_{ST} \leq 0.0025$ ), it is possible that some instances of significant differentiation may have gone undetected. This means that there might be a few more significant comparisons involving our samples than actually detected.

Fourth, we observed a disparity between  $N_e$  and  $N_b$  estimates, with  $N_b$  estimated values being orders of magnitude smaller than  $N_e$ . Although this disparity has been documented for bivalves and crustaceans (Robinson and Moyer, 2013; Waples and Yokota, 2007), several assumptions violations may impact the estimation of  $N_e$  and  $N_b$ . In our specific case, high variability in reproductive success, possible high larval mortality rate, small samples size, sampling error, HWD and migration (the possibility that gene flow has occurred between sampling localities and that offspring at one site might be the result of reproduction of individuals from different geographic origin) could have biased the  $N_e$  and  $N_b$  estimates. Temporal methods are also known to provide downwardly biased estimates when generations are not discrete and fewer than three to five generations have elapsed between samples (in our case, we assumed one generation of distance between small and big clams) (Ruzzante et al., 2016). However, given the complexity of the interaction of all these factors, it is not possible to ascertain the extend or direction (upwards or downwards) of the bias. Given the possible impact of life history traits, non-discrete size classes and deviations from methods assumptions,  $N_e$  and  $N_b$  estimates should always be considered with caution (Ruzzante et al., 2016; Waples et al., 2014). Moreover, since some  $N_e$  and  $N_b$  estimates obtained in this study had no definite CI limits, these results require further confirmation by increasing sampling efforts for both specimens and markers to reduce

bias and accrue definite CI limits when dealing with large  $N_e$  as assumed for mollusks (Hare et al., 2011). However, even in the case of an infinite upper CI limit and overlapping generations, the lower limit on a point estimate can be a useful indicator of the lowest possible level of  $N_e$  (Fraser et al., 2007; Hare et al., 2011). Our hypotheses about the biological conditions leading to the disparity between  $N_e$  and  $N_b$  in *C. gallina* are discussed in Section 4.3 Contemporary effective population size and demographic history (Discussion).

#### 4.2. Gene flow and potential drivers of diversity

Based on  $D_{JOST}$  estimates, *C. gallina* stocks in the northern-central Adriatic Sea are highly connected. As reported for several similar species, we expected that genetic exchange among *C. gallina* populations was high owing mainly to pelagic larval dispersal (and its duration), controlled by large scale hydrodynamics (Munroe et al., 2016; Schiavina et al., 2014). However, based on  $G'_{ST}$  distances, contemporary small significant fluctuations in allelic frequencies occur at small geographic scale and among temporal replicates and size classes. Factors contributing to this pattern include local circulation system, limitations in larval dispersal, genetic drift, high temporal variability in recruitment (i.e. the number of individuals reaching the age of maturity, Demandt, 2010) and a decrease in the number of new recruits due to abiotic factors (such as increasing temperature, low salinity, suboptimal reproduction conditions and the desynchronization of male and female spawning). Larval dispersal is commonly assumed to promote genetic homogenization (Jolly et al., 2014). The larval phase of *C. gallina*, the main life stage when dispersal would occur for this species, lasts for several weeks, probably not more than 20–30 days (Frogliia, 1989; Morello et al., 2011). Larvae are pelagic until settling in the sandy sea-bottom (Casali, 1984; Frogliia, 1989). The northern Adriatic circulation is mainly cyclonic and flows southwards along the western Adriatic coast (Papetti et al., 2013; Vilicic et al., 2013). Our analysis of relative migration network, indeed, indicates that all locations are highly connected, with the gene flow main direction occurring from Porto Caleri towards Chioggia and Ancona. However, the circulation in the northern part of the basin also exhibits transient small-scale spatial structures, high temporal variability, and dynamics that are largely thermohaline in origin (Poulain, 2001; Vilicic et al., 2013). This may cause unequal mixing of larval cohorts of different origins, allowing for small-scale genetic heterogeneity among subpopulations, irrespective of geographic distance (Hogan et al., 2010; Jolly et al., 2014; Selkoe et al., 2006; White et al., 2010), as reflected in the  $G'_{ST}$  differentiation pattern.

High variability in reproductive success and high larval mortality, working in concert with variability in local circulation, present another possible explanation for the weak differences found among our samples at local geographic scales and amongst size classes. High variability in reproductive success, gamete emission (two emission peaks during the spawning season in close geographic areas and possible asynchrony in male and female emissions in *C. gallina*, Milan et al., 2016; Morello et al., 2005a,b) and larval mortality rate (Plough and Hedgecock, 2011) could be a source of genetic differentiation which is not stable on a temporal scale and is also maintained between populations separated by small geographic distances (Hedgecock et al., 2007; Hedgecock and Pudovkin, 2011; Johnson and Black, 1982; Larson and Julian, 1999).

#### 4.3. Contemporary effective population size and demographic history

Our global estimates of  $N_e$  based on the LD method suggest a medium to high effective population size and are similar to those obtained for other exploited mollusks (e.g. *H. corrugata*  $N_e$  range 667–6553, Munguía-Vega et al., 2015). In contrast, the small  $N_b$  estimated by Cn and temporal methods (assuming one generation of distance between small and big clams) implies that animals responsible for the recruitment of small clams (likely the young ones derived from the last reproductive season of the year) are a small fraction of all adults

(Hare et al., 2011; Waples, 2016). This suggests a strong asymmetry in reproductive success, with few individuals reproducing (or producing viable offspring) in every peak of gamete emission during the reproductive season, resulting in offspring of the same age (when counted in years) but born at different times across the reproductive season. In this way, while few clams generate each size class throughout the entirety of the reproductive season, the global  $N_e$  over multiple generations is much higher. The extent of variability in reproductive success in *C. gallina* may vary among years and locations, and result in temporally and geographically variable genetic drift causing differences in  $N_e$  and  $N_b$ . A precise estimation of clams' age and shell growth would clarify if groups of clams of different ages within our samples, born at different times during the same reproductive season, also have similar shell length, thus resulting in overlap among size classes.

The clam mass mortality events occurring since 2005 in the central-northern Adriatic Sea, have been ascribed to recent environmental impacts such as salinity reduction, an increase in the concentration of water pollutants due to river run off (especially in autumn), water temperature and turbidity variability, oxygen depletion and human disturbance (Angioni et al., 2010; Milan et al., 2016). Although it has been documented that clam stocks have undergone multiple random mass mortality events, our analyses failed to detect any bottleneck with the heterozygosity-excess method by Cornuet and Luikart (1996), and showed changes in allele size distribution in several but not all loci with the M-ratio approach, failing indisputably to detect any bottleneck. The program Bottleneck is expected to identify demographic reduction which occurred approximately 0.2–4.0  $N_e$  generations ago (Cornuet and Luikart, 1996). Considering our global  $N_e$  estimates and one year as the generation time for *C. gallina* (Casali, 1984; Froglija, 1989), this would mean that any demographic reduction detected would have occurred more than several hundreds of years ago. It has also been shown that Bottleneck is less powerful in the case of long-term duration of population reduction since the excess of heterozygosity after a bottleneck is detectable only for a short time, after which a new equilibrium between mutation and drift is reached (Luikart and Cornuet, 1998; Peery et al., 2012). For *C. gallina*, it is more likely that a true bottleneck occurred only after it began to be exploited commercially in the 1970s (Froglija, 1989; Morello et al., 2005a,b). The HWD affecting some loci in our dataset may have had an impact on the M-ratio results, since this test is sensitive to assumption violations, limiting the power to detect a bottleneck at all loci and samples (Peery et al., 2012). However, the lack of agreement in the results provided by the two analytical approaches used here suggests that, had it occurred, a bottleneck would not have been detectable with the tools at hand. It could also be that the recovery of the local stocks may have already overcome the demographic drop.

#### 4.4. Implications for stock management and future directions

Our results on population genetic structure, gene flow direction and demographic status ( $N_e$ ) of *C. gallina* in the northern-central Adriatic Sea prompt the need for comprehensive future sampling and collection of biological and physical data (e.g. detailed circulation patterns, realized larval dispersal, adult density, growth rate vs. age and age vs. shell size of clams) over the span of years or decades, for both exploited and unexploited stocks. The integration of this information with data from large databases of catch-rates, would allow for a more precise stock assessment and analyses of population demographic trajectories.

Although local administrations continue to include the development and implementation of different strategies to support the *C. gallina* fishery in their economic plans, these approaches are usually not combined with pre- and post-assessment of genetic variability (Vasi and Bagni, 2009). We propose that future efforts (e.g. fishery suspension, seeding and restoration programs) should aim to limit  $N_e$  fluctuations (especially drops in population size) and increase, or at least maintain, genetic diversity – essential to the long-term sustainability of the resource – while taking into account the need to improve water quality to

avoid mass mortality events.

#### Funding sources

This work was part of the project CLODIA funded by the Veneto Region (Italy) Law 15/2007 (DGR n. 4069) to Mariella Rasotto and LZ. This study results from a post-doctoral fellowship to CP (University of Padova, salary grant GRIC110B82). Financial support of the Hanse-Wissenschaftskolleg, Institute for Advanced Study in Delmenhorst, Germany to CP is also acknowledged.

#### Author contributions

CP and LZ conceived and designed the study, CP performed the experiments. CP and LS performed the statistical analyses and wrote the paper. MM, ML, JAC, MP, EB, IAMM and LC advised on the laboratory protocols and statistical analyses. All authors critically revised and approved the final manuscript.

#### Competing financial interests

The authors declare that they have no conflict of interest and that funding agencies had no role in study design, data collection and analysis, decision to publish, or preparation of the manuscript.

#### Ethics statement

This study does not involve experiments with live animals and has been conducted on invertebrates (mollusks) not subjected to regulations. No specific permits were required for the sampling as the sites were not privately-owned or protected in any way. The target species is not endangered or protected.

#### Data availability statement

Data are made directly available in this paper by providing all allelic frequencies obtained in this study in Table S3 in Supplementary Material.

#### Acknowledgments

Authors would like to thank M. La Mesa (CNR, Institute of Marine Sciences, Ancona, Italy) for providing the clam sample from Ancona, M.G. Marin for providing sampling coordinates and details about the *Chamelea gallina* reproductive cycle and A. Sanchini for useful advice. We thank L. Masiero, G. Rizzo, F. Cernigai and the crew of the hydraulic dredge “Matteo” for their kind support in *C. gallina* samples collection.

#### Appendix A. Supplementary data

Supplementary data associated with this article can be found, in the online version, at <https://doi.org/10.1016/j.fishres.2018.01.006>.

#### References

- Addison, J.A., Hart, M.W., 2005. Spawning: copulation and inbreeding coefficients in marine invertebrates. *Biol. Lett.* 1, 450–453.
- Aglieri, G., Papetti, C., Zane, L., Milisenda, G., Boero, F., Piraino, S., 2014. First evidence of inbreeding, relatedness and chaotic genetic patchiness in the holoplanktonic jellyfish *Pelagia noctiluca* (Scyphozoa, Cnidaria). *PLoS One* 9, e99647.
- Agostini, C., Papetti, C., Patarnello, T., Mark, F., Zane, L., Marino, I.M., 2013. Putative selected markers in the *Chionodraco* genus detected by interspecific outlier tests. *Polar Biol.* 36, 1509–1518.
- Amos, W., Hoffman, J.I., Frodsham, A., Zhang, L., Best, S., Hill, A.V.S., 2007. Automated binning of microsatellite alleles: problems and solutions. *Mol. Ecol. Notes* 7, 10–14.
- Angioni, S.A., Giansante, C., Ferri, N., 2010. The clam (*Chamelea gallina*): evaluation of the effects of solids suspended in seawater on bivalve molluscs. *Vet. Ital.* 46, 101–106.
- Antao, T., Lopes, A., Lopes, R.J., Beja-Pereira, A., Luikart, G., 2008. LOSITAN: a



- workbench to detect molecular adaptation based on a  $F_{ST}$ -outlier method. *BMC Bioinform.* 9, 323.
- Assis, J., Castilho Coelho, N., Alberto, F., Valero, M., Raimondi, P., Reed, D., Alvares Serrão, E., 2013. High and distinct range-edge genetic diversity despite local bottlenecks. *PLoS One* 8, e68646.
- Backeljau, T., Gofas, S., 1994. Genetic variation, systematics and distribution of the venerid clam *Chamelea gallina*. *J. Mar. Biol. Assoc. UK* 74, 211–223.
- Beaumont, M.A., Nichols, R.A., 1996. Evaluating loci for use in the genetic analysis of population structure. *Proc. R. Soc. Lond. B Biol. Sci.* 263, 1619–1626.
- Busch, J.D., Waser, P.M., DeWoody, J.A., 2007. Recent demographic bottlenecks are not accompanied by a genetic signature in banner-tailed kangaroo rats (*Dipodomys spectabilis*). *Mol. Ecol.* 16, 2450–2462.
- Carlsson, J., 2008. Effects of microsatellite null alleles on assignment testing. *J. Hered.* 99, 616–623.
- Carvajal-Rodríguez, A., de Uña-Alvarez, J., 2011. Assessing significance in high-throughput experiments by sequential goodness of fit and q-value estimation. *PLoS One* 6, e24700.
- Casali, C., 1984. Résumé des paramètres biologiques sur *Venus gallina* L. en Adriatique (Synopsis of biological data on *Venus gallina* L. in the Adriatic Sea). *FAO Fish Rep.* 290, 171–173.
- Chapuis, M.-P., Estoup, A., 2007. Microsatellite null alleles and estimation of population differentiation. *Mol. Biol. Evol.* 24, 621–631.
- Coombs, J.A., Letcher, B.H., Nislow, K.H., 2008. Create: a software to create input files from diploid genotypic data for 52 genetic software programs. *Mol. Ecol. Resour.* 8, 578–580.
- Coppe, A., Bortoluzzi, S., Murari, G., Marino, I.A.M., Zane, L., Papetti, C., 2012. Sequencing and characterization of striped venus transcriptome expand resources for clam fishery genetics. *PLoS One* 7, e44185.
- Cornuet, J.M., Luikart, G., 1996. Description and power analysis of two tests for detecting recent population bottlenecks from allele frequency data. *Genetics* 144, 2001–2014.
- Demandt, M.H., 2010. Temporal changes in genetic diversity of isolated populations of perch and roach. *Conserv. Genet.* 11, 249–255.
- Dempster, A., Laird, N., Rubin, D., 1977. Maximum likelihood from incomplete data via the EM algorithm. *J. R. Stat. Soc. Ser. B Stat. Methodol.* 39, 1–38.
- Dharmarajan, G., Beatty, W.S., Rhodes, O.E., 2013. Heterozygote deficiencies caused by a Wahlund effect: dispelling unfounded expectations. *J. Wildl. Res.* 77, 226–234.
- Di Rienzo, A., Peterson, A.C., Garza, J.C., Valdes, A.M., Slatkin, M., Freimer, N.B., 1994. Mutational processes of simple-sequence repeat loci in human populations. *Proc. Natl. Acad. Sci. U. S. A.* 91, 3166–3170.
- Do, C., Waples, R.S., Peel, D., Macbeth, G.M., Tillett, B.J., Ovenden, J.R., 2014. NeEstimator v2: re-implementation of software for the estimation of contemporary effective population size ( $N_e$ ) from genetic data. *Mol. Ecol. Resour.* 14, 209–214.
- Eggleton, J.D., Smith, R., Reiss, H., Rachor, E., Vanden Berghe, E., Rees, H.L., et al., 2007. Species distributions and changes (1986–2000). In: Rees, H.L. (Ed.), *Structure and Dynamics of the North Sea Benthos*. ICES Cooperative Research Report, 288.
- Excoffier, L., Estoup, A., Cornuet, J.M., 2005. Bayesian analysis of an admixture model with mutations and arbitrarily linked markers. *Genetics* 169, 1727–1738.
- Frankham, R., 1995. Effective population size/adult population size ratios in wildlife: a review. *Genet. Res.* 66, 95–107.
- Fraser, D.J., Hansen, M.M., Ostergaard, S., Tessier, N., Legault, M., Bernatchez, L., 2007. Comparative estimation of effective population sizes and temporal gene flow in two contrasting population systems. *Mol. Ecol.* 16, 3866–3889.
- Frasier, T.R., 2008. STORM: software for testing hypotheses of relatedness and mating patterns. *Mol. Ecol. Resour.* 8, 1263–1266.
- Frogliola, C., 1975. Osservazioni sull'accrescimento di *Chamelea gallina* (L.) e *Ensis minor* (Chenu) nel Medio Adriatico (Remarks on the growth of *Chamelea gallina* L. and *Ensis minor* Chenu in the Central Adriatic Sea). *Quad. Lab. Tecnol. Pesca Ancona* 2 (1), 37–48.
- Frogliola, C., 1989. Clam fisheries with hydraulic dredges in the Adriatic Sea. In: Caddy, J. (Ed.), *Marine Invertebrate Fisheries*. J. Wiley.
- Garza, J.C., Williamson, E.G., 2001. Detection of reduction in population size using data from microsatellite loci. *Mol. Ecol.* 10, 305–318.
- Gizzi, F., Caccia, M.G., Simoncini, G.A., Mancuso, A., Reggi, M., Fermani, S., Brizi, L., Fantazzini, P., Stagoni, M., Falini, G., Piccinetti, C., Goffredo, S., 2016. Shell properties of commercial clam *Chamelea gallina* are influenced by temperature and solar radiation along a wide latitudinal gradient. *Sci. Rep.* 6, 36420.
- Hare, M.P., Nunney, L., Schwartz, M.K., Ruzzante, D.E., Burford, M., Waples, R.S., Ruegg, K., Palstra, F., 2011. Understanding and estimating effective population size for practical application in marine species management. *Conserv. Biol.* 25, 438–449.
- Hedgecock, D., Pudovkin, A.I., 2011. Sweepstakes reproductive success in highly fecund marine fish and shellfish: a review and commentary. *Bull. Mar. Sci.* 87, 971–1002.
- Hedgecock, D., Launey, S., Pudovkin, A.I., Naciri, Y., Lapègue, S., Bonhomme, F., 2007. Small effective number of parents ( $N_b$ ) inferred for a naturally spawned cohort of juvenile European flat oysters *Ostrea edulis*. *Mar. Biol.* 150, 1173–1182.
- Hedrick, P.W., 2005. A standardized genetic differentiation measure. *Evolution* 59, 1633–1638.
- Hogan, J.D., Thiessen, R.J., Heath, D.D., 2010. Variability in connectivity indicated by chaotic genetic patchiness within and among populations of a marine fish. *Mar. Ecol. Prog. Ser.* 417, 263–275.
- Hutchings, J.A., Reynolds, J.D., 2004. Marine fish population collapses: consequences for recovery and extinction risk. *Bioscience* 54, 297–309.
- Jensen, H., Moe, R., Hagen, I.J., Holand, A.M., Kekkonen, J., Tufto, J., Sæther, B.E., 2013. Genetic variation and structure of house sparrow populations: is there an island effect? *Mol. Ecol.* 22, 1792–1805.
- Johnson, M.S., Black, R., 1982. Chaotic genetic patchiness in an intertidal limpet, *Siphonaria* sp. *Mar. Biol.* 70, 157–164.
- Jolly, M.T., Thiébaud, E., Guyard, P., Gentil, F., Jollivet, D., 2014. Meso-scale hydrodynamic and reproductive asynchrony affects the source-sink metapopulation structure of the coastal polychaete *Pectinaria koreni*. *Mar. Biol.* 161, 367–382.
- Jorde, P., Ryman, N., 2007. Unbiased estimator for genetic drift and effective population size. *Genetics* 177, 927–935.
- Jost, L., 2008.  $G_{ST}$  and its relatives do not measure differentiation. *Mol. Ecol.* 17, 4015–4026.
- Keenan, K., McGinnity, P., Cross, T.F., Crozier, W.W., Prodöhl, P.A., 2013. diveRst: an R package for the estimation and exploration of population genetics parameters and their associated errors. *Methods Ecol. Evol.* 4, 782–788.
- Larson, R.J., Julian, R.M., 1999. Spatial and temporal genetic patchiness in marine populations and their implications for fisheries management. *Calif. Coop. Oceanic Fish Investig. Rep.* 40, 94–99.
- Li, C.C., Weeks, D.E., Chakravarti, A., 1993. Similarity of DNA fingerprints due to chance and relatedness. *Hum. Hered.* 43, 45–52.
- Luikart, G., Cornuet, J.M., 1998. Empirical evaluation of a test for identifying recently bottlenecked populations from allele frequency data. *Conserv. Biol.* 12, 228–237.
- Lynch, M., Ritland, K., 1999. Estimation of pairwise relatedness with molecular markers. *Genetics* 152, 1753–1766.
- Milan, M., Palazzo, F., Papetti, C., Grotta, L., Marchetti, S., Patarnello, T., Bargelloni, L., Martino, G., 2016. Transcriptomic profiling of *Chamelea gallina* from sites along the Abruzzo coast (Italy), subject to periodic localized mortality events. *Mar. Biol.* 163, 196.
- Milligan, B., 2003. Maximum-likelihood estimation of relatedness. *Genetics* 163, 1153–1167.
- Morello, E.B., Frogliola, C., Atkinson, R.J.A., Moore, P.G., 2005a. Hydraulic dredge discards of the clam (*Chamelea gallina*) fishery in the western Adriatic Sea, Italy. *Fish Res.* 76, 430–444.
- Morello, E.B., Frogliola, C., Atkinson, R.J.A., Moore, P.G., 2005b. Impacts of hydraulic dredging on a macrobenthic community of the Adriatic Sea, Italy. *Can. J. Fish. Aquat. Sci.* 62, 2076–2087.
- Morello, E., Martinelli, M., Antolini, B., Gramitto, M., Arneri, E., Frogliola, C., 2011. Population dynamics of the clam, *Chamelea gallina*, in the Adriatic Sea (Italy). In: Brugnoti, E., Cavarretta, G., Mazzola, S., Trincardi, F., Ravaioli, M., Santoleri, R. (Eds.), *Marine Research at CNR. Dipartimento Terra e Ambiente – CNR (Publisher)*, pp. 1907–1921.
- Moschino, V., Marin, M.G., 2006. Seasonal changes in physiological responses and evaluation of well-being in the Venus clam *Chamelea gallina* from the Northern Adriatic Sea. *Comp. Biochem. Physiol. A Mol. Integr. Physiol.* 145, 433–440.
- Munguía-Vega, A., Sáenz-Arroyo, A., Greenley, A.P., Espinoza-Montes, J.A., Palumbi, S.R., Rossetto, M., Micheli, F., 2015. Marine reserves help preserve genetic diversity after impacts derived from climate variability: lessons from the pink abalone in Baja California. *Glob. Conserv.* 4, 264–276.
- Munroe, D.M., Narváez, D.A., Hennen, D., Jacobson, L., Mann, R., Hofmann, E.E., Powell, E.N., Klinck, J.M., 2016. Fishing and bottom water temperature as drivers of change in maximum shell length in Atlantic surfclams (*Spisula solidissima*). *Estuar. Coast. Shelf Sci.* 170, 112–122.
- Nei, M., Chesser, R.K., 1983. Estimation of fixation indices and gene diversities. *Ann. Hum. Genet.* 47, 253–259.
- Nei, M., Kumar, S., 2000. *Molecular Evolution and Phylogenetics*. Oxford University Press, Oxford.
- Nei, M., Tajima, F., 1981. Genetic drift and estimation of effective population size. *Genetics* 98, 625–640.
- Nei, M., 1987. *Molecular Evolutionary Genetics*. Columbia University Press, New York.
- Nomura, T., 2008. Estimation of effective number of breeders from molecular coancestry of single cohort sample. *Evol. Appl.* 1, 462–474.
- O'Leary, S.J., Hice, L.A., Feldheim, K.A., Frisk, M.G., McElroy, A.E., Fast, M.D., Chapman, D.D., 2013. Severe inbreeding and small effective number of breeders in a formerly abundant marine fish. *PLoS One* 8, e66126.
- Papetti, C., Di Franco, A., Zane, L., Guidetti, P., De Simone, V., Spizzotini, M., Zorica, B., Čikeš Keč, V., Mazzoldi, C., 2013. Single population and common natal origin for Adriatic *Scomber scombrus* stocks: evidence from an integrated approach. *ICES J. Mar. Sci.* 70, 387–398.
- Patwary, M.U., Kenchington, E.L., Bird, C.J., Zouros, E., 1994. The use of random amplified polymorphic DNA markers in genetic studies of the sea scallop *Placopecten magellanicus* (Gmelin, 1791). *J. Shellfish Res.* 13, 547–553.
- Peery, M.Z., Kirby, R., Reid, B.N., Stoelting, R., Doucet-Béer, E., Robinson, S., Vásquez-Carrillo, C., Pauli, J.N., Palsboll, P.J., 2012. Reliability of genetic bottleneck tests for detecting recent population declines. *Mol. Ecol.* 21, 3403–3418.
- Pew, J., Muir, P.H., Wang, J., Frasier, T.R., 2015. related: an R package for analysing pairwise relatedness from codominant molecular markers. *Mol. Ecol. Resour.* 15, 557–561.
- Piry, S., Luikart, G., Cornuet, J.M., 1999. BOTTLENECK: a computer program for detecting recent reductions in the effective population size using allele frequency data. *J. Hered.* 90, 502–503.
- Plough, L.V., Hedgecock, D., 2011. Quantitative trait locus analysis of stage-specific inbreeding depression in the Pacific oyster *Crassostrea gigas*. *Genetics* 189, 1473–1486.
- Pollak, E., 1983. A new method for estimating the effective population size from allele frequency changes. *Genetics* 104, 531–548.
- Poulain, P.M., 2001. Adriatic sea surface circulation as derived from drifter data between 1990 and 1999. *J. Mar. Syst.* 29, 3–32.
- Queller, D., Goodnight, K., 1989. Estimating relatedness using molecular markers. *Evolution* 43, 258–275.
- Raeymaekers, J.A.M., Lens, L., Van Den Broeck, F., Van Dongen, S., Volckaert, F.A.M., 2012. Quantifying population structure on short timescales. *Mol. Ecol.* 21, 3458–3473.

- Raymond, M., Rousset, F., 1995. An exact test for population differentiation. *Evolution* 49, 1280–1283.
- Ritland, K., 1996. Estimators for pairwise relatedness and inbreeding coefficients. *Genet. Res.* 67, 175–186.
- Robinson, J.D., Moyer, G.R., 2013. Linkage disequilibrium and effective population size when generations overlap. *Evol. Appl.* 6, 290–302.
- Romanelli, M., Cordisco, C.A., Giovanardi, O., 2009. The long-term decline of the *Chamelea gallina* L. (Bivalvia: Veneridae) clam fishery in the Adriatic sea: is a synthesis possible? *Acta Adriat.* 50, 171–205.
- Rousset, F., 2008. GENEPOP'007: a complete re-implementation of the GENEPOP software for Windows and Linux. *Mol. Ecol. Resour.* 8, 103–106.
- Ruzzante, D.E., McCracken, G.R., Parmelee, S., Hill, K., Corrigan, A., MacMillan, J., Walde, S.J., 2016. Effective number of breeders, effective population size and their relationship with census size in an iteroparous species, *Salvelinus fontinalis*. *Proc. Biol. Sci.* 283, 20152601.
- Ryman, N., Palm, S., 2006. POWSIM: a computer program for assessing statistical power when testing for genetic differentiation. *Mol. Ecol. Notes* 6, 600–602.
- Schiavina, M., Marino, I.A.M., Zane, L., Melià, P., 2014. Matching oceanography and genetics at the basin scale. Seascape connectivity of the Mediterranean shore crab in the Adriatic Sea. *Mol. Ecol.* 23, 5496–5507.
- Schneider, T.C., Kappeler, P.M., Pozzi, L., 2016. Genetic population structure and relatedness in the narrow-striped mongoose (*Mungotictis decemlineata*), a social Malagasy carnivore with sexual segregation. *Ecol. Evol.* 6, 3734–3749.
- Selkoe, K.A., Gaines, S.D., Caselle, J.E., Warner, R.R., 2006. Current shifts and kin aggregation explain genetic patchiness in fish recruits. *Ecology* 87, 3082–3094.
- Sundqvist, L., Keenan, K., Zackrisson, M., Prodöhl, P., Kleinans, D., 2016. Directional genetic differentiation and relative migration. *Ecol. Evol.* 6, 3461–3475.
- van Oosterhout, C., Hutchinson, W.F., Wills, D.P.M., Shipley, P., 2004. MICRO-CHECKER: software for identifying and correcting genotyping errors in microsatellite data. *Mol. Ecol. Notes* 4, 535–538.
- Vasi, P., Bagni, E., 2009. Progetti di ricerca del Piano Regionale della pesca e dell'acquicoltura 1998–2007 (Regione Emilia-Romagna). Greentime SpA, Bologna, Italy.
- Vilicic, D., Kuzmic, M., Tomazić, I., Ljubešić, Z., Bosak, S., Precali, R., Djakovac, T., Marić, D., Godrijan, J., 2013. Northern Adriatic phytoplankton response to short Po river discharge pulses during summer stratified conditions. *Mar. Ecol.* 34, 451–466.
- Wahlund, S., 1928. Zusammensetzung von Populationen und Korrelationserscheinungen vom Standpunkt der Vererbungslehre aus betrachtet. *Hereditas* 11, 65–106.
- Wang, J., 2002. An estimator for pairwise relatedness using molecular markers. *Genetics* 160, 1203–1215.
- Wang, J., 2007. Triadic IBD coefficients and applications to estimating pairwise relatedness. *Genet. Res.* 89, 135–153.
- Wang, J., 2011. Coancestry: a program for simulating, estimating and analysing relatedness and inbreeding coefficients. *Mol. Ecol. Resour.* 11, 141–145.
- Wang, J., 2016. A comparison of single-sample estimators of effective population sizes from genetic marker data. *Mol. Ecol.* 25, 4692–4711.
- Waples, R.S., Do, C., 2008. LDNE: a program for estimating effective population size from data on linkage disequilibrium. *Mol. Ecol. Resour.* 8, 753–756.
- Waples, R.S., Do, C., 2010. Linkage disequilibrium estimates of contemporary  $N_e$  using highly variable genetic markers: a largely untapped resource for applied conservation and evolution. *Evol. Appl.* 3, 244–262.
- Waples, R.S., Yokota, M., 2007. Temporal estimates of effective population size in species with overlapping generations. *Genetics* 175, 219–233.
- Waples, R.S., Antao, T., Luikart, G., 2014. Effects of overlapping generations on linkage disequilibrium estimates of effective population size. *Genetics* 197, 769–780.
- Waples, R.S., 1989. A generalized approach for estimating effective population size from temporal changes in allele frequency. *Genetics* 121, 379–391.
- Waples, R.S., 2015. Testing for Hardy-Weinberg proportions: have we lost the plot? *J. Hered.* 106, 1–19.
- Waples, R.S., 2016. Tiny estimates of the  $N_e/N$  ratio in marine fishes: are they real? *J. Fish Biol.* 89, 2479–2504.
- Weir, B., Cockerham, C., 1984. Estimating F-statistics for the analysis of population structure. *Evolution* 38, 1358–1370.
- Weir, B., 1996. *Genetic Data Analysis 2: Methods for Discrete Population Genetic Data*. Sinauer Associates, Sunderland (Massachusetts).
- White, C., Selkoe, K.A., Watson, J., Siegel, D.A., Zacherl, D.C., Toonen, R.J., 2010. Ocean currents help explain population genetic structure. *Proc. R. Soc. Lond. B Biol. Sci.* 277, 1685–1694.
- Whitlock, M., Schluter, D., 2009. *The Analysis of Biological Data*. Roberts and Co, Greenwood Village, Colorado.

# Supplementary Information **Papetti *et al.* 2018**

1 **Electronic Supplementary Material for Fisheries Research**

2  
3 **Genetic variability of the striped venus *Chamelea gallina* in the northern Adriatic Sea**

4  
5 Chiara Papetti<sup>1,4,#\*</sup>, Luca Schiavon<sup>1#</sup>, Massimo Milan<sup>2</sup>, Magnus Lucassen<sup>3</sup>, Jilda Alicia Caccavo<sup>1,4</sup>, Marta Paterno<sup>1,4</sup>, Elisa Boscari<sup>1,4</sup>,  
6 Ilaria Anna Maria Marino<sup>1,4</sup>, Leonardo Congiu<sup>1,4</sup>, Lorenzo Zane<sup>1,4</sup>

7  
8 **Postal Addresses**

9 <sup>1</sup> Department of Biology, University of Padova - 35121 Padova, Italy

10 <sup>2</sup> Department of Comparative Biomedicine and Food Science, University of Padova - 35020 Legnaro, Italy

11 <sup>3</sup> Alfred Wegener Institute Helmholtz Centre for Polar and Marine Research - D-27570 Bremerhaven, Germany

12 <sup>4</sup> Consorzio Nazionale Interuniversitario per le Scienze del Mare (CoNISMa) - 00196 Roma, Italy

13  
14 # These authors equally contributed to this study

15  
16 **Corresponding author**

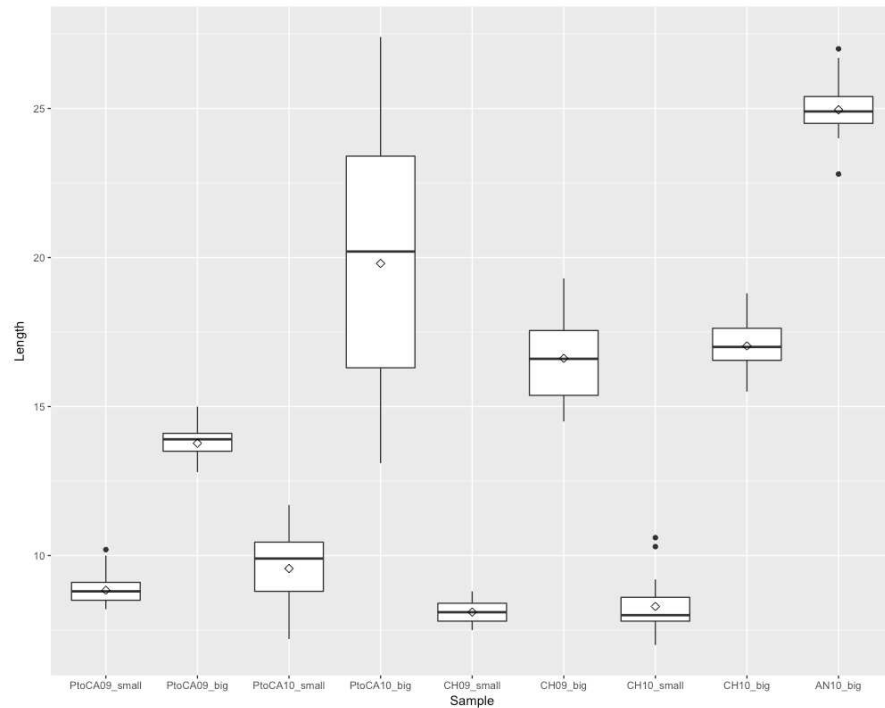
17 \* Chiara Papetti, Department of Biology, University of Padova, via G. Colombo, 3 - 35121 Padova, Italy – phone +39 0498276259, –  
18 chiara.papetti@unipd.it; ORCID: 0000-0002-4567-459X

20  
21  
22  
23  
24  
25  
26  
27  
28  
29  
30  
31  
32  
33  
34

**Figure S1a and b. Box plots and histograms showing the distribution of length (along the anterior-posterior axis) of left shell in *Chamelea gallina* samples genotyped in this study.** a) Box plot of the mean length (in mm) of the left shell of each specimen. Each box plot visualises six summary statistics (the median as a horizontal bold line, two hinges, two whiskers and the mean as a diamond symbol), and all "outlying" points individually. The lower and upper hinges correspond to the first and third quartiles (the 25th and 75th percentiles) of the distribution. The upper whisker extends from the hinge to the largest value. The lower whisker extends from the hinge to the smallest value. Data beyond the end of the whiskers are "outlying" points and are plotted individually; b) histograms showing the distribution of length (in mm) in each sample per location and year (bins of 0.5 mm). We point out that the length distribution in each sample is not necessarily representative of the real distribution in nature, during sampling specimens were picked, randomly, to be smaller or larger than 12 mm (see Materials and Methods section 2.2 for a detailed explanation of the sampling approach).

Each figure reports the sample acronym on the x-axis (see main text and Table 1 for explanation of samples acronyms and size classes subdivision). Box plots and histograms were obtained with R (ver. 3.3.2) package ggplot2.

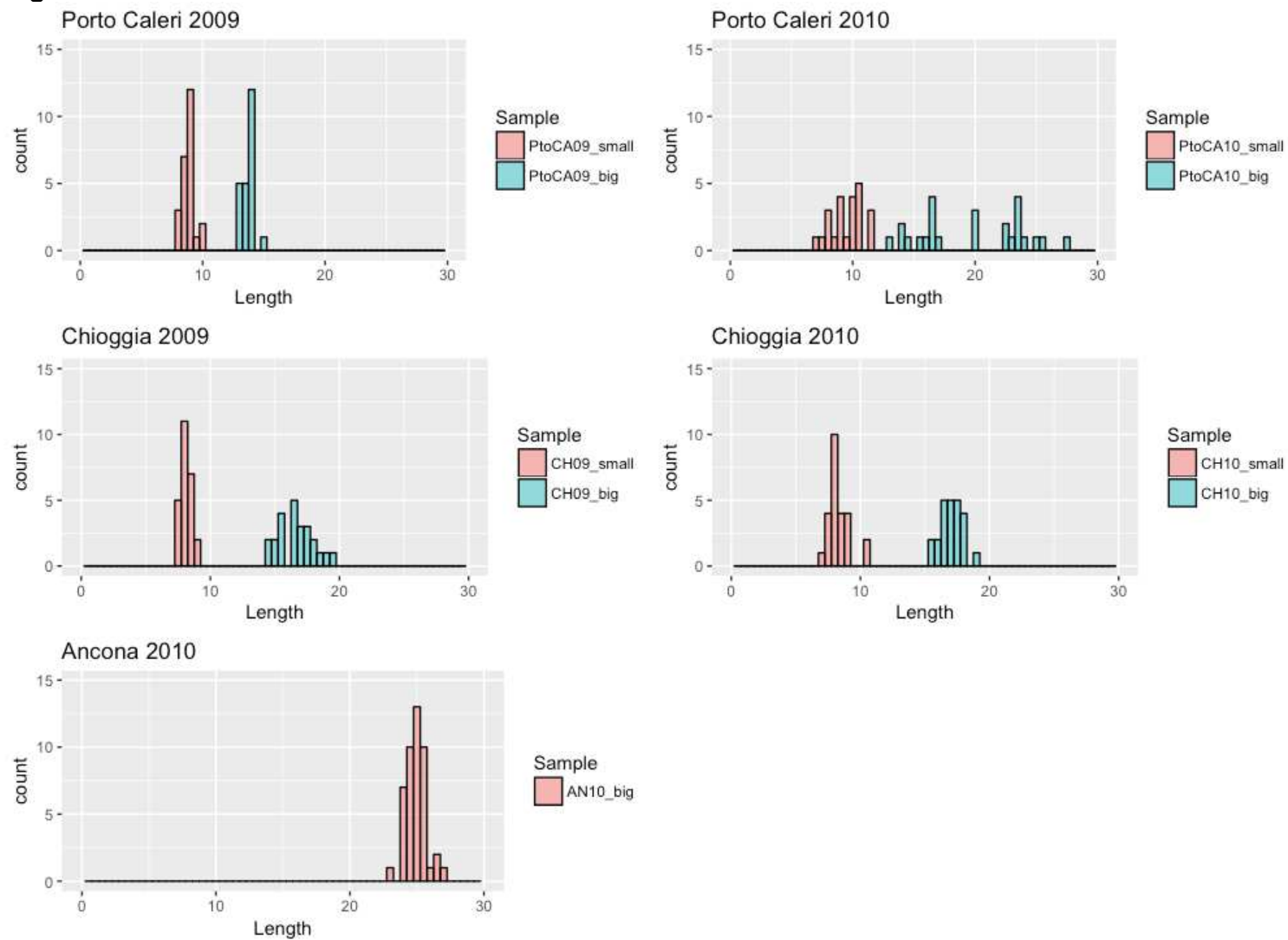
**Fig. S1a**



35

36  
37

**Fig. S1b**



38  
39

40 **Table S1. Loci genotyped in *Chamelea gallina* for this study.** The table reports: locus name (Locus), repeat content (Repeat, in  
 41 bp), primer sequences (5'-3', forward and reverse), fluorescent label, final concentration of each primer in the multiplex PCR reaction  
 42 mix (see note below table), size range (in bp) as found for the specimens analysed in this study, allelic range in number of repeats,  
 43 total number of alleles (total alleles, over the whole dataset of 239 individuals).  
 44

Locus	Repeat (bp)	Primer forward	Primer reverse	Fluorescent label	Primer final concentration ( $\mu\text{M}$ ) <sup>a</sup>	Size range (bp)	Allelic range (repeats)	Total alleles
260	2	TGGAGTTGACGATGTAACCCA	TGCTCATAACGGCAAAGTACA	FAM	0.2	84.02 - 97.18	1 - 8	7
1088	2	GCAACTTCCGACATAATGGGA	ATCGGAAGACGACGATGCATG	FAM	0.2	150.2 - 175.7	1 - 13	11
1243	2	GTAGAAGGAAGCCAGACTCAC	AGTTATGGAACAGGCATAGCA	VIC	0.6	88.56 - 130.49	1 - 25	11
9969	3	TGCATTCTCATTACTGTCCTCA	TGGAACCAAAATTCACAGGTGA	NED	0.2	123.38 - 142.22	1 - 7	7
10343	3	AGCAAATTGGCACTTGTGAGC	AACGTTACACCTGTGATTCTT	VIC	0.2	231.34 - 253.43	1 - 8	7
18241	3	ACTAGGTGTTATCCAGCCATCA	GAGTTGGGAGAAGGGTGACAC	PET	0.2	106.93 - 132.91	1 - 10	10
20447	2	GTAAGGCCCAAAGCGGTGTGT	TGCCCTTTAGCACATTGAGCT	PET	0.2	205.56 - 233	14 - 16	3
20467 <sup>b</sup>	4	GGGACCAGAACTATTTGGCT	CGTCCATCCTAACTGTAACACT	NED	0.4	90.17 - 114.56	1 - 7	7
26069	3	CTGAACAACGTCTGCATGAC	CGCCCAAAGAAGTCTTGATGA	VIC	0.4	163.1 - 197.93	1 - 10	9
33835	4	CCGACTATATCAGACGTTTCAGG	CATGATTATGGACCCCTTCAC	FAM	0.4	193.36 - 337.56	1 - 38	36
41629	2	TGCCTTTGTTCTGAAAGCAGT	ACCTTGAGCAAGTTAGCTGGCT	NED	0.6	228.17 - 290.58	1 - 31	16
41630	2	TGCTCCTTAGCATCACAGAAC	CGCTCTTACCAATGCATCCA	PET	0.2	155.78 - 210.98	1 - 32	14

45 <sup>a</sup> Reaction mix and thermal profile optimized for the amplification in multiplex of the 12 microsatellites. *Reaction mix*: Multiplex PCR amplifications were performed in 10  $\mu\text{L}$  total volume containing: 1X  
 46 QIAGEN Multiplex PCR Master mix (QIAGEN, HotStarTaq DNA Polymerase, Multiplex PCR Buffer, dNTPs Mix), 1  $\mu\text{L}$  primer mix (final concentration of each primer as in this table) and 100 ng of  
 47 template DNA. *Thermal profile*. A standard multiplex thermal profile for microsatellite loci was used according to the following scheme: (i) initial activation step: 95°C 15 min; (ii) 35 cycles: denaturation  
 48 94°C 30 s, annealing 57°C 90 s, extension 72°C 90 s; and (iii) final extension for 30 min at 60°C.

49 <sup>b</sup> Removed from dataset (see main text).  
 50

51 **Table S2. *Chamelea gallina* basic statistics for each locus (11 microsatellite loci in 9 samples).** The table reports for each  
 52 sample and for each locus: the number of individuals typed per locus (N, in the last column overall value is the mean number of  
 53 individuals typed), number of alleles observed per locus (A), percentage of total observed alleles per locus per sample (%), allelic  
 54 richness per locus (Ar, overall value is the mean allelic richness), observed and expected heterozygosity ( $H_o$  and  $H_e$ , overall value is  
 55 the mean heterozygosity across loci). All values reported in this table were calculated with the R (ver. 3.3.2) package diveRsity ver.  
 56 1.9.90 (Keenan et al., 2013). Samples acronyms as in Table 1 (main text).  
 57

Samples and basic statistics	Loci												
	PtoCA09_small	260	1088	1243	9969	10343	18241	20447	26069	33835	41629	41630	Overall
N	25	25	24	25	25	25	24	25	24	25	25	25	24.73
A	5	7	5	5	5	7	3	6	22	9	7		
%	71.43	63.64	45.45	71.43	71.43	70	100	66.67	61.11	56.25	50		66.13
Ar	4.75	5.93	4.31	4.67	4.49	6.13	2.98	4.9	16.63	6.6	5.11		6.1
$H_o$	0.76	0.4	0.17	0.52	0.64	0.88	0.21	0.48	0.92	0.52	0.32		0.53
$H_e$	0.57	0.64	0.54	0.59	0.6	0.69	0.41	0.51	0.92	0.66	0.29		0.58
<b>PtoC09_big</b>	<b>260</b>	<b>1088</b>	<b>1243</b>	<b>9969</b>	<b>10343</b>	<b>18241</b>	<b>20447</b>	<b>26069</b>	<b>33835</b>	<b>41629</b>	<b>41630</b>	<b>Overall</b>	
N	23	22	22	23	23	23	23	23	21	22	23		22.55
A	5	7	3	3	4	6	3	8	18	8	7		
%	71.43	63.64	27.27	42.86	57.14	60	100	88.89	50	50	50		60.11
Ar	4.56	6.08	2.87	2.63	3.84	5.23	2.99	6.6	13.97	6.44	5.35		5.52
$H_o$	0.74	0.27	0.14	0.39	0.52	0.78	0.3	0.43	0.48	0.27	0.35		0.43
$H_e$	0.65	0.62	0.39	0.32	0.54	0.64	0.53	0.53	0.92	0.7	0.38		0.57
<b>PtoCA10_small</b>	<b>260</b>	<b>1088</b>	<b>1243</b>	<b>9969</b>	<b>10343</b>	<b>18241</b>	<b>20447</b>	<b>26069</b>	<b>33835</b>	<b>41629</b>	<b>41630</b>	<b>Overall</b>	
N	23	23	20	23	23	23	23	23	22	20	23		22.36
A	4	6	2	5	5	7	3	4	14	8	3		
%	57.14	54.55	18.18	71.43	71.43	70	100	44.44	38.89	50	21.43		54.32
Ar	3.52	5.58	1.96	4.25	4.61	5.86	2.63	3.51	11.73	6.7	2.52		4.79
$H_o$	0.52	0.48	0.05	0.35	0.57	0.43	0.48	0.22	0.59	0.5	0.13		0.39
$H_e$	0.49	0.65	0.22	0.43	0.65	0.59	0.43	0.39	0.9	0.76	0.12		0.51



<b>PtoCA10_big</b>	<b>260</b>	<b>1088</b>	<b>1243</b>	<b>9969</b>	<b>10343</b>	<b>18241</b>	<b>20447</b>	<b>26069</b>	<b>33835</b>	<b>41629</b>	<b>41630</b>	<b>Overall</b>
<b>N</b>	25	24	22	25	25	25	24	25	22	22	24	23.91
<b>A</b>	4	4	4	4	4	5	3	4	19	7	2	
<b>%</b>	57.14	36.36	36.36	57.14	57.14	50	100	44.44	52.78	43.75	14.29	49.95
<b>Ar</b>	3.44	3.42	3.45	3.22	3.62	4.15	2.61	3.54	14.77	5.79	1.85	4.56
<b>H<sub>o</sub></b>	0.4	0.29	0.23	0.28	0.56	0.16	0.17	0.2	0.77	0.45	0.08	0.33
<b>H<sub>e</sub></b>	0.36	0.4	0.5	0.4	0.61	0.5	0.47	0.37	0.92	0.51	0.08	0.47
<b>CH09_small</b>	<b>260</b>	<b>1088</b>	<b>1243</b>	<b>9969</b>	<b>10343</b>	<b>18241</b>	<b>20447</b>	<b>26069</b>	<b>33835</b>	<b>41629</b>	<b>41630</b>	<b>Overall</b>
<b>N</b>	25	25	24	25	25	25	25	25	23	25	25	24.73
<b>A</b>	4	7	4	3	4	7	3	5	19	9	4	
<b>%</b>	57.14	63.64	36.36	42.86	57.14	70	100	55.56	52.78	56.25	28.57	56.39
<b>Ar</b>	3.6	5.68	3.71	2.86	3.64	5.72	2.93	4.08	14.57	7.5	3.38	5.24
<b>H<sub>o</sub></b>	0.6	0.4	0.17	0.4	0.8	0.44	0.56	0.32	0.7	0.56	0.24	0.47
<b>H<sub>e</sub></b>	0.48	0.59	0.59	0.33	0.61	0.69	0.48	0.42	0.93	0.76	0.22	0.56
<b>CH09_big</b>	<b>260</b>	<b>1088</b>	<b>1243</b>	<b>9969</b>	<b>10343</b>	<b>18241</b>	<b>20447</b>	<b>26069</b>	<b>33835</b>	<b>41629</b>	<b>41630</b>	<b>Overall</b>
<b>N</b>	24	24	21	24	24	23	21	24	20	18	21	22.18
<b>A</b>	5	5	4	4	5	7	3	5	16	6	6	
<b>%</b>	71.43	45.45	36.36	57.14	71.43	70	100	55.56	44.44	37.5	42.86	57.47
<b>Ar</b>	4.27	4.18	3.22	3.81	4.45	6.12	2.96	4.81	12.26	4.54	4.39	5.01
<b>H<sub>o</sub></b>	0.62	0.38	0.1	0.38	0.67	0.35	0.29	0.42	0.45	0.22	0.24	0.37
<b>H<sub>e</sub></b>	0.51	0.55	0.45	0.38	0.62	0.7	0.46	0.55	0.92	0.46	0.3	0.53
<b>CH10_small</b>	<b>260</b>	<b>1088</b>	<b>1243</b>	<b>9969</b>	<b>10343</b>	<b>18241</b>	<b>20447</b>	<b>26069</b>	<b>33835</b>	<b>41629</b>	<b>41630</b>	<b>Overall</b>
<b>N</b>	25	25	23	25	25	25	25	25	25	24	25	24.73
<b>A</b>	5	5	7	5	5	7	3	5	18	9	3	72
<b>%</b>	71.43	45.45	63.64	71.43	71.43	70	100	55.56	50	56.25	21.43	61.51
<b>Ar</b>	4.11	4.11	5.29	4.4	4.56	6.21	2.99	4.46	14.75	7.01	2.23	5.46
<b>H<sub>o</sub></b>	0.64	0.24	0.17	0.4	0.64	0.52	0.24	0.28	0.8	0.67	0.08	0.43

<b>H<sub>e</sub></b>	0.49	0.47	0.44	0.53	0.6	0.64	0.44	0.57	0.93	0.76	0.08	0.54
<b>CH10_big</b>	<b>260</b>	<b>1088</b>	<b>1243</b>	<b>9969</b>	<b>10343</b>	<b>18241</b>	<b>20447</b>	<b>26069</b>	<b>33835</b>	<b>41629</b>	<b>41630</b>	<b>Overall</b>
<b>N</b>	24	24	23	22	24	23	23	24	23	20	23	23
<b>A</b>	5	4	5	5	4	7	3	5	18	7	3	
<b>%</b>	71.43	36.36	45.45	71.43	57.14	70	100	55.56	50	43.75	21.43	56.6
<b>Ar</b>	4.82	3.74	4.2	3.86	3.95	5.86	2.87	4.59	14.32	6	2.23	5.15
<b>H<sub>o</sub></b>	0.83	0.21	0.35	0.36	0.62	0.65	0.35	0.58	0.7	0.5	0.09	0.48
<b>H<sub>e</sub></b>	0.68	0.39	0.48	0.43	0.62	0.65	0.36	0.6	0.92	0.69	0.08	0.54
<b>AN10_big</b>	<b>260</b>	<b>1088</b>	<b>1243</b>	<b>9969</b>	<b>10343</b>	<b>18241</b>	<b>20447</b>	<b>26069</b>	<b>33835</b>	<b>41629</b>	<b>41630</b>	<b>Overall</b>
<b>N</b>	45	45	44	44	42	40	44	45	39	37	44	42.64
<b>A</b>	7	6	4	5	6	7	3	4	23	8	9	
<b>%</b>	100	54.55	36.36	71.43	85.71	70	100	44.44	63.89	50	64.29	67.33
<b>Ar</b>	5.64	4.87	3.17	4.36	4.51	4.95	2.89	3.39	14.08	6.92	5.69	5.51
<b>H<sub>o</sub></b>	0.8	0.38	0.16	0.39	0.57	0.35	0.36	0.36	0.46	0.43	0.41	0.42
<b>H<sub>e</sub></b>	0.67	0.54	0.44	0.48	0.57	0.48	0.46	0.5	0.93	0.7	0.39	0.56

58  
59

60 **Table S3. Microsatellite allele frequencies for each sample of *Chamelea gallina* genotyped in this study.** The table reports  
61 single allele frequencies for each locus and each sample. Alleles are coded in number of repeats. See main text, Table 1 for  
62 explanation of samples acronyms.  
63

Locus	Allele	Samples								
		PtoCa09_small	PtoCa09_big	PtoCa10_small	PtoCa10_big	CH09_small	CH09_big	CH10_small	CH10_big	AN10_big
260	1	0.060	0.152	0.000	0.000	0.080	0.104	0.040	0.208	0.189
	3	0.060	0.065	0.000	0.000	0.000	0.021	0.020	0.000	0.033
	4	0.000	0.000	0.043	0.040	0.000	0.000	0.000	0.063	0.022
	5	0.600	0.522	0.652	0.780	0.680	0.667	0.660	0.479	0.500
	6	0.240	0.217	0.283	0.160	0.220	0.188	0.260	0.188	0.211
	7	0.040	0.043	0.022	0.020	0.020	0.021	0.020	0.063	0.033
	8	0.000	0.000	0.000	0.000	0.000	0.000	0.000	0.000	0.011
1088	1	0.000	0.000	0.000	0.021	0.000	0.000	0.000	0.000	0.000
	3	0.560	0.591	0.543	0.750	0.600	0.604	0.700	0.771	0.656
	4	0.040	0.114	0.087	0.042	0.140	0.063	0.040	0.042	0.133
	5	0.060	0.023	0.000	0.000	0.020	0.021	0.000	0.083	0.067
	6	0.000	0.068	0.000	0.000	0.040	0.021	0.000	0.000	0.000
	7	0.180	0.091	0.174	0.188	0.160	0.292	0.180	0.104	0.111
	8	0.000	0.091	0.065	0.000	0.000	0.000	0.000	0.000	0.011
	9	0.080	0.023	0.109	0.000	0.020	0.000	0.040	0.000	0.022
	10	0.060	0.000	0.022	0.000	0.020	0.000	0.000	0.000	0.000
	11	0.000	0.000	0.000	0.000	0.000	0.000	0.040	0.000	0.000
13	0.020	0.000	0.000	0.000	0.000	0.000	0.000	0.000	0.000	
1243	1	0.000	0.000	0.000	0.000	0.000	0.000	0.000	0.022	0.000
	8	0.042	0.045	0.000	0.000	0.000	0.000	0.000	0.109	0.011
	9	0.042	0.000	0.000	0.000	0.000	0.000	0.000	0.000	0.000
	12	0.625	0.750	0.875	0.659	0.521	0.714	0.739	0.696	0.716
	13	0.250	0.205	0.125	0.250	0.354	0.190	0.109	0.130	0.216
	14	0.000	0.000	0.000	0.068	0.083	0.048	0.022	0.043	0.000
	15	0.000	0.000	0.000	0.000	0.042	0.000	0.065	0.000	0.057

	16	0.000	0.000	0.000	0.000	0.000	0.048	0.022	0.000	0.000
	18	0.042	0.000	0.000	0.023	0.000	0.000	0.000	0.000	0.000
	24	0.000	0.000	0.000	0.000	0.000	0.000	0.022	0.000	0.000
	25	0.000	0.000	0.000	0.000	0.000	0.000	0.022	0.000	0.000
9969	1	0.000	0.000	0.000	0.000	0.000	0.000	0.000	0.023	0.000
	2	0.040	0.022	0.065	0.000	0.000	0.042	0.020	0.000	0.057
	3	0.040	0.000	0.022	0.020	0.040	0.063	0.080	0.023	0.023
	4	0.300	0.174	0.152	0.220	0.160	0.125	0.220	0.205	0.193
	5	0.560	0.804	0.739	0.740	0.800	0.771	0.640	0.727	0.693
	6	0.060	0.000	0.022	0.020	0.000	0.000	0.040	0.000	0.034
	7	0.000	0.000	0.000	0.000	0.000	0.000	0.000	0.023	0.000
10343	1	0.000	0.000	0.000	0.000	0.000	0.000	0.000	0.000	0.012
	3	0.000	0.000	0.022	0.000	0.000	0.021	0.020	0.000	0.012
	4	0.060	0.065	0.065	0.120	0.120	0.042	0.120	0.125	0.060
	5	0.320	0.283	0.326	0.360	0.400	0.354	0.220	0.292	0.298
	6	0.540	0.609	0.478	0.500	0.460	0.500	0.580	0.521	0.583
	7	0.060	0.043	0.109	0.020	0.020	0.083	0.060	0.063	0.036
	8	0.020	0.000	0.000	0.000	0.000	0.000	0.000	0.000	0.000
18241	1	0.000	0.000	0.000	0.000	0.000	0.000	0.000	0.022	0.000
	2	0.000	0.000	0.000	0.000	0.000	0.000	0.000	0.022	0.0125
	3	0.100	0.217	0.022	0.000	0.020	0.022	0.000	0.152	0.025
	4	0.180	0.022	0.130	0.100	0.100	0.087	0.080	0.087	0.025
	5	0.120	0.130	0.109	0.160	0.220	0.152	0.140	0.152	0.150
	6	0.500	0.543	0.609	0.680	0.480	0.500	0.560	0.543	0.700
	7	0.060	0.065	0.087	0.040	0.120	0.087	0.120	0.000	0.0625
	8	0.020	0.022	0.000	0.000	0.020	0.043	0.020	0.022	0.000
	9	0.020	0.000	0.022	0.020	0.040	0.109	0.040	0.000	0.025
	10	0.000	0.000	0.022	0.000	0.000	0.000	0.040	0.000	0.000
20447	14	0.146	0.239	0.239	0.292	0.280	0.238	0.120	0.152	0.227
	15	0.750	0.630	0.717	0.667	0.660	0.690	0.720	0.783	0.693
	16	0.104	0.130	0.043	0.042	0.060	0.071	0.160	0.065	0.080

26069	1	0.000	0.043	0.022	0.020	0.000	0.104	0.040	0.021	0.000
	2	0.040	0.043	0.000	0.000	0.020	0.042	0.000	0.125	0.000
	3	0.000	0.000	0.000	0.000	0.020	0.000	0.040	0.000	0.000
	4	0.000	0.022	0.000	0.000	0.000	0.000	0.000	0.000	0.000
	5	0.220	0.087	0.174	0.140	0.180	0.146	0.120	0.188	0.189
	6	0.660	0.674	0.761	0.780	0.740	0.646	0.620	0.583	0.667
	7	0.020	0.087	0.043	0.060	0.040	0.063	0.180	0.083	0.133
	8	0.040	0.022	0.000	0.000	0.000	0.000	0.000	0.000	0.011
	10	0.020	0.022	0.000	0.000	0.000	0.000	0.000	0.000	0.000
	33835	1	0.021	0.000	0.000	0.000	0.000	0.000	0.000	0.000
4		0.021	0.000	0.023	0.023	0.000	0.000	0.020	0.000	0.013
5		0.021	0.048	0.000	0.023	0.022	0.000	0.000	0.065	0.013
6		0.000	0.048	0.045	0.091	0.022	0.025	0.020	0.043	0.026
7		0.021	0.000	0.000	0.023	0.022	0.000	0.080	0.000	0.013
8		0.063	0.048	0.182	0.091	0.065	0.000	0.040	0.087	0.103
9		0.125	0.048	0.045	0.023	0.152	0.125	0.120	0.130	0.115
10		0.042	0.095	0.091	0.045	0.043	0.100	0.080	0.087	0.128
11		0.083	0.024	0.114	0.045	0.043	0.100	0.080	0.022	0.077
12		0.021	0.048	0.091	0.068	0.109	0.050	0.060	0.087	0.064
13		0.167	0.000	0.000	0.068	0.043	0.025	0.060	0.065	0.051
14		0.042	0.048	0.068	0.159	0.065	0.075	0.080	0.022	0.038
15		0.042	0.024	0.000	0.045	0.043	0.000	0.080	0.022	0.000
16		0.042	0.119	0.091	0.114	0.087	0.100	0.100	0.109	0.064
17		0.042	0.024	0.000	0.023	0.065	0.100	0.060	0.065	0.013
18		0.083	0.143	0.114	0.045	0.043	0.050	0.040	0.065	0.077
19		0.021	0.048	0.045	0.023	0.000	0.000	0.000	0.022	0.077
20		0.000	0.024	0.000	0.045	0.000	0.000	0.000	0.000	0.000
21		0.021	0.000	0.000	0.023	0.022	0.050	0.020	0.000	0.000
22		0.021	0.024	0.000	0.000	0.000	0.000	0.000	0.022	0.013
23		0.042	0.000	0.023	0.000	0.043	0.000	0.000	0.000	0.013
24		0.021	0.000	0.000	0.000	0.043	0.025	0.000	0.000	0.000

	25	0.000	0.000	0.023	0.000	0.043	0.050	0.020	0.000	0.000
	26	0.021	0.000	0.000	0.000	0.000	0.050	0.000	0.000	0.013
	27	0.000	0.000	0.000	0.000	0.000	0.000	0.020	0.000	0.026
	28	0.000	0.000	0.000	0.000	0.000	0.050	0.000	0.000	0.000
	29	0.000	0.000	0.000	0.000	0.000	0.000	0.000	0.000	0.013
	30	0.000	0.095	0.000	0.000	0.000	0.000	0.000	0.000	0.026
	31	0.000	0.000	0.000	0.023	0.022	0.000	0.000	0.022	0.000
	32	0.000	0.048	0.000	0.000	0.000	0.025	0.000	0.043	0.000
	33	0.000	0.000	0.045	0.000	0.000	0.000	0.000	0.022	0.000
	34	0.000	0.048	0.000	0.000	0.000	0.000	0.000	0.000	0.000
	35	0.000	0.000	0.000	0.000	0.000	0.000	0.000	0.000	0.013
	36	0.021	0.000	0.000	0.000	0.000	0.000	0.000	0.000	0.000
	37	0.000	0.000	0.000	0.000	0.000	0.000	0.020	0.000	0.000
	38	0.000	0.000	0.000	0.000	0.000	0.000	0.000	0.000	0.013
<b>41629</b>	1	0.000	0.000	0.000	0.000	0.000	0.028	0.000	0.000	0.000
	9	0.000	0.000	0.000	0.000	0.040	0.000	0.000	0.000	0.000
	15	0.020	0.000	0.000	0.023	0.000	0.000	0.000	0.000	0.000
	16	0.020	0.000	0.000	0.000	0.000	0.000	0.000	0.000	0.000
	18	0.000	0.000	0.025	0.000	0.000	0.000	0.000	0.050	0.000
	19	0.020	0.045	0.025	0.000	0.060	0.000	0.021	0.000	0.054
	20	0.460	0.500	0.375	0.682	0.420	0.722	0.375	0.500	0.500
	21	0.340	0.136	0.175	0.068	0.140	0.000	0.229	0.125	0.149
	22	0.020	0.045	0.050	0.000	0.040	0.028	0.083	0.100	0.068
	23	0.000	0.091	0.000	0.000	0.040	0.000	0.000	0.000	0.000
	24	0.080	0.136	0.225	0.091	0.080	0.111	0.188	0.175	0.108
	25	0.000	0.023	0.000	0.023	0.000	0.028	0.021	0.000	0.027
	27	0.000	0.023	0.000	0.000	0.000	0.000	0.000	0.000	0.000
	28	0.020	0.000	0.100	0.068	0.160	0.083	0.042	0.025	0.068
30	0.020	0.000	0.025	0.045	0.020	0.000	0.021	0.025	0.027	
31	0.000	0.000	0.000	0.000	0.000	0.000	0.021	0.000	0.000	
<b>41630</b>	1	0.000	0.043	0.000	0.000	0.000	0.000	0.000	0.000	0.000

4	0.000	0.000	0.000	0.000	0.000	0.048	0.000	0.000	0.000
7	0.000	0.000	0.000	0.000	0.000	0.024	0.000	0.000	0.000
9	0.020	0.000	0.000	0.000	0.000	0.000	0.000	0.000	0.000
10	0.040	0.000	0.043	0.042	0.060	0.048	0.020	0.000	0.091
12	0.000	0.000	0.000	0.000	0.000	0.000	0.000	0.000	0.023
13	0.000	0.022	0.000	0.000	0.000	0.024	0.000	0.000	0.034
14	0.840	0.783	0.935	0.958	0.880	0.833	0.960	0.957	0.773
15	0.020	0.000	0.000	0.000	0.040	0.024	0.020	0.000	0.011
16	0.040	0.043	0.000	0.000	0.000	0.000	0.000	0.000	0.011
20	0.020	0.022	0.022	0.000	0.000	0.000	0.000	0.000	0.000
28	0.020	0.065	0.000	0.000	0.020	0.000	0.000	0.022	0.034
29	0.000	0.022	0.000	0.000	0.000	0.000	0.000	0.022	0.011
32	0.000	0.000	0.000	0.000	0.000	0.000	0.000	0.000	0.011

64  
65

**Table S4. *Chamelea gallina* Hardy–Weinberg equilibrium probabilities for 11 microsatellite loci in 9 samples for the original and corrected dataset (corrected with Micro-Checker ver. 2.2.3 (van Oosterhout et al., 2004)).** Probabilities of deviation from Hardy–Weinberg equilibrium were calculated with the R package diveRsity ver. 1.9.90 (Keenan et al., 2013) and are presented at each locus for each sample (acronyms in the first column). Values in bold indicate significant HWE deviations after SGoF+ correction (Carvajal-Rodriguez and de Uña-Alvarez 2011). Samples acronyms as in Table 1 (main text).

Samples	Dataset	Loci											
		260	1088	1243	9969	10343	18241	20447	26069	33835	41629	41630	Overall
PtoCA09_small	Original	0.239316	<b>0.013015</b>	<b>P&lt; 0.0001</b>	0.287655	0.167110	0.283264	<b>0.016474</b>	0.601307	0.261400	0.149257	1.000000	<b>P&lt; 0.0001</b>
	Corrected	0.239316	<b>0.048100</b>	<b>0.000219</b>	0.287655	0.167110	0.283264	0.687523	0.601307	0.268600	0.149257	1.000000	<b>0.005000</b>
PtoCA09_big	Original	0.024764	<b>0.000006</b>	<b>0.000456</b>	0.645546	0.198439	0.027265	0.023627	0.258766	<b>P&lt; 0.0001</b>	<b>0.000048</b>	0.289723	<b>P&lt; 0.0001</b>
	Corrected	0.024764	<b>0.002360</b>	0.053168	0.645546	0.198439	0.027265	0.750243	0.258766	<b>P&lt; 0.0001</b>	<b>0.041300</b>	0.289723	<b>P&lt; 0.0001</b>
PtoCA10_small	Original	0.516145	0.045125	<b>0.010395</b>	0.536746	0.843019	0.451261	<b>0.005548</b>	0.030041	<b>0.000300</b>	0.131641	1.000000	<b>P&lt; 0.0001</b>
	Corrected	0.516145	0.098840	0.160590	0.536746	0.843019	0.346987	<b>0.005548</b>	0.181963	<b>0.002500</b>	0.746400	1.000000	<b>0.012000</b>
PtoCA10_big	Original	0.202838	0.127157	<b>0.007402</b>	0.419540	0.386759	<b>0.000073</b>	<b>0.000230</b>	<b>0.007569</b>	0.023300	0.115367	1.000000	<b>P&lt; 0.0001</b>
	Corrected	0.202838	0.127157	0.271339	0.419540	0.386759	0.073162	<b>0.024198</b>	0.100258	<b>0.021700</b>	0.115367	1.000000	<b>0.005000</b>
CH09_small	Original	0.069330	0.156477	<b>0.000006</b>	0.614252	0.047194	<b>0.010503</b>	0.836244	0.217435	<b>0.002400</b>	0.033800	1.000000	<b>P&lt; 0.0001</b>
	Corrected	0.069330	0.888107	<b>0.044104</b>	0.614252	0.047194	<b>0.015300</b>	0.836244	0.217435	<b>0.003000</b>	0.070600	1.000000	<b>0.001000</b>
CH09_big	Original	0.175875	0.272878	<b>0.000055</b>	0.854555	0.092147	<b>0.005430</b>	<b>0.002137</b>	<b>0.003187</b>	<b>0.000300</b>	<b>0.011761</b>	0.154066	<b>P&lt; 0.0001</b>
	Corrected	0.175875	0.272878	<b>0.001820</b>	0.854555	0.092147	0.106100	<b>0.002137</b>	<b>0.003187</b>	0.073000	<b>0.035967</b>	0.154066	<b>P&lt; 0.0001</b>
CH2010_small	Original	0.144095	<b>0.001099</b>	<b>0.000030</b>	0.094280	0.218290	0.168596	<b>0.006608</b>	<b>0.000005</b>	0.060300	0.342325	1.000000	<b>P&lt; 0.0001</b>
	Corrected	0.144095	<b>0.011010</b>	<b>0.001600</b>	0.094280	0.218290	0.168596	0.529289	<b>0.000969</b>	0.060900	0.342325	1.000000	<b>P&lt; 0.0001</b>
CH10_big	Original	<b>0.000931</b>	<b>0.002459</b>	<b>0.009099</b>	0.181670	0.370490	0.054144	0.059679	0.244275	<b>P&lt; 0.0001</b>	<b>0.007152</b>	1.000000	<b>P&lt; 0.0001</b>
	Corrected	<b>0.000931</b>	<b>0.005239</b>	<b>0.009099</b>	0.181670	0.370490	0.054144	0.059679	0.244275	<b>P&lt; 0.0001</b>	<b>0.017917</b>	1.000000	<b>P&lt; 0.0001</b>
AN10_big	Original	<b>0.000518</b>	0.024879	<b>0.000002</b>	0.232005	0.812437	<b>0.014069</b>	<b>0.000154</b>	<b>0.013634</b>	<b>P&lt; 0.0001</b>	<b>0.006500</b>	0.590994	<b>P&lt; 0.0001</b>
	Corrected	<b>0.000518</b>	0.061800	<b>0.048863</b>	0.232005	0.812437	0.050400	<b>0.000154</b>	0.579795	<b>0.031700</b>	0.238800	0.590994	<b>P&lt; 0.0001</b>

66  
67  
68  
69  
70  
7172  
73



74  
75  
76  
77  
78

**Table S5. *Chamelea gallina* inbreeding values ( $F_{IS}$ ) for 11 microsatellite loci in 9 samples for the original (O) and corrected (C) dataset (corrected with Micro-Checker ver. 2.2.3, (van Oosterhout et al., 2004)).  $F_{IS}$  estimates and their 95% confidence interval (CI) were calculated with the R package diveRsity ver. 1.9.90 (Keenan et al., 2013) and are presented at each locus for each sample (acronyms in the first column, as in Table 1, main text).**

Samples	Data set	Loci											Overall
		260	1088	1243	9969	10343	18241	20447	26069	33835	41629	41630	
PtoCA09_small	O	-0.325 [-0.4867, -0.1651]	0.3734 [0.068, 0.6648]	0.6923 [0.4201, 0.9262]	0.118 [-0.1792, 0.4276]	-0.0695 [-0.3188, 0.1961]	-0.2776 [-0.3961, -0.1473]	0.4861 [0.0643, 0.842]	0.0625 [-0.2166, 0.3834]	0.0075 [-0.1044, 0.1409]	0.2169 [-0.0272, 0.4738]	-0.105 [-0.1816, 0.0415]	0.0955 [0.0051, 0.1857]
	C	-0.325 [-0.4864, -0.1653]	0.0731 [-0.1808, 0.3296]	-0.0087 [-0.2691, 0.2578]	0.118 [-0.1745, 0.4216]	-0.0695 [-0.3232, 0.1907]	-0.2776 [-0.3995, -0.1468]	-0.0526 [-0.2963, 0.2132]	0.0625 [-0.2138, 0.3704]	0.0075 [-0.1036, 0.1413]	0.2169 [-0.03, 0.4725]	-0.105 [-0.1814, 0.0414]	-0.0263 [-0.113, 0.0593]
PtoCA09_big	O	-0.135 [-0.3983, 0.1578]	0.557 [0.2978, 0.8187]	0.6535 [0.2115, 1.0233]	-0.2141 [-0.3701, -0.0933]	0.04 [-0.2549, 0.3562]	-0.2321 [-0.4649, 0.0265]	0.424 [0.0279, 0.7615]	0.1727 [-0.0691, 0.4454]	0.4847 [0.2539, 0.7105]	0.61 [0.3167, 0.8687]	0.08 [-0.1807, 0.4654]	0.2472 [0.1466, 0.3469]
	C	-0.135 [-0.3979, 0.1557]	0.0154 [-0.2091, 0.2432]	-0.0388 [-0.353, 0.2743]	-0.2141 [-0.3578, -0.0886]	0.04 [-0.2485, 0.3511]	-0.2321 [-0.4638, 0.0251]	-0.0073 [-0.2678, 0.2703]	0.1727 [-0.0753, 0.4523]	0.3876 [0.1632, 0.6177]	0.008 [-0.2361, 0.2516]	0.08 [-0.1772, 0.4817]	0.028 [-0.0842, 0.1268]
PtoCA10_small	O	-0.0595 [-0.3489, 0.2524]	0.2645 [-0.0344, 0.5632]	0.7714 [-0.0043, 1.0483]	0.1822 [-0.1626, 0.5531]	0.1283 [-0.1632, 0.4297]	0.2652 [-0.0828, 0.6085]	-0.122 [-0.4567, 0.2944]	0.4404 [0.0717, 0.7961]	0.3448 [0.1163, 0.5803]	0.3453 [0.0518, 0.6362]	-0.0534 [-0.1205, -0.0129]	0.2337 [0.1175, 0.3375]
	C	-0.0595 [-0.3387, 0.2642]	0.1459 [-0.1229, 0.4215]	-0.0336 [-0.3778, 0.3467]	0.1822 [-0.1698, 0.5673]	0.1283 [-0.1668, 0.4376]	0.0813 [-0.2046, 0.376]	-0.122 [-0.4569, 0.285]	-0.0645 [-0.269, 0.1293]	0.3 [0.0766, 0.529]	0.1331 [-0.1183, 0.393]	-0.0534 [-0.1214, -0.0138]	0.089 [-0.0321, 0.2043]
PtoCA10_big	O	-0.0989 [-0.277, 0.1111]	0.2711 [-0.1013, 0.6456]	0.5436 [0.1492, 0.872]	0.3056 [-0.1134, 0.6984]	0.0753 [-0.2124, 0.3703]	0.68 [0.3259, 0.9415]	0.6444 [0.2559, 0.9349]	0.4565 [0.09, 0.8081]	0.1614 [-0.0052, 0.3503]	0.1165 [-0.1539, 0.4163]	-0.0435 [-0.1086, -0.0127]	0.2981 [0.1855, 0.3995]
	C	-0.0989 [-0.2786, 0.1139]	0.2711 [-0.1039, 0.6549]	-0.0329 [-0.3113, 0.2647]	0.3056 [-0.11, 0.6892]	0.0753 [-0.2174, 0.3788]	-0.0601 [-0.3345, 0.2128]	-0.0866 [-0.3672, 0.2115]	0.0085 [-0.2421, 0.265]	0.1614 [-0.0097, 0.3484]	0.1165 [-0.1545, 0.4209]	-0.0435 [-0.1094, -0.0135]	0.0569 [-0.0559, 0.1634]
CH09_sm all	O	-0.2438 [-0.4266, -0.0572]	0.3243 [0.023, 0.6197]	0.7197 [0.4459, 0.941]	-0.2019 [-0.3456, -0.0946]	-0.3038 [-0.5442, -0.0604]	0.3664 [0.0402, 0.6635]	-0.1609 [-0.4292, 0.152]	0.2337 [-0.1134, 0.5844]	0.2497 [0.0459, 0.4677]	0.2662 [-0.0095, 0.5307]	-0.0909 [-0.1735, -0.0224]	0.1532 [0.0834, 0.2196]
	C	-0.2438 [-0.4228, -0.0566]	0.0196 [-0.2001, 0.2609]	-0.1014 [-0.3456, 0.1497]	-0.2088 [-0.35, -0.1024]	-0.3038 [-0.5428, -0.0651]	0.1127 [-0.1646, 0.3801]	-0.1609 [-0.4222, 0.1456]	0.2337 [-0.1141, 0.5856]	0.2395 [0.0476, 0.4447]	0.1935 [-0.0672, 0.4515]	-0.0909 [-0.1732, -0.0221]	0.005 [-0.1028, 0.1191]
CH09_big	O	-0.2287 [-0.3939, -0.0533]	0.3121 [0.0063, 0.6276]	0.7879 [0.4012, 1.0188]	0.0248 [-0.2153, 0.3929]	-0.0832 [-0.3783, 0.2148]	0.5014 [0.2179, 0.7705]	0.3808 [0.0606, 0.7155]	0.2357 [-0.106, 0.557]	0.5115 [0.2653, 0.7465]	0.5135 [-0.0499, 0.9096]	0.2045 [-0.1143, 0.6922]	0.3037 [0.2049, 0.3949]
	C	-0.2287 [-0.3937, -0.0509]	0.3121 [0.0019, 0.6255]	-0.0262 [-0.3865, 0.3206]	0.0248 [-0.2123, 0.3959]	-0.0832 [-0.3725, 0.21]	0.0624 [-0.1822, 0.3105]	0.3808 [0.0604, 0.7181]	0.2357 [-0.0988, 0.5525]	0.2463 [0.0158, 0.4745]	0.192 [-0.2387, 0.5717]	0.2045 [-0.1154, 0.6869]	0.1194 [-0.0053, 0.2353]
CH2010_small	O	-0.2945 [-0.5008, -0.0988]	0.4924 [0.1166, 0.8199]	0.6009 [0.2721, 0.9013]	0.2504 [-0.0752, 0.5686]	-0.0724 [-0.2639, 0.1159]	0.1905 [-0.0752, 0.4706]	0.4565 [0.0405, 0.8166]	0.505 [0.1952, 0.7868]	0.1372 [-0.0218, 0.3122]	0.1243 [-0.1234, 0.3847]	-0.0309 [-0.0816, 0.0103]	0.2132 [0.127, 0.2941]
	C	-0.2945	0.0062	0.0543	0.2504	-0.0724	0.1905	-0.0681	0.0857	0.1372	0.1243	-0.0309	0.0521

		[-0.5019, -0.1]	[-0.2767, 0.2991]	[-0.2576, 0.3544]	[-0.0729, 0.5754]	[-0.2582, 0.1129]	[-0.0752, 0.4739]	[-0.2877, 0.19]	[-0.1809, 0.3474]	[-0.0244, 0.3133]	[-0.1323, 0.3829]	[-0.0811, -0.0098]	[-0.0368, 0.1325]
<b>CH10_big</b>	<b>O</b>	-0.2183 [-0.4645, 0.0483]	0.4607 [-0.0497, 0.8502]	0.2827 [-0.1426, 0.6609]	0.1498 [-0.1571, 0.4942]	-0.0014 [-0.2664, 0.2754]	-0.0044 [-0.2793, 0.2844]	0.0341 [-0.2818, 0.4594]	0.0303 [-0.2282, 0.3077]	0.2474 [0.0513, 0.4595]	0.2754 [-0.0426, 0.5818]	-0.0337 [-0.0876, -0.01]	0.1137 [0.0236, 0.2009]
	<b>C</b>	-0.2183 [-0.465, 0.0465]	0.1206 [-0.2379, 0.4693]	0.2827 [-0.1354, 0.6589]	0.1498 [-0.1589, 0.4974]	-0.0014 [-0.2711, 0.2704]	-0.0044 [-0.2739, 0.2818]	0.0341 [-0.276, 0.4607]	0.0303 [-0.2262, 0.3084]	0.2474 [0.0506, 0.4564]	0.1376 [-0.1615, 0.4264]	-0.0337 [-0.0887, -0.0095]	0.0774 [-0.0192, 0.171]
<b>AN10_big</b>	<b>O</b>	-0.1996 [-0.3369, -0.056]	0.294 [0.0658, 0.5228]	0.6364 [0.3615, 0.8694]	0.1905 [-0.0483, 0.4372]	-0.0095 [-0.211, 0.2027]	0.2732 [-0.0022, 0.5398]	0.2121 [-0.0923, 0.496]	0.2917 [0.018, 0.5607]	0.5016 [0.3258, 0.6692]	0.3846 [0.1826, 0.59]	-0.0455 [-0.1961, 0.187]	0.2409 [0.1761, 0.3048]
	<b>C</b>	-0.1996 [-0.3401, -0.0556]	0.0378 [-0.142, 0.2275]	-0.055 [-0.2571, 0.1532]	0.1905 [-0.0424, 0.4334]	-0.0095 [-0.217, 0.2063]	-0.0159 [-0.1843, 0.1705]	0.2121 [-0.0971, 0.504]	0.0339 [-0.1661, 0.2483]	0.2063 [0.0544, 0.3639]	0.0629 [-0.0988, 0.2321]	-0.0455 [-0.1956, 0.1839]	0.0407 [-0.0247, 0.1071]

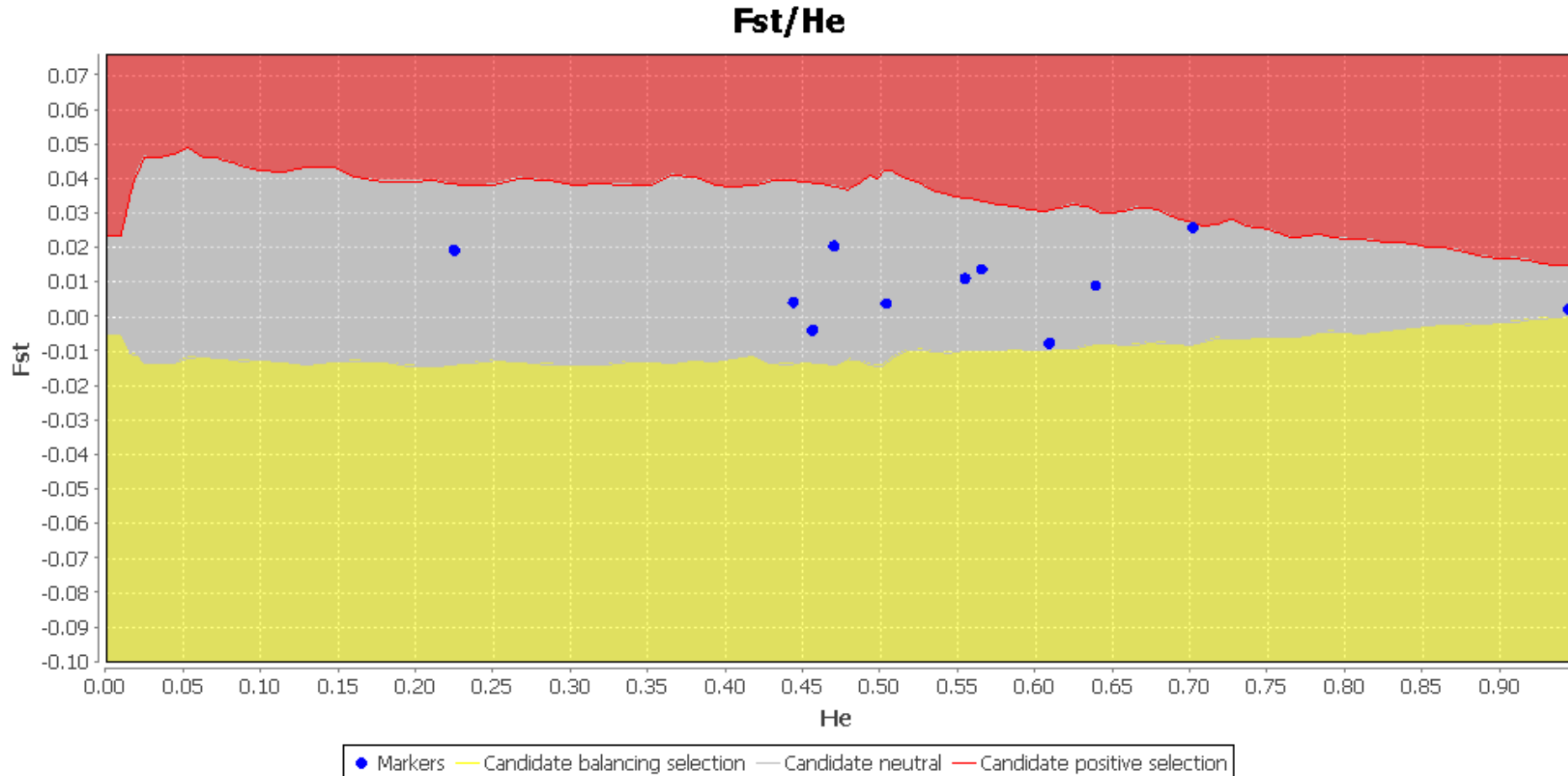
79  
80

81 **Table S6. Estimation of loci under selection for *Chamelea gallina* over all samples.** The table reports p-values obtained with  
82 LOSITAN ver. 1.0.0 (Antao et al., 2008) after 1,000,000 simulations, imposing the stepwise mutation model and subsample size of 45  
83 individuals following Agostini et al., (2013). None of the estimates fall outside the 99% confidence interval (CI) of the  $F_{ST}$  vs.  $H_{Exp}$   
84 (expected heterozygosity) expected distribution.  
85

Locus	P-value
260	0.726973
1088	0.630626
1243	0.838501
9969	0.451706
10343	0.062326
18241	0.579058
20447	0.210198
26069	0.419716
33835	0.130647
41629	0.967692
41630	0.815641

86  
87  
88

89 **Figure S2. Estimation of loci under selection for *Chamelea gallina* over all samples.** The graphic reports results from LOSITAN  
 90 ver. 1.0.0 (Antao et al., 2008) after 1,000,000 simulations, imposing the stepwise mutation model and subsample size of 45 individuals  
 91 following Agostini et al., (2013). Shown in grey (centre) is the 99 % confidence interval (CI) of the  $F_{ST}$  vs.  $H_{Exp}$  (expected  
 92 heterozygosity) expected distribution. Loci outside this interval are potential candidates for being subject to directional selection (red,  
 93 top) or balancing selection (yellow, bottom). None of the loci used in this study fall outside the 99% (CI).  
 94



95  
96

97  
 98  
 99  
 100  
 101  
 102  
 103  
 104  
 105  
 106  
 107  
 108  
 109  
 110  
 111  
 112  
 113  
 114  
 115  
 116  
 117  
 118

**Table S7a, b, c. Relatedness within *Chamelea gallina* samples based on seven different relatedness estimators.** The R package related ver. 1.0 (Pew et al., 2015; Wang 2011) allows for an explicit comparison across seven different relatedness estimators: five moment estimators (Li et al., 1993; Lynch and Ritland 1999; Queller and Goodnight 1989; Ritland 1996; Wang 2001) and two likelihood-based estimators (the dyadic likelihood estimator – dyadml, Milligan 2003; Schneider et al., 2016; and the triadic likelihood estimator – trioml, Wang 2007). To identify the most appropriate of these seven estimators, we first generated a dataset of pairs of individuals of known relatedness (100 parent-offspring pairs, 100 full-sib pairs, 100 half-sib pairs, and 100 unrelated pairs, with the function *familysim*) using the allele frequencies observed in our dataset, a genotyping error rate of 5% and considering inbreeding (Schneider et al., 2016). We then estimated the relatedness within this dataset using all estimators (with the function *coancestry*). For each estimator, a correlation coefficient between observed and expected values was calculated. The method associated with the highest correlation coefficient was selected for subsequent analysis. We calculated the average within-group relatedness and the associated p-values by comparing them with a distribution of expected values (generated by randomly shuffling individuals between category groups for 1,000 permutations and keeping size constant, with the function *grouprel*, (Pew et al., 2015)). If the observed mean relatedness was greater than that of the permuted data ( $P > 0.95$ ), then the null hypothesis, that the mean within-category relatedness is random, was rejected (Schneider et al., 2016). The table a) reports correlation coefficients between observed and expected values for each method. Trioml was selected as the method associated with the highest correlation coefficient. Table b) reports relatedness values obtained for all seven methods. Table c) reports p-values associated with relatedness estimates. In bold: significantly higher relatedness than expected by random combination of individuals after correction for multiple tests with SGoF+ (Carvajal-Rodriguez and de Uña-Alvarez 2011), negative relatedness values indicate lower relatedness than expected by random combination.

**Table S7a**

	Method						
	dyadml	lynchli	lynchrd	quellergt	ritland	trioml	wang
<b>Correlation coefficient</b>	0.810853	0.734128	0.723722	0.747724	0.46127	0.811714	0.763571

119  
 120  
 121

**Table S7b**

Samples	Relatedness values per each method						
	dyadml	lynchli	lynchrd	quellergt	ritland	trioml	wang

<b>PtoCA09_small</b>	0.110119	-0.14043	0.000274	-0.06258	-0.00103	0.085082	-0.03971
<b>PtoCA09_big</b>	0.129425	-0.14609	0.003771	-0.03169	0.001731	0.102129	-0.10092
<b>PtoCA10_small</b>	0.153239	-0.03165	0.005744	0.052422	0.000168	0.112261	-0.0418
<b>PtoCA10_big</b>	0.24568	0.028307	0.015962	0.128678	0.005515	0.203289	-0.03804
<b>CH09_small</b>	0.138351	-0.06138	-0.00629	-0.01282	-0.00183	0.104825	-0.05057
<b>CH09_big</b>	0.16062	-0.12216	-0.00109	-0.00471	-0.00573	0.126278	-0.11743
<b>CH2010_small</b>	0.12899	-0.12083	-0.00202	0.006886	-0.0017	0.097195	-0.0505
<b>CH10_big</b>	0.141469	-0.05433	0.00697	0.000951	0.010229	0.108259	-0.04098
<b>AN10_big</b>	0.159701	-0.12306	-0.00234	-0.01445	-0.00249	0.127173	-0.10245
<b>Average</b>	0.151955	-0.08574	0.002332	0.006965	0.000542	0.118499	-0.06471

122  
123  
124  
125  
126

**Table S7c**

Samples	P-values						
	dyadml	lynchli	lynchrdr	quellergt	ritland	trioml	wang
<b>PtoCA09_small</b>	0.878	0.686	0.295	0.809	0.165	0.849	0.344
<b>PtoCA09_big</b>	0.681	0.682	0.132	0.693	0.096	0.624	0.682
<b>PtoCA10_small</b>	0.355	0.313	0.091	0.233	0.185	0.444	0.316
<b>PtoCA10_big</b>	0.021	0.142	<b>0.004</b>	0.02	<b>0.017</b>	0.024	0.277
<b>CH09_small</b>	0.56	0.449	0.651	0.587	0.253	0.563	0.372
<b>CH09_big</b>	0.277	0.655	0.363	0.502	0.637	0.254	0.772

<b>CH2010_small</b>	0.672	0.621	0.396	0.472	0.239	0.687	0.403
<b>CH10_big</b>	0.493	0.386	0.058	0.511	<b>0.001</b>	0.504	0.299
<b>AN10_big</b>	0.26	0.699	0.336	0.666	0.111	0.199	0.807
<b>Average</b>	0.318	0.436	<b>0.001</b>	0.445	<b>0.001</b>	0.275	0.384

127  
128  
129  
130  
131  
132  
133  
134  
135  
136  
137  
138  
139

**Table S8. Results of power analysis for the Fisher's and Chi-square tests by using POWSIM ver. 4.1 (Ryman and Palm 2006).**  $F_{ST}$  in POWSIM refers to Nei's  $G_{ST}$  modified to be independent of the number of subpopulations (Nei 1987; Nei and Kumar 2000; Ryman and Palm 2006) and therefore we referred to our  $G_{ST}$  estimates to identify which genetic distance thresholds to test (see main text). To assess the statistical power of our 11 markers to detect  $F_{ST}$  ( $G_{ST}$ ) values  $\leq 0.01$ , we employed observed sample sizes and allele frequencies taken from our 9 samples and 1000 replicates. Following the POWSIM manual, we tested several combinations of  $N_e$  (100-3000) and generations ( $t = 1-60$ ) to account for the variability in  $N_e$  estimation. Power is given in % for Fisher's and Chi-square test.

$N_e$	$F_{ST} = 0.01$			$F_{ST} = 0.005$			$F_{ST} = 0.0025$			$F_{ST} = 0.001$		
	$t$	Fisher	Chi-square	$t$	Fisher	Chi-square	$t$	Fisher	Chi-square	$t$	Fisher	Chi-square
<b>100</b>	2	100	100	1	98.60	99.40	1	98.60	99.40	-	-	-
<b>500</b>	10	100	100	5	98.30	99.40	3	79.50	86.80	1	24.40	24.50
<b>1000</b>	20	100	100	10	98.40	99.70	5	66.90	73.90	2	23.30	22.30
<b>1500</b>	30	100	100	15	99.90	99.90	8	72.50	80.60	3	23.60	23.50
<b>3000</b>	60	100	100	30	98.90	99.60	15	65.90	74.70	6	22.40	23.40

140  
141

142 **Table S9. Sample pairwise unbiased  $F_{ST}$  (Weir 1996) estimates calculated with FreeNA (Chapuis and Estoup 2007) with and**  
143 **without correction for null alleles for each pair of samples of *Chamelea gallina*.** The software estimates null allele frequencies for  
144 each locus and sample, implementing the so-called excluding null allele (ENA) correction to provide accurate estimation of  $F_{ST}$  in the  
145 presence of null alleles (Dempster et al., 1977; Weir 1996). 95% confidence intervals (CI) for each  $F_{ST}$  estimate were obtained using  
146 10,000 bootstrap iterations. Differences at 95% CI associated with  $F_{ST}$  estimates obtained with and without applying the ENA algorithm  
147 were detected by visually comparing each CI for overlap.  
148

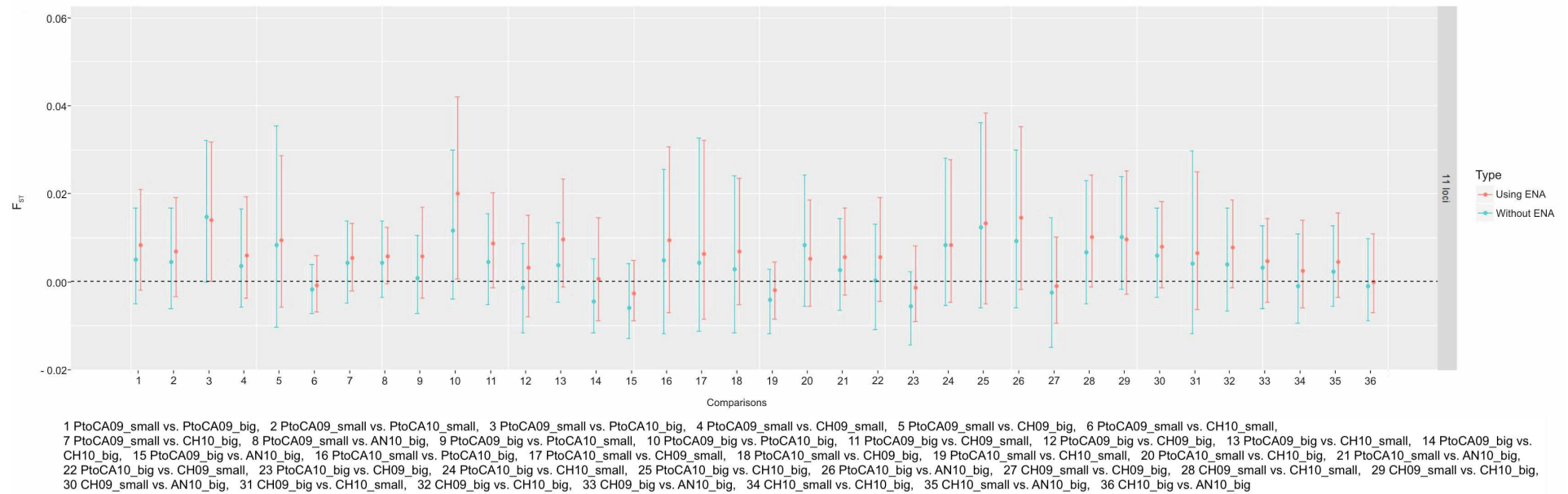


Samples	Method	PtoCA09_small	PtoCA09_big	PtoCA10_small	PtoCA10_big	CH09_small	CH09_big	CH10_small	CH10_big	AN10_big
PtoCA09_small	Without ENA									
	Using ENA									
PtoCA09_big	Without ENA	0.004958 [-0.005042, 0.016686]								
	Using ENA	0.008278 [-0.001907, 0.020854]								
PtoCA10_small	Without ENA	0.004516 [-0.006174, 0.016803]	0.000772 [-0.00723, 0.010454]							
	Using ENA	0.006808 [-0.00335, 0.019125]	0.00567 [-0.003762, 0.0169]							
PtoCA10_big	Without ENA	0.01474 [-0.000103, 0.032107]	0.011566 [-0.003936, 0.02994]	0.004905 [-0.011775, 0.025529]						
	Using ENA	0.013904 [0.000088, 0.03167]	0.019951 [0.000633, 0.041973]	0.009461 [-0.007052, 0.030713]						
CH09_small	Without ENA	0.003534 [-0.005781, 0.016457]	0.004493 [-0.00531, 0.015409]	0.004272 [-0.01126, 0.032664]	0.000221 [-0.01091, 0.01315]					
	Using ENA	0.005917 [-0.003835, 0.019336]	0.008636 [-0.001398, 0.020159]	0.006238 [-0.008461, 0.032154]	0.005597 [-0.004588, 0.019064]					
CH09_big	Without ENA	0.008394 [-0.01038, 0.03539]	-0.001335 [-0.011578, 0.008652]	0.00282 [-0.011615, 0.023976]	-0.005558 [-0.014415, 0.00223]	-0.002552 [-0.015023, 0.014606]				
	Using ENA	0.009338 [-0.005732, 0.028579]	0.00326 [-0.007988, 0.01515]	0.006855 [-0.005191, 0.023454]	-0.001348 [-0.009005, 0.008109]	-0.000998 [-0.009472, 0.010207]				
CH10_small	Without ENA	-0.001818 [-0.007295, 0.003922]	0.003677 [-0.004786, 0.013432]	-0.004095 [-0.011801, 0.002741]	0.008357 [-0.005456, 0.028002]	0.006731 [-0.005113, 0.022885]	0.004011 [-0.011915, 0.029743]			
	Using ENA	-0.00091 [-0.006803, 0.005978]	0.0096 [-0.00113, 0.023362]	-0.001897 [-0.008531, 0.004454]	0.008214 [-0.004715, 0.027669]	0.01005 [-0.001279, 0.024257]	0.006415 [-0.006275, 0.024927]			
CH10_big	Without ENA	0.00419 [-0.00489, 0.013782]	-0.004478 [-0.011628, 0.005231]	0.008246 [-0.005617, 0.024237]	0.012273 [-0.005999, 0.036197]	0.010112 [-0.00174, 0.023889]	0.003829 [-0.006728, 0.016674]	-0.001006 [-0.009395, 0.010885]		

	Using ENA	0.005306 [-0.00213, 0.013252]	0.000699 [-0.008866, 0.014491]	0.005213 [-0.00553, 0.018649]	0.013288 [-0.005105, 0.038335]	0.009548 [-0.002868, 0.025082]	0.007751 [-0.001462, 0.018514]	0.002424 [-0.00594, 0.013989]		
<b>AN10_big</b>	Without ENA	0.004355 [-0.003506, 0.013888]	-0.00592 [-0.012988, 0.004075]	0.002552 [-0.006442, 0.014303]	0.009225 [-0.005908, 0.029833]	0.005865 [-0.003676, 0.016818]	0.003241 [-0.006142, 0.012749]	0.002174 [-0.005626, 0.012619]	-0.001114 [-0.008885, 0.00973]	
	Using ENA	0.005815 [-0.000481, 0.012349]	-0.0027 [-0.008852, 0.004814]	0.005589 [-0.00312, 0.016796]	0.014491 [-0.001838, 0.035144]	0.007946 [-0.00143, 0.018203]	0.004619 [-0.004633, 0.014416]	0.004478 [-0.003631, 0.01559]	-0.00004 [-0.007084, 0.01095]	

150  
151

152 **Figure S3. Visualization of the  $F_{ST}$  (Weir 1996) estimates calculated with FreeNA (Chapuis and Estoup 2007) with and without**  
 153 **correction for null alleles for each pair of samples of *Chamelea gallina*.** The software estimates null allele frequencies for each  
 154 locus and population, implements the so-called excluding null allele (ENA) correction to provide accurate estimation of  $F_{ST}$  in the  
 155 presence of null alleles (Dempster et al., 1977; Weir 1996). 95% confidence intervals (CI) for each  $F_{ST}$  estimate were obtained using  
 156 10,000 bootstrap iterations. Differences at 95% CI associated with  $F_{ST}$  estimates obtained with and without applying the ENA algorithm  
 157 were detected by visually comparing each CI for overlap.



158  
 159

160 **Table S10 *Chamelea gallina*  $F_{ST}$  and  $G_{ST}$  estimates of pairwise genetic distance between samples and corresponding 95%**  
 161 **confidence intervals (95% CI).** The table reports the genetic distances calculated with the R package diveRsity ver. 1.9.90 (Keenan  
 162 et al., 2013). Below the diagonal is the genetic distance  $F_{ST}$  (Weir and Cockerham 1984) with corresponding 95% CI (in brackets) and  
 163 above the diagonal is the genetic distance  $G_{ST}$  (Nei and Chesser 1983) with corresponding 95% CI (in brackets). Genetic distances in  
 164 bold indicate significantly different sample pairs (where the 95% CI does not contain the zero).  
 165

Samples	PtoCA09_small	PtoCA09_big	PtoCA10_small	PtoCA10_big	CH09_small	CH09_big	CH10_small	CH10_big	AN10_big
<b>PtoCA09_small</b>		0.0046 [-0.0005, 0.0103]	0.0045 [-0.0016, 0.0118]	<b>0.0097</b> <b>[0.0025, 0.0184]</b>	0.0032 [-0.0017, 0.0097]	0.0072 [-0.003, 0.0224]	0.0009 [-0.0023, 0.0045]	0.0035 [-0.0012, 0.0087]	0.0037 [0.0000, 0.0083]
<b>PtoCA09_big</b>	0.0049 [-0.0048, 0.0166]		0.0034 [0.0000, 0.0071]	<b>0.0089</b> <b>[0.0017, 0.0169]</b>	0.0047 [-0.0003, 0.0106]	0.003 [-0.0024, 0.009]	<b>0.0045</b> <b>[0.0008, 0.0087]</b>	0.0000 [-0.0038, 0.0051]	-0.0007 [-0.0042, 0.0041]
<b>PtoCA10_small</b>	0.005 [-0.006, 0.0174]	0.0006 [-0.0073, 0.0099]		0.0063 [-0.0029, 0.0169]	0.005 [-0.0042, 0.0212]	0.0058 [-0.0033, 0.0184]	0.0006 [-0.0036, 0.0046]	0.0062 [-0.0005, 0.0138]	0.0036 [-0.0008, 0.009]
<b>PtoCA10_big</b>	0.0147 [-0.0005, 0.032]	0.0112 [-0.0047, 0.0286]	0.0061 [-0.0124, 0.0265]		0.0028 [-0.0034, 0.0097]	0.0007 [-0.0034, 0.0042]	<b>0.0073</b> <b>[0.0001, 0.0175]</b>	0.0084 [-0.0002, 0.0197]	0.0071 [-0.0001, 0.0171]
<b>CH09_small</b>	0.0034 [-0.006, 0.0164]	0.0045 [-0.0054, 0.0152]	0.0052 [-0.0112, 0.0348]	0.0004 [-0.0113, 0.0132]		0.0019 [-0.0056, 0.0122]	0.0056 [-0.001, 0.0146]	<b>0.0067</b> <b>[0.0005, 0.014]</b>	<b>0.0048</b> <b>[0.0001, 0.0101]</b>
<b>CH09_big</b>	0.0094 [-0.0104, 0.0384]	-0.0012 [-0.0115, 0.0094]	0.0046 [-0.0113, 0.0276]	-0.006 [-0.0155, 0.0015]	-0.0018 [-0.0153, 0.0167]		0.0057 [-0.0026, 0.0201]	0.0047 [-0.0006, 0.0112]	0.0043 [-0.0005, 0.0097]
<b>CH10_small</b>	-0.0018 [-0.0073, 0.0038]	0.0035 [-0.0049, 0.0132]	-0.0043 [-0.0119, 0.0026]	0.0088 [-0.0054, 0.0288]	0.0069 [-0.0056, 0.0228]	0.0053 [-0.0121, 0.033]		0.0014 [-0.0023, 0.0063]	0.0031 [-0.0004, 0.0077]
<b>CH10_big</b>	0.0042 [-0.0046, 0.0136]	-0.0047 [-0.0121, 0.0047]	0.0078 [-0.0055, 0.0236]	0.0119 [-0.006, 0.0356]	0.0099 [-0.0021, 0.0235]	0.004 [-0.0068, 0.0163]	-0.0012 [-0.0094, 0.0104]		0.0012 [-0.0027, 0.0065]
<b>AN10_big</b>	0.0044 [-0.0035, 0.0143]	-0.006 [-0.013, 0.0044]	0.0023 [-0.0066, 0.0138]	0.0088 [-0.0062, 0.0286]	0.0057 [-0.0039, 0.0165]	0.0034 [-0.0063, 0.0134]		-0.0014 [-0.0092, 0.0093]	

166  
167

168 **Table S11a, b and c. *Chamelea gallina* effective population size ( $N_e$ ) estimates.** Different methods were applied following Do et  
 169 al., (2014) as implemented in NeEstimator 2. Table a) displays global  $N_e$  estimates based on all individuals, global temporal and  
 170 geographic  $N_e$  estimates based on sample pools, all estimates were calculated with the Linkage Disequilibrium method (Waples and  
 171 Do 2010). Table b) shows single sample  $N_e$  estimates for each sample.  $N_b$  estimates were calculated only for the small size class  
 172 samples as they are considered the offspring of the latest reproductive season. Table c) provides  $N_b$  estimates based on temporal  
 173 methods. In brackets the 95% parametric confidence interval (CI). Sample acronym names as in Table 1 (main text). N sample size.  
 174  
 175

**Table S11a**

Methods	Samples pools				
	All	Porto Caleri	Chioggia	2009	2010
<b>N</b>	239	96	98	97	99
<b>LD<sup>a</sup></b>	1994.9 [452.6, ∞]	830.8 [180.3, ∞]	2197.3 [220.0, ∞]	304.7 [126.0, ∞]	344.9 [134.6, ∞]

<sup>a</sup>LD Linkage Disequilibrium method (Waples and Do 2010), the lowest allele frequency considered is 0.05

**Table S11b**

Methods	Samples								
	PtoCA09_small	PtoCA09_big	PtoCA10_small	PtoCA10_big	CH09_small	CH09_big	CH10_small	CH10_big	AN10_big
<b>N</b>	25	23	23	25	25	24	25	24	45
<b>LD<sup>a</sup></b>	373.7 [43.3, ∞]	59.9 [24.0, ∞]	77.1 [26.2, ∞]	26.4 [12.9, 101.3]	∞ [151.8, ∞]	138.8 [34.7, ∞]	1295.4 [49.0, ∞]	∞ [67.4, ∞]	73.4 [39.4, 246.8]
<b>Cn<sup>b</sup></b>	56.5 [0.1, 283.6]		8.7 [1.4, 22.4]		∞ [∞, ∞]		6.4 [1.1, 16.5]		

<sup>a</sup>LD Linkage Disequilibrium method (Waples and Do 2010), the lowest allele frequency considered is 0.05

<sup>b</sup>Cn Coancestry method (Nomura 2008)

**Table S11c**

Methods	Combination of samples and generation											
	Gen <sup>d</sup> . 0	Gen. 1	Gen. 0	Gen. 1	Gen. 0	Gen. 1	Gen. 0	Gen. 1	Gen. 0	Gen. 1	Gen. 0	Gen. 1
	PtoCA09_bi g	PtoCA09_sma ll	CH09_bi g	CH09_sma ll	PtoCA10_bi g	PtoCA10_sma ll	CH10_bi g	CH10_sma ll	PtoCA09_bi g	PtoCA10_sma ll	CH09_bi g	CH10_sma ll
<b>N</b>	23	25	24	25	25	23	24	25	23	23	24	25
<b>Pollak<sup>a</sup></b>	23.3 [7.8, ∞]		215.1 [16.2, ∞]		42.7 [10.1, ∞]		32.5 [9.8, ∞]		17.5 [6.4, 124.4]		143.4 [15.1, ∞]	
<b>Nei/Tajima<sup>b</sup></b>	27.1 [8.4, ∞]		187.0 [15.7, ∞]		32.8 [9.0, ∞]		54.3 [12.1, ∞]		20.5 [7.1, 392.2]		61.7 [12.1, ∞]	
<b>Jorde/Ryman<sup>c</sup></b>	27.3 [16.3, 41.0]		60.8 [37.1, 90.2]		18.6 [11.1, 28.1]		326.2 [200.7, 481.8]		23.6 [14.1, 35.5]		23.9 [14.5, 35.6]	

- 183 <sup>a</sup>Method by Pollak (Pollak 1983)  
184 <sup>b</sup>Nei/Tajima (Nei and Tajima 1981)  
185 <sup>c</sup>Jorde/Ryman (Jorde and Ryman 2007)  
186 <sup>d</sup>Gen. Generation, for all estimates the lowest allele frequency considered is 0.05  
187

188 **Table 12a and b. Garza and Williamson Index for *Chamelea gallina* and  $M_c$  critical values for each set of starting conditions**  
 189 **as described in the main text.** This analysis follows the principle that the ratio of the number of alleles to the range in allele size for a  
 190 sample of microsatellite loci can be used to detect reductions in effective population size (Garza and Williamson 2001). This method is  
 191 based on the premise that during a bottleneck, rare alleles are more likely to be lost, and the number of observed allelic states ( $k$ )  
 192 reduces faster than the range of allele size ( $r$ ), which results in a reduced M-ratio ( $M = k/r$ ). Table a) reports for all samples and loci the  
 193 modified M-ratio values calculated with Arlequin 3.5.1.3 (Excoffier and Lischer 2010). Values below the critical threshold are in bold.  
 194 Table b) reports the  $M_c$  (critical value) for samples with 25 individuals and for the Ancona sample with 45 individuals respectively were  
 195 calculated with Critical\_M (Garza and Williamson 2001) imposing two possible values of pre-bottleneck  $N_e$  and percentage of one-step  
 196 model (90 and 80%). The lowest value obtained (0.62) was used as the conservative threshold for bottleneck evaluation. The highest  
 197 and lowest values for each N group are in bold.

198  
 199 **Table S12a**  
 200

Locus	PtoCA09_small	PtoCA09_big	PtoCA10_small	PtoCA10_big	CH09_small	CH09_big	CH10_small	CH10_big	AN10_big	Mean	SD <sup>a</sup>
260	0.6250	0.6250	<b>0.5000</b>	<b>0.5000</b>	<b>0.5000</b>	0.6250	0.6250	0.6250	0.8750	0.6111	0.1160
1088	<b>0.5385</b>	<b>0.5385</b>	<b>0.4615</b>	<b>0.3077</b>	<b>0.5385</b>	<b>0.3846</b>	<b>0.3846</b>	<b>0.3077</b>	<b>0.4615</b>	0.4359	0.0942
1243	<b>0.2000</b>	<b>0.1200</b>	<b>0.0800</b>	<b>0.1600</b>	<b>0.1600</b>	<b>0.1600</b>	<b>0.2800</b>	<b>0.2000</b>	<b>0.1600</b>	0.1689	0.0558
9969	0.7143	<b>0.4286</b>	0.7143	<b>0.5714</b>	<b>0.4286</b>	<b>0.5714</b>	0.7143	0.7143	0.7143	0.6191	0.1237
10343	0.6250	<b>0.5000</b>	0.6250	<b>0.5000</b>	<b>0.5000</b>	0.6250	0.6250	<b>0.5000</b>	0.7500	0.5833	0.0884
18241	0.7000	<b>0.6000</b>	0.7000	<b>0.5000</b>	0.7000	0.7000	0.7000	0.7000	0.7000	0.6667	0.0707
20447	1.0000	1.0000	1.0000	1.0000	1.0000	1.0000	1.0000	1.0000	1.0000	1.0000	0.0000
26069	<b>0.6000</b>	0.8000	<b>0.4000</b>	<b>0.4000</b>	<b>0.5000</b>	<b>0.5000</b>	<b>0.5000</b>	<b>0.5000</b>	<b>0.4000</b>	0.5111	0.1269
33835	<b>0.5790</b>	<b>0.4737</b>	<b>0.3684</b>	<b>0.5000</b>	<b>0.5000</b>	<b>0.4211</b>	<b>0.4737</b>	<b>0.4737</b>	<b>0.6053</b>	0.4883	0.0722
41629	<b>0.2903</b>	<b>0.2581</b>	<b>0.2581</b>	<b>0.2258</b>	<b>0.2903</b>	<b>0.1936</b>	<b>0.2903</b>	<b>0.2258</b>	<b>0.2581</b>	0.2545	0.0340
41630	<b>0.2188</b>	<b>0.2188</b>	<b>0.0938</b>	<b>0.0625</b>	<b>0.1250</b>	<b>0.1875</b>	<b>0.0938</b>	<b>0.0938</b>	<b>0.2813</b>	0.1528	0.0757
Mean	0.5537	0.5057	0.4728	0.4297	0.4765	0.4880	0.5169	0.4854	0.5641		
SD*	0.2379	0.2558	0.2778	0.2509	0.2430	0.2552	0.2520	0.2677	0.2717		

<sup>a</sup> SD, Standard Deviation

201  
 202

203 **Table S12b**  
 204

	For samples from Chioggia and Porto Caleri				For sample from Ancona			
<b>N (samples size x 2)</b>	50	50	50	50	90	90	90	90
<b>Pre-bottleneck <math>\Theta</math> (<math>4N_e\mu^a</math>)</b>	6	6	2	2	6	6	2	2
<b>Mean size of non-stepwise mutations <math>\Delta_g</math></b>	3.5	3.5	3.5	3.5	3.5	3.5	3.5	3.5
<b>% larger mutations <math>p_s</math></b>	0.2	0.1	0.2	0.1	0.2	0.1	0.2	0.1
<b>Critical value (<math>M_c</math>)</b>	<b>0.620484</b>	0.693621	0.663494	<b>0.749058</b>	<b>0.649436</b>	0.718571	0.671954	<b>0.755447</b>

<sup>a</sup> mutation rate from Estoup and Angers (1998)

205  
 206



207 **Table S13 Probability results of one tailed Wilcoxon signed-rank test for heterozygosity excess as implemented in the**  
 208 **software Bottleneck ver. 1.2.02 (Cornuet and Luikart 1996; Piry et al., 1999).** The analyses were conducted for each sample using  
 209 a 70% Stepwise Mutation Model (SMM) and 30% Infinite Allele Model (IAM) in the Two Phase Model (TPM) (Di Rienzo et al., 1994),  
 210 and a TPM variance of 12, as recommended for microsatellites (Jensen et al., 2013; Piry et al., 1999) with 10,000 replications.  
 211

Samples	Probability		
	IAM	TPM	SMM
PtoCA09_small	0.71143	1.00000	1.00000
PtoCA09_big	0.55078	0.98950	0.99829
PtoCA10_small	0.58447	0.99390	0.99878
PtoCA10_big	0.79346	0.99658	0.99951
CH09_small	0.35010	0.95850	0.99390
CH09_big	0.76758	0.99390	0.99927
CH2010_small	0.76758	0.99658	0.99951
CH10_big	0.61768	0.97314	0.99756
AN10_big	0.48291	0.99927	0.99976

212  
 213

214  
215  
216  
217  
218  
219  
220  
  
221  
222  
  
223  
224  
  
225  
  
226  
227  
  
228  
229  
  
230  
231  
  
232  
233  
  
234  
235  
  
236  
237  
  
238

## References

- Agostini, C.; Papetti, C.; Patarnello, T.; Mark, F.; Zane, L.; Marino, I.M. Putative selected markers in the *Chionodraco* genus detected by interspecific outlier tests. *Polar Biol.* 36:1509-1518; 2013
- Antao, T.; Lopes, A.; Lopes, R.J.; Beja-Pereira, A.; Luikart, G. LOSITAN: A workbench to detect molecular adaptation based on a  $F_{st}$ -outlier method. *BMC Bioinformatics.* 9:323; 2008
- Carvajal-Rodriguez, A.; de Uña-Alvarez, J. Assessing significance in high-throughput experiments by sequential goodness of fit and q-value estimation. *PLoS ONE.* 6:e24700; 2011
- Chapuis, M.-P.; Estoup, A. Microsatellite null alleles and estimation of population differentiation. *Mol Biol Evol.* 24:621-631; 2007
- Cornuet, J.M.; Luikart, G. Description and power analysis of two tests for detecting recent population bottlenecks from allele frequency data. *Genetics.* 144:2001-2014; 1996
- Dempster, A.; Laird, N.; Rubin, D. Maximum likelihood from incomplete data via the EM algorithm. *J R Stat Soc Series B Stat Methodol.* 39:1-38; 1977
- Di Rienzo, A.; Peterson, A.C.; Garza, J.C.; Valdes, A.M.; Slatkin, M.; Freimer, N.B. Mutational processes of simple-sequence repeat loci in human populations. *Proc Natl Acad Sci U S A.* 91:3166-3170; 1994
- Do, C.; Waples, R.S.; Peel, D.; Macbeth, G.M.; Tillett, B.J.; Ovenden, J.R. NeEstimator v2: Re-implementation of software for the estimation of contemporary effective population size ( $N_e$ ) from genetic data. *Mol Ecol Resour.* 14:209-214; 2014
- Estoup, A.; Angers, B. Microsatellites and minisatellites for molecular ecology: theoretical and empirical considerations. *Advances in molecular ecology.* Amsterdam: IOS Press; 1998
- Excoffier, L.; Lischer, H.E.L. Arlequin suite ver 3.5: A new series of programs to perform population genetics analyses under Linux and Windows. *Mol Ecol Resour.* 10:564-567; 2010
- Garza, J.C.; Williamson, E.G. Detection of reduction in population size using data from microsatellite loci. *Mol Ecol.* 10:305-318; 2001

- 239 Jensen, H.; Moe, R.; Hagen, I.J.; Holand, A.M.; Kekkonen, J.; Tufto, J.; Sæther, B.E. Genetic variation and structure of house sparrow  
240 populations: Is there an island effect? *Mol Ecol.* 22:1792-1805; 2013
- 241 Jorde, P.; Ryman, N. Unbiased estimator for genetic drift and effective population size. *Genetics.* 177:927-935; 2007
- 242 Keenan, K.; McGinnity, P.; Cross, T.F.; Crozier, W.W.; Prodöhl, P.A. *diveR*sity: An R package for the estimation and exploration of  
243 population genetics parameters and their associated errors. *Methods Ecol Evol.* 4:782-788; 2013
- 244 Li, C.C.; Weeks, D.E.; Chakravarti, A. Similarity of DNA fingerprints due to chance and relatedness. *Hum Hered.* 43:45-52; 1993
- 245 Lynch, M.; Ritland, K. Estimation of pairwise relatedness with molecular markers. *Genetics.* 152:1753-1766; 1999
- 246 Milligan, B. Maximum-likelihood estimation of relatedness. *Genetics.* 163:1153-1167; 2003
- 247 Nei, M. *Molecular Evolutionary Genetics.* New York: Columbia University Press; 1987
- 248 Nei, M.; Chesser, R.K. Estimation of fixation indices and gene diversities. *Ann Hum Genet.* 47:253-259; 1983
- 249 Nei, M.; Kumar, S. *Molecular evolution and phylogenetics.* Oxford: Oxford University Press; 2000
- 250 Nei, M.; Tajima, F. Genetic drift and estimation of effective population size. *Genetics.* 1981:625-640; 1981
- 251 Nomura, T. Estimation of effective number of breeders from molecular coancestry of single cohort sample. *Evol Appl.* 1:462-474; 2008
- 252 Pew, J.; Muir, P.H.; Wang, J.; Frasier, T.R. *related*: An R package for analysing pairwise relatedness from codominant molecular  
253 markers. *Mol Ecol Resour.* 15:557-561; 2015
- 254 Piry, S.; Luikart, G.; Cornuet, J.M. *BOTTLENECK*: A computer program for detecting recent reductions in the effective population size  
255 using allele frequency data. *J Hered.* 90:502-503; 1999
- 256 Pollak, E. A new method for estimating the effective population size from allele frequency changes. *Genetics.* 104:531-548; 1983
- 257 Queller, D.; Goodnight, K. Estimating relatedness using molecular markers. *Evolution.* 43:258-275; 1989
- 258 Ritland, K. Estimators for pairwise relatedness and inbreeding coefficients. *Genet Res.* 67:175-186; 1996

- 259 Ryman, N.; Palm, S. POWSIM: A computer program for assessing statistical power when testing for genetic differentiation. *Mol Ecol*  
260 *Notes*. 6:600-602; 2006
- 261 Schneider, T.C.; Kappeler, P.M.; Pozzi, L. Genetic population structure and relatedness in the narrow-striped mongoose (*Mungotictis*  
262 *decemlineata*), a social Malagasy carnivore with sexual segregation. *Ecol Evol*. 6:3734-3749; 2016
- 263 van Oosterhout, C.; Hutchinson, W.F.; Wills, D.P.M.; Shipley, P. MICRO-CHECKER: Software for identifying and correcting  
264 genotyping errors in microsatellite data. *Mol Ecol Notes*. 4:535-538; 2004
- 265 Wang, J. An estimator for pairwise relatedness using molecular markers. *Genetics*. 160:1203-1215; 2001
- 266 Wang, J. Triadic IBD coefficients and applications to estimating pairwise relatedness. *Genet Res*. 89:135-153; 2007
- 267 Wang, J. Coancestry: A program for simulating, estimating and analysing relatedness and inbreeding coefficients. *Mol Ecol Resour*.  
268 11:141-145; 2011
- 269 Waples, R.S.; Do, C. Linkage disequilibrium estimates of contemporary  $N_e$  using highly variable genetic markers: A largely untapped  
270 resource for applied conservation and evolution. *Evol Appl*. 3:244-262; 2010
- 271 Weir, B. Genetic data analysis 2: methods for discrete population genetic data. Sunderland (Massachusetts): Sinauer Associates;  
272 1996
- 273 Weir, B.; Cockerham, C. Estimating F-statistics for the analysis of population structure. *Evolution*. 38:1358-1370; 1984  
274

**FIN**